SURFACE SYNOPTIC FLOW TYPES AND THEIR RELATION TO RAINFALL OVER THE ISLAND OF TAIWAN

A DISSERTATION SUBMITTED TO THE GRADUATE DIVISION OF THE UNIVERSITY OF HAWAII IN PARTIAL FULFILLMENT OF THE REQUIREMENTS FOR THE DEGREE OF

DOCTOR OF PHILOSOPHY

IN GEOGRAPHY

DECEMBER 1974

by

Gong-yuh Lin

Dissertation Committee:

Jen-hu Chang, Chairman
R.W. Armstrong
Wilfrid Bach
Sen-dou Chang
Paul C. Ekern
John M. Street

We certify that we have read this dissertation and that in our opinion it is satisfactory in scope and quality as a dissertation for the degree of Doctor of Philosophy in Geography.

DISSERTATION COMMITTEE

_____
Chairman

_____

_____

_____

_____

_____

ABSTRACT

In this paper, spatial and temporal variation in rainfall characteristics over Taiwan are investigated in the light of synoptic and general circulations, ocean-surface temperatures in the Pacific, the extent of the Arctic sea ice, and solar activity. Eleven synoptic flow types over Taiwan are recognized, based on daily weather maps for the eleven years from 1959 through 1969. Mean rainfall-annual, monthly, and daily--and the probability of rainy days associated with those synoptic flow types show distinct spatial variation. The Mongolian and Mongolian cutoff anticyclones, and the Taiwan low prevail over Taiwan in winter, fall, and early spring, respectively. They contribute rainfall mainly to northern and eastern Taiwan. In late spring and early summer, polar fronts dominate Taiwan and cause the "plum rains" over the entire island. The onset of the "plum rains" is associated with the increase in the 500-mb geopotential height and temperature, and with the weakening of the westerlies over Taiwan. In summer, the North Pacific subtropical anticyclone and the southwest monsoon dominate Taiwan, but they are most frequently associated with dry days. Typhoons tend to visit Taiwan during periods of intense negative height anomalies over Siberia and the east China seaboard at

the 700-mb level. Based on stepwise multiple regression analysis, it is found that the center of action, such as the North Pacific subtropical anticyclone, accounts for most of the variation in annual rainfall over Taiwan.

In terms of the general circulation, low zonal-index favors Taiwan with heavy rainfall due to more active Mongolian anticyclone, Taiwan low, and typhoons. The low zonal-index with the belt of the strongest westerlies in low latitudes favors only northern and eastern Taiwan with wet periods, whereas the low zonal-index with distinct blocking patterns favors the entire island with wet periods. The secular rainfall variation over Taiwan follows the 80-year solar-climatic cycle, and is related to ocean-surface temperatures and the extent of the Arctic sea ice.

The drought period of 1962 to 1965 over Taiwan was associated with the warming of the eastern equatorial Pacific and the central North Pacific. It is also associated with the decrease in the annual frequencies of the Mongolian cutoff anticyclone and the North Pacific subtropical anticyclone.

The dirunal rainfall variation over Taiwan shows distinct spatial and temporal variation, as a result of the combined effect of the synoptic-scale prevailing winds, land

and sea breezes, and topography.

The daily rainfall occurrence at various Taiwan stations follows either the Markov chain model or the logarithmic series. The occurrence of synoptic flow types follows the Markov chain model, but only that of summer types follows the logarithmic series.

The spatial distribution of water surplus and water deficit over Taiwan resembles that of rainfall regimes resulting from various synoptic flow types. The significant decreases in annual rice yields over Taiwan are associated with large-scale droughts.

TABLE OF CONTENTS

ABSTRACT iii

LIST OF TABLES ix

LIST OF ILLUSTRATIONS. xi

CHAPTER I. INTRODUCTION

Background of the Study. 1
Objectives and Expected Significance 3
Literature Review. 4
Methods. 8
Data 17

CHAPTER II. FREQUENCY OF SYNOPTIC FLOW TYPES

Mean Monthly Frequency 18
Mean Annual Frequency. 23
Solar Activity 25
Air-Sea Interaction. 32
Summary of Significant Results 40

CHAPTER III. RAINFALL ASSOCIATED WITH THE MONGOLIAN ANTICYCLONE AND THE MONGOLIAN CUTOFF ANTICYCLONE

The Mongolian Anticyclone. 43
The Mongolian Cutoff Anticyclone . . . 55
Summary of Significant Results 61

CHAPTER IV. RAINFALL ASSOCIATED WITH THE TAIWAN LOW AND THE POLAR FRONT

The Taiwan Low 64
Polar Fronts 70
The Plum Rains 75
Summary of Significant Results 104

CHAPTER V. RAINFALL ASSOCIATED WITH THE NORTH PACIFIC SUBTROPICAL ANTICYCLONE AND THE SOUTHWEST MONSOON

The North Pacific Subtropical Anticyclone 107
The Southwest Monsoon 110
Summary of Significant Results. . . . 113

CHAPTER VI. RAINFALL ASSOCIATED WITH TYPHOONS

Mean Annual and Monthly Frequencies . 116
Mean Monthly 700-mb Circulation Associated with Typhoon Frequency . 121
Rainfall Associated with Typhoon Visiting Taiwan 136
Rainfall Associated with the Kyushu-type Typhoon 138
Rainfall Associated with the Monsoon Trough. 140
Summary of Significant Results. . . . 141

CHAPTER VII. STATISTICAL MODELS OF DAILY RAINFALL AND SYNOPTIC FLOW TYPE OCCURRENCES

The Simple Markov Chain Probability Model 144
Logarithmic Series. 160
Synoptic Flow Types 163
Summary of Significant Results. . . . 173

CHAPTER VIII. DIURNAL RAINFALL VARIATIONS

Theories. 178
Winter. 185
Spring. 192
Summer. 193
Fall. 195
Summary of Significant Results. . . . 195

CHAPTER IX. ANNUAL RAINFALL

The Stability of Means and Median. . . 199
Skewness and Rainfall Probability Chart. 202
Synoptic Aspects of Inter-Annual Rainfall Variations. 208
Floods and Droughts. 217
Summary of Significant Results 225

CHAPTER X. SECULAR RAINFALL VARIATIONS

Method 228
Regionalization. 233
Physical Causes. 240
Summary of Significant Results 249

CHAPTER XI. SUMMARY. 255

APPENDIX. 269

BIBLIOGRAPHY. 335

LIST OF TABLES

Table		Page
1	Mean, standard deviation, and coefficients of variation of frequencies of synoptic flow types	26
2	Frequency of polar fronts which last for 3 days or longer for the period 1959 to 1969	72
3	Dates of the onset and the end of the plum rains for the period 1959 to 1969	87
4	Mean annual thunderstorm frequencies associated with different synoptic flow types over Taiwan	115
5	Frequency distribution of typhoons visiting Taiwan (1897-1969)	119
6	Total and mean monthly frequency of typhoons in the western North Pacific for the period 1940 to 1969	120
7	Total and mean monthly frequency of typhoons visiting Taiwan for the period 1897 to 1969	120
8	Estimates of wet-day (0.1 mm or more) occurrences	148
9	Monthly variations in conditional probabilities of wet-day occurrences	150
10	Return periods (in days) of wet-spells derived from the simple Markov chain probability model	158
11	Return periods (in days) of dry-spells derived from the simple Markov chain probability model	159

Table		Page
12	Four parameters for the estimation of wet-spells and dry-spells according to the logarithmic series	162
13	The argument between the frequency distribution of wet and dry spells derived from the simple Markov chain probability model or from the logarithmic series, and that derived from observation.	175
14	The agreement between the frequency distribution of synoptic flow types derived from the simple Markov chain probability model or from the logarithmic series, and that derived from observation.	176
15	Mean and median values of annual and monthly rainfall at various Taiwan stations	203
16	Coefficients of determination between annual frequencies of synoptic flow types and annual rainfall.	210
17	Coefficients of correlation between annual frequencies of synoptic flow types and annual rainfall.	212
18	Coefficients of correlation among all synoptic flow types.	214
19	Residuals between the computed and observed annual rainfall	218
20	The frequencies of floods and droughts over Taiwan and their relations to the positions of the Aleutian low, the Mongolian anticyclone, the monsoon trough, and to zonal-index	220

LIST OF ILLUSTRATIONS

Figure		Page
1	Models of synoptic flow patterns in the vicinity of Taiwan	12
2	The mean monthly frequency of various synoptic flow types.	19
3	The mean annual frequency of various synoptic flow types.	24
4	Variations in the annual frequency of various synoptic flow types.	30
5	Time history of zonal and meridional indices.	31
6	Time series of monthly sea-surface temperature anomalies in the tropical Pacific.	34
7	Seasonal mean sea-surface temperature departures from normal for 10° square centered at 40°N, 150°W (A), and at 35°N, 170°W (B).	38
8	Mean monthly rainfall variations at the various Taiwan stations.	41
9	Vertical variations in temperatures and winds associated with the Mongolian and Pacific anticyclones, at Taoyuan	47
10	Mean annual rainfall associated with the eleven synoptic flow types	48
11	Mean daily rainfall associated with the eleven synoptic flow types	51
12	Standard deviation of daily rainfall associated with the eleven synoptic flow types	52

	and Tongkang during the plum rain period of 1960	96
26	Daily rainfall variations at Keelung and Kaoshiung, 500-mb height variations at Taoyuan, and 500-mb height differences between Taoyuan and Tongkang during the plum rain period of 1964.	97
27	Daily rainfall variations at Keelung and Kaoshiung, 500-mb height variations at Taoyuan, and 500-mb height differences between Taoyuan and Tongkang during the plum rain period of 1965.	98
28	Daily 500-mb temperature variations at Taoyuan during the plum rain period of 1964 and 1965.	100
29	Daily 590-mb temperature variations at Taoyuan during the plum rain period of 1960	101
30	Mean daily rainfall associated with the latitudinal positions polar fronts . . .	102
31	Variations in the annual frequency of typhoons in the western North Pacific and those visiting Taiwan, 1897-1969	117
32	Mean 700-mb contours and height anomalies of the Northern Hemisphere for August of 1959, 1960, 1961, and 1962	123
33	Mean 700-mb contours of the Northern Hemisphere for August of 1963, 1964, and 1968	129
34	Mean 700-mb height anomalies of the Northern Hemisphere for August of 1963, 1964, and 1968	130
35	Mean 700-mb height anomalies of the North Pacific and East Asia associated with active typhoon months of August in Taiwan.	134

13	Probability of rainy days associated with the eleven synoptic flow types.	54
14	Vertical variations in temperatures and winds associated with the Mongolian and Mongolian cutoff anticyclones, at Taoyuan	57
15	Vertical variations in temperatures and winds associated with the Mongolian anticyclone and Taiwan low, at Taoyuan . . .	66
16	Vertical wind variations at Taoyuan during the frequent Taiwan low period. . . .	67
17	Vertical variations in temperatures and winds associated with the southwest monsoon and polar front, at Taoyuan.	71
18	Daily rainfall variations at the various Taiwan stations during the plum rain period of 1967	83
19	Vertical wind variations at Taoyuan during the plum rain period of 1960.	89
20	Vertical wind variations at Tongkang during the plum rain period of 1960.	90
21	Vertical wind variations at Taoyuan during the plum rain period of 1964.	91
22	Vertical wind variations at Tongkang during the plum rain period of 1964.	92
23	Vertical wind variations at Taoyuan during the plum rain period of 1965.	93
24	Vertical wind variations at Tongkang during the plum rain period of 1965.	94
25	Daily rainfall variations at Keelung (curves) and Kaoshiung (straight lines), 500-mb height variations at Taoyuan, and 500-mb height differences between Taoyuan	

36 Mean 700-mb height anomalies of the North Pacific and East Asia ssso-ciated with inactive typhoon months of August in Taiwan. 135

37 The cumulative conditional prob-abilities (curves) derived from the simple Markov chain model and the cumulative unconditional prob-abilities (dots) of wet spells of various length. 151

38 The cumulative conditional probabilities (curves) derived from the simple Markov chain model and the cumulative uncondi-tional probabilities (dots) of dry-spells of various length 153

39 The frequency distribution of wet-spells by the simple Markov chain model (curves) and by observation (dots) 154

40 The frequency distribution of dry-spells by the simple Markov chain model (curves) and by observation (dots) 156

41 The frequency distribution of wet-spells by the logarithmic series (curves) and by observation (dots) 164

42 The frequency distribution of dry-spells by the logarithmic series (curves) and by observation (dots) 165

43 The cumulative conditional probabilities (curves) derived from the simple Markov chain model and the cumulative uncondi-tional probabilities (dots) of occurrences of the eleven synoptic flow types 167

44 The frequency distribution of the eleven synoptic flow types by the simple Markov chain model (curves) and by observation (dots). 169

45	The frequency distribution of the eleven synoptic flow types by the logarithmic series (curves) and by observation (dots).	171
46	Diurnal rainfall variations at various Taiwan stations	187
47	Diurnal rainfall variations at Keelung. . .	188
48	The prevailing winds over Taiwan in January	190
49	The prevailing winds over Taiwan in July.	194
50	The stability of mean and median at various Taiwan stations	201
51	Cumulative frequency distribution of the mean annual rainfall at the six Taiwan stations	205
52	Spatial variations in the skewness of rainfall	206
53	The rainfall probability chart based on the eight Taiwan stations.	209
54	The inter-annual variation in Wolf's sunspot number and flood years at various Taiwan stations	223
55	The inter-annual variation in Wolf's sunspot number and drought years at various Taiwan stations	224
56	The annual rainfall residual-mass curves at various Taiwan stations	234
57	The rainfall residual-mass curves in summer (full lines) and in winter (dotted lines) at various Taiwan stations.	235

CHAPTER I

INTRODUCTION

Background of the Study

Quick and accurate forecasting cannot be achieved without criteria which provide objective means for the analysis of daily weather maps. It has long been recognized that the classification of weather into synoptic flow types serves as an invaluable tool for forecasting with a moderate degree of accuracy (Elliott, 1949). The classification of synoptic flow types is essentially the cataloguing of past weather. Strictly speaking, it is not possible to find two identical synoptic flow patterns at different times. However, on the basis of similarity, synoptic flow patterns can be classified into several types in terms of selected criteria. Once this is done, current and future weather can be objectively analyzed by referring to the classified types.

Since climate can be defined as the statistical collective of individual conditions of weather (Landsberg, 1951), it is obvious that the dominance of a given synoptic flow type serves to a large degree to explain the climate of a given area. Consequently, the classification of

synoptic flow types provides a convenient tool for the study of both synoptic and dynamic climatology over a given area.

The technique of the classification of synoptic flow patterns has been used to analyze rainfall for the islands of Puerto Rico, central Cuba, and Hawaii, and has produced significant results. A study of this kind is particularly important to Taiwan because of the fluctuations in time and space of monsoons, trades, and typhoons, and of topographic characteristics of the island which favor recurrent floods and droughts. Local daily rainfall amounts caused by typhoons often reach several hundred millimeters. A noted example of heavy rain occurred on August 7, 1959, which resulted in a great inundation in the middle and south parts of Taiwan--covering 43% of total cultivated lands (Cheng, 1959). On the other hand, Taiwan frequently suffers from droughts due to the absence of the unpredictable typhoons in summer and the unusual persistence of the Mongolian anticyclone in winter.

Although an adequate data bank is available, a review of the literature indicated that no extensive study of synoptic flow types in relation to rainfall over Taiwan has as yet been made. Therefore, this study will undertake

to clarify synoptic flow patterns and dynamic weather activities, with the aim of establishing some basis for the improvement of forecasting, as well as an understanding of climatic variation over Taiwan.

Objectives and Expected Significances

A number of statistical studies of Taiwan regarding distribution and variation in rainfall characteristics such as mean rainfall amount, median, and mean rainy days and intensity, persistence, and trend of rainfall, have been made (Chiang, 1954; Chen, 1959; Kang, 1968). For the most part, these studies were descriptive, and little attempt was made to explain the distribution and variation in rainfall characteristics over Taiwan by means of objective synoptic analysis of flow types. Consequently, the main purpose of this study is to determine the synoptic flow types and their relationship to rainfall over Taiwan by using daily data over an extended number of years.

As early as 1931, Willett (1931) pointed out the importance of the classification of weather pattern as a tool for weather forecasting and the study of climatic variation. It is hoped that the results of this investigation will fill the critical need of understanding the various synoptic flow types and their relation to rainfall which

affect Taiwan. The results themselves will constitute a framework upon which future studies of climatic variation of synoptic flow types may be built.

Literature Review

In the past, many efforts have been devoted to the classification of synoptic flow patterns over regions ranging in scale from the hemisphere to small islands. Since the turn of this century, various methodologies have been employed in such classifications.

Baur (1941) classified the weather for the summer months over western Europe into thirty types. He used surface pressure distribution as a criterion for his classification. He tabulated the frequency and persistence of weather types from 1885 to 1939. Other studies regarding the classification of weather types for European areas have been presented by Hess and Brezowsky (1952) and Burger (1952).

In North America, two of the earliest studies of weather pattern classification were those made by Bowie and Weightman (1914), who defined storm types of the United States, and by Reed (1932), who classified weather types of the North Pacific in terms of prevailing wind directions. During the late thirties, a group of scholars in the

Department of Meteorology, California Institute of Technology, made a number of studies of the six-day North American weather types. The results were presented in a series of papers. The weather types they defined were based on the distribution of semi-permanent elements of circulation such as the Pacific anticyclone, the Aleutian low, trajectories of polar outbreaks, and cyclonic paths. One of the later papers by Elliott (1949) is the most extensive. He defined sixteen weather types for North America in terms of meridional and zonal flows at the upper level and the associated surface distribution of cyclones and anticyclones. Rainfall and temperature distributions associated with individual weather types were analyzed.

Various studies regarding synoptic weather patterns over China have been made by Chu (1926) and Cheng (1949). These studies were based on daily surface pressure distribution charts. Cheng (1949) defined synoptic weather types by daily isobaric charts for the year 1948. He presented the spatial distribution of rainfall over China associated with individual weather types. Hsueh (1963a and b) classified flow patterns over China and East Asia into five types based on the composition of jet streams at the 500-mb level and the distribution of ridges and troughs at the 700-mb

level. Surface distribution and movement of anticyclones and cyclones were discussed for individual types. He found that the periodicity of these types is around six days which confirmed the earlier findings of the California Institute of Technology on weather types.

In South Africa, Vowinckel (1956) defined seven weather types based on the surface pressure distribution.

The above-mentioned studies dealt with synoptic weather patterns over large areas in middle latitudes. Similar techniques have been applied to tropical and subtropical islands with varying degrees of success in explaining the occurrence and quantity of rainfall which is the most significant weather element in lower latitudes.

Synoptic flow patterns in relation to rainfall have been made for the islands of Puerto Rico, central Cuba, and Hawaii by Riehl and Schacht (1947), Howell (1954), and Yeh, et al. (1951a), respectively. Riehl and Schacht, using forty years of records, determined the total daily rainfall associated with various synoptic flow types during January and March. They found that days with 0.25 inch (6.35 mm) or more of rainfall are usually the result of major synoptic disturbances, while days with 0.2 inch (0.51 mm) or less represent undisturbed atmospheric flow with frequent light

showers. Howell defined nine types of synoptic flow patterns for central Cuba in terms of the surface distribution and shape of anticyclones, polar fronts, and tropical disturbances for the period 1946-1950. The occurrence and quantity of rainfall in relation to the accompanying surface synoptic flow types was examined. In addition, Howell classified flow patterns at the 700-mb level into four subtypes and discussed the wind speed and direction at three levels, i.e., surface, 1000 feet, and 700 mb, and the lapse rate in relation to the amount of rainfall. In terms of the distribution of cyclones and anticyclones for the period 1916-1940, Yeh, et al. classified the surface synoptic flow patterns near Hawaii into eight types. These workers analyzed the frequency and variability of these types and their relationship to annual, monthly, and daily rainfall over Oahu. In addition, they investigated rainfall anomaly patterns for various wind directions at 3 km with a given surface flow pattern. In another study, Yeh, et al. (1951b) attempted to explain the effect of the jet stream at the 700-mb level on the surface circulation and rainfall. Their surface synoptic flow types have been adopted by Samarakkody (1969) in a study of the synoptic climatology of Hawaii for the period 1937-1966. Based on Yeh, et al.'s study,

Worthley (1967) calculated the mean number, and the maximum and minimum number of frontal passages for the four major islands of Hawaii by months and by winter seasons. Lee (1967) correlated the frequencies of thunderstorms over four major islands of Hawaii with Yeh, et al.'s synoptic flow types and concluded that they are somehow related.

Dzerdzeevskii (1963) classified the Northern Hemisphere weather into six types based on the relative strength of zonal and meridional flows. However, classifications of hemispheric weather patterns do not provide sufficient information for the study of local climate.

Methods

There are two general schemes for the classification of synoptic flow patterns. One is essentially based on the distribution of cyclones, anticyclones, fronts, and various synoptic disturbances as shown on daily weather charts for a given area. Hsueh (1963a) has given the term "static" to this approach. The studies by Riehl, et al. (1947), Howell (1954), and Yeh, et al. (1951a) adopted this classification scheme. In contrast, synoptic flow types can also be defined in terms of the movement of surface cyclones and anticyclones, which are steered by upper air circulations such as zonal, meridional flows, and the composition of jet

streams, within a given large region over a sequence of days. Hsueh (1963a and b) has given the term "dynamic" to this approach which was developed initially by a group of scholars in the Department of Meteorology, California Institute of Technology. Elliott (1949) and Hsuch (1963a and b) based their studies on this classification scheme. This study of Taiwan will use the "Static" approach, since the dynamic method is essentially useful for studies of extensive areas and is therefore not applicable. The method that will be used is essentially based on the technique developed by Riehl and Schact (1947), Howell (1954), and Yeh, et al. (1951a and b), with various additions and modifications.

In Taiwan, eleven synoptic flow types have been identified based on daily surface isobaric charts for eleven years from 1959 through 1969 (Figure 1):

1. The Mongolian anticyclone (type 1)
   A polar continental anticyclone is centered on Mongolia or near Lake Baikal.
2. The Mongolian cutoff anticyclone (type 2)
   The center of the Mongolian anticyclone moves to the east of the 120°E meridian, most frequently over the East China Sea or the Yellow Sea.

3. The Taiwan low (type 3)

   An extratropical cyclone originates over the sea surfaces off Taiwan.

4. The polar front over Taiwan (type 4)

   A polar front, frequently associated with a cyclonic family, extends from the Aleutian low southwestward across Taiwan, roughly between 21°-26°N along 120°E, to south China or Indochina, where a distinct low is identifiable.

5. The polar front south of Taiwan (type 5)

   A polar front is located south of 21°N along 120°E.

6. The North Pacific subtropical anticyclone (type 6)

   Taiwan is situated under or south of the North Pacific subtropical anticyclone.

7. The southwest monsoon (type 7)

   A polar front is located north of 26°N along 120°E. Southwest winds prevail over the entire South China Sea, the Philippines, and Taiwan.

8. The northern-type typhoon (type 8)

   A typhoon is over Taiwan or over the sea surface within 300 miles off the Taiwan coast and is centered north of Hwalien.

9. The southern-type typhoon (type 9)

   A typhoon is over Taiwan or over the sea surface within 300 miles off the Taiwan coast and is centered south of Hwalien.

10. The Kyushu-type typhoon (type 10)

    An intense typhoon is centered near Kyushu, Japan.

11. Monsoon trough (type 11)

    Taiwan is situated south of the North Pacific subtropical anticyclone with a family of tropical cyclones near 20^{o}N in the western North Pacific and the South China Sea. Winds shift from southwest over the Philippines to southeast over Taiwan.

Synoptic flow types and daily rainfall at ten Taiwan stations have been punched on IBM cards and a computer program has been used to calculate the following items:

1. Frequency of each synoptic flow type for the period 1959-1969 and its monthly variation.
2. Mean annual rainfall, both amounts and percentages, associated with each synoptic flow tape.
3. Mean monthly rainfall, both amounts and percentages, associated with each synoptic flow type.
4. Mean, standard deviation, and maximum of daily rainfall associated with each synoptic flow type.

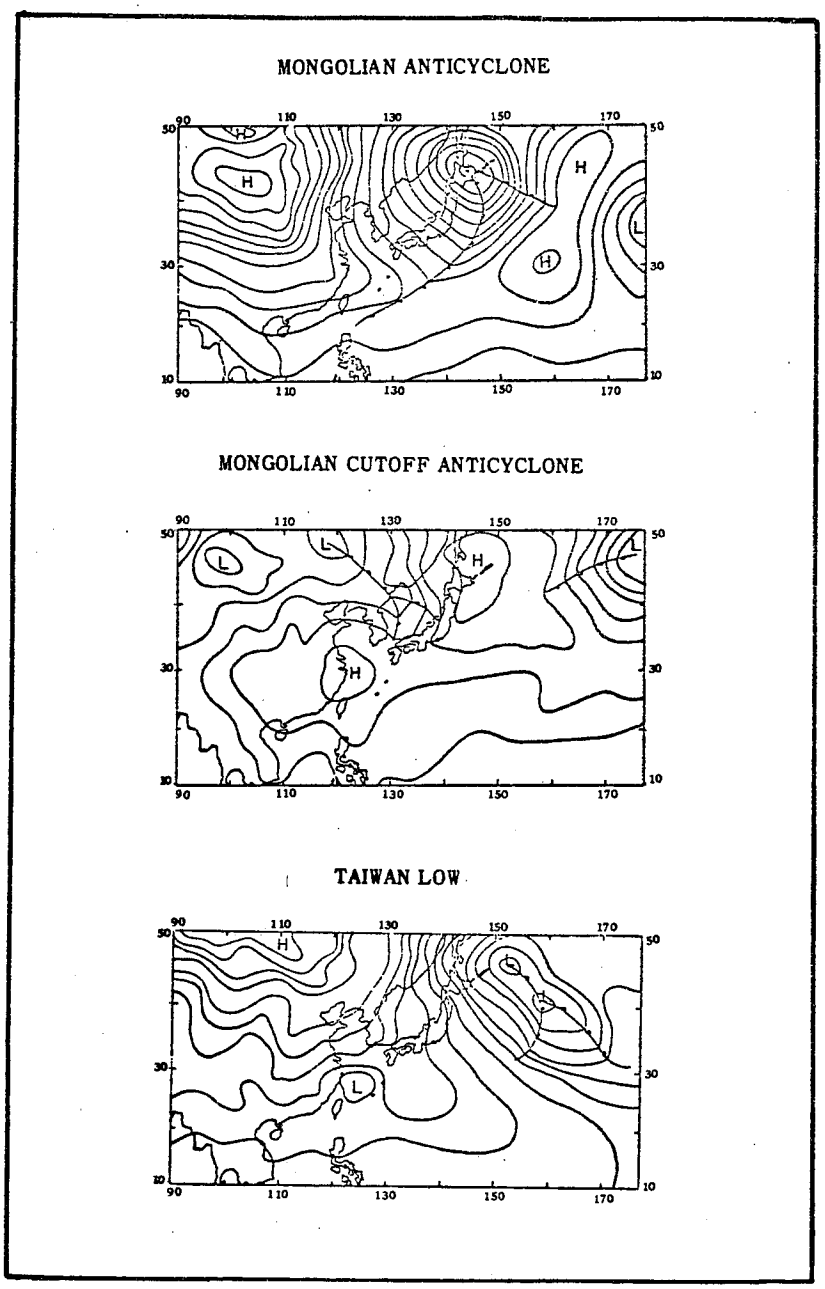

Figure 1. Models of synoptic flow patterns in the vicinity of Taiwan.

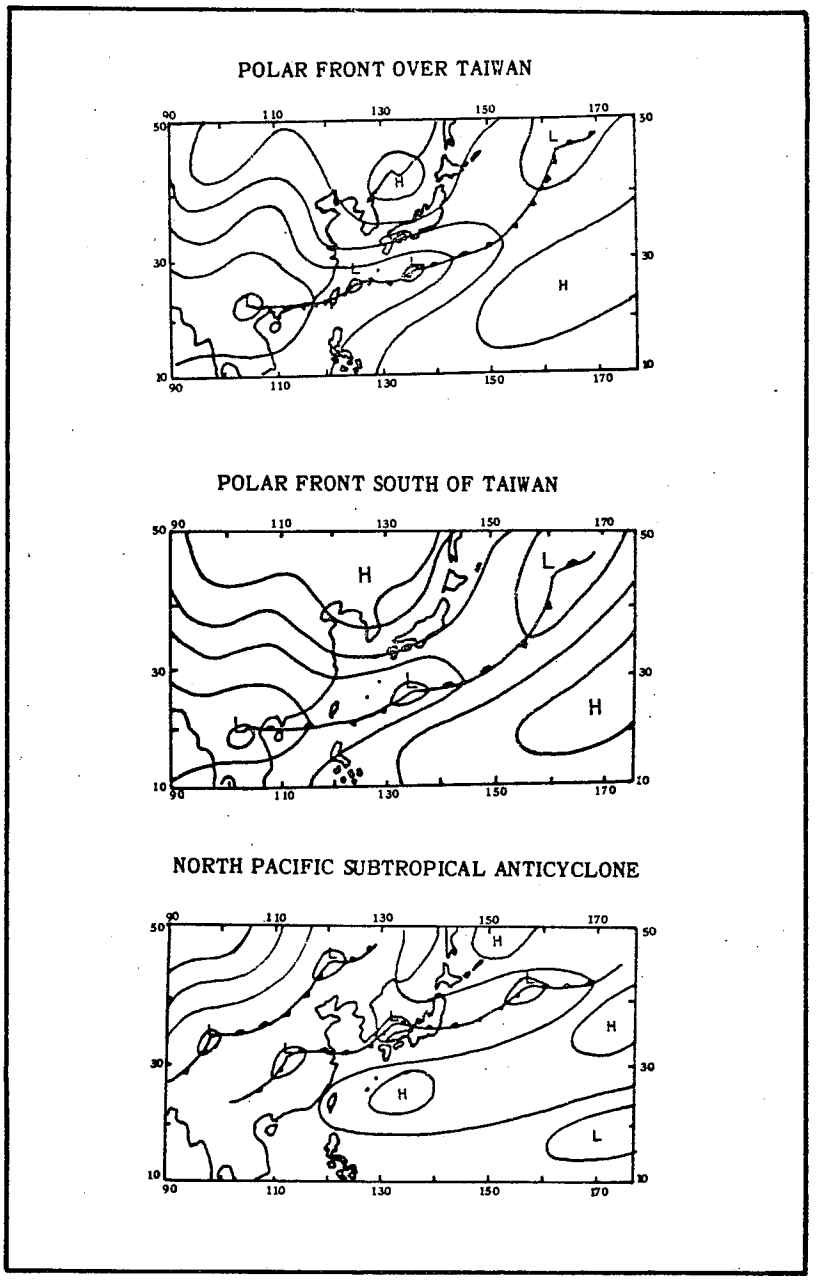

Figure 1. Continued.

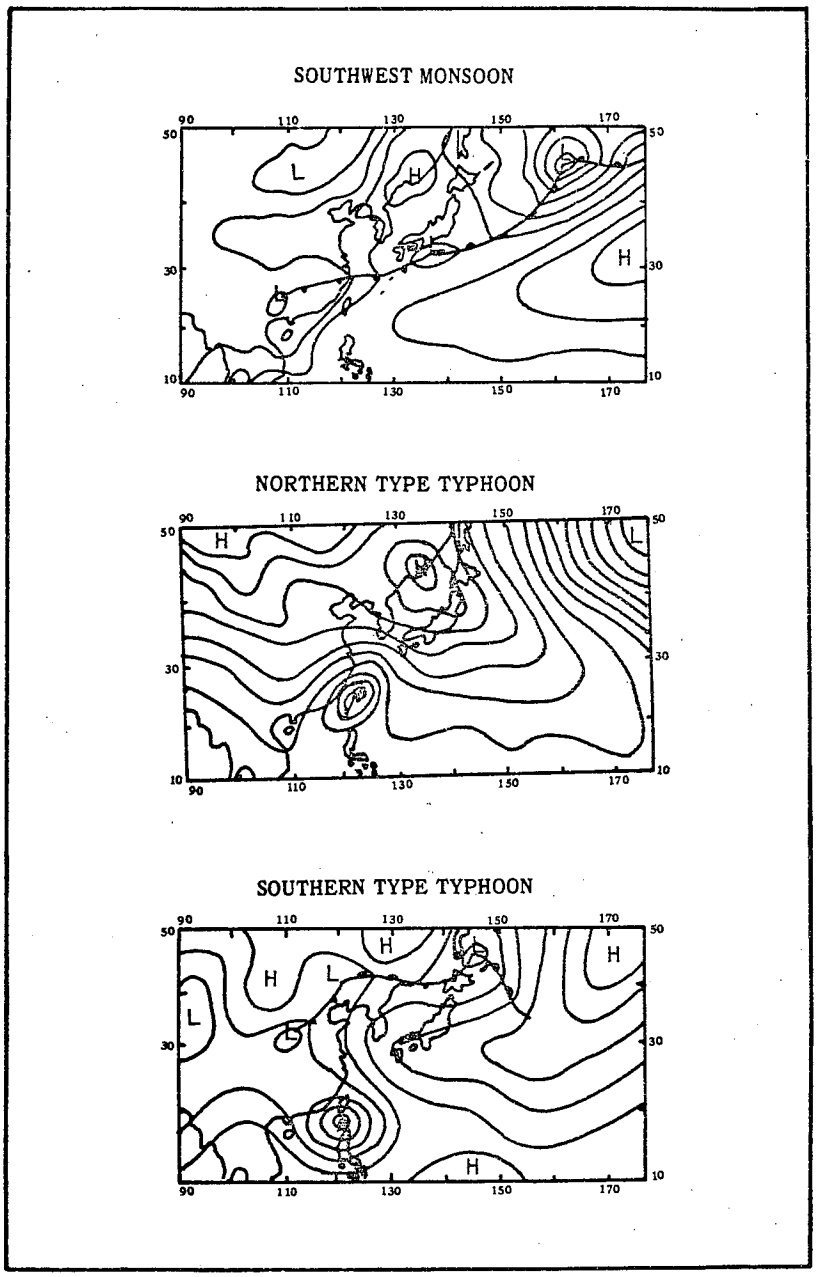

Figure 1. Continued.

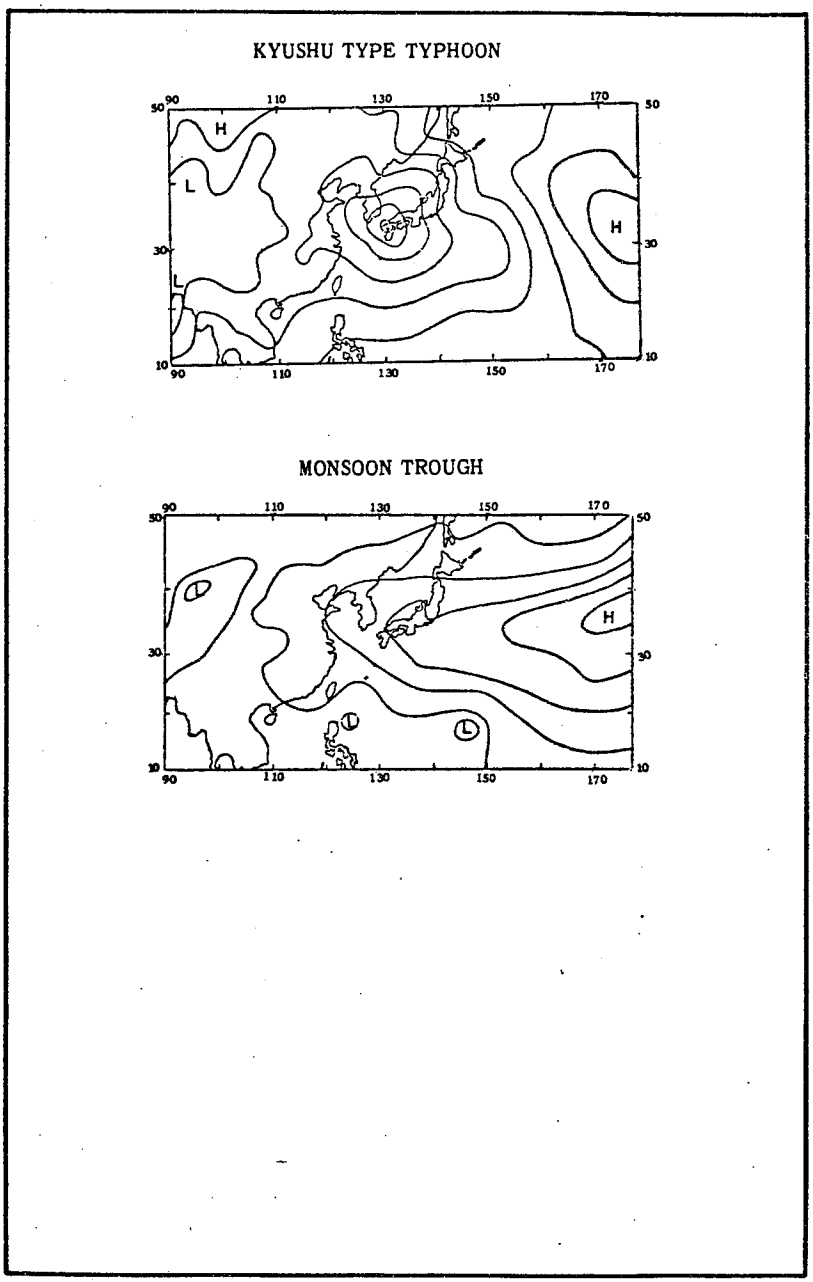

Figure 1. Continued.

5. The probability of rainy days associated with each synoptic flow type.

Where possible, the descriptive work of previous investigators has been examined and evaluated in the light of this study.

Data

The following data have been used for this study:

1. Daily surface-weather charts (i.e., 0000Z) for eleven years from 1959 through 1969, published by Japan Meteorological Agency.
2. Daily rainfall at ten stations: Keelung, Taipei, Taichung, Tainan, Kaoshiung, Hengchun, Taitung, Hwalien, Yilan, and Alishan.
3. Hourly rainfall at nine stations: Keelung, Taipei, Taichung, Kaoshiung, Hengchun, Taitung, Hwalien, Yilan, and Alishan.
4. Annual and monthly rainfall for the period 1897-1968 at seven stations: Keelung, Taipei, Taichung, Tainan, Hengchun, Taitung, and Hwalien.
5. IGC OBSERVATION DATA, Chinese National Committee, 1960.
6. IQSY OBSERVATION DATA, Chinese National Committee, 1964 and 1965.

7. Annual Wolf's sun-spot numbers for 1897 through 1969, World Data Center, U.S.A.

CHAPTER II

FREQUENCY OF SYNOPTIC FLOW TYPES

Mean Monthly Frequency

The rainfall regime in an area can be explained mainly by the frequency of different synoptic weather systems, which in turn are associated with change of the general circulation, particularly the strength of the westerlies. The purpose of this chapter is to investigate the seasonal frequency and inter-annual variation of different synoptic flow types in Taiwan, based on daily weather maps for eleven years from 1959 through 1969.

The strength and pattern of the atmospheric circulation are related to solar activity and ocean-surface temperatures. An attempt is hence made to study the influence of these factors on the variation in the frequency of synoptic flow types in Taiwan.

Figure 2 shows the mean monthly frequency of different synoptic flow types. In winter, the Mongolian anticyclone dominates Taiwan, with a maximum mean monthly frequency in December and in January of about 50% or 15 days. The Mongolian anticyclone tends to invade Taiwan when the westerlies over East Asia are weak. Chang (1959) has stated

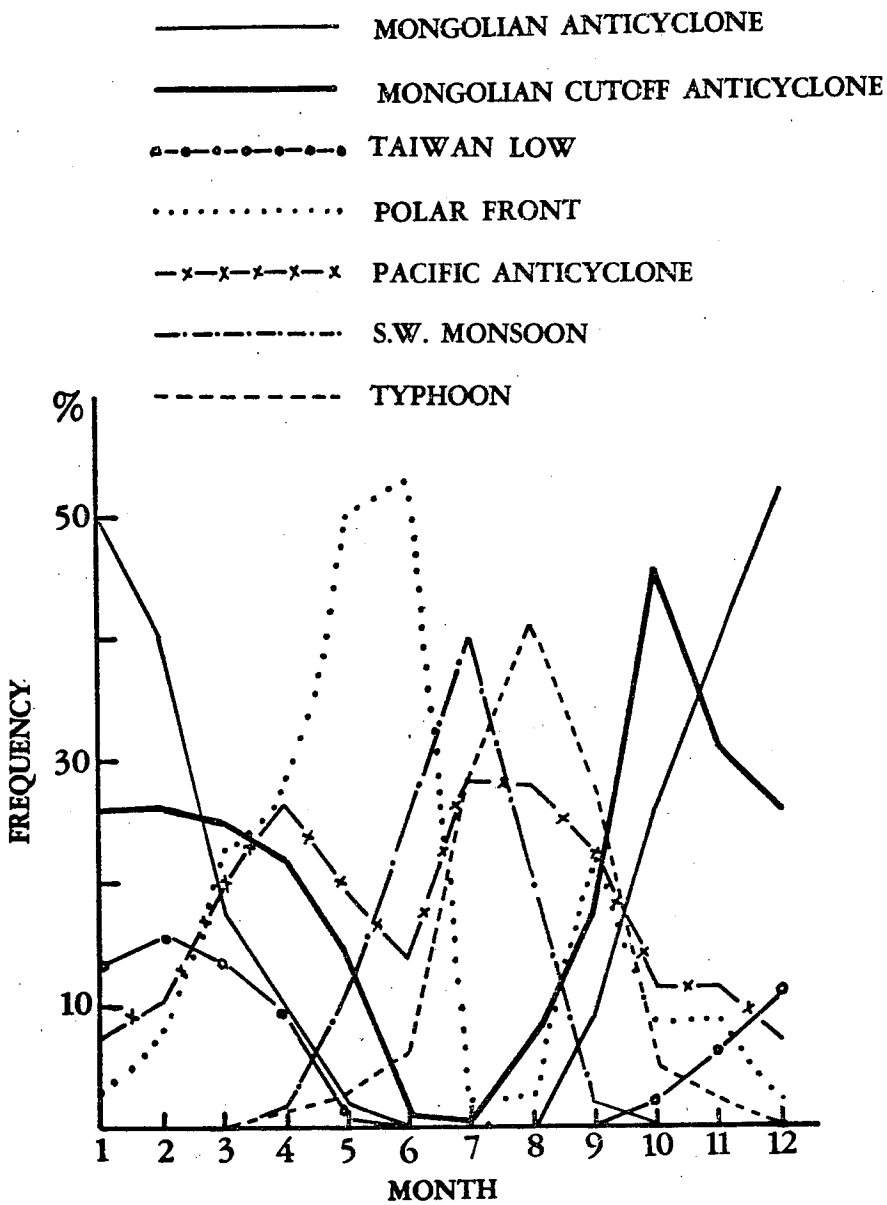

Figure 2. The mean monthly frequency of various synoptic flow types.

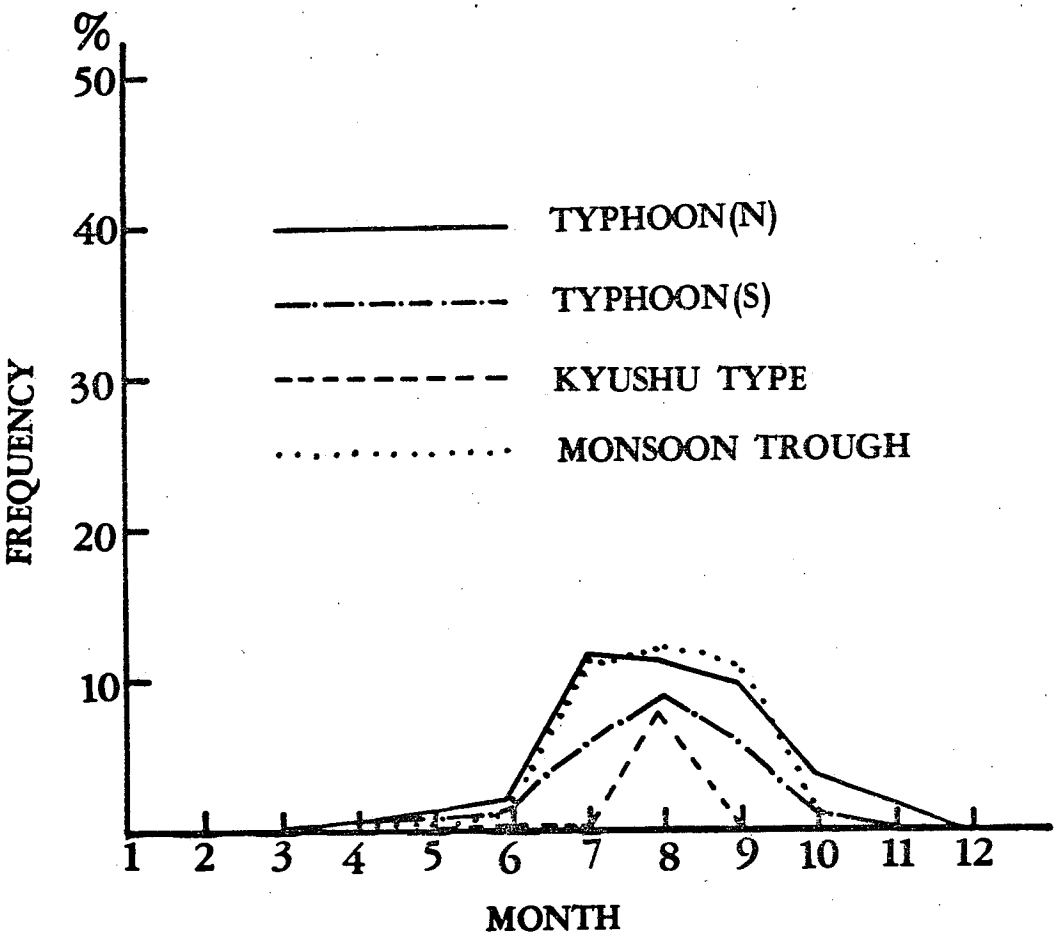

Figure 2. Continued.

that, in winter, periods of low zonal-index are associated with the strengthening of the monsoon circulation over China. In summer, June through August, the Mongolian anticyclone retreats northward to high latitudes and no longer threatens Taiwan. In spring, the mean monthly frequency of the Mongolian anticyclone drops sharply, from 40% in February to 18% in March and to less than 1% in May (Appendix A).

Similarly, the Mongolian cutoff anticyclone also occurs most frequently in the cold season, with a maximum frequency in fall of about 45% or 14 days in October. In contrast to the Mongolian anticyclone, over Taiwan the Mongolian cutoff anticyclone is persistent throughout spring with no significant decrease in monthly frequency. The frequency of the Mongolian cutoff anticyclone drops sharply in early summer, from 22% in April to 12% in May, and to less than 1% in June.

In Taiwan, polar fronts have two frequency maxima, one in May or June, and the other in September. The mean monthly frequency of polar fronts reaches 53% in June and 23% in September. Frequency is only 3% per month both in midsummer, July and August, and in mid-winter, December and January.

The Taiwan low occurs only in winter, between October and May, with a maximum frequency in February when the hemispheric circulation is at a minimum (Namias, 1950). In summer, both the southwest monsoon and typhoons dominate the island. In Taiwan, the southwest monsoon begins in April and ends in October, with a maximum frequency in July of about 40% or 12 days.

Typhoons commence in April and reach a maximum frequency in August, also of about 40%. In December, typhoons may occasionally travel within 300 miles of the Taiwan coasts, but did not come inland in the 11 years from 1959 through 1969. Typhoons can be grouped into four subtypes according to geographic position. All these four subtypes may visit Taiwan in spring, April and May. The northern-type typhoon visits Taiwan most frequently in July on about 12% or 3 days, and may come closely to Taiwan even in December, whereas the southern-type typhoon visits Taiwan most frequently in August, with a frequency of about 9% or 3 days. Both the Kyushu-type typhoon and the monsoon trough occur only in summer, with maximum mean monthly frequencies in August of about 8% and 12%, respectively.

The North Pacific subtropical anticyclone is the only synoptic flow type with a significant mean monthly frequency

during the entire year. It has two frequency maxima annually, one in April and the other in August, about 27% and 28%, respectively.

The sum of the mean monthly frequencies of the Mongolian and Mongolian cutoff anticyclones amounts to more than 40% from late fall through early spring, October through March, with a maximum mean monthly frequency in December of about 80% or 24 days. This agrees with the previous finding that in Taiwan winds from the northeast quadrant account for about 80% of the frequency in December (Chi, 1969).

Mean Annual Frequency

Figure 3 shows the mean annual frequency of different synoptic flow types in Taiwan. The Mongolian cutoff anticyclone has the highest frequency, followed by the Mongolian anticyclone; the two account for slightly greater than 40%. Next are polar fronts (both over and south of Taiwan) and the North Pacific subtropical anticyclone; each account for about 18%. The southwest monsoon accounts for less than 10% of mean annual frequency. The northern-type and southern-type typhoons also account for less than 10% although they are main rainfall sources in summer. The mean annual frequency of the Kyushu-type typhoon is less than 1%. The

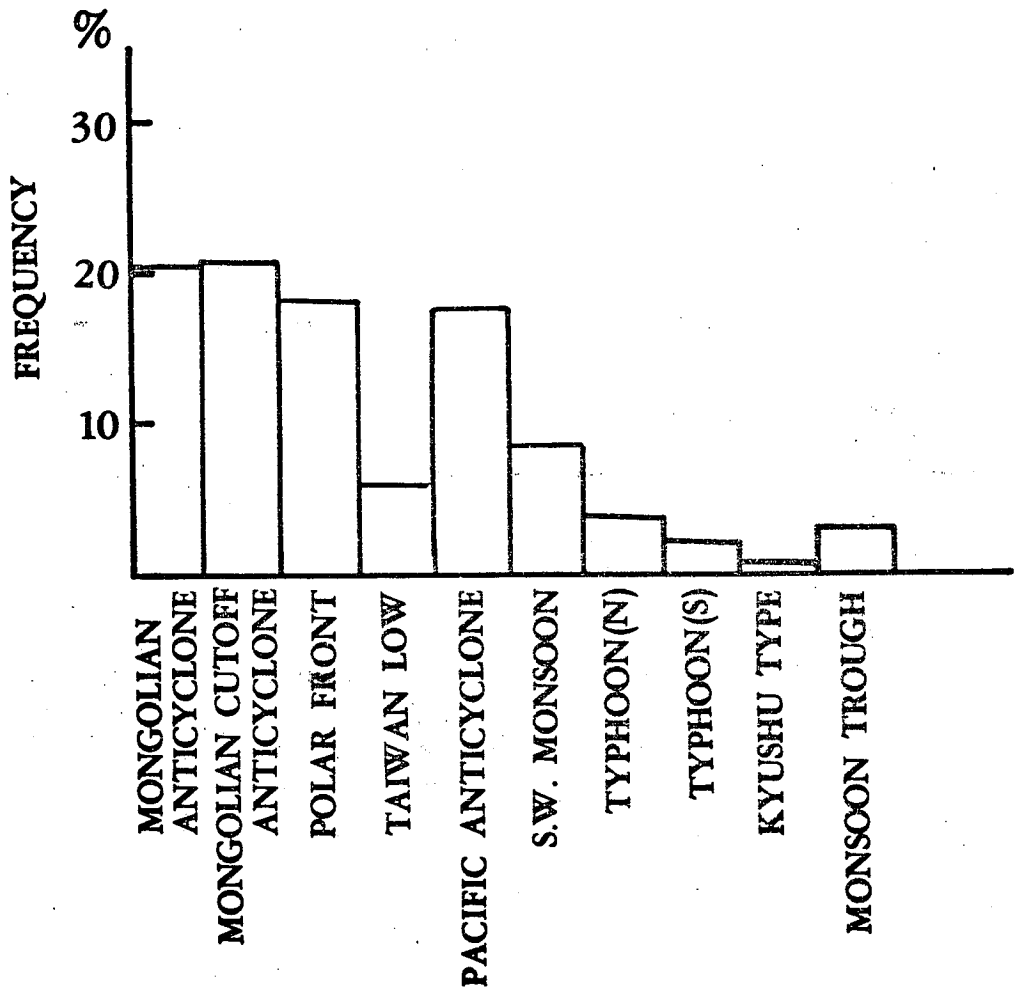

Figure 3. The mean annual frequency of various synoptic flow types.

monsoon trough has a mean annual frequency of about 3%.

It can be seen from Table 1 that in general the synoptic flow type with a higher mean annual frequency also has a higher standard deviation. The North Pacific subtropical anticyclone has the highest standard deviation of 3.64 whereas the Kyushu-type typhoon has the lowest standard deviation of 0.58. If annual frequencies of the polar fronts both over and south of Taiwan are combined together, the standard deviation is highest, reaching 4.17.

However, the coefficient of variation is a better indicator of frequency variability. The coefficient of variation is defined as the ratio between the standard deviation and mean. It can be seen from Table 1 that the coefficient of variation is highest for the Kyushu-type typhoon although its standard deviation is lowest. In addition, summer synoptic flow types have higher values of the coefficient of variation than winter synoptic flow types. This suggests that winter synoptic flow types are more persistent and vary less in frequency from year to year than summer synoptic flow types.

Solar Activity

Solar activity frequently is used to explain

TABLE 1

MEAN, STANDARD DEVIATION, AND COEFFICIENT OF VARIATION OF FREQUENCIES OF SYNOPTIC FLOW TYPES

Types	Mean	Standard Deviation	Coefficient of Variation
1	20.22	2.97	0.15
2	20.31	3.25	0.16
3	6.15	2.27	0.37
4	15.49	3.00	0.19
5	2.15	1.59	0.74
4+5	17.64	4.17	0.24
6	17.38	3.64	0.21
7	8.55	1.73	0.20
8	3.68	2.06	0.56
9	2.17	1.11	0.51
8+9	5.85	2.82	0.48
10	0.73	0.58	0.80
11	3.09	1.70	0.55

inter-annual or secular fluctuations in meteorological elements such as temperature, pressure, wind, and rainfall. Some climatologists assume that fluctuations in solar activity may affect the strength of the atmospheric circulation through the change in ultraviolet emission (Willett, 1961). Willett (1949) found that correlations, both simultaneous and with lag, among various indices of the strength of the atmospheric circulation had little or no statistical significance. The subsequent state of the atmospheric circulation is not determined simply by the preceding state but rather is induced by external influences. Julian (1966) found no evidence for sequential variations and correlations of the strength of the westerlies at various latitudes with any preferred range of period. Rather, significant relationships hold over a very broad range period. Willett (1949) remarked that long-period circulation changes ran parallel in both hemispheres and revealed a pattern similar to that of week-to-week fluctuations between high- and low-index circulations. These facts suggest solar activity as the most probable primary cause of all climatic fluctuations. However, correlation between solar phenomena and the strength of the atmospheric circulation is not statistically high; perhaps the zonal index chosen does not completely represent

the strength of the atmospheric circulation. Forsdyke (1958) has stated that it is only when zonal indices take extreme values that they give any indication of associated circulations.

Of several established indices of solar phenomena, sun-spot number is most common. Sun-spot number undergoes cyclical variations of different time-length, i.e., 11-year, 20-24 year (double sun-spot cycle), 32-35 year (Bruckner cycle), and 80-90 year (century cycle). In a study of the solar climatic relationship for the Northern Hemisphere, Willett (1965) has confirmed that latitudinal variations in pressure and virtual temperature during the period 1900-1959 appear to be in direct response to the 80-90 year cycle of sun-spot activity. In terms of the double sun-spot solar-climatic cycle, increases in solar activity tend to be associated with weaker circulations, while decreases are accompanied by stronger circulations.

The increase in sun-spot number from minimum to major maximum usually is accompanied by a predominance of polar anticyclones in winter, an usual case in the first quarter of the 80-90 year cycle. Increase from minimum to minor maximum is associated with equatorward displacement of storm tracks, a common case in the last quarter of the 80-90 year

cycle. On the other hand, a decrease in sun-spot number from maximum to minimum is associated with poleward displacement of prevailing storm tracks and precipitation, a high zonal-index atmospheric circulation pattern.

Figure 4 shows variations in the annual frequency of synoptic flow types in Taiwan for the period 1959-1969, including an active-sun year of 1959 and a quiet-sun period of 1963-1965. The frequency of the Mongolian anticyclone and typhoons in Taiwan decreased from 1963 to 1965 when the sun-spot number was at a minimum, and was accompanied by an increase in the strength of the westerlies (Figure 5). It appears that both the Mongolian anticyclone and typhoons visit Taiwan more frequently during a period of weakening atmospheric circulation. The frequencies of the southwest monsoon and polar fronts also show a minimum in 1963. In contrast, both the North Pacific subtropical anticyclone and the Mongolian cutoff anticyclone visted Taiwan most frequently in 1963. The minimum sun-spot number in 1963 was associated with the strengthening of the westerlies. The North Pacific subtropical anticyclone was well developed and invaded Taiwan more frequently than usual.

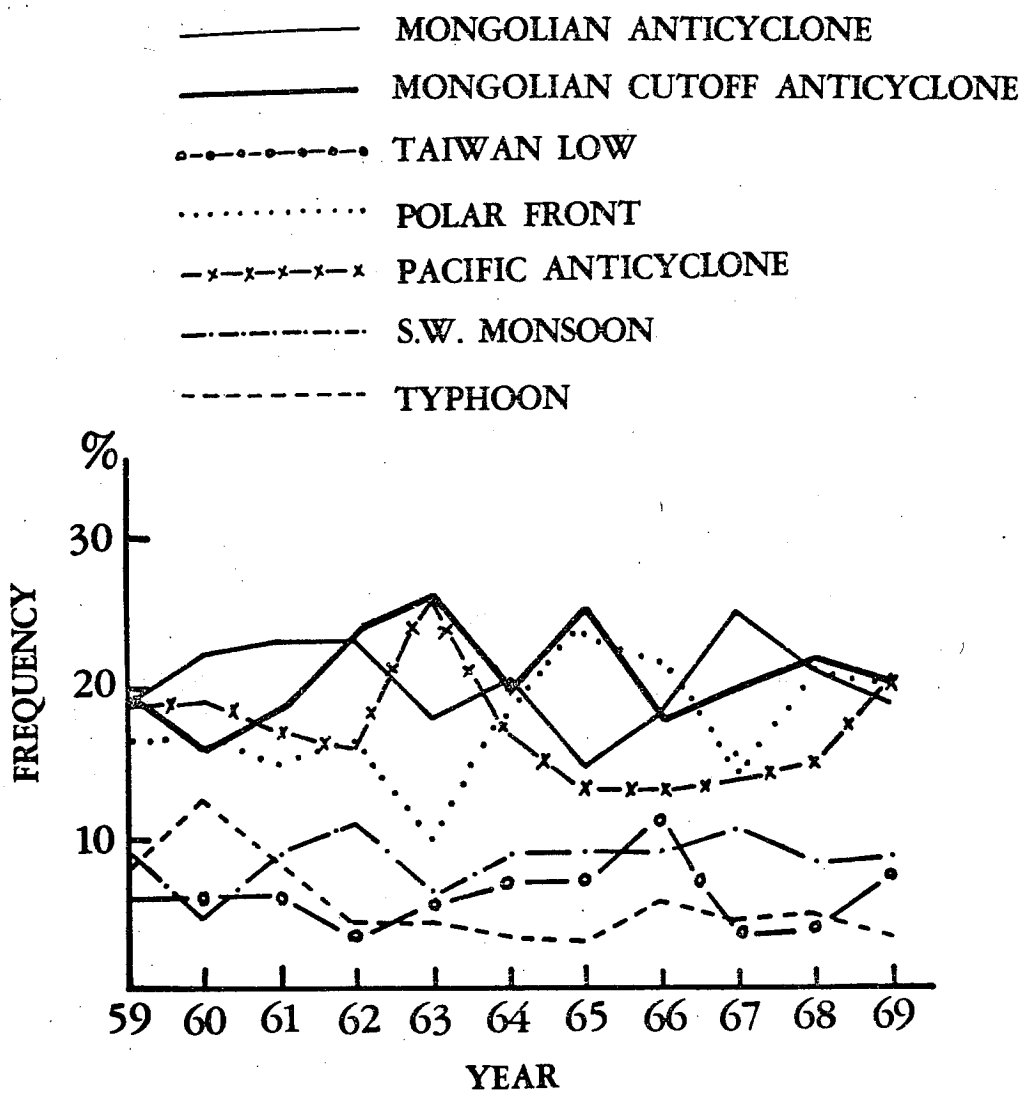

Figure 4. Variations in the annual frequency of various synoptic flow types.

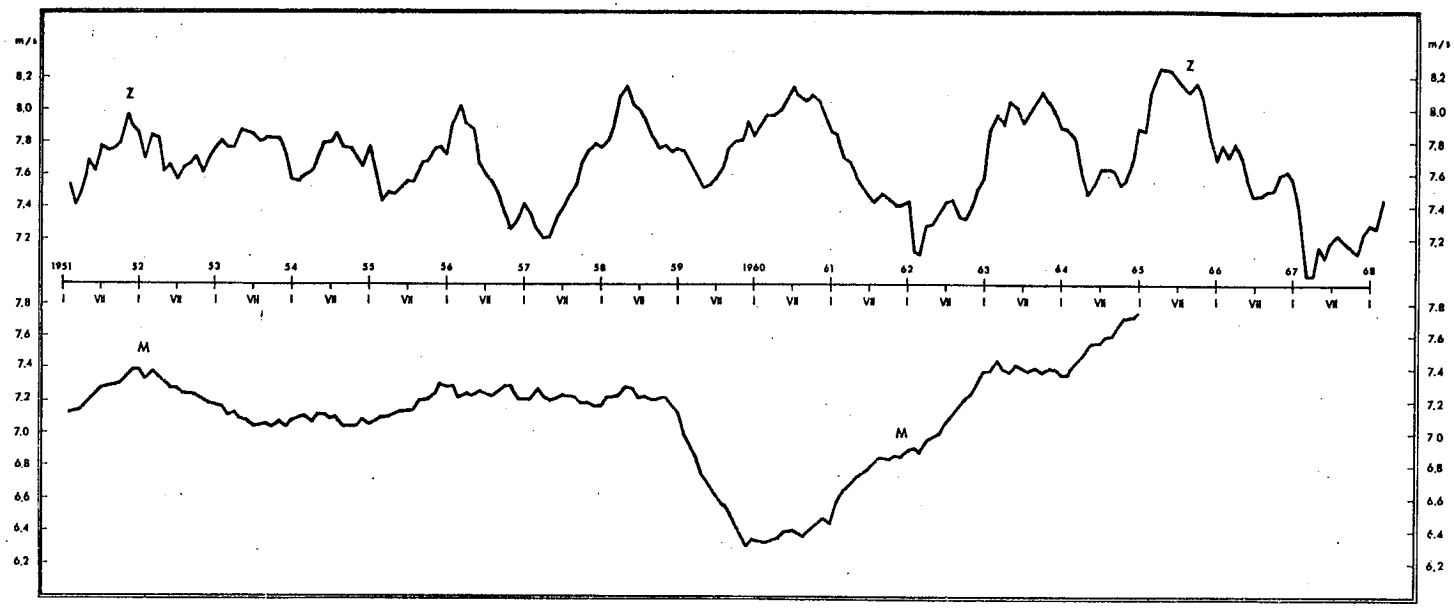

Figure 5. Time history of zonal and meridional indices. Running 12-month averages are plotted against the first month of "year", e.g., the value plotted at 1951 I represents year 1951 I-XII, that at 1951 VII is year 1951 VII - 1952 VI, etc. (after Wahl, 1972).

Air-Sea Interaction

Many climatologists have noted that a narrow dry belt extends from the coast of South America westward to about 165°E, approximately along the equator in central east Pacific. This dry zone is underlain by a cold-water tongue, formed primarily by upwelling and the cold Peru ocean current. The upwelling in this dry zone is caused by the Ekman drift of the tropical easterlies in both hemispheres. To the west of the dry zone, ocean water is warm and climate is normally humid. This warm-water pool between 5°N and 10°N in the western equatorial Pacific supplies thermal energy to drive the Hadley circulation in both hemispheres.

Bjerknes (1969) has demonstrated the presence of a longitudinal atmospheric circulation overlying the cold-water zone in the eastern equatorial Pacific as a part of "Walker's Southern Oscillation." He named this isolated circulation cell "Walker Circulation" and ascribed it to longitudinal temperature gradient.

The narrow cold-water tongue in the eastern equatorial Pacific is subject to periods of abnormal warming in response to change in the strength of prevailing winds. Prior to the establishment of abnormal warming of the ocean water in the eastern equatorial Pacific, trade winds weaken in both

hemispheres. As a result, upwelling in the dry zone also weakens or even disappears. This may result in abnormal warming of the ocean water which supplies energy to the overlying atmosphere by means of sensible heat transfer and evaporation. The Hadley circulation is thus accelerated, and it in turn intensifies the Ferrel westerlies by transporting absolute angular momentum poleward from the tropics. Over South America, the Intertropical Convergence Zone (ITCZ) may be displaced southward more than usual and establishes a heavy rainy and warm period over the Peruvian coast, a phenomenon known as El Nino (Caviedes, 1973).

The years of 1958, 1963, and 1965 were characterized by ocean temperature maxima in the eastern equatorial Pacific (Figure 6). Coincidentally, high zonal-index circulations were observed in those years, whereas low zonal-index circulations were observed in 1962, 1964, 1966, and 1967 when the ocean temperatures were at minima (Figure 5). Wyrtki's (1973) index of transport of the equatorial countercurrent also reached maxima in 1958, 1963, and 1965, in contrast to minima in 1962, 1964, 1966, and 1967, indicating that there was a strong association between the strength of the countercurrent and sea temperatures in the eastern equatorial Pacific. Namias (1973) suggested that the weak trade

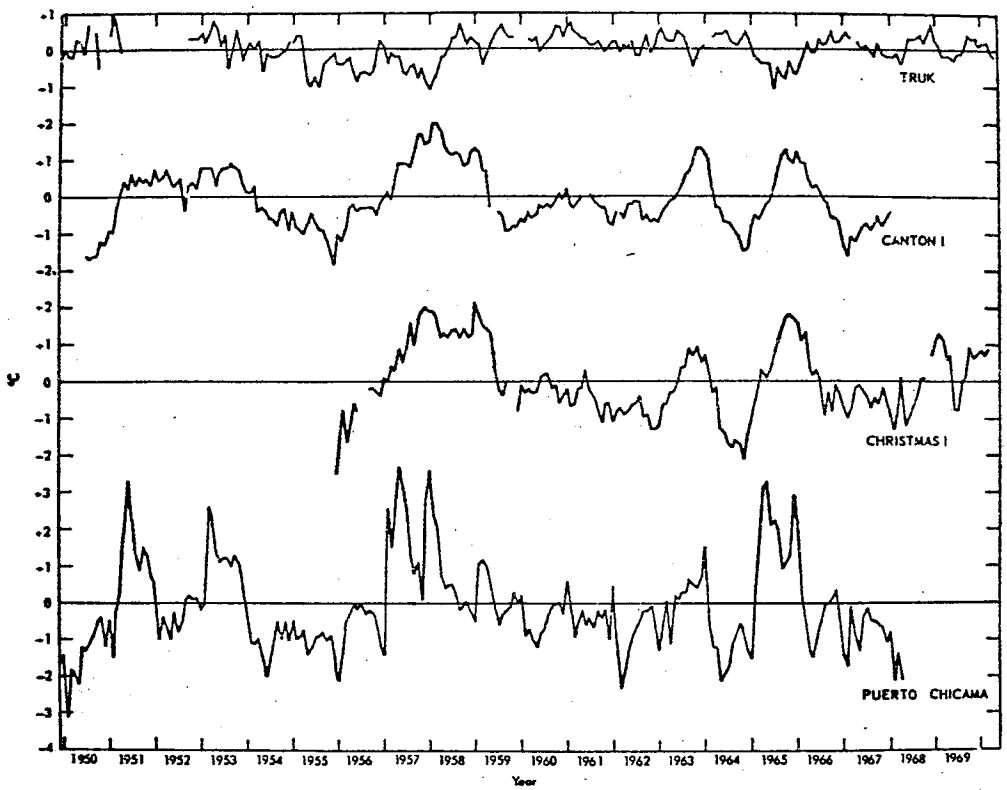

Figure 6. Time series of monthly sea surface temperature anomalies in the tropical Pacific (after Rowntree, 1972).

winds associated with the strong subtropical upper westerlies increased the strength of the countercurrent bringing warm water about eight months later off Central America. This may favor the occurrence of the El Nino.

Ramage (1968) has found that in January 1963 the zonal circulation was weak and meridional flow was pronounced over the North Pacific. At mean sea level, both the Mongolian anticyclone and Aleutian low were unusually intense. As a result, the monsoon circulation intensified. In Indonesia, rainfall was well above normal. Meanwhile, on Canton Island, in the eastern equatorial Pacific, a severe dry month occurred (Bjerknes, 1969). A year later in January 1964, the meridional circulation was weaker (Ramage, 1968). Rainfall was far below normal in Indonesia but far above normal on Canton Island. According to "Walker's circulation," there is a negative correlation in meteorological elements between the eastern tropical Pacific and Indonesia.

In Taiwan, the frequency of the Mongolian anticyclone was slightly above normal in January 1963 when the westerlies over the North Pacific were weak. This confirms the previous conclusion that the Mongolian anticyclone is prone to visit Taiwan when the westerlies weaken.

On a yearly basis, ocean temperatures in the eastern equatorial Pacific rose in 1963 and 1965, accompanied by strengthening of the westerlies in the Northern Hemisphere (Figures 5 and 6). In Taiwan, the Mongolian cutoff anticyclone shows two frequency maxima in 1963 and in 1965. In addition, the North Pacific subtropical anticyclone also shows an annual frequency maximum in 1963. On the other hand, both the Mongolian anticyclone and typhoons reached their lowest frequencies in those two years.

Namias (1959, 1963, 1965, 1968, 1969a and b) has paid much attention to air-sea interaction in the North Pacific and associated teleconnections in the Northern Hemisphere. Namias (1969b) noted that the period 1961-1967 was one of a unique climatic regime in the North Pacific, characterized by a stronger than normal Pacific anticyclone overlying a warm-water pool. Prior to the rapid warming of ocean temperatures in the fall of 1961, a cold-water pool developed in the same position as it was in 1957. This cold-water pool enhanced atmospheric stability which prevented the leakage of air and thus favored the development of the anticyclone. Once an intense Pacific anticyclone was established in the fall of 1961, ocean temperatures remained warm because of the poleward advection of warm air and the decrease or

absence of upwelling. The development of a positive pressure anomaly in the central North Pacific during the period of a pronounced water warming from 1962 through 1965 (Figure 7) implied the strengthening of the westerlies.

Coincidentally, the frequency of the Mongolian cutoff anticyclone in Taiwan revealed a peak during the period of the pronounced warming of the ocean surface at 35°N and 170°W in the central North Pacific (Figure 7). In contrast, both the Mongolian anticyclone and typhoons invaded Taiwan less frequently during the same period, probably in association with the strengthening of the North Pacific subtropical anticyclone. Typhoons tend to visit Taiwan during periods of weak circulation in the North Pacific, a subject which will be evaluated in Chapter VI.

In summary, the frequency of certain synoptic flow types appears to be related to solar activity and ocean-surface temperatures in the central North Pacific and the eastern equatorial Pacific. During years of quiet-sun activity, frequencies of the Mongolian anticylone and typhoons decrease in contrast to an increase in frequencies of the North Pacific and Mongolian cutoff anticyclone.

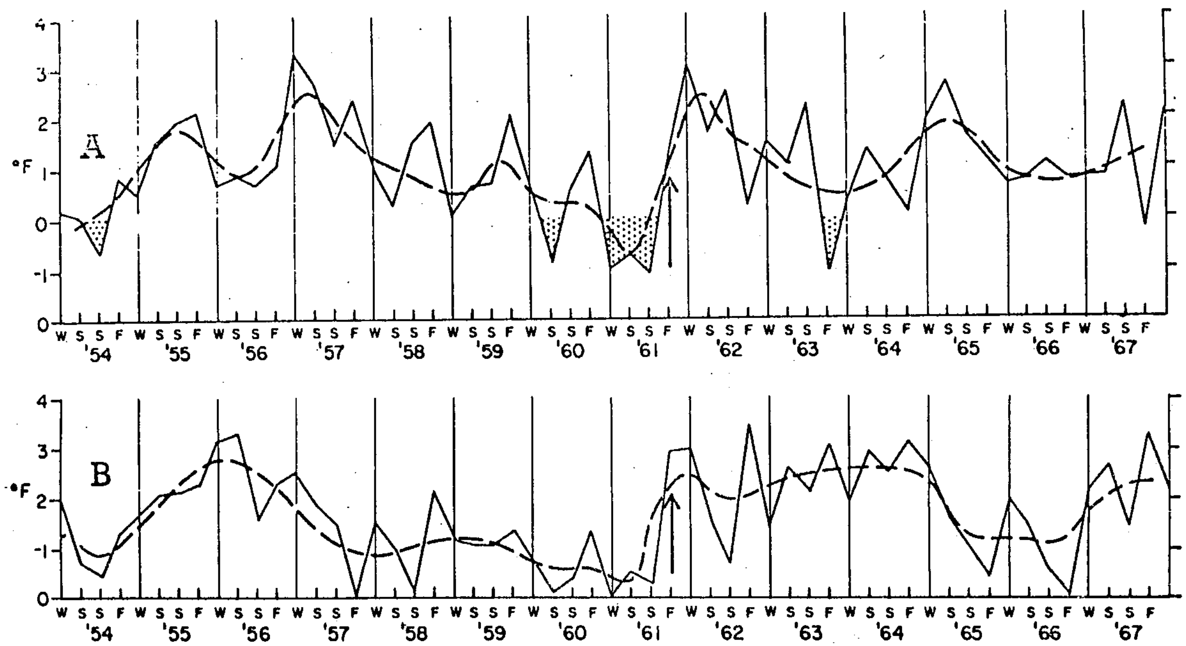

Figure 7. Seasonal mean sea-surface temperature departures from normal for 10^{o} square centered at $40^{o}N$, $150^{o}W$ (A), and at $35^{o}N$, $170^{o}W$ (B). Broken curves are smoothed with the help of three-season overlapping means. Shaded area in (A) denotes below-normal temperatures. Arrows denote change in climatic regime (after Namias, 1969b).

As already discussed, the North Pacific subtropical anticyclone is one of the major centers of action which significantly affect weather in Taiwan. The strength of this anticyclone has been found to be correlated to ocean-surface temperatures in both the eastern equatorial Pacific and central North Pacific. Bjerknes (1966, 1969) has proposed that fluctuations of ocean temperature in the eastern equatorial Pacific are responsible for major variations in locations of upper troughs and ridges, the Aleutian low, and the North Pacific subtropical anticyclone. His theory has been confirmed both by Rowntree (1972) and by Krueger and Gray (1969) in their studies of the influence of tropical east Pacific temperatures on atmosphere. Namias (1968, 1969a and b) has found that fluctuations of ocean temperature can be correlated with variations in tracks of cyclones and anticyclones in the North Pacific.

The current study indicates that ocean-surface temperatures in both the eastern equatorial Pacific and central North Pacific influence the frequencies of synoptic flow types in Taiwan. The relationships hold best for years of extreme change in the North Pacific ocean temperatures. One such period occurred from 1962 to 1965 when ocean-surface temperatures in the central North Pacific were abnormally warm.

Summary of Significant Results

The significant results of this chapter lie in several aspects. Barry and Perry (1973) defined synoptic climatology as the study of the relationships between the atmospheric circulation and local climate. Rainfall is one of the most distinct climatic elements. Rainfall regimes over an area are usually expressed by their monthly and inter-annual variations. Although some climatologists have studied mean monthly and annual rainfall over Taiwan, no statistical figures of synoptic flow types have been presented. The current study is the first attempt to classify the atmospheric circulation into synoptic flow types and to tabulate their monthly and annual frequencies. It appears that frequencies of the eleven synoptic flow types are useful in the study of rainfall characteristics. A comparison between Figure 2 and Figure 8 indicates that monthly rainfall maxima at various stations result from frequency maxima of different synoptic flow types. The coefficients of variation of different synoptic flow types are useful in explaining the spatial variation in rainfall variability, a subject which will be discussed in Chapter IX. One of the major goals of climatology is to find out variables or indices in hope that they can be used for weather or climatic forecasting. It is

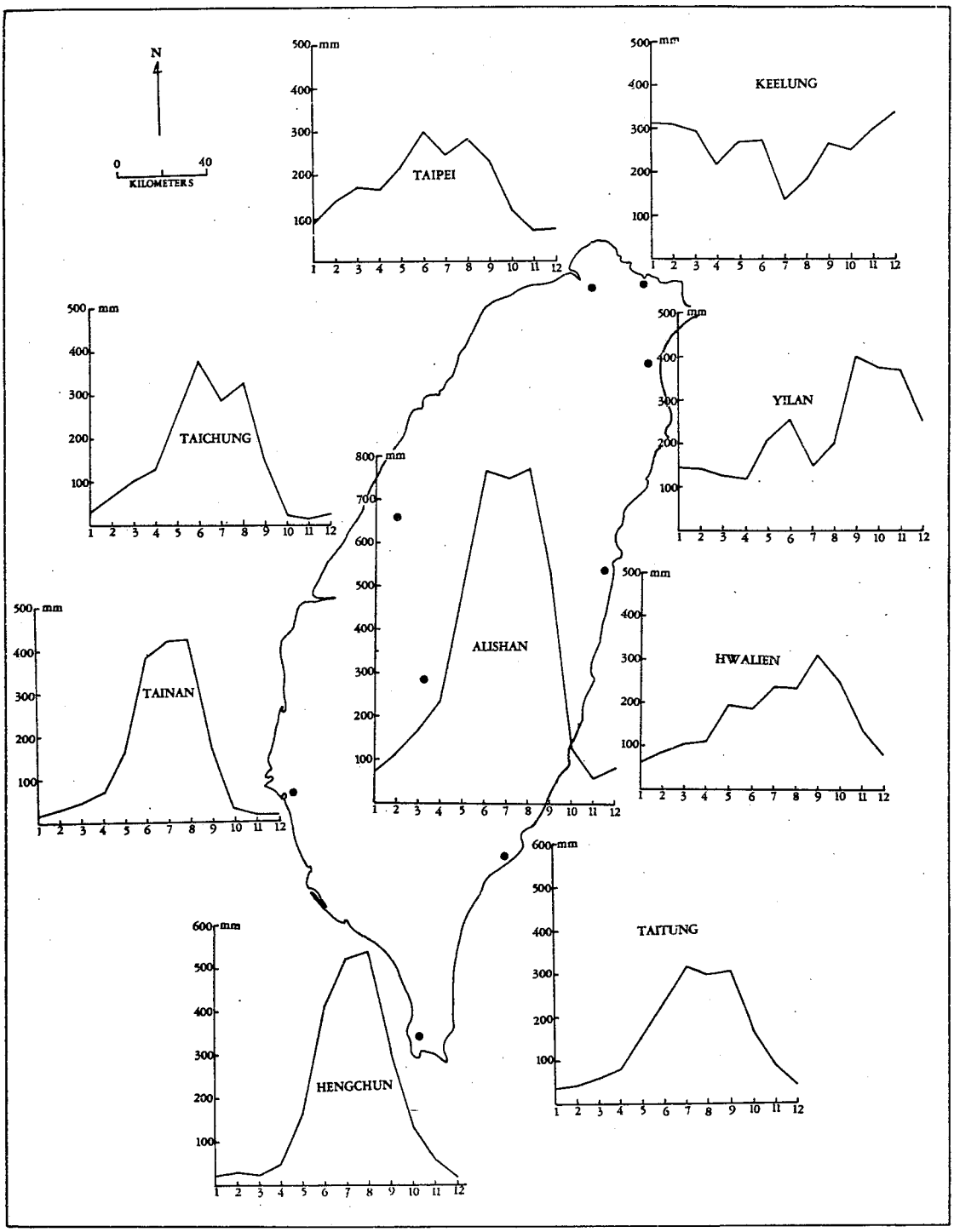

Figure 8. Mean monthly rainfall variations at the various Taiwan stations. The abscissa is month and the ordinate mean monthly rainfall.

found that the annual frequencies of some major synoptic flow types over Taiwan are related to solar activity and ocean-surface temperatures over the central North Pacific and eastern equatorial Pacific. This suggests that the inter-annual or secular rainfall variation over Taiwan is not a local phenomenon but rather is the result of the hemispheric circulation. Therefore, indices of the strength of the westerlies and solar activity, and ocean-surface temperatures can be used as aids for weather or climatic forecasting.

CHAPTER III

RAINFALL ASSOCIATED WITH THE MONGOLIAN ANTICYCLONE AND THE MONGOLIAN CUTOFF ANTICYCLONE

The Mongolian Anticyclone

As pointed out in the preceding chapter, the Mongolian anticyclone dominates Taiwan in winter. The formation and intensification of this polar anticyclone is often introduced by the passage of an upper-air trough or an occluded cyclone from Siberia, the Kara Sea, the Barents Sea, or Greenland (Chang, 1972). Dzerdzeevskii (1962) attributed the polar anticyclone to the meridional advection of the Arctic cold air to lower latitudes in one or several directions and called this type of circulation the violation of zonality. A group of Chinese meteorologists (Staff Members, 1958) pointed out that the Mongolian polar outbreak may be caused by arctic intrusion of cold air either from the west of Novaya Zemlya by way of north Europe and west Siberia to Mongolia, or, from the Arctic Sea north of the Asiatic continent through west Siberia to China. In addition, the polar anticyclone may originate in Siberia or Mongolia due to radiative cooling effect, usually accompanied by a blocking high over the Urals, or it may develop

from a high pressure wedge behind a weak cold front over Ukraine. Ramage (1971) examined Petterson's equation of the advection of vorticity and remarked that vigorous anti-cyclogenesis may occur in the area of intensive surface divergence associated with upper tropospheric convergence. He also pointed out that the mountains immediately to the south and east of the basin of Lake Baikal reduced the inhibiting effect of the subsidence in Petterson's equation, by retarding outflow, and hence terrain favored the intensification of the polar anticyclone there. Mintz (1965), in a simulated study of the global general circulation, found that the winter Siberian anticyclone would be absent at sea level if the Himalaya-Tibetan mountains were to be removed. This elevated massif prevents the northward advection of the convectively heated air out of India from reducing the effect of the radiative cooling over Siberia.

The advance of cold air associated with the invasion of the Mongolian anticyclone over China is usually called polar outbreak, cold surge, or cold wave. Polar outbreaks follow one another rather irregularly and are sometimes presenced by a cold front but on many occasions they may be observed without any well-organized frontal systems (Chin, 1969).

A polar outbreak usually starts with the deepening of a 500-mb trough approximately along 120°E, frequently accompanied by the intensification of an underlying surface cyclone over Manchuria or the Yellow Sea. The polar outbreak dissipates when the long-wave trough moves eastward into the North Pacific. A second weak polar outbreak may be triggered in accordance with the westward retrogression of the long-wave trough over north China.

However, a severe polar outbreak may also occur without the presence of a coastal long-wave trough at the 500-mb level. At such time it is associated with a breakdown of the equilibrium field at the 850-mb level (Wang, 1958a and b).

During periods of polar outbreaks over Taiwan, strong mid-tropospheric westerlies with speeds exceeding 100 knots are frequently observed as a result of the presence of a jet stream which fluctuates between 20°N and 35°N (Hsu and Wang, 1956, 1958). The development of this subtropical jet stream at 500 mb is attributed to the southward displacement of the northern branch of the westerlies over East Asia, a circulation pattern similar to Namias and Clapp's (1949) confluence theory of the jet stream formation.

Double inversion layers over Taiwan are frequently observed in connection with polar outbreaks, one near 900-800 mb and the other near 700-500 mb (Figure 9). The lower inversion layer is caused by a warm southerly air current overlying the cold monsoon layer, whereas the upper inversion layer results from the subsidence of the northwesterly air current of the northern branch of the westerlies over China. This upper inversion layer associated with polar outbreaks in winter is also frequently observed over south China and is called the dynamic stable layer. Its frequency over Taiwan reaches 20 days in January (Yu, 1965).

The Mongolian anticyclone frequently contributes rainy days to Taiwan, especially to the windward stations in the northern part of the island due to the orographic uplifting. Figure 10 shows the amounts of mean annual rainfall contributed by the eleven synoptic flow types over Taiwan. Obviously, the Mongolian anticyclone contributes a considerable amount of rainfall to the northern and eastern sectors of the island. About one-third of the mean annual rainfall at Keelung and one-fifth that at Yilan are contributed by the Mongolian anticyclone (Tables 22a and 23b in Appendix B). In contrast, the Mongolian anticyclone contributes an almost negligible amount of rainfall to the

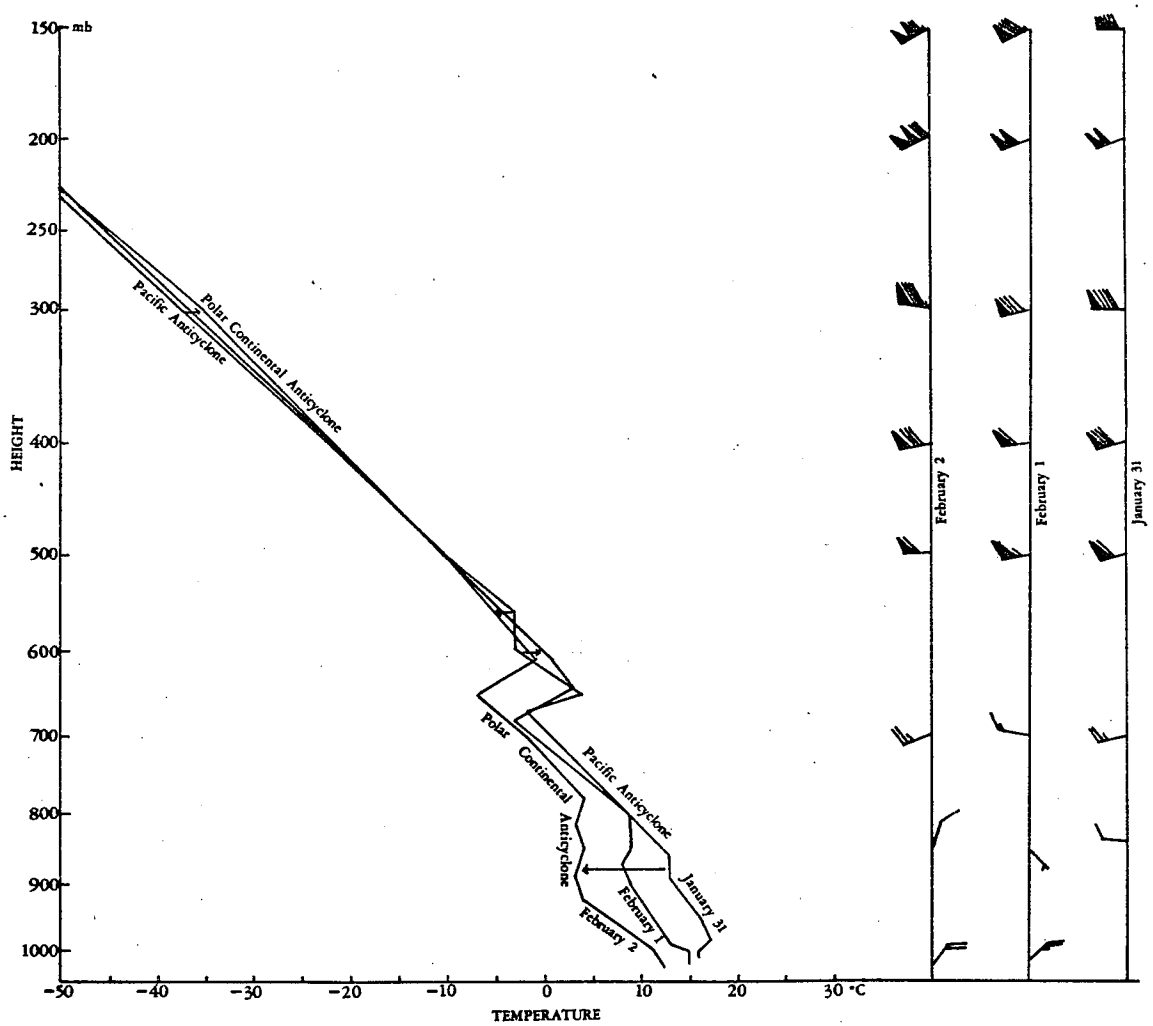

Figure 9. Vertical variations in temperatures and winds associated with the Mongolian and Pacific anticyclones, at Taoyuan. Arrows denote warm or cold air advection.

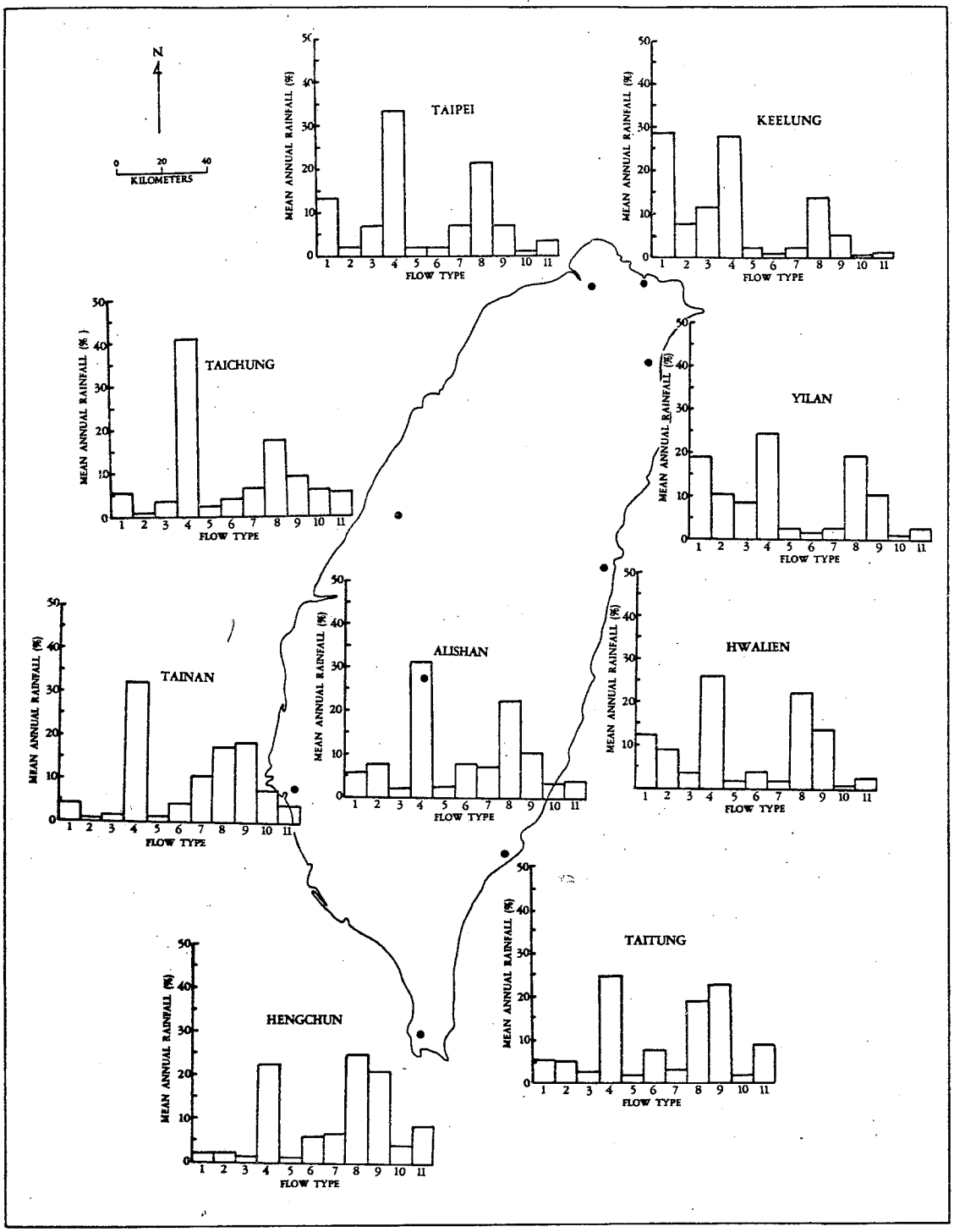

Figure 10. Mean Annual rainfall associated with the eleven synoptic flow types.

southern and southwestern portions of the island, i.e., less than 50 mm or 2 inches in a year. The mean annual rainfall at Taipei and Hengchun are almost equal. However, the Mongolian anticyclone annually contributes more than eight times as much rainfall to Taipei as to Hengchun. The percentage of mean annual rainfall associated with the Mongolian anticyclone reaches 13% at Taipei but is less than 2% at Hengchun. At Keelung, in contrast to other stations, the mean annual rainfall contributed by the Mongolian anticyclone is much more than that contributed by any other synoptic flow types.

Mean monthly rainfall contributed by the Mongolian anticyclone also shows a distinct regional pattern (Tables 23a and 23b in Appendix B). The percentage of mean monthly rainfall associated with the Mongolian anticyclone reaches more than 50% in winter, December through February, at Keelung, Yilan, Taipei, and Hwalien, in the northern and eastern sectors of the island. It decreases to about 40% at Taichung, in the central west sector, and to about 30% at Hengchun and Taitung, in the southern sector. Although the percentage of mean monthly rainfall associated with the Mongolian anticyclone in winter may reach nearly 50% at Kaoshiung and Tainan, in the southwest sector, its

contributions in amounts are almost negligible. Its contribution reaches about 200 mm (7.9 inches) at Keelung in December through February and drops to less than 10 mm (0.39 inches) at Kaoshiung, Tainan, and Hengchun. Both the amount and the percentage of mean monthly rainfall associated with the Mongolian anticyclone show peaks in February at most stations. The peaks are probably associated with a primary zonal-index cycle, which is defined as a pronounced transformation of the intensity of the westerlies from low to high during late February and early March, year after year (Namias, 1950). The decrease in zonal-index in February is associated with the intensification of the subtropical jet stream and the occurrence of polar outbreaks. Consequently, winter rainfall is directly associated with the strength of the westerlies.

Figures 11 and 12 show pronounced spatial variations in the mean and standard deviation of daily rainfall associated with different synoptic flow types over Taiwan. The mean daily rainfall contributed by the Mongolian anticyclone is about 16 mm (0.63 inches) at Keelung but is only about 2 mm (0.08 inches) at Hengchun (Table 24 in Appendix B). It appears that there is a direct relation between mean daily rainfall and the standard deviation of daily rainfall. With

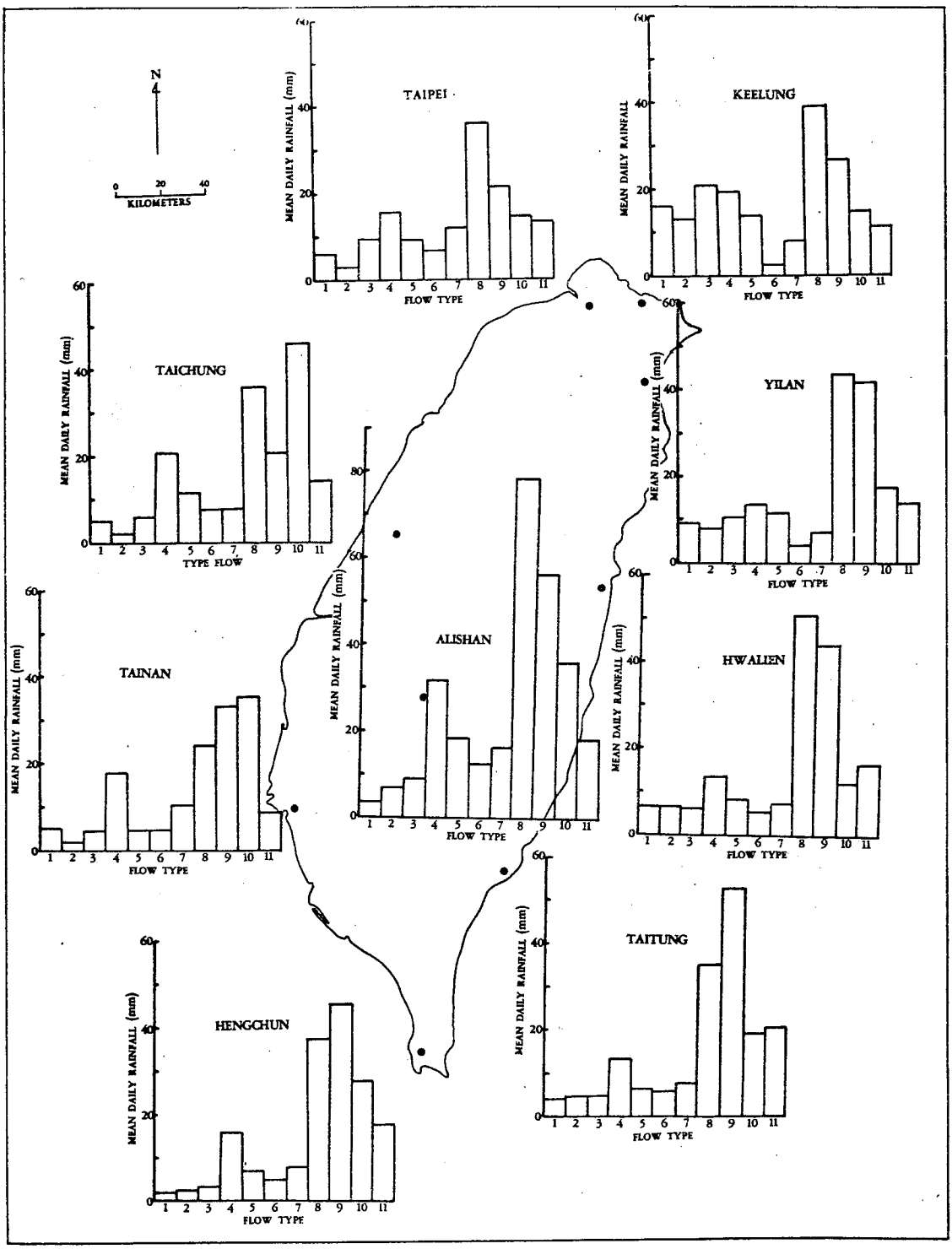

Figure 11. Mean daily rainfall associated with the eleven synoptic flow types.

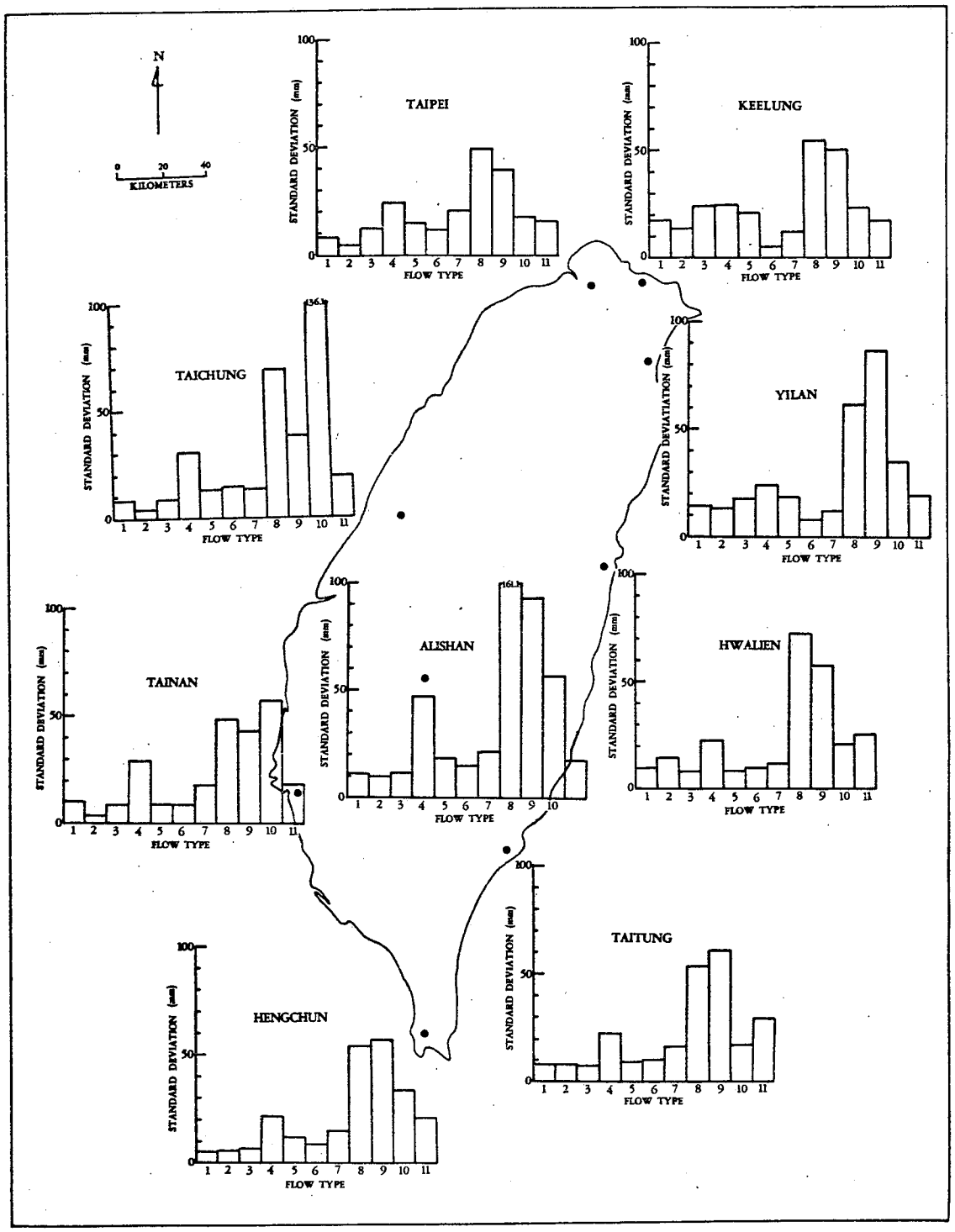

Figure 12. Standard deviation of daily rainfall associated with the eleven synoptic flow types.

the exception of Tainan, the standard deviation shows higher values in northern and northeastern sectors than in any other sectors of the island. The maximum daily rainfall reaches more than 100 mm (3.94 inches) at both Keelung and Yilan. Although the Mongolian anticyclone produces rainfall mainly in the northern and eastern sectors of the island, the maximum daily rainfall is over 50 mm (1.97 inches) at all stations.

As expected, the probability of rainy days associated with the Mongolian anticyclone decreases from nearly 78% at Keelung to about 11% at both Kaoshiung and Tainan (Figure 13 and Table 25 in Appendix B). The probability of rainy days is defined as the ratio between the number of rainy days and all days for a given synoptic flow type. The rainfall intensity associated with the Mongolian anticyclone occurs most frequently between 0.1 mm (0.003 inches) and 12.6 mm (0.5 inches) per day at all stations. The probability of rainy days with rainfall between 12.7 mm (0.5 inches) and 25.3 mm (1 inch) is about 20% at Keelung but is less than 1% at Kaoshiung, Tainan, and Hengchun. With the exception of Keelung where 16% of the Mongolian anticyclone days produces rainfall between 25.4 mm (1 inch) and 76.2 mm (3 inches) per day, the chances of having such a rainfall intensity are

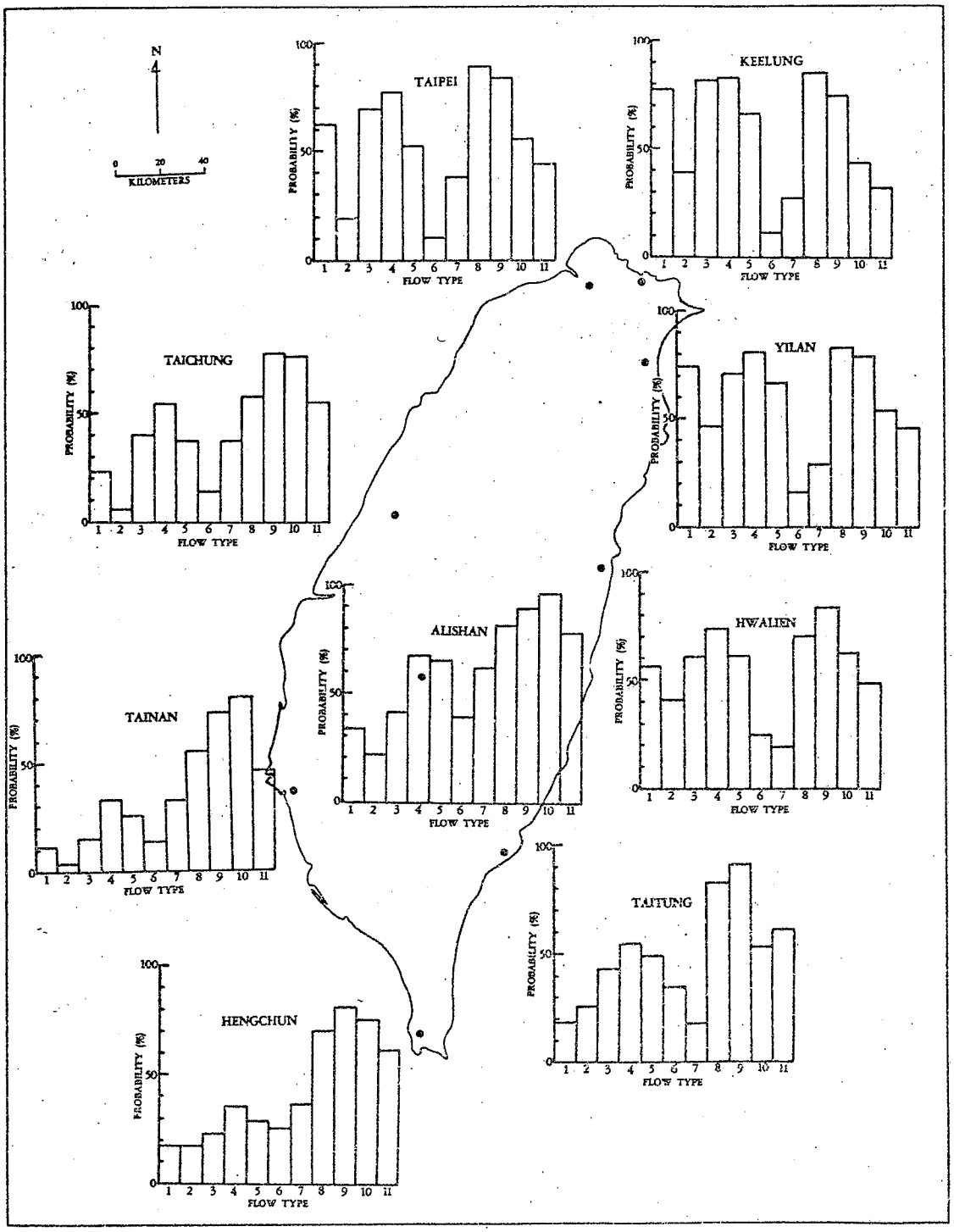

Figure 13. Probability of rainy days associated with the eleven synoptic flow types.

very small, about 2% or less, at other stations. Although the Mongolian anticyclone is a main rainfall contributor at stations in the northern and eastern sectors of the island, the chances of having daily rainfall over 76.2 mm (3 inches) are very small. In an eleven-year period there was such an intensity on only six days at Keelung and Yilan, on one day at Taipei and Taichung, and on no days at other stations. It is concluded that the Mongolian anticyclone seldom produces heavy rainfall over Taiwan despite its high probability of rainfall in winter in the northern and eastern sectors of the island.

The Mongolian Cutoff Anticyclone

Many efforts have been made to study the source and surges of the Mongolian anticyclone, but little attention has been paid to its behavior after a cold surge. Chang and Sh (1957) have classified tracks of the anticyclone into two groups:

1. The first group travels from Siberia to Mongolia southeastward through north and central China to the Yangtze River Valley and then swings progressively northeastward to Japan by way of the East China Sea.

2. The second group proceeds from Siberia or Mongolia eastward to Japan through the Sea of Japan. The speed of the anticyclones of both groups is accelerated after they migrate beyond the China coast and recurve northward to Japan.

Wu (1971) has found that only 42% of the anticyclones migrate across 125°E. The Mongolian cutoff anticyclone is normally associated with warm advection in the lower troposphere (Figure 14). Double inversion layers are frequently observed.

In contrast to the Mongolian anticyclone, the cutoff anticyclone is more frequently accompanied by improving weather, although light drizzle or fog may occasionally occur over Taiwan. As a rule of thumb, clear weather can be expected as soon as the center of the cutoff anticyclone moves off the East China coast south of the Yangtze River Valley. Chow and Cheng (1971) have observed that 53% of the foggy days at Taipei in winter are attributable to the proximity of the Mongolian cutoff anticyclone. Light surface winds and strong nocturnal radiation accompanying it favor the formation of fog in the early morning in Taiwan (Lee, 1971).

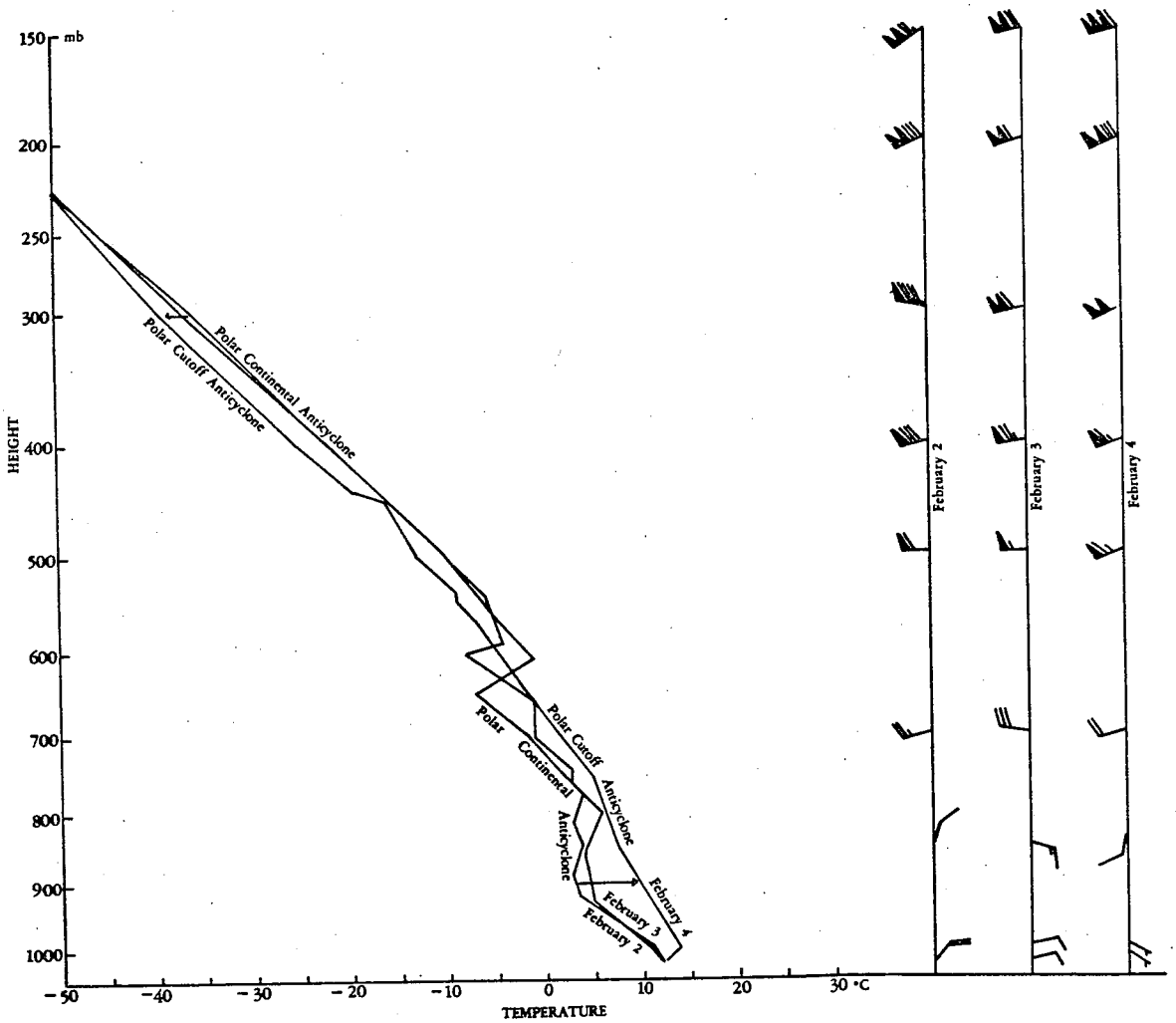

Figure 14. Vertical variations in temperature and winds associated with the Mongolian and Mongolian cutoff anticyclones, at Taoyuan.

Ramage (1954) has found that the Mongolian cutoff anticyclone over the Yellow Sea and the East China coast favors the development of "crachin" along the coasts of south China and north Indochina, approximately between 17°N and 28°N. "Crachin" is defined as a humid period of fog and light rains in winter and spring in those regions. Air originating from the Mongolian cutoff anticyclone travels over the warm Kurioshio ocean current and then moves progressively southwestward to the southeast China coast where a cold coastal current occurs. Fog and drizzle set in as a result of the surface cooling of moist air. "Crachins" appear most frequently in spring when the air-sea temperature difference reaches a maximum in the year.

It can be seen from Tables 22a and 22b in Appendix B that the Mongolian cutoff anticyclone produces much less rainfall than the Mongolian anticyclone in northern Taiwan but almost equal amounts of rainfall in eastern Taiwan. The cutoff anticyclone contributes higher percentages and amounts of mean annual rainfall to Yilan than to Keelung. This indicates a decreasing topographic effect in the northern sector in contrast to an increasing topographic effect in the eastern sector when winds veer from northeast to east and southeast with the advent of the cutoff

anticyclone.

Both the Mongolian and Mongolian cutoff anticyclones contribute very small amounts of rainfall to western and southern Taiwan due to the rain shadow effect. Hence, the difference between rainfall amounts contributed by both anticyclones is small at various stations in these areas. The spatial variation in mean annual rainfall contributed by the cutoff anticyclone can be seen clearly in Figure 10.

It is noteworthy that except for Keelung and Taitung, other stations show that the percentage of mean monthly rainfall associated with the Mongolian cutoff anticyclone is highest in October (Tables 26a and 26b in Appendix B). As shown in the preceding chapter, the frequency of the cutoff anticyclone is at a maximum in October.

Mean daily rainfall associated with the cutoff anticyclone is about half that associated with the Mongolian anticyclone at stations on the west coast. The two sources contribute almost equal mean daily rainfall at stations on the east coast and mountains (Figures 11 and 12, and Table 27 in Appendix B). The mean daily rainfall contributed by the cutoff anticyclone is slightly greater than that contributed by the anticyclone at Taitung, on the windward side with respect to east and southeast winds but on the leeward

side with respect to northeast wind. With the exception of Tainan, the standard deviation of daily rainfall contributed by the cutoff anticyclone is smaller than that contributed by the anticyclone. This is because the frequency of extremely high daily rainfall is less for the former than for the latter synoptic flow types.

The maximum daily rainfall associated with the cutoff anticyclone is smaller than that associated with the anticyclone at most stations except for Yilan and Hwalien. In these two cases east and southeast winds may contribute significant amounts of rainfall despite the decrease in pressure gradients and wind speeds accompanied by the cutoff anticyclone.

As expected, the probability of rainy days associated with the cutoff anticyclone is highest in the east and lowest in the west and southwest of the island. The probability of rainy days is about 47% at Yilan but is only 4% at Tainan. At Keelung, the probability is about 39% for the cutoff anticyclone as contrasted with 78% for the anticyclone (Figure 13 and Table 28 in Appendix B). This suggests the importance of the topographic effect on rainfall. The improved weather associated with the cutoff anticyclone is attributable not only to the decrease in pressure

gradients and wind speeds but also to the veering of winds from northeast to east and southeast. The daily rainfall associated with the cutoff anticyclone seldom reaches over 50 mm (1.97 inches) at all stations. Daily rainfall totals of 76.3 mm (3 inches) or higher occur only at Keelung, Yilan, and Hwalien, with a frequency of one to three days during the eleven-year period.

Summary of Significant Results

It can be concluded that the Mongolian cutoff anticyclone contributes less rainfall than the Mongolian anticyclone over Taiwan. It contributes significant amounts of rainfall only to the northern and eastern sectors of the island. The probability of rainy days associated with the cutoff anticyclone is much lower than that associated with the anticyclone.

In this chapter, the distinct spatial variations in mean rainfall characteristics associated with the Mongolian and Mongolian cutoff anticyclones over Taiwan are recognized. The statistical figures presented in this chapter can be used for the daily rainfall forecast over different parts of the island. The important role of topography on spatial distributions of rainfall characteristics is evidenced by higher annual, monthly, and daily rainfall in the northern

and eastern sectors than in the western and southern sectors of Taiwan. With the exception of the eastern sector, the Mongolian anticyclone is a more important rainmaker than the cutoff anticyclone, as seen by its higher probability of rainy days and by its higher mean, standard deviation, and maximum of daily rainfall. Both anticyclones play almost the same role in contributing rainfall to the eastern sector, suggesting that the prevailing wind direction appears to be more important than wind speed and pressure gradient in triggering rainfall over Taiwan. Unique rainfall regimes over northern and eastern Taiwan are observed as a result of the persistence of the anticyclone and the cutoff anticyclone in winter. It is a well known fact that in monsoon Asia winter is a dry season. However, northernmost Taiwan is characterized by a wet winter and by a less wet summer, whereas eastern Taiwan shows a rainfall maximum in fall. Unlike the other parts of Taiwan, northern and eastern Taiwan show water surplus even in winter (Chen, 1959). Although the Mongolian anticyclone visits Taiwan most frequently in December and January, it contributes the greatest amount of rainfall to Taiwan in February. In terms of the hemispheric circulation, the strength of the westerlies reaches a minimum in February. This shows that the low

zonal-index circulation favors Taiwan with a heavier rainfall than does the high zonal-index circulation. The strength of the westerlies thus provides an important guide for both weather and climatic forecastings over Taiwan.

Both the Mongolian and Mongolian cutoff anticyclones contribute almost negligible amounts of rainfall to western and southern Taiwan, but those synoptic flow types dominate Taiwan in winter. As a result, long dry winters occur year after year. During the eleven-year period from 1959 through 1969, the longest dry spell reached 88 days at Taichung, 109 days at Kaoshiung, and 37 days at Hengchun. Significant water deficits in these areas are expected in almost every year. Consequently, rice growth in these areas requires irrigation. In western and southern Taiwan, rice field soils become dry in November and December. It is necessary to soak soils before the first rice crop seed beds are planted in January. The first rice crop is normally harvested in June. During the early growth cycle of the first rice crop, February through May, water needs in rice fields are most serious and the irrigation canals are characterized by lowest water level (VanderMeer, 1968).

CHAPTER IV

RAINFALL ASSOCIATED WITH THE TAIWAN LOW AND POLAR FRONTS

The Taiwan Low

The Taiwan low is an extratropical cyclone originating in the eastern and northern sea surface off Taiwan. It appears occasionally from late autumn to early spring, with a maximum mean frequency in February (Figure 2). Two conditions near Taiwan provide a favorable cyclogenesis field for the Taiwan low. First, the Kuroshio warm ocean-current travels northward over the sea surfaces east and north off Taiwan, whereas a cold ocean-current flows southward along the east China coast. The boundary between these two currents is located over the East China Sea in the vicinity of northern Taiwan. It is characterized by a sharp temperature gradient and hence is favorable for cyclogenesis. Second, the establishment of a dynamic trough over central high mountains in Taiwan frequently favors cyclogenesis (P. I. Wang, 1971).

Several attempts have been made to study the development of the Taiwan low. According to the First Weather Wing (1966), the Taiwan low is usually accompanied by two

surface synoptic flow types:

1. The normal type

   The Taiwan low is concurrent with a Mongolian or a Mongolian cutoff anticyclone.

2. The double-eye type

   The Taiwan low is located in a col between two anticyclones, i.e., a Mongolian anticyclone and a Pacific anticyclone.

The Taiwan low is usually accompanied by a 500-mb trough along 110°E-120°E over central China (First Weather Wing, 1966). It is also associated with low-level warm advection and upper-level cold advection over Taiwan (Figure 15).

Based on the analysis of 700-1000 mb thickness charts, Hsu (1969) has found that a Taiwan low frequently develops in the area where the most concentrated isopycnic lines are arcuate with the ends bending toward the southeast and southwest, respectively.

Figure 16 shows daily variations in winds at different levels over Taoyuan during the period late February to early March 1965 when there were nine days with the Taiwan low. It shows that the Taiwan low is usually accompanied by a slight strengthening of the northeast monsoon at the surface.

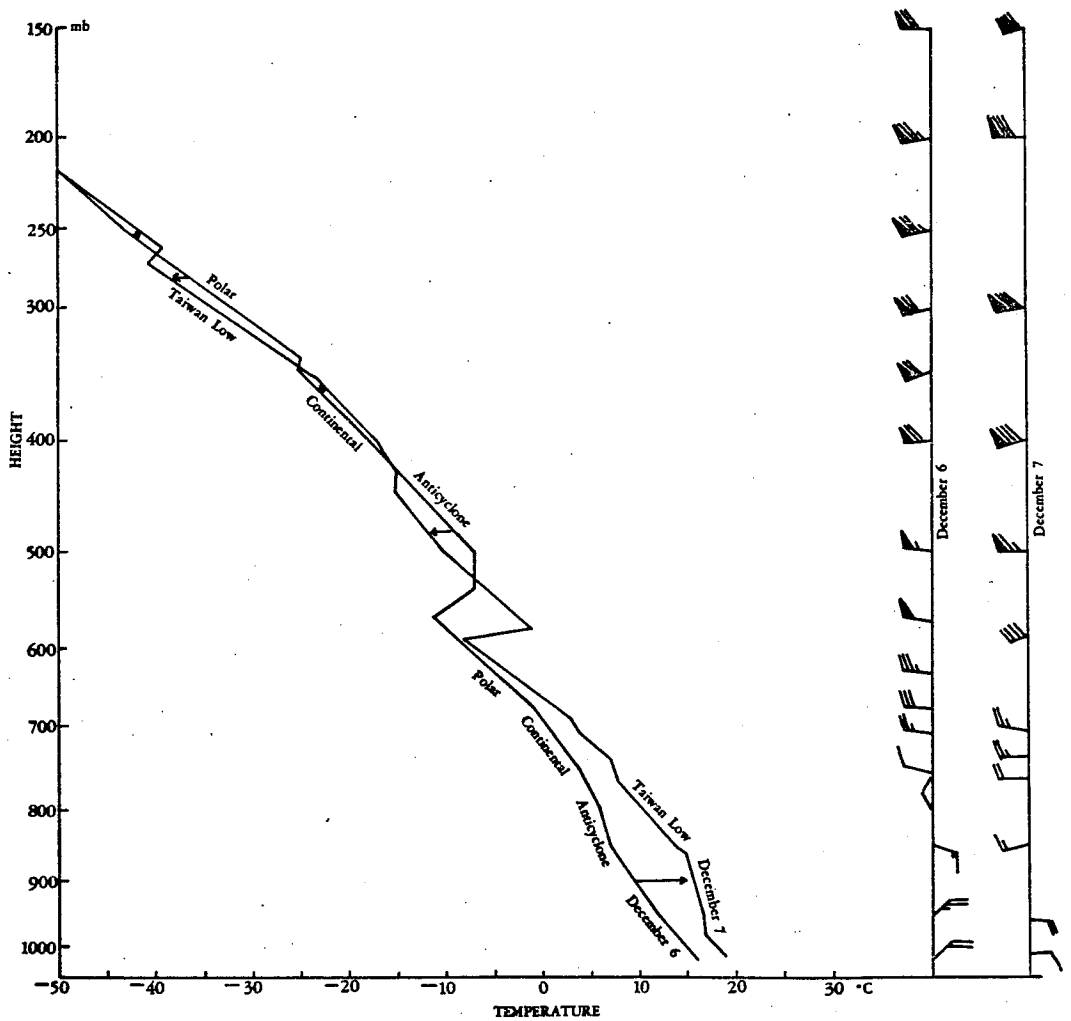

Figure 15. Vertical variations in temperatures and winds associated with the Mongolian anticyclone and Taiwan low, at Taoyuan.

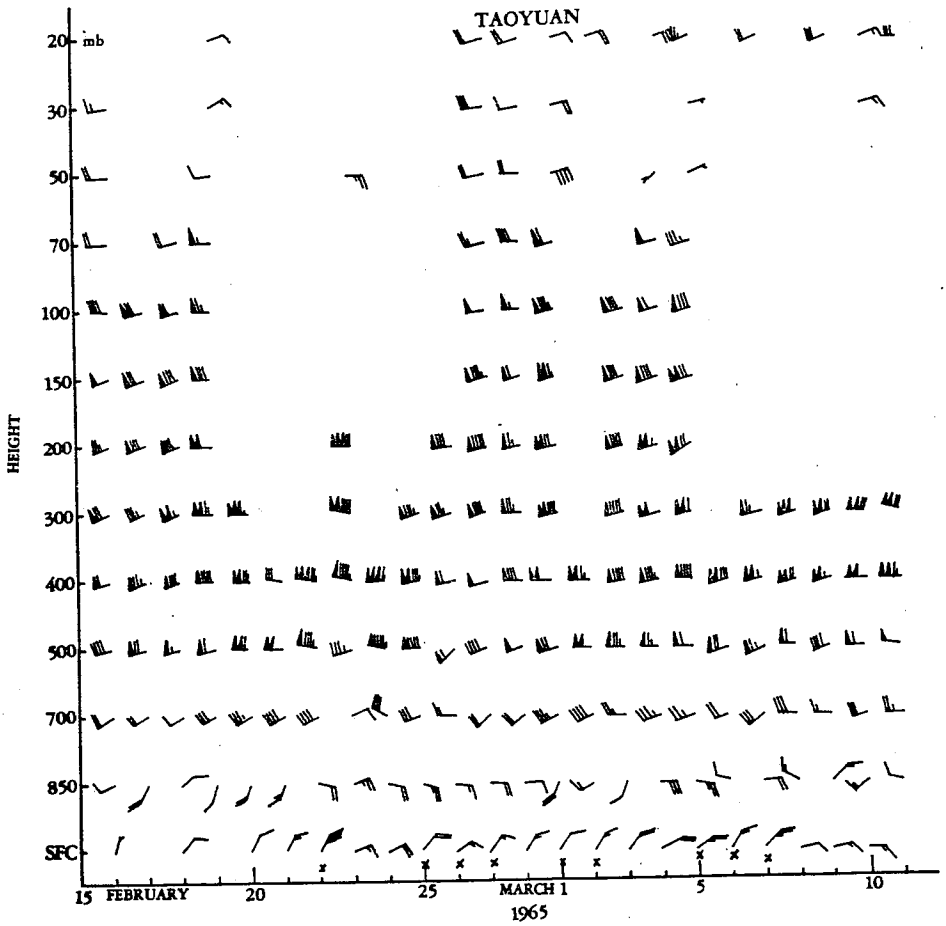

Figure 16. Vertical wind variations at Taoyuan during the frequent Taiwan low period. X denotes the Taiwan low day.

At the 850-mb level, an east wind is frequently observed in association with the Taiwan low. At the 700-mb and 500-mb levels, pronounced wind shift from west to southwest is concurrent with the Taiwan low. This is in agreement with the First Weather Wing's (1966) finding that the Taiwan low is correlated with the northward displacement of the subtropical jet stream and the southward displacement of the polar front jet stream.

On the average, a Taiwan low persists for 36-48 hours, moving toward southern Japan at a speed of 25 knots. In rare cases, the Taiwan low may travel eastward across Okinawa into the Pacific or it may travel northward across Korea into the Sea of Japan.

As expected, the Taiwan low contributes a fairly large proportion of the mean monthly rainfall to northern Taiwan (Figure 10 and Tables 22a and 22b in Appendix B), about 11% of the mean monthly rainfall at Keelung, but only about 1% of the mean annual rainfall at the more southerly stations of Kaoshiung and Tainan.

The Taiwan low also contributed a greater amount of mean monthly rainfall to north than to south, but it contributes a greater proportion of mean monthly rainfall to south than to north (Tables 29a and 29b in Appendix B). In the southwestern sector of the island where winter is dry,

the Taiwan low contributes a high percentage of mean monthly rainfall in winter, although the amount of mean monthly rainfall contributed is very small. At Hengchun, the percentage of mean monthly rainfall contributed by the low is highest among all surface synoptic flow types in January. At Taichung, more than 50% of mean monthly rainfall in December is derived from the low. Except for Hengchun, the mean monthly rainfall contributed by the low reaches a maximum in February. However, the percentage of mean monthly rainfall contributed by the low reaches a peak in December or January at various stations in the southern and western sectors of the island.

As with the Mongolian anticyclone, the mean, standard deviation, and maximum daily rainfall associated with the Taiwan low are higher in the northeastern sector than in the southwestern sector of the island. However, the mean daily rainfall is slightly smaller than that contributed by the Mongolian anticyclone at all stations (Figures 11 and 12 and Table 30 in Appendix B). At Keelung and Yilan, the mean daily rainfall is more than 10 mm and the maximum daily rainfall is more than 100 mm.

The probability of rainy days associated with the Taiwan low is more than 70% in the north and east but is

only 15% in the southwest. At Keelung, the probability of rainy days reaches 82% and the percentage of rainy days with rainfall exceeding 76.2 mm (3 inches) is 3.3%, the highest value among all surface synoptic flow types in winter (Figure 13 and Table 31 in Appendix B).

Polar Fronts

The polar front is one of the major synoptic flow types contributing heavy rainfall over the entire island. In winter, polar fronts usually precede polar outbreaks. Passages of polar fronts over Taiwan are normally accompanied by cold advection in the lower troposphere (Figure 17).

Table 2 shows the frequency of polar fronts which persist for three days or more over Taiwan. The table indicates that polar fronts become stationary in spring and early summer. During the eleven-year period from 1959 through 1969, not a single polar front lasting more than two days has ever been observed over Taiwan in mid-winter, December and January. Stationary polar fronts lasting more than four days over Taiwan occur most frequently in May and June, when the entire island enjoys a period of heavy rainfall. Stationary polar fronts also occur frequently in September when the summer monsoon gives way to the winter

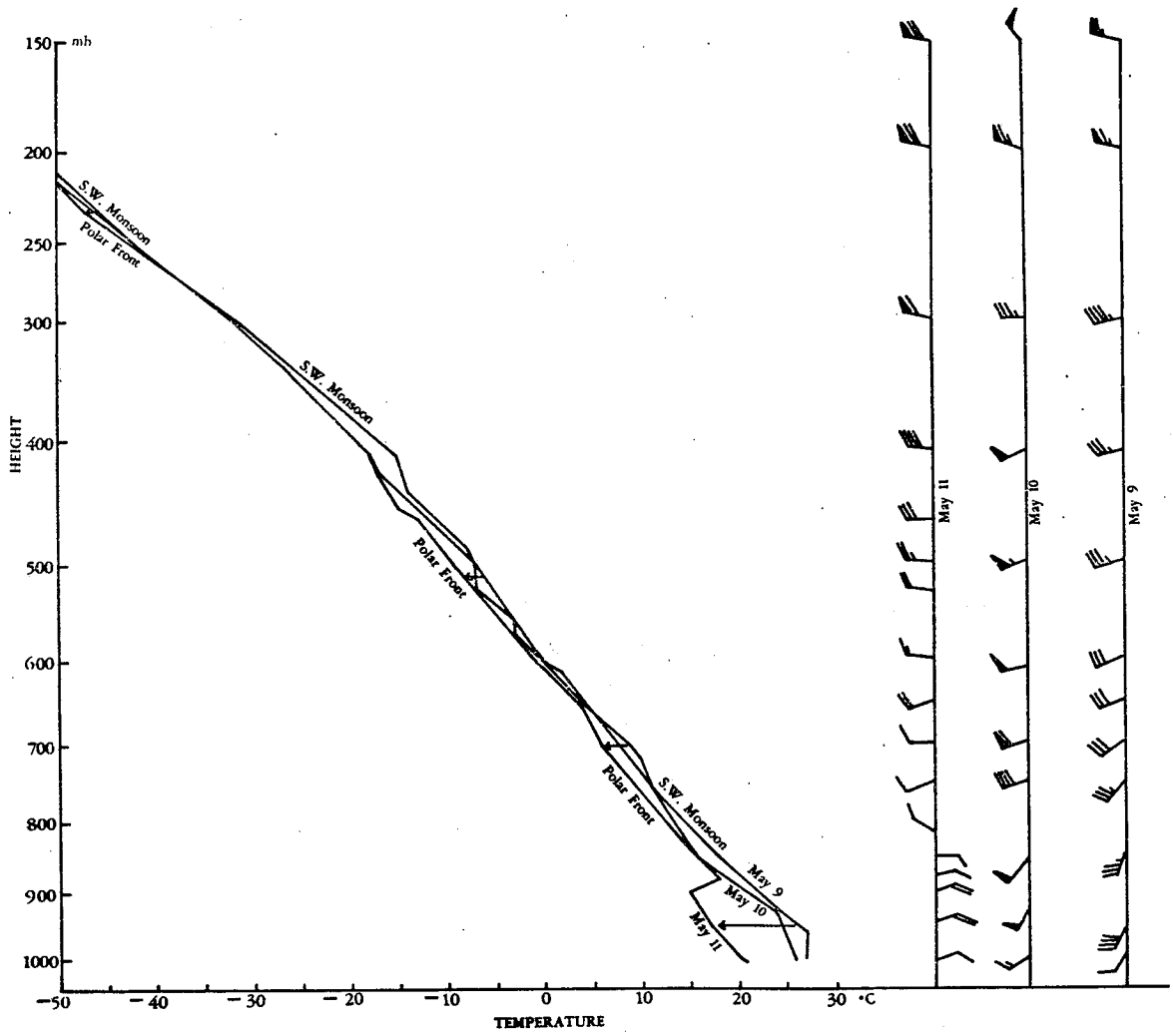

Figure 17. Vertical variations in temperatures and winds associated with the southwest monsoon and polar front, at Taoyuan.

TABLE 2

FREQUENCY OF POLAR FRONTS WHICH LAST FOR 3 DAYS OR LONGER FOR THE PERIOD 1959 TO 1969

Months	1	2	3	4	5	6	7	8	9	10	11	12
1959		1		2	2	4						
1960			1	1	3	1			1	1		
1961			2	2	1	1			1			
1962			2		3	2					1	
1963				1		2			2			
1964					4	1			1	2		
1965			1	3	4	3			1		1	
1966				4	1	1	1	1	1		1	
1967			1	1	1	1			1			
1968		1	1	1	4	3		1				
1969		1	1		2	1			1		1	
Total		3	9	15	24	20	1	2	9	3	4	

monsoon.

Remarkably, the amount of mean annual rainfall associated with polar fronts is more than 400 mm (15.75 inches) at all stations (Figure 10 and Tables 22a and 22b in Appendix B). It appears that except for mountain stations polar fronts contribute more rainfall to the north than to the south. With the exception of Keelung, where both polar fronts and the Mongolian anticyclone produce almost equal amounts of rainfall, polar fronts contribute more mean annual rainfall than does the Mongolian anticyclone to other stations. In contrast to the Mongolian anticyclone, polar fronts account for more than 20% of the mean annual rainfall at all Taiwan stations, with values higher in the west and southwest than in the north and east. The mean annual rainfall contributed by polar fronts is 41% at Taichung, a value even higher than that (26%) contributed by typhoons (Figure 10 and Tables 22a and 22b in Appendix B).

As expected, the amount and percentage of mean monthly rainfall associated with polar fronts is highest in June and is lowest in December at all stations (Tables 32a and 32b in Appendix B). The mean monthly rainfall contributed by polar fronts in June reaches more than 100 mm (3.94 inches), at all stations, with the highest value at Alishan followed

by Taichung. In June, many stations received more than 80% of their mean monthly rainfall from polar fronts.

The mean, standard deviation, and maximum daily rainfall associated with polar fronts are much higher than those associated with the Mongolian anticyclone or the Mongolian cutoff anticyclone (Figures 11 and 12 and Table 33 in Appendix B). The mean daily rainfall associated with polar fronts is more than 10 mm (0.39 inches) at all stations. The highest values are in the west and southwest, and the lowest in the south and east. The maximum daily rainfall reaches more than 150 mm (5.91 inches) at all stations; it reaches about 296 mm (11.65 inches) per day at Yilan and nearly 350 mm (13.78 inches) per day at Alishan.

The probability of rainy days associated with polar fronts is highest among all winter synoptic flow types and is second only to typhoons among all synoptic flow types over the entire year (Figure 13). As with the Mongolian anticyclone, the probability of rainy days associated with polar fronts is much higher in the north than in the south. The chances of polar fronts producing heavy rainfall are greater than any other winter synoptic flow type. At Keelung, in the eleven-year period 1959-1969, there were seventeen polar front days contributing daily rainfall of

more than 76.2 mm (3 inches). But there were only six Mongolian anticyclone days with comparable rainfall intensity. In western and southern Taiwan, where the Mongolian anticyclone contributes less than 1% of rainy days with rainfall of more than 50.8 mm (2 inches), the probability of having such a rainfall intensity associated with polar fronts is about 3% or higher. Hence, it can be concluded that polar fronts are associated with a greater frequency of rainy days over the entire island and with a heavy rainfall intensity in late spring and early summer (Table 34 in Appendix B).

The foregoing discussion refers to polar fronts over Taiwan (between 21°N and 26°N along 120°E). The rainfall in Taiwan contributed by polar fronts south of Taiwan (south of 21°N along 120°E) was also studied. It was found that the spatial variation in annual, monthly, and daily rainfall in Taiwan is essentially similar for both groups of fronts. The only difference is that polar fronts south of Taiwan show lower rainfall intensities and less probabilities of rainy days (Tables 35a through 37 in Appendix B).

The Plum Rains[1]

It has long been recognized that the rainy belt in East Asia advances step by step from south to north during

late spring and early summer (Dao, et al., 1958; Yoshino, 1965a and b, 1966). In June and July, the rainy belt is over the Yangtze River Basin and normally persists for five to twenty days. The plum rain period over the Yangtze River Basin is concurrent with the setting-in of a stationary polar front at the surface (Zou, et al., 1964; Chu, 1962). The plum rains are large-scale atmospheric phenomena and pronounced climatic singularities, usually appearing simultaneously with the onset of the southwest monsoon over India (Suda and Asakura, 1955; Dao and Chen, 1957). The rains mark the transition from a winter to a summer circulation pattern in the upper atmosphere (Yeh, et al., 1958, 1959). In Arizona (U.S.A.), Bryson and Lowry (1955) observed the same abrupt change in the upper atmospheric circulation and the associated increase in rainfall in late June and early July.

A number of studies have been made to relate the plum rains to the large-scale change in atmospheric circulation patterns over Asia. Jet streams, blocking highs, mid-latitude ridges and troughs, and subtropical ridgelines have

---

[1]The plum rains are also called Mai-yü or mold rains in Chinese, with reference to the season when plums ripen and to the effects of continued dampness.

constituted topics for exploration. Yin (1949) has discovered that the onset of the summer monsoon in India is characterized by the following changes in the general circulation:

1. The sudden absence of the subtropical jet stream south of the Tibetan Plateau.
2. The westward displacement of the subtropical trough from 90°E to 80°E.
3. The change in long-wave numbers from 3 to 4 in the Northern Hemisphere.
4. The establishment of a monsoon trough near 23°N over India.

Some Chinese meteorologists have conformed that the onset of the plum rains over the Yangtze River Basin is accompanied by an abrupt dissipation of the subtropical jet stream at 65°E and the weakening of the subtropical jet stream by half at 140°E (Yeh, et al., 1952; Dao and Chen, 1957; Liu and Wu, 1956).

The plum rains have been attributed to the development of the Okhotsk blocking high. Zou, et al. (1964) have studied the 500-mb circulation during the plum rain period over the middle and lower Yangtze River Basin and have concluded that stable blocking highs along 50°N - 70°N over

Siberia favor the development of a short-wave trough between 35°N and 45°N over East Asia. Chen (1957) found that a record heavy rainfall in early summer 1954 was associated with the Okhotsk blocking high. Over Manchuria, a cutoff low was triggered by this high. As a result, the polar front jet stream over East Asia split into two branches, one being displaced southward to the Yangtze River Basin, about 10 degrees of latitude south of its normal position. However, Liu and Wu (1956) have stated that the onset of the plum rains is accompanied by the presence of the Ural blocking high which establishes a stable strong westerly wind belt along 30°N-40°N over China. The plum rains may start without the presence of the Okhotsk high, which plays a more important role in increasing the duration and intensity of rainfall than in triggering the plum rains. The development of the Okhotsk high during the plum rain period is probably in response to the adjusting process of long-wave numbers from 3 to 4 as the season shifts from winter to summer (Yeh, et al., 1958; Chu, 1962).

Dao, et al. (1958) and Zou, et al. (1964) have discovered that the plum rain period becomes established when the North Pacific subtropical ridge appears between 20°N and 25°N. As a result, a polar front moves from the Nan Ling

Mountains to the Yangtze River Basin and creates a long rainy period. The "jumping" behavior of the North Pacific subtropical ridge is found to be related to the setting-in of a warm blocking high from west Siberia to the East Asia coast. In addition, when the plum rains begin over China and Japan, the upper-air winds shift from west to east at subtropical stations and an easterly jet stream develops over South Asia.

Cessation of the plum rain period is characterized by northward displacement of the polar front jet stream from 30-40°N to 40-50°N along 120°E and 140°E while the North Pacific subtropical ridge advances northward to 30-40°N. Meanwhile, the polar front zone retreats northward from the Yangtze River Basin to the Yellow River Valley (Liu and Wu, 1956). Dao, et al. (1958) have discovered that the onset of the plum rains over China can be correlated with the diminution of the subtropical jet stream south of the Tibetan Plateau, accompanied by the presence of a polar front jet stream in high latitudes near 70°N over East Asia. Yoshino (1965a and b) also has noted that two polar front jet streams develop over Japan during the plum rain period. The plum rain period ends when the northern jet stream near 70°N disappears and the southern jet stream advances to

north of 40°N over Japan. Chen (1957) has conformed that the plum rain period over China ends when the North Pacific subtropical ridge advances northward to 35°N and the jet stream south of 40°N along 140°E moves to 42-47°N. In addition, typhoons start to invade the east China coast and the Yellow Sea. The westerlies at 200 mb over southern Japan are replaced by the easterlies. As a result of the northward push of the North Pacific subtropical ridge near 40°N after the end of the plum rain period, the Okhotsk high also dissipates and is replaced by a trough (Chu, 1962; Chen, 1957). Furthermore, a polar trough appears to the north of the Tibetan Plateau and a firm summer circulation pattern is established with four wave-numbers in the Northern Hemisphere at the 500-mb level. At the 200-mb level, the summer circulation pattern also differs greatly from the winter pattern. In winter, the westerlies extend over the subtropics with three major highs, over the northwestern part of South America, over central Africa, and around Borneo and Indonesia (Krishnamurti, et al, 1973a). These regions are characterized by strong convective activity in winter. In summer, the blocking effect of the thermal Tibetan high acts as a barrier, providing the dynamic mechanism for the formation of the Mexican high, the African high, the mid-Pacific

trough, and the mid-Atlantic trough. Many studies of the numerical simulation models also show the occurrence of these primary entities of the large-scale circulation over the northern summer hemisphere (Krishnamurti, et al. 1973b; Manabe and Hahn, 1973; and Abbott, 1973).

As already discussed, the plum rain period over the Yangtze River Basin is concurrent with the abrupt change in the atmospheric circulation in the Northern Hemisphere. Many studies have been made to determine the dates of the onset and recess of the plum rains over China and Japan based on the discontinuities of daily meteorological elements such as rainfall, pressure, temperature, wind, vapor flux, and isobaric surface heights (Hsu and Kao, 1962; Neyama, 1963; Yoshino, 1965a and b; Mizukoshi, 1962; Gangopadhyaya, et al., 1963). An attempt is made in this study to determine the dates of the onset and retreat of the plum rains over Taiwan based on some of those criteria.

It has long been recognized that most Taiwan stations show mean monthly rainfall peaks in June when polar fronts visit Taiwan most frequently. Chi (1964) has attributed the heavy rainfall in June to the convection caused by solar heating and orographic uplifting of the southwest monsoon. This is intensified by the passage of a polar front and the

convergence between the southwest monsoon and the southeast trade. A careful study of the daily rainfall and weather maps over Taiwan indicates that the persistence of a polar front over Taiwan does, in fact, account for the heavy rainfall in June. For example, in 1963 the heavy rainy periods from June 1 to June 5 and from June 14 to June 20 were concurrent with polar fronts over Taiwan.

The dates of the onset and cessation of the plum rains in Taiwan can be determined by plotting daily rainfall curves from May through July at various stations. The onset of the plum rains is evidenced by an abrupt increase in daily rainfall at almost all stations. A typical 1967 case is presented in Figure 18. It shows that the plum rains started on May 22 when a heavy daily rainfall was observed at all stations. The daily rainfall on May 23 reached almost 350 mm (13.78 inches) at Kaoshiung. The maximum daily rainfall at many stations exceeded 100 mm (3.94 inches) during this plum rain period. In the northern and eastern portions of the island and mountain areas where winter is wet, rainfall occurred several days ahead of the onset of the plum rains.

The date of the cessation of the plum rains in Taiwan is much better defined than that of the onset of the plum

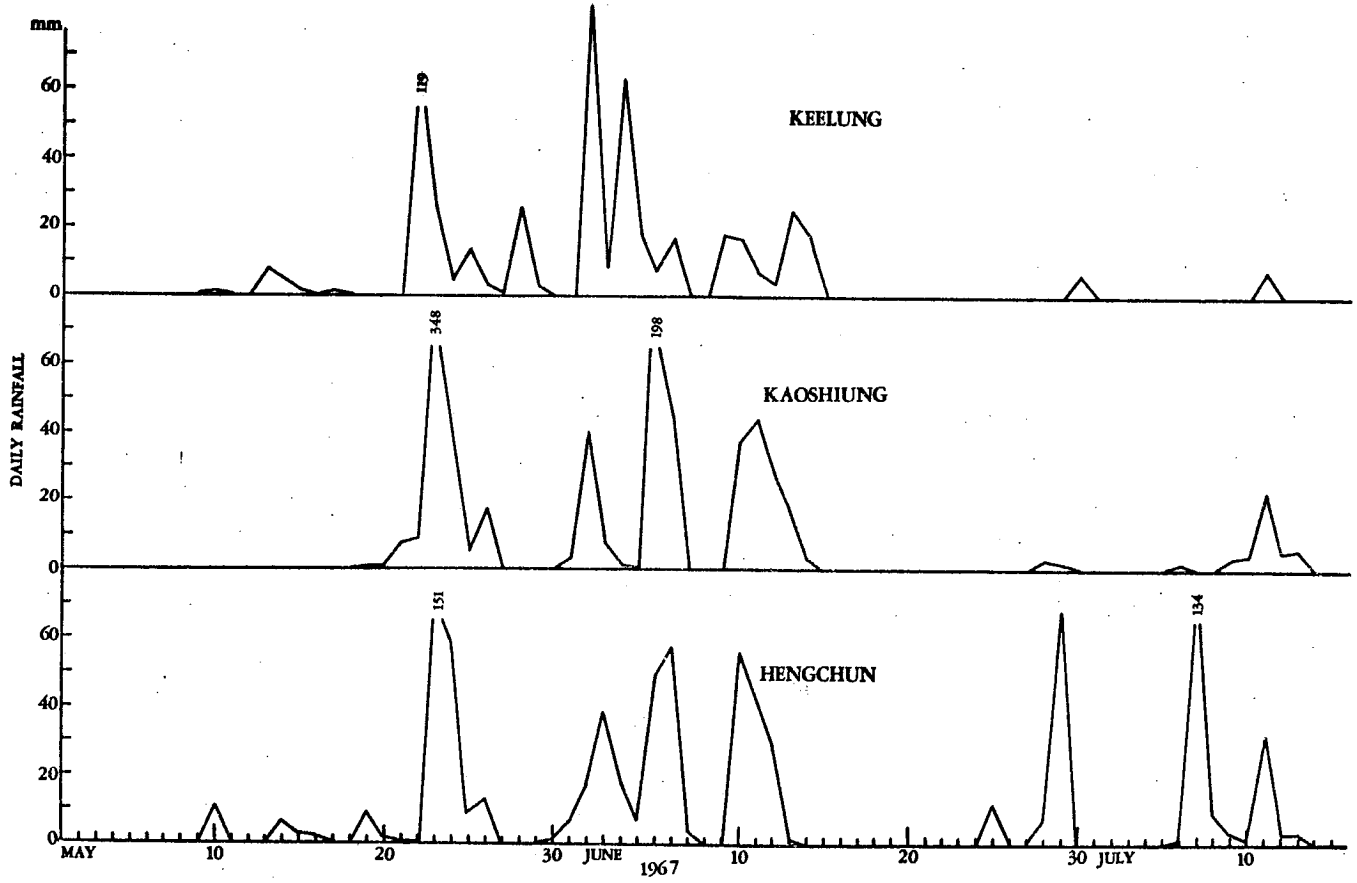

Figure 18. Daily rainfall variations at the various Taiwan stations during the plum rain period of 1967.

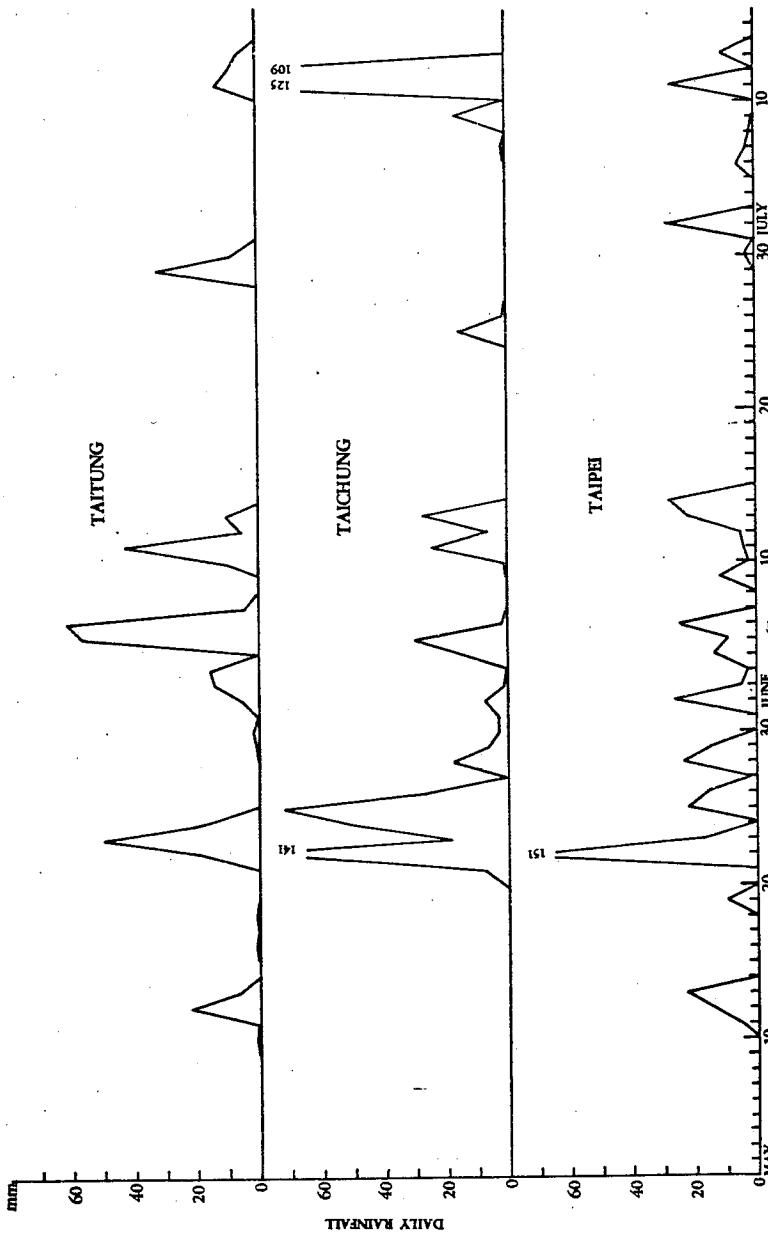

Figure 18. Continued.

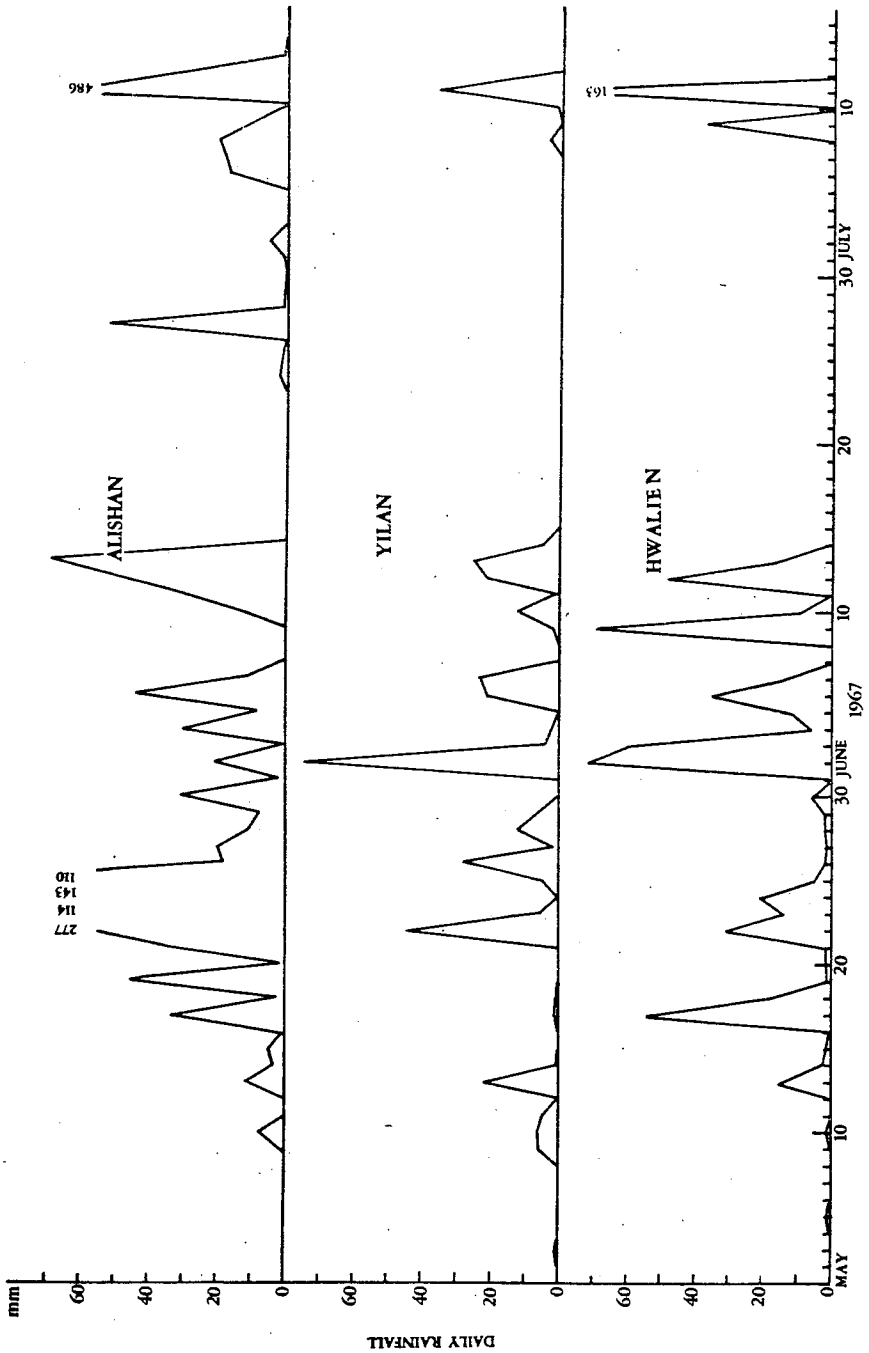

Figure 18. Continued.

rains. The plum rains in 1967 persisted for more than twenty days. An abrupt halt was clearly observed on June 15 at most stations. Although the rainy period at some stations ended one day earlier, i.e., June 14, a persistent polar front dominated Taiwan from May 22 to June 14. Consequently, June 15 is considered as the date of the cessation of the plum rains.

Based on daily rainfall curves and stationary polar fronts for the period 1959-1969, the dates of the onset and cessation of the plum rains in Taiwan have been determined as shown in Table 3. These dates vary greatly from year to year, although the average duration is about twenty-five days. The plum rains can arrive on Taiwan as early as May 17 or as late as June 6. They can leave Taiwan anywhere between June 5 and July 2.

The onset of the plum rains in Taiwan has been found to be associated with a persistent polar front that separates a Mongolian cutoff anticyclone over the East China Sea from a North Pacific subtropical anticyclone south of Taiwan. According to Dao, et al. (1958), the first stage of the plum rains in East Asia is characterized by the presence of a persistent polar front over south China; the current study agrees with their findings.

TABLE 3

DATES OF THE ONSET AND THE END OF THE PLUM RAINS FOR THE PERIOD 1959 TO 1969

	Onset	End	Duration (days)
1959	May 27	June 15	20
1960	May 19	June 19	32
1961	May 17	June 15	30
1962	June 6	July 2	27
1963	June 1 and June 14	June 5 June 20	12
1964	May 20	June 28	40
1965	June 1	June 30	30
1966	May 28	June 14	18
1967	May 22	June 14	23
1968	May 19	June 14	26
1969	May 20	June 23	35
Average	May 25	June 20	27

At the 500-mb level, the synoptic flow patterns associated with the plum rains over Taiwan indicate that an isolated subtropical anticyclone is developed over the South China Sea near 20°N and the North Pacific subtropical ridge extends from the central North Pacific to the south of Taiwan in a northeast-southwest orientation. A polar trough over Taiwan separates these two subtropical anticyclones.

Figures 19 through 24 indicate daily variations in winds at different levels during the period May through July of 1960, 1964, and 1965 at Taoyuan (25°N) and Tongkang (22°N). Some remarkable features are observed. The onset of the plum rains over Taiwan is associated with an abrupt downward intrusion of the easterlies from the stratosphere to the upper and middle tropospheres. Winds in the troposphere become more variable and weaken during the plum rain period. Prior to the onset of the plum rains, a persistent subtropical jet stream with wind speed exceeding 50 knots is observed at 200 mb. During the period, wind speeds equal to 5 knots are frequently observed at that level. Although the jet stream may reappear during the period, it lasts for only a few days. On the other hand, the plum rains end when the easterlies extend from the stratosphere all the way down to ground surface, as a result of the displacement of

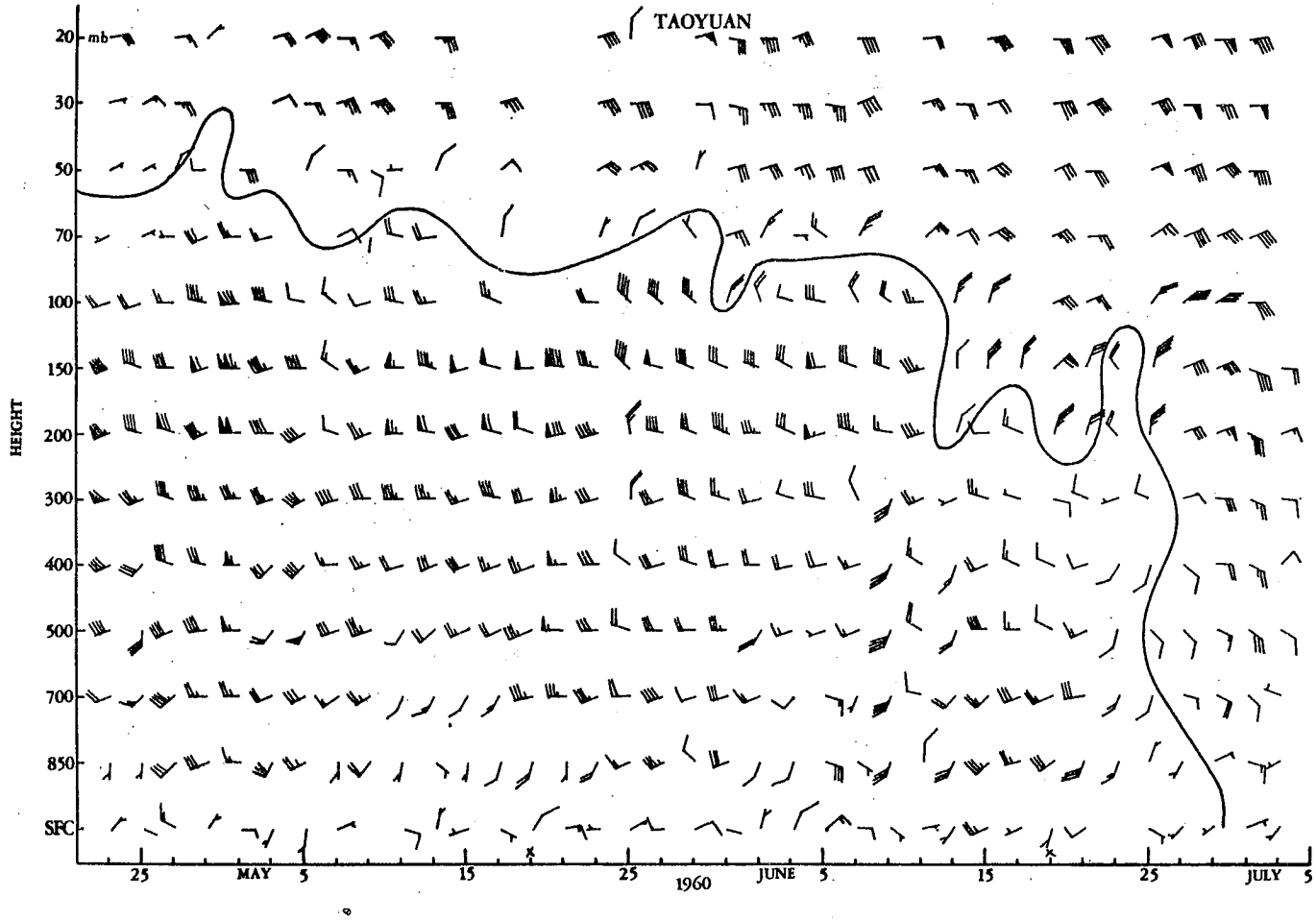

Figure 19. Vertical wind variations at Taoyuan during the plum rain period of 1960. X denotes the onset and end of the plum rains.

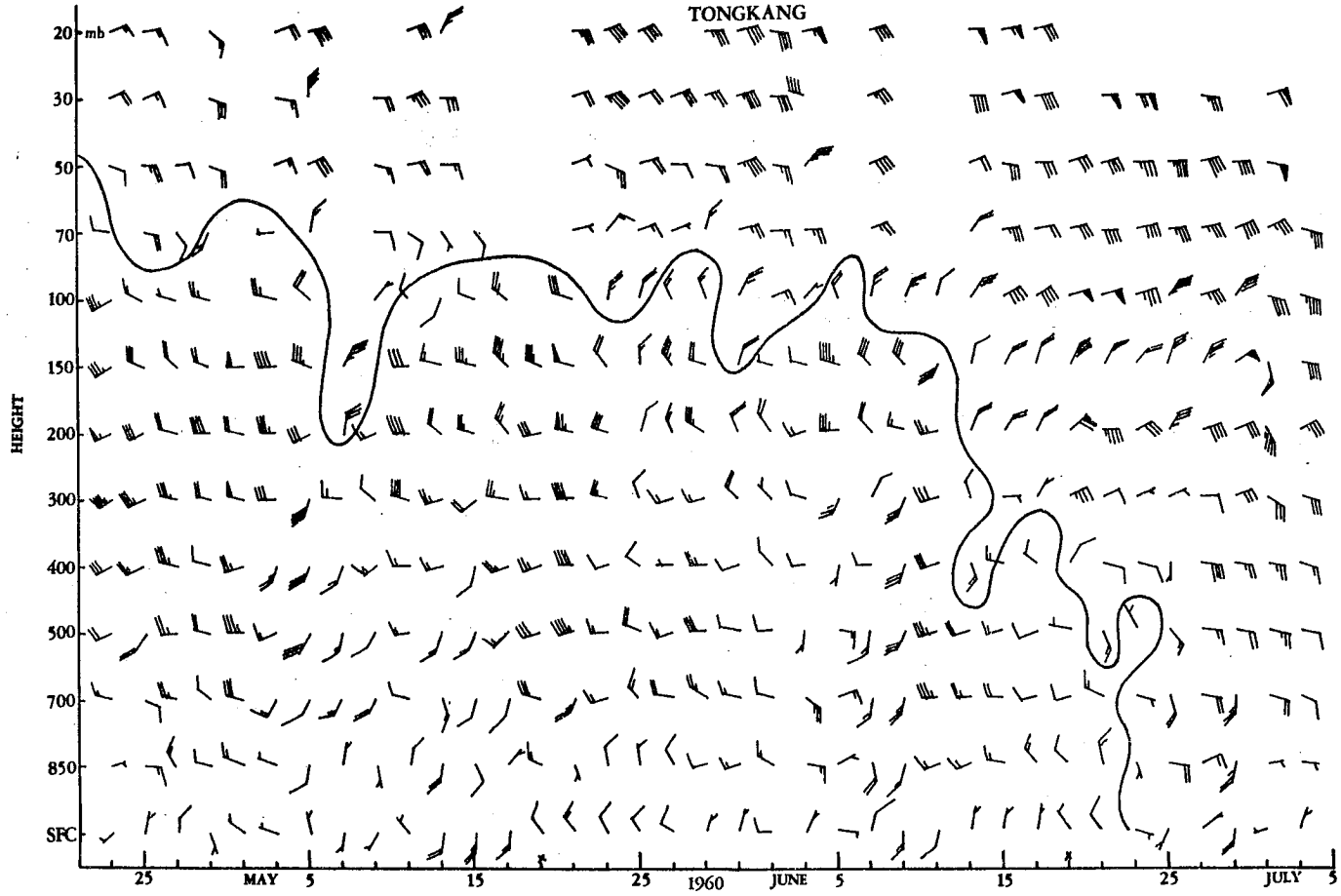

Figure 20. Vertical wind variations at Tongkang during the plum rain period of 1960.

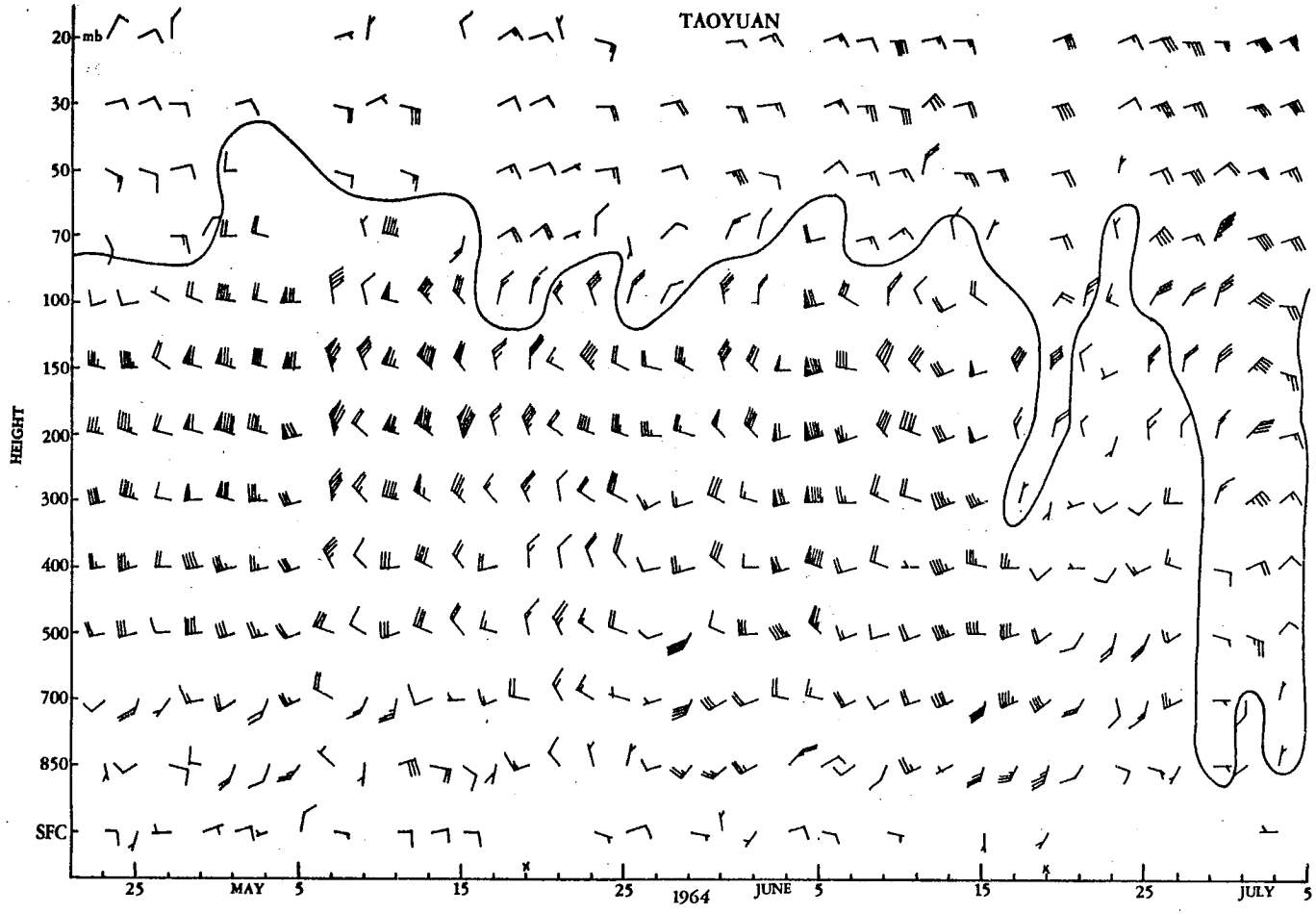

Figure 21. Vertical wind variations at Taoyuan during the plum rain period of 1964.

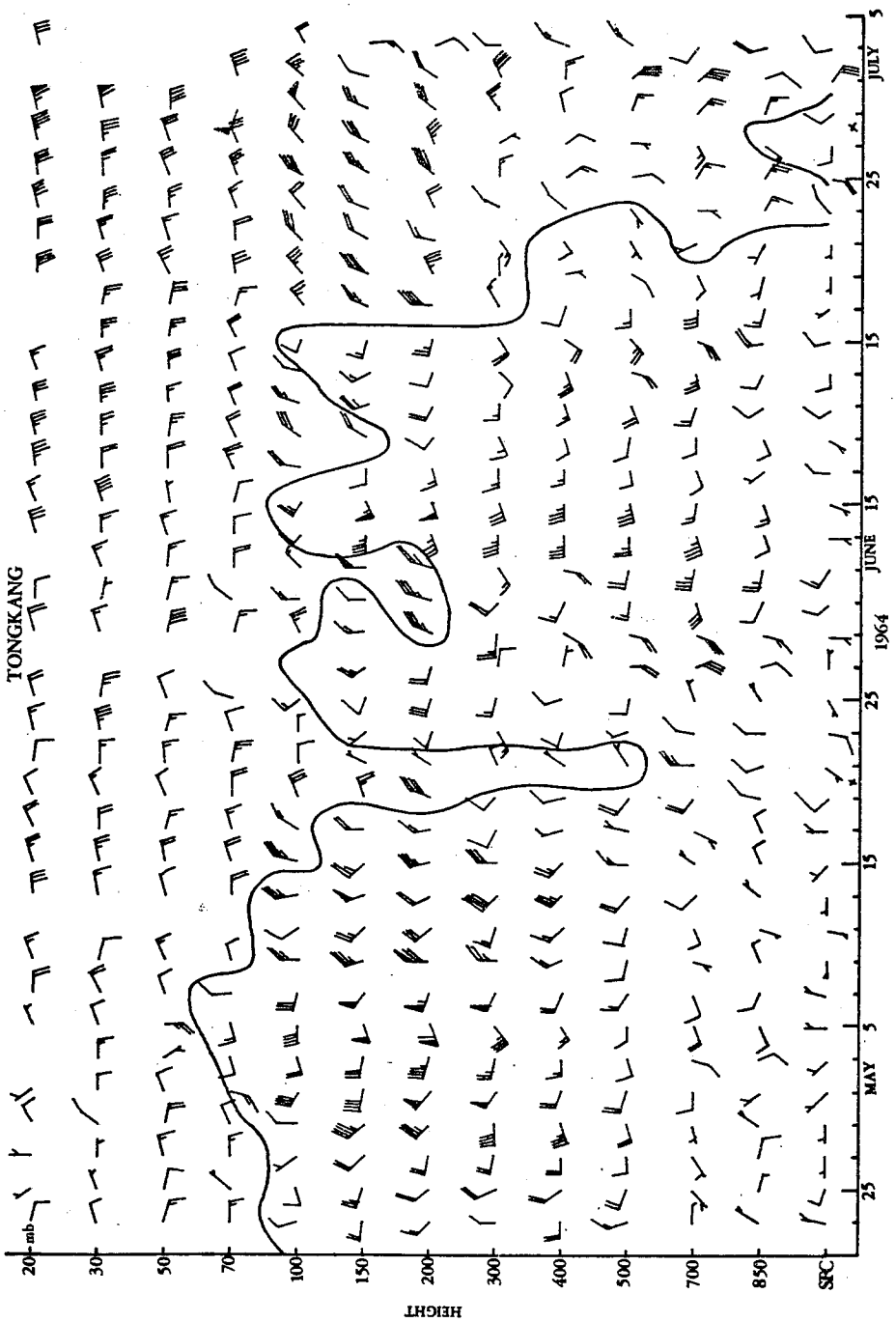

Figure 22. Vertical wind variations at Tongkang during the plum rain period of 1964.

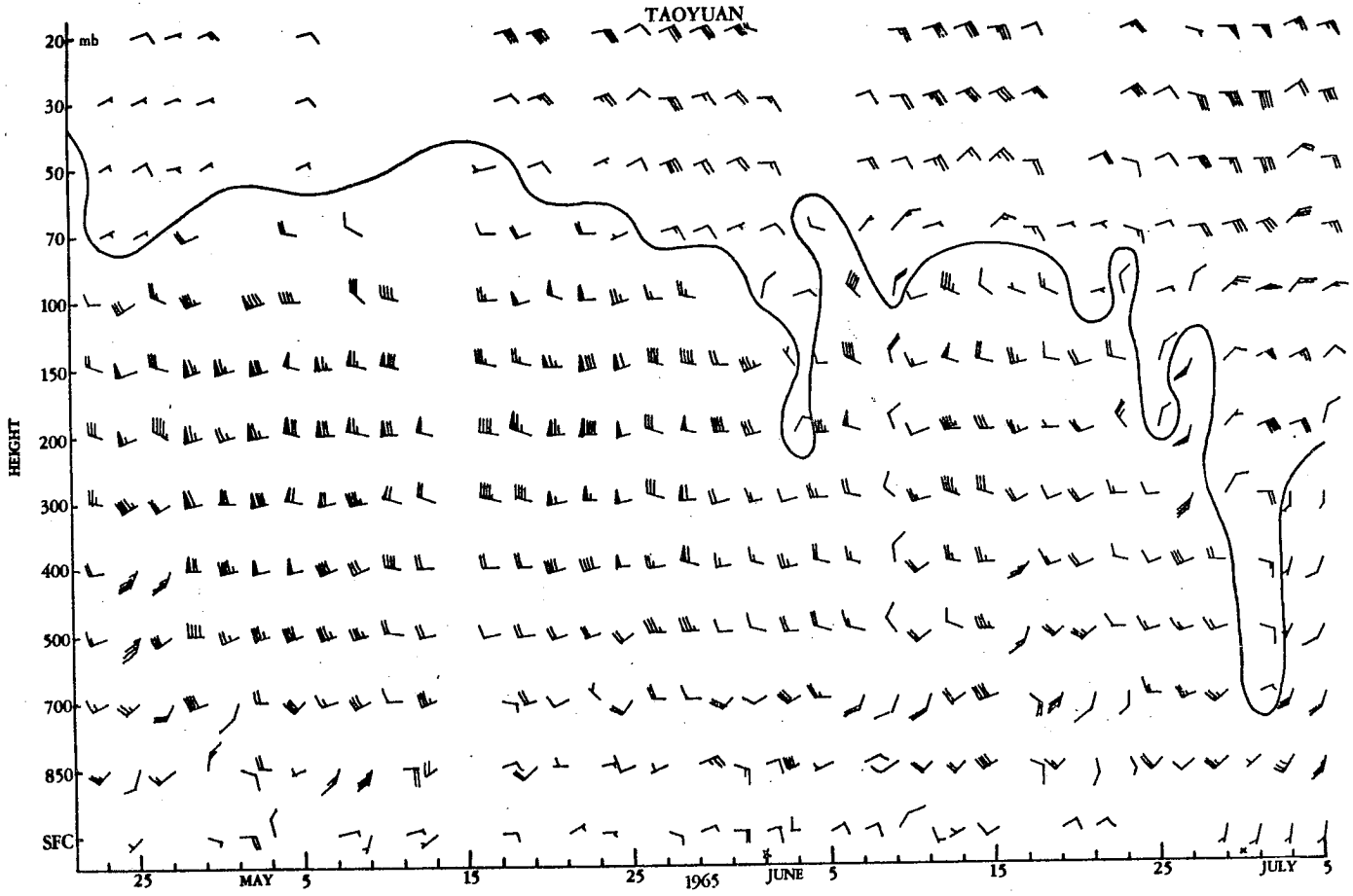

Figure 23. Vertical wind variations at Taoyuan during the plum rain period of 1965.

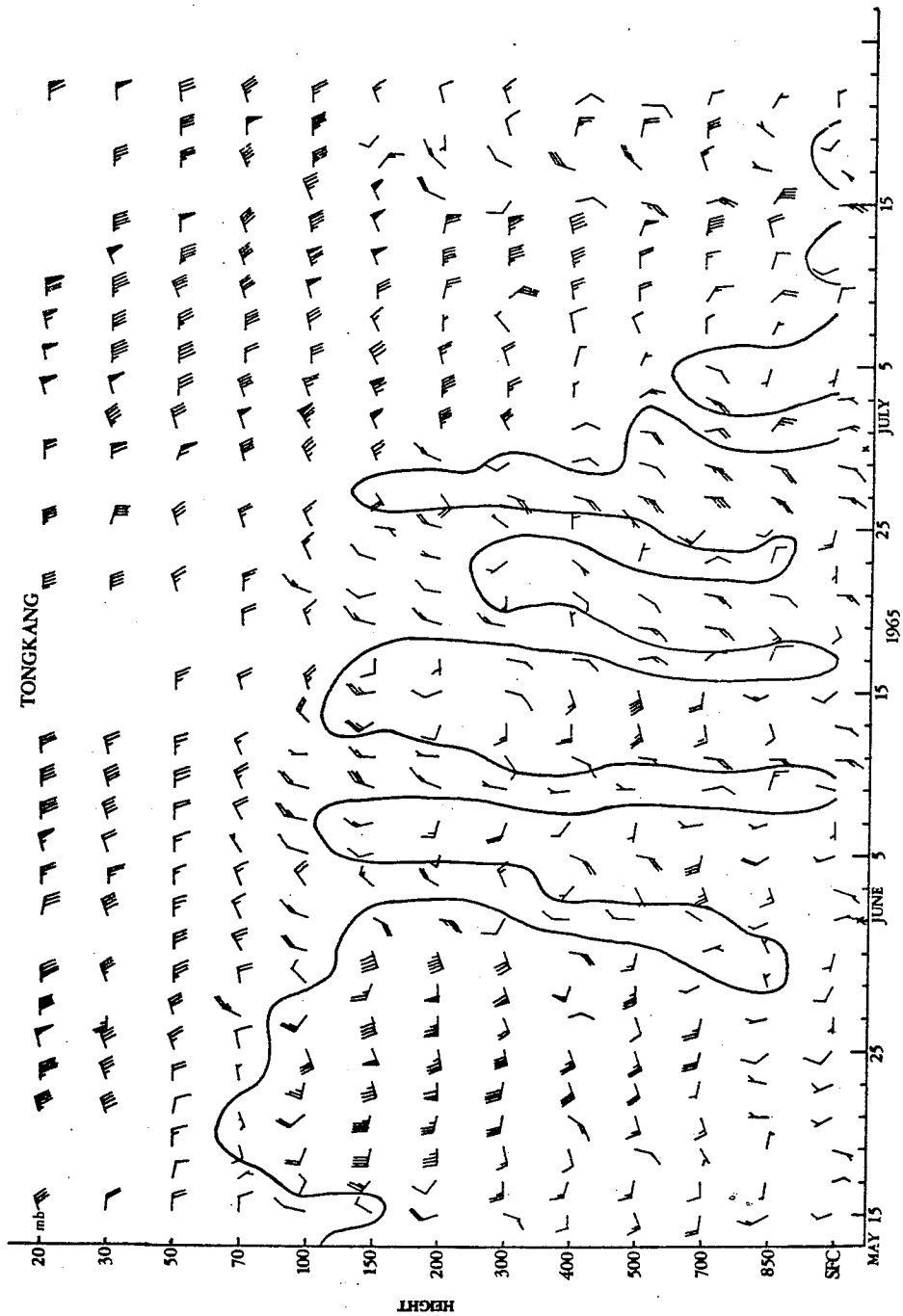

Figure 24. Vertical wind variations at Tongkang during the plum rain period of 1965.

the North Pacific subtropical ridge to the north of Taiwan. Meanwhile, an easterly jet stream with wind speeds exceeding 50 knots is observed upon the cessation of the plum rains over Taiwan.

The relationship between the onset of the plum rains and variations in geopotential height at the 500-mb level over Taoyuan for 1960, 1964, and 1965 is shown in Figures 25 through 27. It appears that the onset of these rains is correlated with a pronounced increase in the geopotential height at the 500-mb level. The rains end also in connection with an abrupt increase in the 500-mb geopotential height. The 500-mb height difference between Taoyuan and Tongkang also shows the same character. Preceding the plum rains, the subtropical ridgeline is located far south of Taiwan and the geopotential height at the 500-mb level is greater at Tongkang than at Taoyuan as seen by negative height differences in Figures 25 through 27. During the plum rain period, the subtropical ridgeline advances northward and fluctuates over Taiwan. In most cases, the 500-mb geopotential height is greater at Taoyuan than at Tongkang. After the plum rain period, the 500-mb geopotential height is persistently greater at Taoyuan than at Tongkang because the North Pacific subtropical ridgeline advances to the

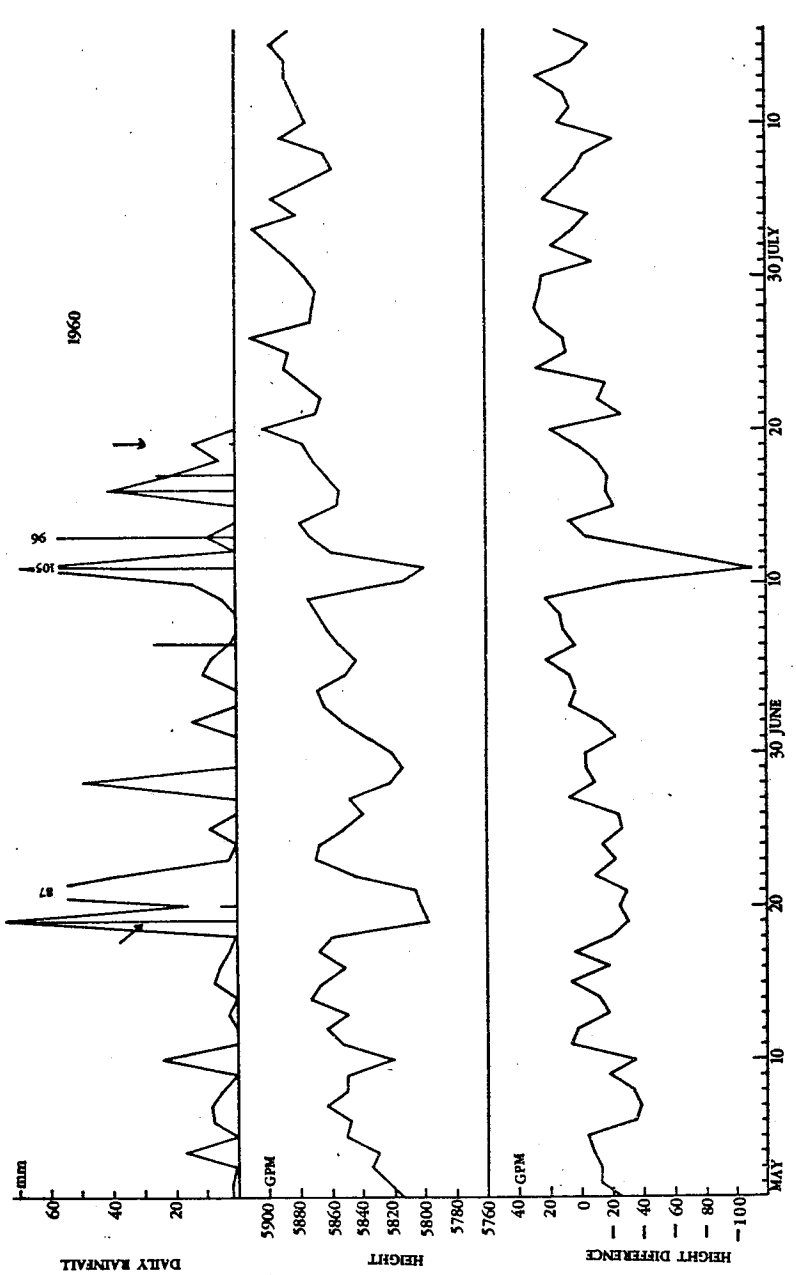

Figure 25. Daily rainfall variations at Keelung (curves) and Kaoshiung (straight lines), 500-mb height variations at Taoyuan, and 500-mb height differences between Taoyuan and Tongkang during the plum rain period of 1960.

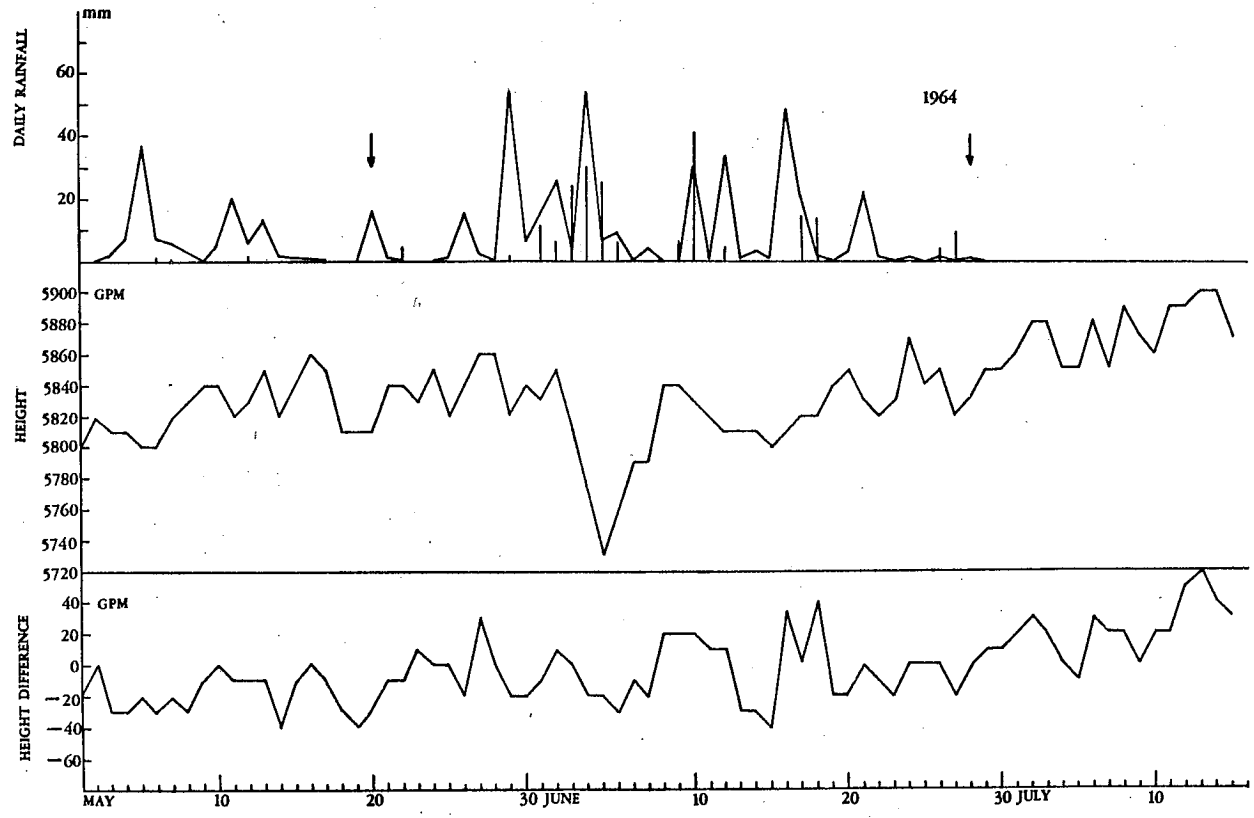

Figure 26. Daily rainfall variations at Keelung and Kaoshiung, 500-mb height variations at Taoyuan, and 500-mb height differences between Taoyuan and Tongkang during the plum rain period of 1964.

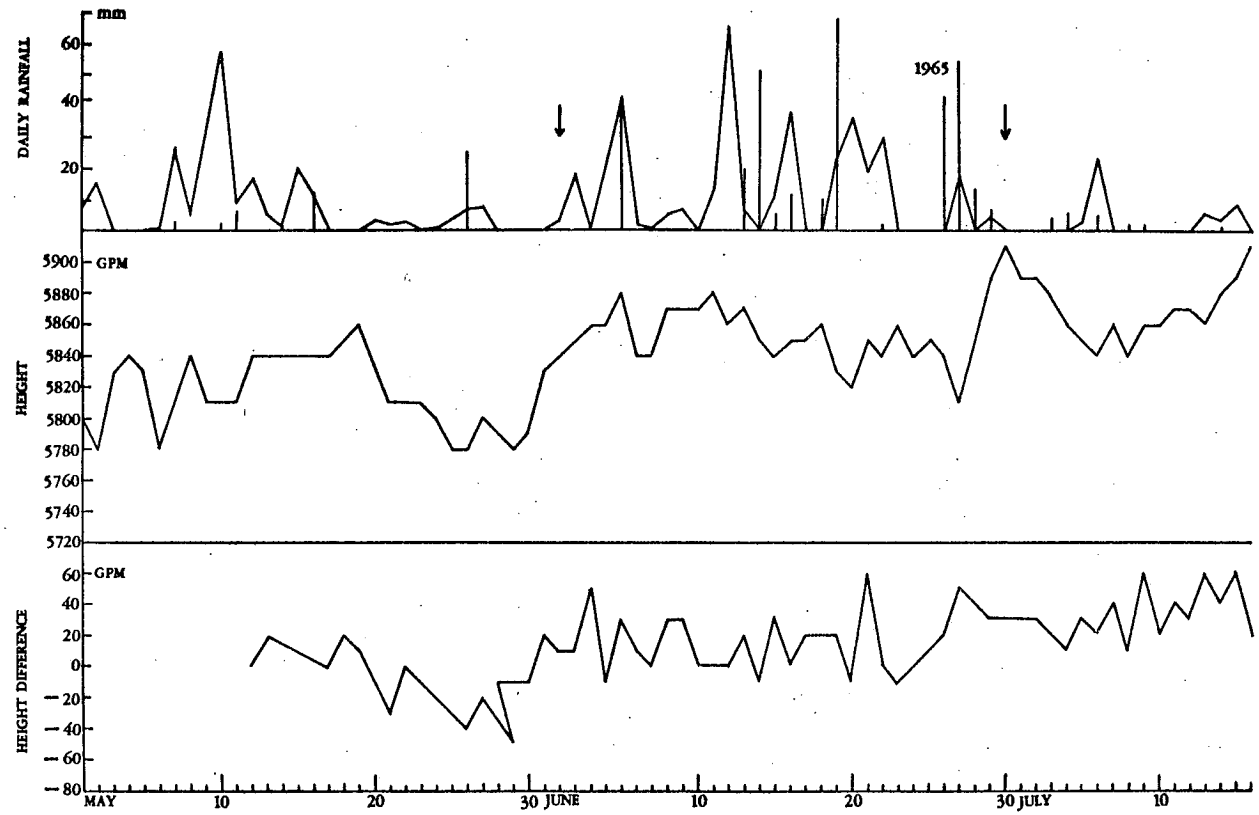

Figure 27. Daily rainfall variations at Keelung and Kaoshiung, 500-mb height variations at Taoyuan, and 500-mb heights differences between Taoyuan and Tongkang during the plum rain period of 1965.

north of Taiwan.

It appears that there is a significant relationship between the daily rainfall and the 500-mb geopotential height over Taiwan. The increase in daily rainfall is frequently concurrent with the significant drop in the 500-mb geopotential height because of the passage of a trough over Taiwan.

Temperature at the 500-mb level over Taoyuan in 1964 and 1965 increased during and after the plum rains (Figure 28). However, in 1960 it decreased when the plum rains ceased (Figure 29).

Figure 30 shows the relationship between the mean daily rainfall and the latitudinal position of polar fronts at the various Taiwan stations. Strikingly, the mean daily rainfall reaches a peak at all stations when polar fronts are located at 23^{o}N along 120^{o}E. With the exception of Tainan, Kaoshiung, and Hengchun, in the southwest and south of the island, the mean daily rainfall is highest when polar fronts are one to two degrees of latitude south of stations. Bell (1969) has found the same characteristic in Hong Kong. At Tainan, Kaoshiung, and Hengchun, the mean daily rainfall is at a peak when polar fronts are located at 25^{o}N, probably due to the strengthening of the southwest monsoon and southeast trade

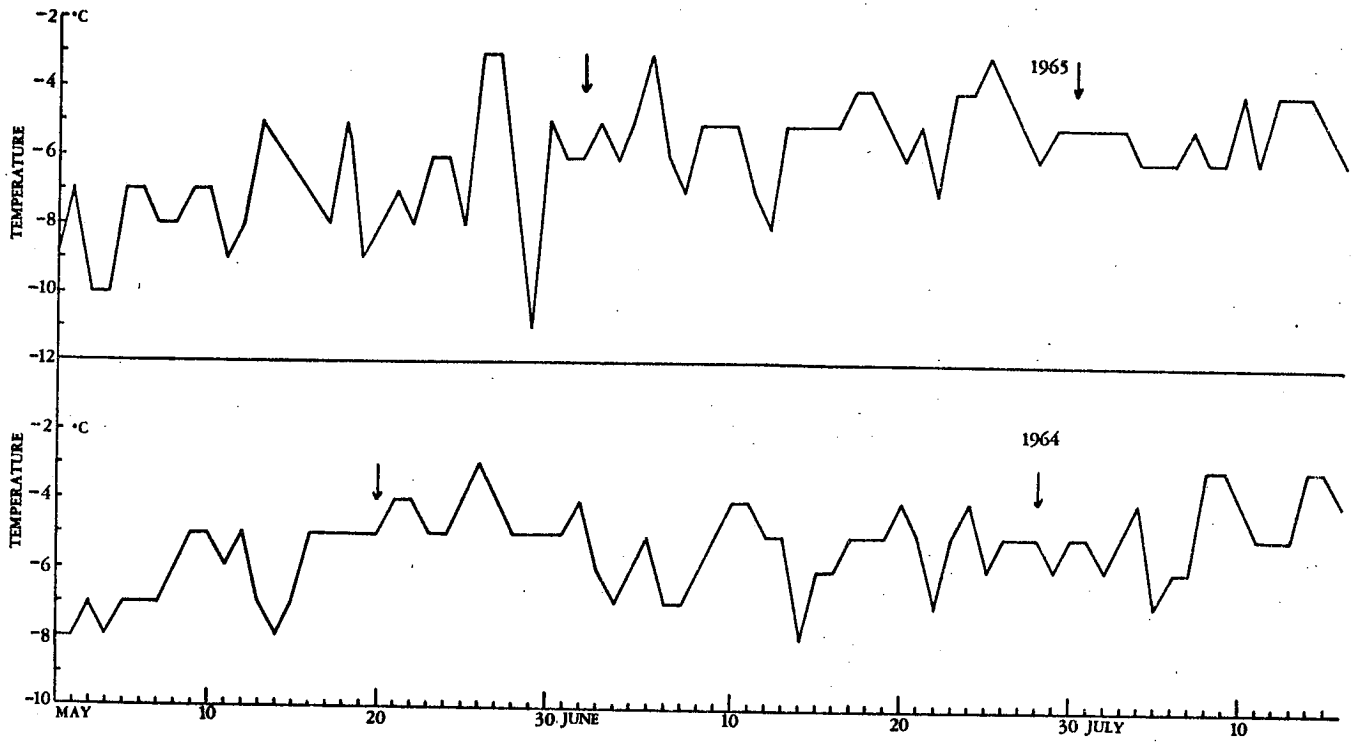

Figure 28. Daily 500-mb temperature variations at Taoyuan during the plum rain period of 1964 and 1965. Arrows denote the onset and end of the plum rains.

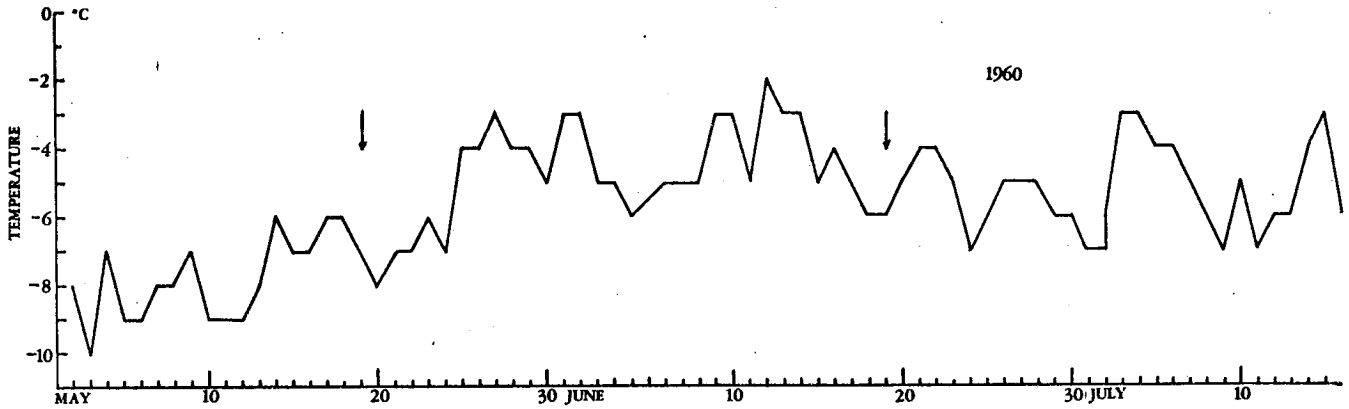

Figure 29. Daily 500-mb temperature variations at Taoyuan during the plum rain period of 1960.

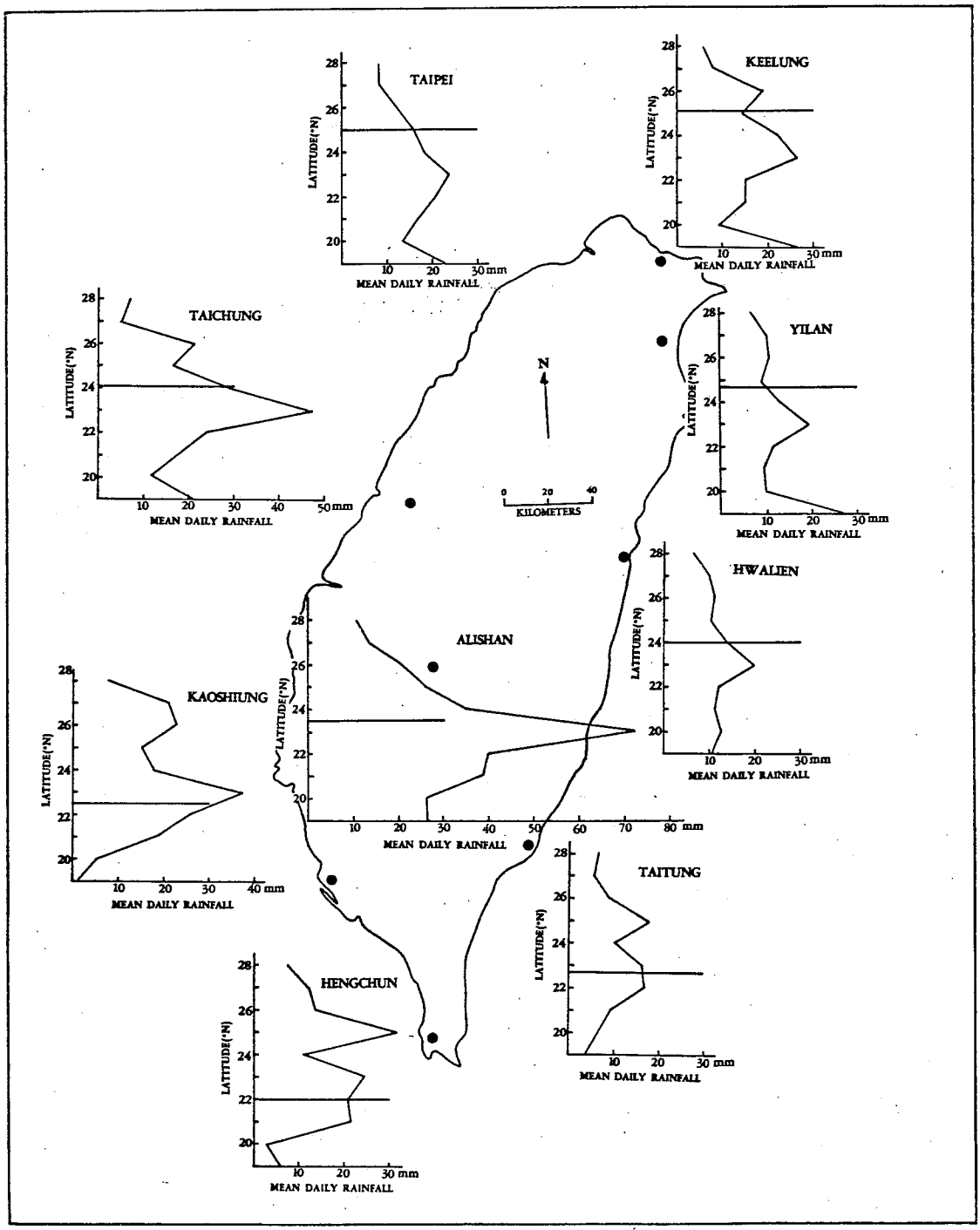

Figure 30. Mean daily rainfall associated with the latitudinal positions of polar fronts.

when a polar front is to the north of Taiwan.

In summary, in Taiwan the onset and cessation of the plum rains are related to a persistent polar front and changes in rainfall intensities, winds, 500-mb geopotential height, and temperature. The plum rains arrive in Taiwan in accordance with the following conditions:

1. A persistent polar front is over Taiwan. As a result, rainfall occurs over the entire island. At many stations, the daily rainfall exceeds 100 mm (3.94 inches).
2. The easterlies penetrate downward from the stratosphere to the upper and middle tropospheres. The subtropical jet stream weakens and is displaced northward as seen by a sudden decrease in upper-level wind speeds over Taiwan.
3. The 500-mb geopotential height over Taiwan increases. The 500-mb height difference between Taoyuan and Tongkang changes from negative to positive.
4. Temperature at the 500-mb level decreases.

On the other hand, the end of the plum rains over Taiwan is associated with the following conditions:

1. The polar front retreats northward to the north of Taiwan.
2. The westerlies are replaced by the easterlies in the troposphere over Taiwan. This is accompanied by an easterly jet stream with wind speeds of more than 50 knots in the stratosphere.
3. The 500-mb geopotential height increases significantly over Taiwan due to warm air advection below. In addition, the 500-mb level becomes consistently higher over Taoyuan than over Tongkang.

Summary of Significant Results

The significant results of the study of this chapter are evidenced by the following findings. As with the case of the Mongolian anticylone, the Taiwan low also occurs and contributes greatest amounts of rainfall to Taiwan in February, indicating that the climatic regime over Taiwan is significantly controlled by the strength of the westerlies. It is found that wind variations at ground surface, 850-mb, 700-mb, and 500-mb levels may provide an aid for the forecasting of the low.

The polar front is one of the major rainfall sources over Taiwan, as evidenced by its high contribution to mean annual, monthly, and daily rainfall and by its high chance

of producing heavy daily rainfall. Almost all stations show rainfall peaks in June when the polar front is most active over Taiwan. According to Chen's (1959) calculation, the soil moisture changes from deficit to surplus in May and June over western Taiwan. The plum rains are helpful in crop production. They supply sufficient water for the ripening of the first rice crop and provide moist soil for the planting of the second rice crop. The absence of the plum rains may result in severe drought. For example, the 1963 drought was mainly caused by a short plum rain period. In this year, the plum rains started later than usual and they lasted for only twelve days, much shorter than the normal duration of twenty-seven days. Almost all crops showed significant reduction of yields in this year (Republic of China, 1970).

Although the plum rains over the Yangtze River Basin have attracted climatologists' attention and many studies have been made to find their physical causes, no particular effort has been made to focus study on the plum rains over Taiwan. The current study finds that variations in wind speeds and directions in the troposphere are significantly related to the onset and cessation of the plum rains. In addition, variations in the 500-mb geopotential height and

temperature provide helpful guides for the forecasting of the plum rains. Daily rainfall appears to be correlated well with the variation in the 500-mb geopotential height during the plum rain period over Taiwan. Mean daily rainfall at various Taiwan stations in relation to the latitudinal position of the polar front, presented in this chapter, provides additional information for the forecasting of daily rainfall during the plum rain period.

CHAPTER V

RAINFALL ASSOCIATED WITH THE NORTH PACIFIC SUBTROPICAL ANTICYCLONE AND THE SOUTHWEST MONSOON

The North Pacific Subtropical Anticyclone

Unlike other synoptic flow types, the North Pacific subtropical anticyclone may invade Taiwan with a significant frequency in every month. As with the Mongolian cutoff anticyclone, the North Pacific subtropical anticyclone is usually accompanied by warm-air advection in the lower troposphere. Lower tropospheric inversion layers are frequently observed. At the surface and 850 mb, it is usually calm when the North Pacific subtropical anticyclone invades Taiwan (Figure 9). Wind directions associated with this anticyclone vary from east to southeast at the surface. In summer, the thermodynamic properties of the North Pacific subtropical anticyclone are similar to those of the southwest monsoon. The trade and the southwest monsoon prevail over Taiwan in June and July. At 850 mb, the mixing ratio and pseudo-equivalent potential temperature of these two synoptic flow types are equal (Saito, 1968).

The behavior of the North Pacific subtropical anticyclone has been found to be closely related to change in

seasons. In summer, the North Pacific subtropical anticyclone is not identifiable at 100 mb. In contrast, a well-developed thermal anticyclone is centered on the Tibetan Plateau and extends eastward with its eastern edge over the western North Pacific (Mason and Anderson, 1963). The intensification of this Tibetan anticyclone at about 80°E is in accordance with the onset of the southwest monsoon over South Asia and the plum rains over the Yangtze River Basin. Dao and Chu (1964) have found that the plum rains over the Yangtze River Basin end when the Tibetan anticyclone splits into two centers, of which one is near 110°E and the other near 50°E, and a deep trough replaces the original position of the Tibetan anticyclone. The North Pacific subtropical ridge at 500 mb advances northward from 20°N to 30°N in association with this adjustment of the circulation at 100 mb. On the other hand, when the split anticyclone returns to its original position, the North Pacific subtropical ridge at 500 mb retreats southward to 20°N and the Yangtze River Basin may enjoy a rainy period again.

In general, the North Pacific subtropical anticyclone favors Taiwan with clear days except for the southeast sector where the easterly trade associated with this anticyclone frequently causes a fairly large amount of rainfall

due to topographic uplifting.

In contrast to winter synoptic flow types, the North Pacific subtropical anticyclone contributes greater mean annual rainfall to the south than to the north of the island. At Taitung, about 8% of mean annual rainfall is derived from the North Pacific subtropical anticyclone, whereas at Keelung it is only 0.6% (Figure 10 and Table 22b in Appendix B).

Although the North Pacific subtropical anticyclone may invade Taiwan in every month, it contributes only small amounts of mean monthly rainfall to the east and almost nothing to the west (Tables 38a and 38b in Appendix B). At Taitung and Hwalien, the contribution reaches a peak in April. At other stations, it is rarely greater than 25.4 mm (1 inch).

Aside from the northeastern part of the island, the mean and the standard deviation of daily rainfall contributed by the North Pacific subtropical anticyclone are slightly greater than for the contributions of the Mongolian and Mongolian cutoff anticyclones. However, the daily maximum rainfall associated with the North Pacific subtropical anticyclone is smaller than that associated with either the Mongolian or Mongolian cutoff anticyclone (Figures 11 and 12 and Table 39 in Appendix B).

The North Pacific subtropical anticyclone is a dry synoptic flow type. The probability of rainy days associated with this anticyclone is only about 10% in the north and the southwest of the island. At Taitung and Alishan, it is higher, about 35% and 42%, respectively, due to topographic effect. With the exception of Keelung, the North Pacific subtropical anticyclone has never contributed daily rainfall greater than 76.2 mm (3 inches) at other stations (Figure 13 and Table 40 in Appendix B).

The Southwest Monsoon

There are controversial theories regarding sources of the southwest monsoon over Asia. The traditional concept regards the southwest monsoon as originating in the southeast trade in the Southern Hemisphere which is deflected by the coriolis force when traveling across the equator. It is also believed that the monsoon is a large-scale land or sea breeze caused by the differential heating between continent and ocean. Those concepts have recently been challenged by some meteorologists. Flohn (1960a) noted the existence of the westerlies in the equatorial area of the Southern Hemisphere. The coriolis force is too small near the equator to deflect wind directions from southeast to

southwest. In addition, pronounced monsoonal wind shifts are absent over the eastern coast of North America, but are frequently observed over the western equatorial Pacific. In summer, the water vapor transport over East Asia is directed from continent to ocean (Saito, 1966). Flohn (1960b) hence attributed monsoons primarily to thermally controlled seasonal migration of the planetary pressure and wind belts in the continental section of the globe.

Palmen (1951) has regarded the equatorial westerlies as a statistical result of cyclonic vortices moving westward near the equator. Fletcher (1945) has observed that the westerlies exist between the two intertropical convergence zones which migrate northward and southward seasonally.

Koteswaram (1960) has regarded the summer monsoon over Asia as a low-level return current of the upper-level easterlies in a meridional circulation system caused by the elevated heating effect of the Tibetan Plateau. However, Subbaramayya and Ramanadhem (1966) have insisted that the southwest monsoon air comes from the Southern Hemisphere. This air, after ascending to the upper troposphere in the northern tropics, forms the easterlies and swings back across the equator, finally subsiding in the southern subtropical ridge. The amount of air subsiding north of the

equator--as proposed by Koteswaram (1960)--would be very small compared to the total monsoon air.

It has been recognized that over Asia the onset of the southwest monsoon is accompanied by abrupt changes in the general circulation. The onset of the southwest monsoon over Taiwan is usually associated with a heavy rainy period, caused by persistent polar fronts, in May and June, as discussed in the previous chapter. In summer, the southwest monsoon frequently invades Taiwan. But the monsoon layer is shallow and is overlain by an easterly layer extending all the way up to the stratosphere.

Although the southwest monsoon is moist and unstable, it causes significant amounts of rainfall only in the southwestern sector of the island, because of its windward position. However, the mean annual rainfall contributed by the southwest monsoon is only 10% in this region. The mean annual rainfall contributed by the southwest monsoon is very small in the north and east of the island (Figure 10 and Tables 22a and 22b in Appendix B).

The mean monthly rainfall contributed by the southwest monsoon reaches maxima in July and August at most stations (Tables 41a and 41b in Appendix B). Although the southwest monsoon is moist, it causes rainfall only when the mechanisms

of condensation exist, i.e., solar heating and topographic uplifting. Except for Taipei and Alishan, the mean monthly rainfall associated with the southwest monsoon is less than 50 mm at other stations.

The mean and the standard deviation of daily rainfall associated with the southwest monsoon are highest at Alishan and Taipei, probably because of stronger thunderstorm activity. The maximum daily rainfall exceeds 100 mm (3.94 inches) at most stations in the western part of the island (Figures 11 and 12 and Table 42 in Appendix B).

The probability of rainy days associated with the southwest monsoon varies from slightly less than 30% in the north to about 40% in the south of the island. In contrast to the trades associated with the North Pacific subtropical anticyclone, the southwest monsoon has a lowest probability of rainy days in the eastern sector of the island, slightly less than 20% (Figure 13 and Table 43 in Appendix B).

Summary of Significant Results

In summary, both the North Pacific subtropical anticyclone and the southwest monsoon are poor rain-contributors over Taiwan. The persistence of these two synoptic flow types may cause severe drought. For example, the 1963 drought was associated with peak frequencies of these two

synoptic flow types (Figure 4). In summer, thermal convection is an important rainfall mechanism. Table 4 shows mean annual frequencies of thunderstorms associated with different synoptic flow types over Taiwan. It appears that thunderstorms accompany polar fronts most frequently at all stations. It is also found that over the southwestern Taiwan thunderstorms are more frequently associated with typhoons or monsoon troughs than with either the North Pacific subtropical anticyclone or the southwest monsoon despite the fact that the latter two flow types dominate Taiwan in summer. The traditional concept attributes the heavy summer rainfall over Taiwan to the southwest monsoon and the southeast trade. The current study indicates that this is not true, as evidenced by their low mean daily rainfall and low rainfall probabilities. In northern Taiwan, thunderstorms are more frequently associated with the southwest monsoon than with either typhoons or monsoon troughs (Table 4). This probably accounts for high mean daily rainfall and standard deviation associated with the southwest monsoon at Taipei.

TABLE 4

MEAN ANNUAL THUNDERSTORM FREQUENCIES ASSOCIATED WITH DIFFERENT SYNOPTIC FLOW TYPES OVER TAIWAN (UNIT: %)

Flow types	1	2	3	4	5	6	7	8	9	10	11
Keelung	3.4	0.7	0.7	38.4	0.6	8.2	28.8	3.4	6.9	4.1	4.8
Taipei	2.4	5.4	2.0	26.9	0.9	11.2	27.8	6.8	3.4	3.9	9.3
Taichung	2.1	2.4	1.2	28.9	1.2	19.1	17.3	8.2	4.0	2.1	13.4
Tainan	2.1	1.8	0.6	23.7	1.2	25.2	15.2	8.8	7.3	4.3	9.4
Kaoshiung	5.9	3.9	3.3	25.7	0.7	17.1	10.5	8.6	6.5	4.6	13.2
Hengchun	1.9	1.9	0.6	27.3	1.9	13.0	9.9	14.3	8.7	4.3	16.1
Taitung	4.8	3.4	1.4	32.2	1.4	7.5	10.3	9.6	12.3	2.7	13.7
Hwalien	5.3	7.3	2.0	30.5	0.0	12.6	17.2	11.9	4.0	2.0	7.3
Yilan	3.2	6.3	1.1	29.6	0.0	10.1	25.9	9.0	6.3	3.7	4.8
Alishan	4.5	5.8	0.6	26.9	1.5	29.1	17.4	4.8	1.8	1.8	5.8

CHAPTER VI

RAINFALL ASSOCIATED WITH TYPHOONS

Mean Annual and Monthly Frequencies

The frequency of typhoon days in Taiwan and its relationship to the westerlies, sea-surface temperatures in the Pacific, and solar activity have been discussed in Chapter II. In this chapter, attention is paid to the monthly number of typhoons which affect Taiwan and its relation to mean monthly 700-mb circulations.

Figure 31 shows the annual number of typhoons that occurred in the western North Pacific and those which visited Taiwan for the period 1897-1969. The number of typhoons includes all tropical cyclones with wind speeds exceeding 34 knots. It appears that there has been a substantial increase in the annual number of typhoons in the western North Pacific since 1940. This is probably due to the sparse aircraft reconnaissances and ship observations prior to World War II and many typhoons may have developed without being detected. It also appears that there has been a reverse relationship between the annual number of typhoons which have occurred in the western North Pacific and those which have visited Taiwan during the past thirty years. Two

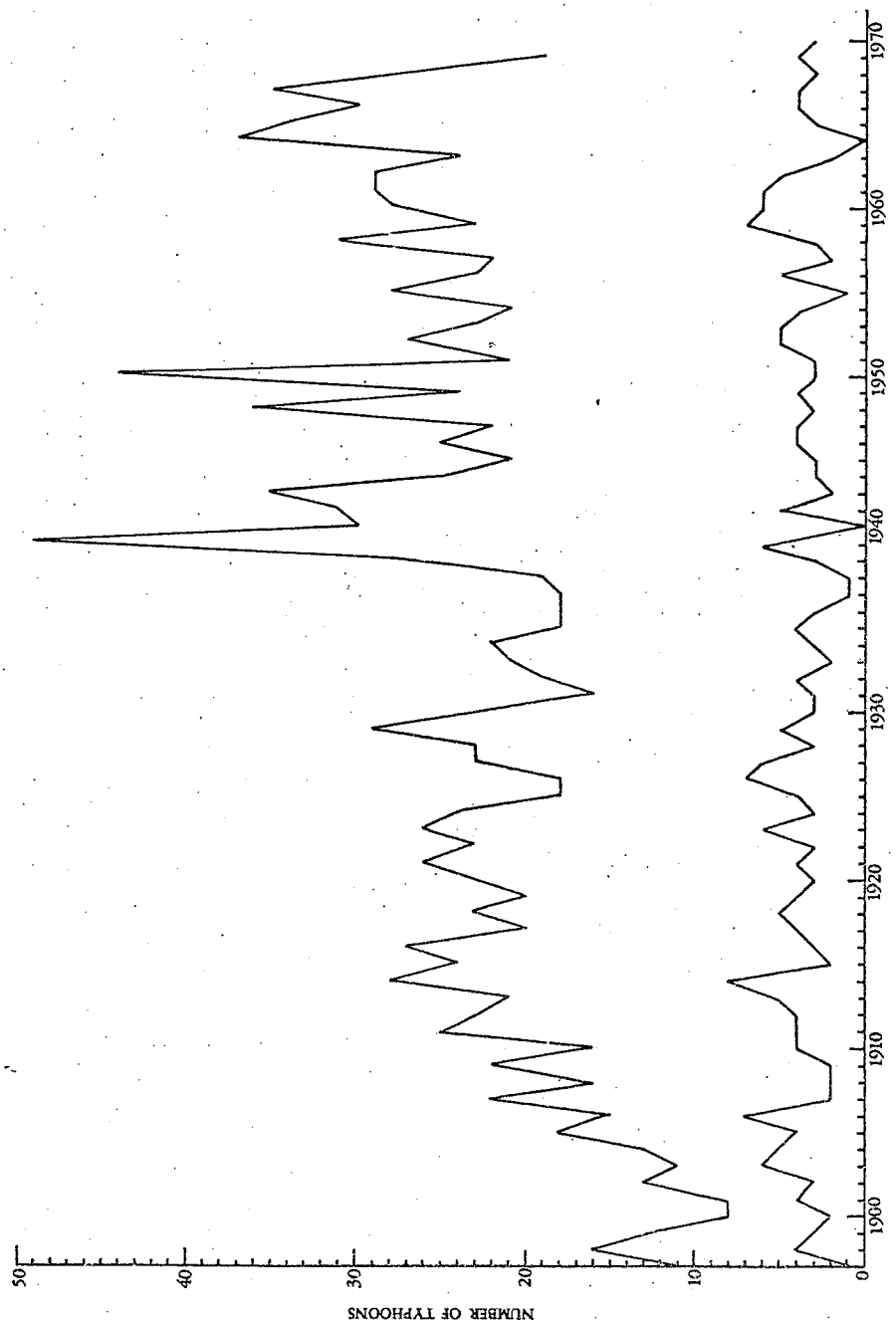

Figure 31. Variations in the annual frequency of typhoons in the western North Pacific and those visiting Taiwan, 1897-1969.

hundred and seventy typhoons visited Taiwan during the 73-year period 1897 to 1969 (Table 5). Three to four typhoons visited Taiwan per year on about 53% of years. As many as eight typhoons may visit Taiwan per year.

Table 6 illustrates the mean monthly number and percentage of typhoons which occurred in the western North Pacific for the period 1940-1969. The mean annual number of typhoons in the western North Pacific reaches about twenty-nine, the highest value among various oceanic regions of the world. The western North Pacific is characterized by a large warm ocean surface along with a more northerly mean position of the subtropical ridge. Therefore, the tropical easterly layer is, on the average, deeper, and the vertical wind shear is weaker than over other oceans; conditions favorable for typhoon development (Yeh, 1950; Ramage, 1959; Gray, 1968). As a result of this situation, typhoons have been observed in every month in the western North Pacific, with highest frequencies in August. In the western North Pacific, typhoons which form from July through December account for more than half of the annual total. Likewise, typhoons visit Taiwan most frequently in August (Table 7). According to the Taiwan Weather Bureau, a typhoon is said to be visiting when it invades the island or comes within 200

TABLE 5

FREQUENCY DISTRIBUTION OF TYPHOONS VISITING TAIWAN (1897-1969)

Number of Typhoons Per Year	Number of Years	Total Number of Typhoons
0	2	0
1	4	4
2	9	18
3	20	60
4	19	76
5	9	45
6	6	36
7	3	21
8	1	8

TABLE 6

TOTAL AND MEAN MONTHLY FREQUENCY OF TYPHOONS IN THE WESTERN NORTH PACIFIC FOR THE PERIOD 1940 TO 1969

Months	1	2	3	4	5	6	7	8	9	10	11	12	Total
Total	15.0	11.0	11.0	27.0	29.0	55.0	132.0	194.0	149.0	118.0	69.0	44.0	854.0
Mean	0.5	0.4	0.4	1.0	1.8	4.4	6.5	5.0	3.9	2.3	1.5	1.5	28.5
Percent	1,8	1.3	1.3	3.2	3.4	6.4	15.5	22.7	17.4	13.8	8.1	5.2	100.0

TABLE 7

TOTAL AND MEAN MONTHLY FREQUENCY OF TYPHOONS WHICH VISITED TAIWAN FOR THE PERIOD 1897 TO 1969

Months	1	2	3	4	5	6	7	8	9	10	11	12	Total
Total				2.0	11.0	17.0	65.0	83.0	62.0	21.0	8.0		269.0
Mean				0.03	0.15	0.2	0.9	1.1	0.9	0.3	0.1		3.7
Percent				0.7	4.1	6.3	24.2	30.9	23.0	7.8	3.0		100.0

km of the Taiwan coasts. The number of typhoons which visit Taiwan from July through September accounts for almost 80% of the annual total. Typhoons have not visited Taiwan in winter, December through March, during the past 73 years.

Mean Monthly 700-mb Circulation Associated with Typhoon Frequency

Typhoon tracks have been of great concern to Taiwanese meteorologists because Taiwan is subject to typhoon attack on an average of four times a year. From July through September, typhoons visit Taiwan, on the average, of once a month.

Synoptic studies of individual typhoons have been presented in various publications. Tracks of all observed typhoons plotted on a map usually show no recognizable pattern. The classification of typhoon tracks based on synoptic circulation patterns often leads to an extremely large number of categories, yet the behavior of individual typhoons may deviate greatly from the generalized condition. However, Namias (1955a and b) and Ballenzweig (1959) have remarked that tropical storms tend to follow preferred courses during a given month of a given year and that patterns of height anomalies at the 700-mb level are useful for storm-track studies. The frequency and track of tropical storms in the

western Atlantic have been found to be strongly influenced by the position and intensity of great centers of action. An attempt is made here to test both Namias (1955a and b) and Ballenzweig's (1959) theory relating monthly frequency of typhoons to changes in the general circulation over the western North Pacific. Since August is the month with the highest frequency of typhoons and sometimes three typhoons may visit Taiwan, attention is paid to the typhoon activity in this month.

Three typhoons visited Taiwan in August of 1959 and 1960, respectively, but the mean monthly circulation patterns of these two months were quite different. In general, August 1959 was characterized by blocking situations in high latitudes in the Northern Hemisphere. In the western North Pacific, a distinct blocking high was centered over the Sea of Okhotsk at the 700-mb level (Figure 32). The mid-Pacific trough was located at its normal position between 150°E and 180°E and slightly intensified, as seen by a deeper than normal negative anomaly to the east of Hokkaido, Japan. The Siberian trough also intensified and extended from east of Lake Baikal southeastward to the east China seaboard. The western portion of the North Pacific subtropical ridge was located at its normal position, but slightly weakened. In

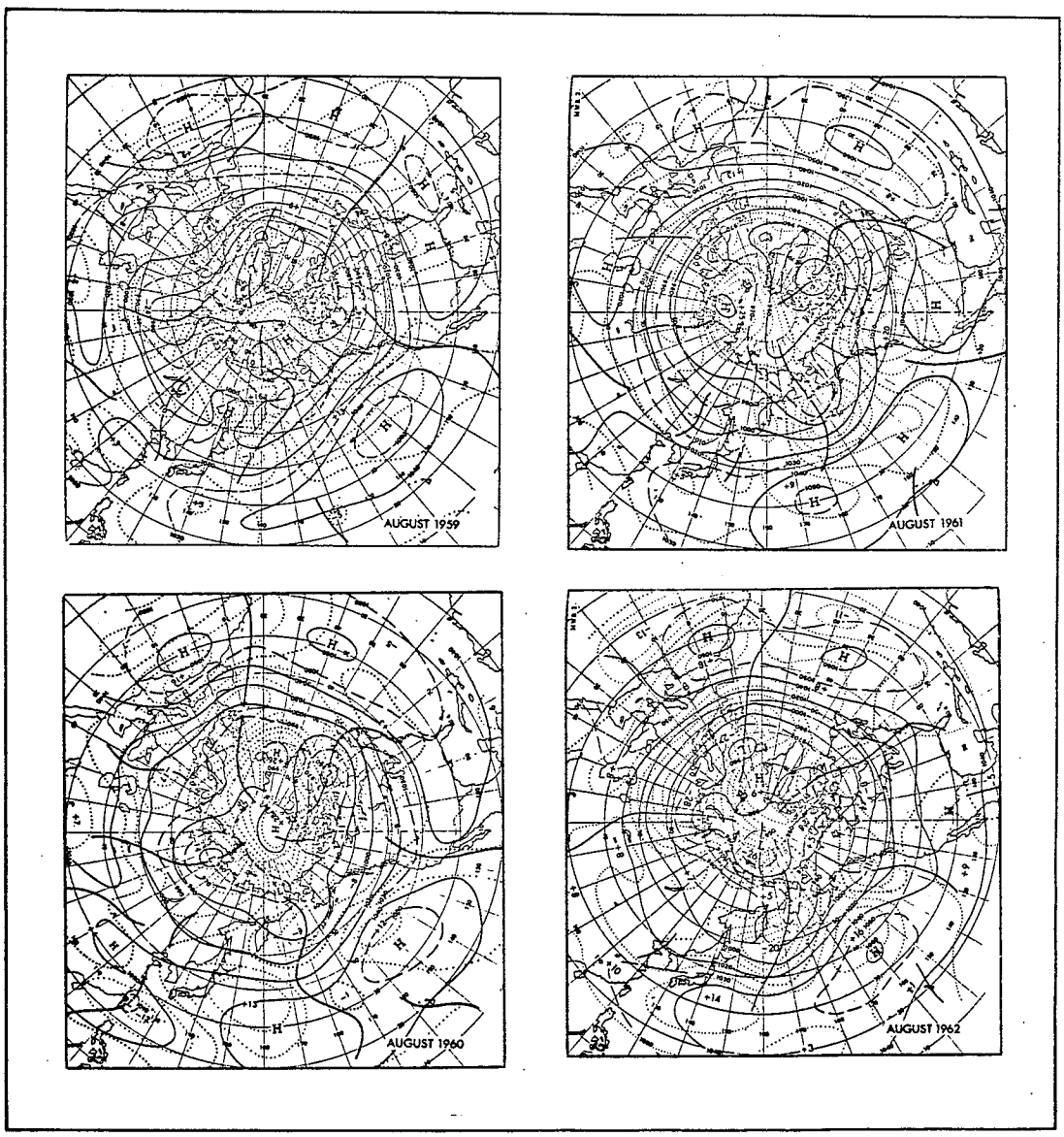

Figure 32. Mean 700-mb contours and height anomalies of the Northern Hemisphere for August of 1959, 1960, 1961, and 1962 (after Monthly Weather Review, 1959, 1960, 1961, and 1962).

addition, the monsoon trough in the South China Sea slightly intensified and was displaced northward and eastward. The slight intensification of the mid-Pacific trough and monsoon trough was probably responsible for six typhoons, near normal frequency, in the western North Pacific in that month. Orgill (1960, 1961) has pointed out that the intensification of the mid-Pacific trough, frequently associated with blocking highs in high latitudes, tends to enhance the release of the perturbation energy in the tropics and hence triggers tropical cyclones. The monsoon trough also plays an important role in typhoon development.

There have been controversies regarding the origin of tropical storms, especially since satellite pictures have been used for weather analysis in the tropics. It is generally believed that most tropical storms in the Atlantic originate in easterly waves (Fett, 1966; Simpson, et al., 1968, 1969), whereas those in the Pacific originate in the intertropical convergence zone or monsoon trough (Sadler, 1964; Gray, 1970). Shieh, et al. (1963) have found that most typhoons in the western North Pacific develop from vortices in the eastern end of a shearline separating the equatorial westerlies and tropical trades. The expansion of the equatorial westerlies associated with the extension

of the shearline north and east is accompanied by more typhoons over the western North Pacific.

The high frequency of typhoons visiting Taiwan in August 1959 was associated with the development of the Siberian trough, the Okhotsk high, and monsoon trough. It has been recognized that tropical storms tend to recurve northward into an approaching polar trough from the west (Riehl and Shafer, 1944; Fett, 1968). Based on the synoptic study of typhoon tracks in the western North Pacific in 1962 and 1963, L. S. Chen (1965) has found that the development of the Okhotsk high and Siberian trough are evidence of strong meridional flow in the subtropical latitudes of East Asia and typhoons tend to recurve northward to threaten the east China seaboard.

In contrast to 1959, the circulation in August 1960 was stronger, about 2 to 5 m.p.s. above normal in the North Pacific (Stark, 1960). This was reflected by the increase in spacings between the mid-Pacific and Siberian troughs. The mid-Pacific trough was slightly displaced east of its normal position and its intensity was higher than normal, as seen by a negative anomalous area centered over the Bering Sea (Figure 32). The Siberian trough extended southward along the east China seaboard into a well-developed

monsoon trough which penetrated eastward to about 140°E along 25°N. This was accompanied by a pronounced northward displacement of the western North Pacific subtropical ridge. The positive anomaly east of Japan was well above normal and the negative anomaly near Taiwan was unusually deep. This prominent high zonal index circulation in the western North Pacific resulted in remarkable typhoon activity during this month. A total of eight typhoons developed in the western North Pacific and three of them visited Taiwan. The intrusion of the Siberian polar trough into the monsoon trough near Taiwan was probably responsible for the three typhoons visiting Taiwan.

August 1961 was an inactive typhoon month in the western North Pacific. A total of only three typhoons was observed, two of which visited Taiwan. The mean 700-mb circulation for this month showed a markedly meridional character in the North Pacific (Figure 32). The circumpolar vortex was displaced southward with the development of the mid-Pacific trough east of its normal position. A well-developed ridge was over the Sea of the Okhotsk with a polar trough to the south. The planetary wavelengths of the middle latitude westerlies shortened. The westerlies in the western North Pacific and East Asia weakened and

their positions shifted southward, primarily as a result of the blocking situation in higher latitudes. Meanwhile, the North Pacific subtropical ridge was displaced southward and weakened. In addition, the positive anomaly south of Japan was weaker than normal. There was no evidence of the penetration of the monsoon trough from the South China Sea into the western North Pacific. This low-zonal index circulation probably accounted for the diminished typhoon activity in the western North Pacific. Namias (1969c) has stated that seasons rich in hurricane in the North Atlantic are generally associated with the northward displacement of the Atlantic centers of action, while more southward displacement is associated with a decrease in hurricanes. Simpson, et al. (1969) have attributed the inactive hurricane year of 1968 in the North Atlantic to the southward displacement of the westerlies, accompanied by the increase in vertical wind shear over the tropical Atlantic.

Although typhoon activity was weak in the western North Pacific in August 1960, the intensification of the Okhotsk high and Siberian trough was associated with two typhoons visiting Taiwan.

In August 1962, the westerlies in the western North Pacific were strong (Figure 32). The wavelengths along

50°N to 60°N increased. The mid-Pacific trough was located at its normal position and its intensity was much stronger than normal. Meanwhile, the North Pacific subtropical ridge was also well-developed, as seen by an intense positive anomaly to the southeast of Japan. As expected, this high zonal-index circulation favored typhoon development. There were eight typhoons in the western North Pacific in this month. On the other hand, the penetration of the Siberian trough southward into the east China seaboard was responsible for two typhoons visiting Taiwan.

In contrast to August of 1959 through 1962, when two or three typhoons visited Taiwan in a single month, not a single typhoon visited Taiwan in August of 1963, 1964, or 1968. An effort is hence made to study the mean monthly 700-mb circulations for those three months.

August 1963 was a unique month for typhoon activity in the western North Pacific. Only three typhoons were observed, and none of them visited Taiwan. The mean 700-mb circulation in August 1963 showed that the western North Pacific subtropical ridge was displaced southward by five degrees of latitude from its normal position. This was reflected by positive anomalies covering from 100°E to 150°E along 25°N (Figures 33 and 34). The mid-Pacific trough

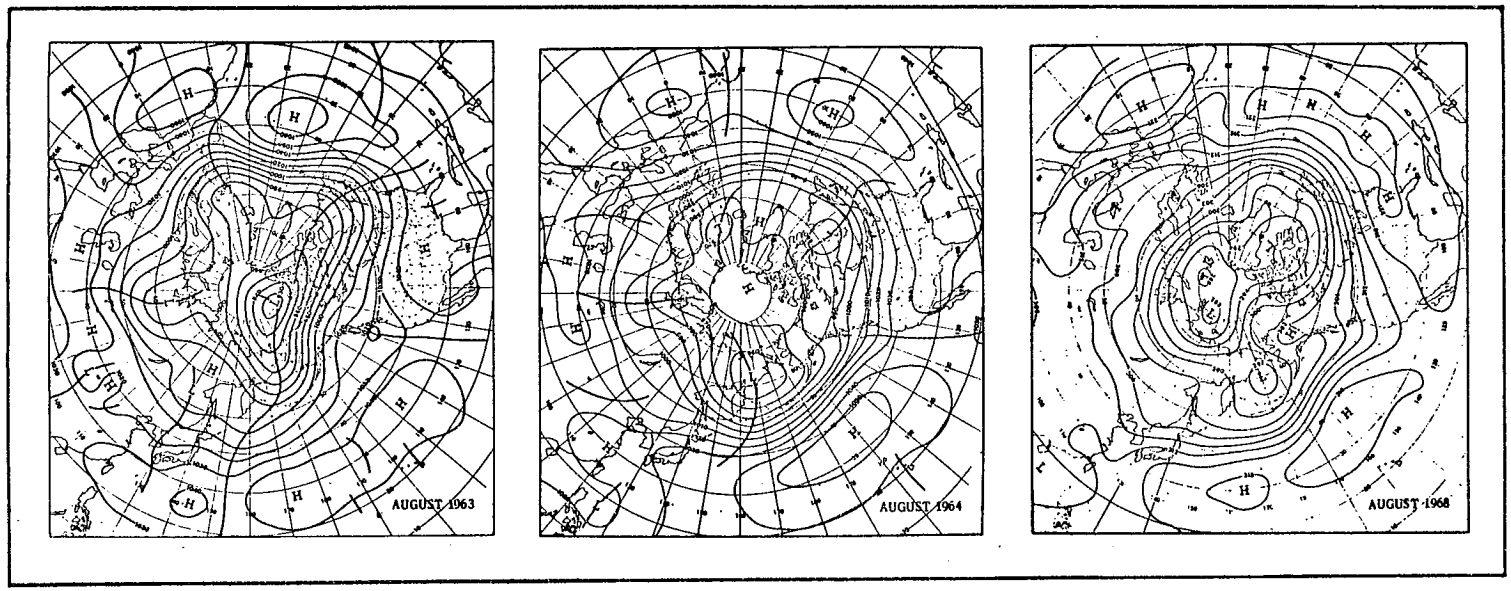

Figure 33. Mean 700-mb contours of the Northern Hemisphere for August of 1963, 1964, and 1968 (after Monthly Weather Review, 1963, 1964, and 1968).

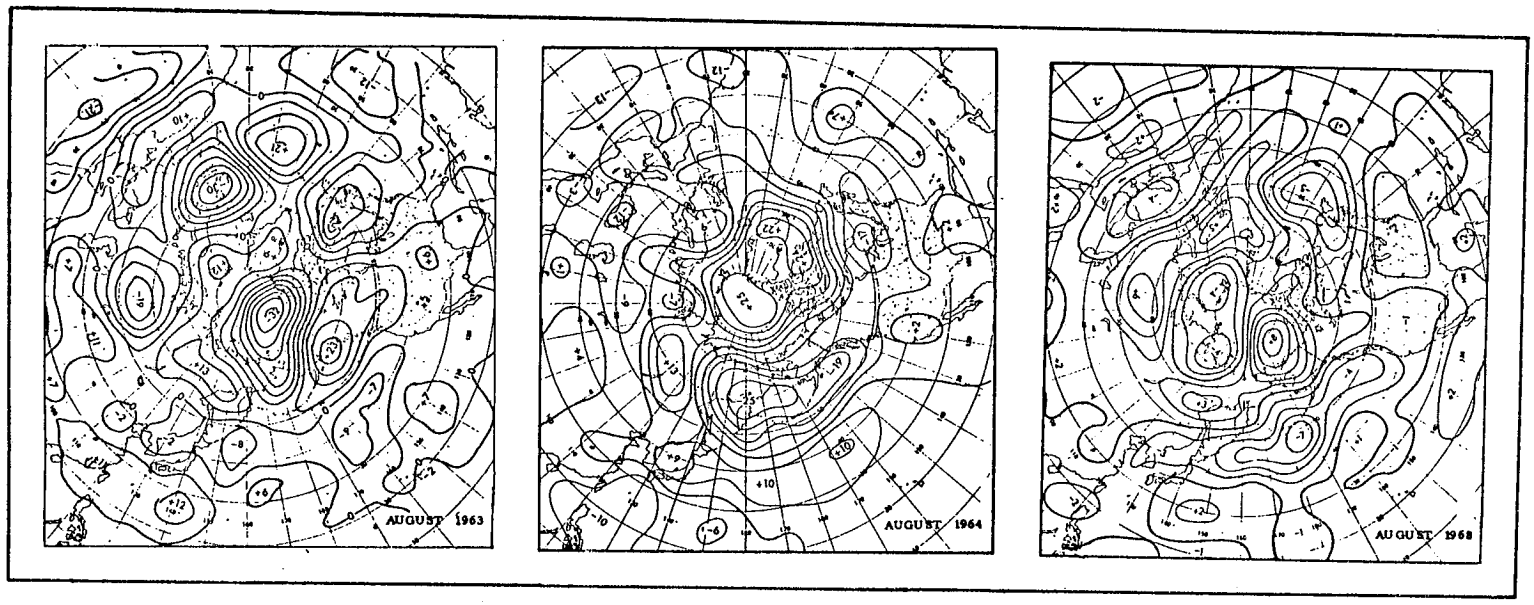

Figure 34. Mean 700-mb height anomalies of the Northern Hemisphere for August of 1963, 1964, and 1968 (after Monthly Weather Review, 1963, 1964, and 1968).

slightly intensified. The wavelengths of the middle latitude westerlies in the western North Pacific shortened as a result of the eastward displacement of the Siberian trough to 130°E. The westerlies in the North Pacific weakened and were displaced south of their normal position. This low zonal-index circulation prevented typhoon development in the western North Pacific. An intense positive anomaly over Taiwan apparently prevented typhoons from visiting the island.

In August 1964, there were six typhoons in the western North Pacific but none of them visited Taiwan. The mean 700-mb circulation showed that both the mid-Pacific trough and the North Pacific subtropical ridge slightly intensified. In addition, the monsoon trough penetrated eastward to about 130°E along 20°N and a tropical vortex developed east of the Philippines. The slight strengthening of the westerlies and northward displacement of the North Pacific subtropical ridge, together with the penetration of the monsoon trough from the South China Sea to the western North Pacific, were associated with normal typhoon frequency in this month. On the other hand, the monsoon trough was limited south of 20°N and the Siberian polar trough was displaced westward about 20 degrees of longitude from the east China seaboard. This

circulation pattern probably prevented typhoons from attacking Taiwan (Figures 33 and 34).

August 1968 was another month without a typhoon visiting Taiwan, although eight typhoons were observed in the western North Pacific. The mean 700-mb circulation for this month was marked by the stronger than normal westerlies (Figures 33 and 34). The mid-Pacific trough was slightly displaced east of its normal position. The subtropical ridge weakened slightly. However, the monsoon trough penetrated eastward approximately to 125°E along 20°N. This probably accounted for the active typhoon month in the western North Pacific. On the other hand, the Siberian trough progressed toward the east and penetrated southward to the east of Taiwan. As a result, typhoons recurved northward before reaching Taiwan.

From the foregoing discussion, it is obvious that, in August, typhoon activity in the western North Pacific is related to the mean 700-mb circulation. Normally, high zonal-index circulations are associated with high typhoon frequencies in the western North Pacific. During active typhoon months, the circulation is characterized by the strengthening and northward displacement of the westerlies, mid-Pacific trough, North Pacific subtropical ridge, and

monsoon trough.

Active typhoon months in the western North Pacific are not always concurrent with a high frequency of typhoons visiting Taiwan. Mean 700-mb circulations associated with frequent typhoon months in Taiwan are listed below (Figure 35):

1. The Okhotsk blocking high is well-developed. An intensive negative anomaly is centered on the Sea of Okhotsk.
2. The Siberian trough is also well-developed. A large area of negative anomalies covers Siberia and extends southward into tropical latitudes approximately along 120°E or the east China seaboard.
3. The monsoon trough intensifies and advances northward to the vicinity of Taiwan.

On the other hand, inactive typhoon months in Taiwan are characterized by conditions the opposite of frequent-typhoon months (Figure 36):

1. The Okhotsk blocking high is absent.
2. The Siberian polar trough weakens and is displaced to the east of Taiwan. Pronounced positive anomalies cover Siberia and the east China seaboard.

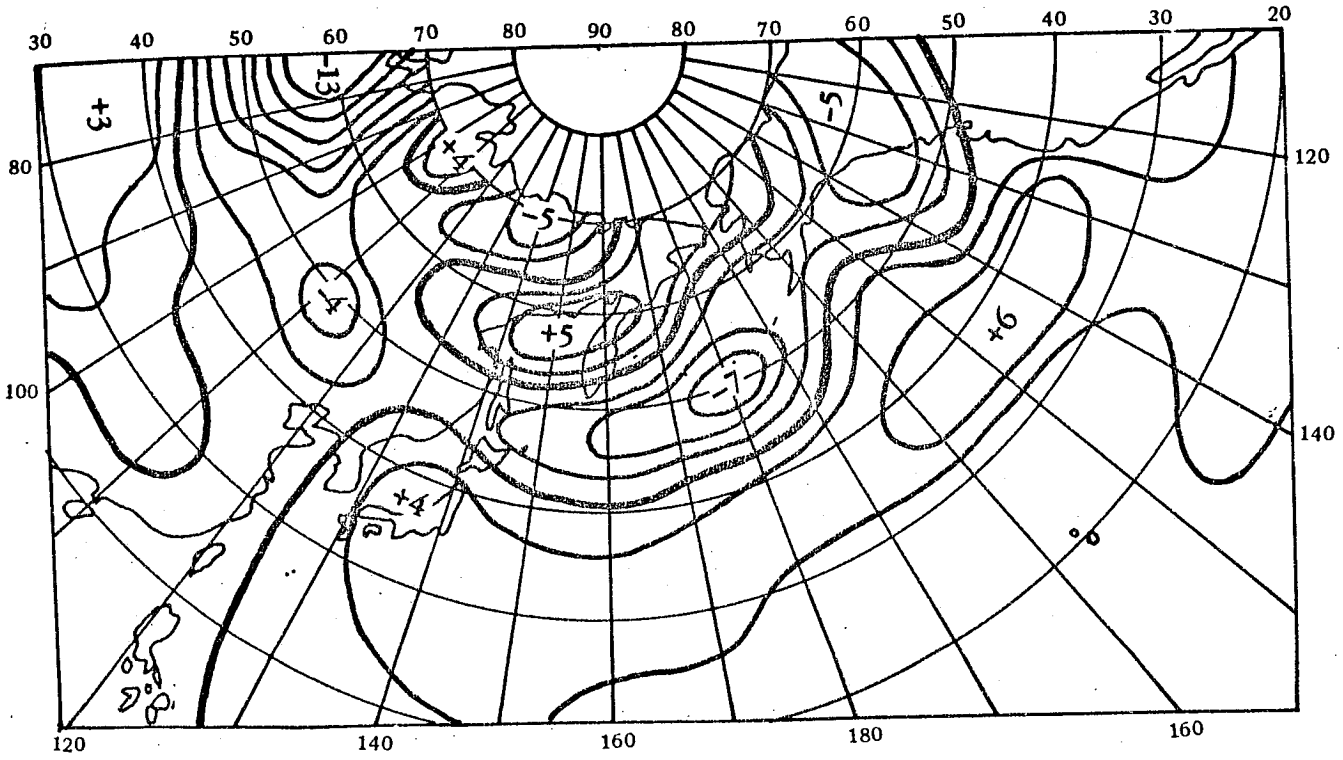

Figure 35. Mean 700-mb height anomalies of the North Pacific and East Asia associated with active typhoon months of August in Taiwan.

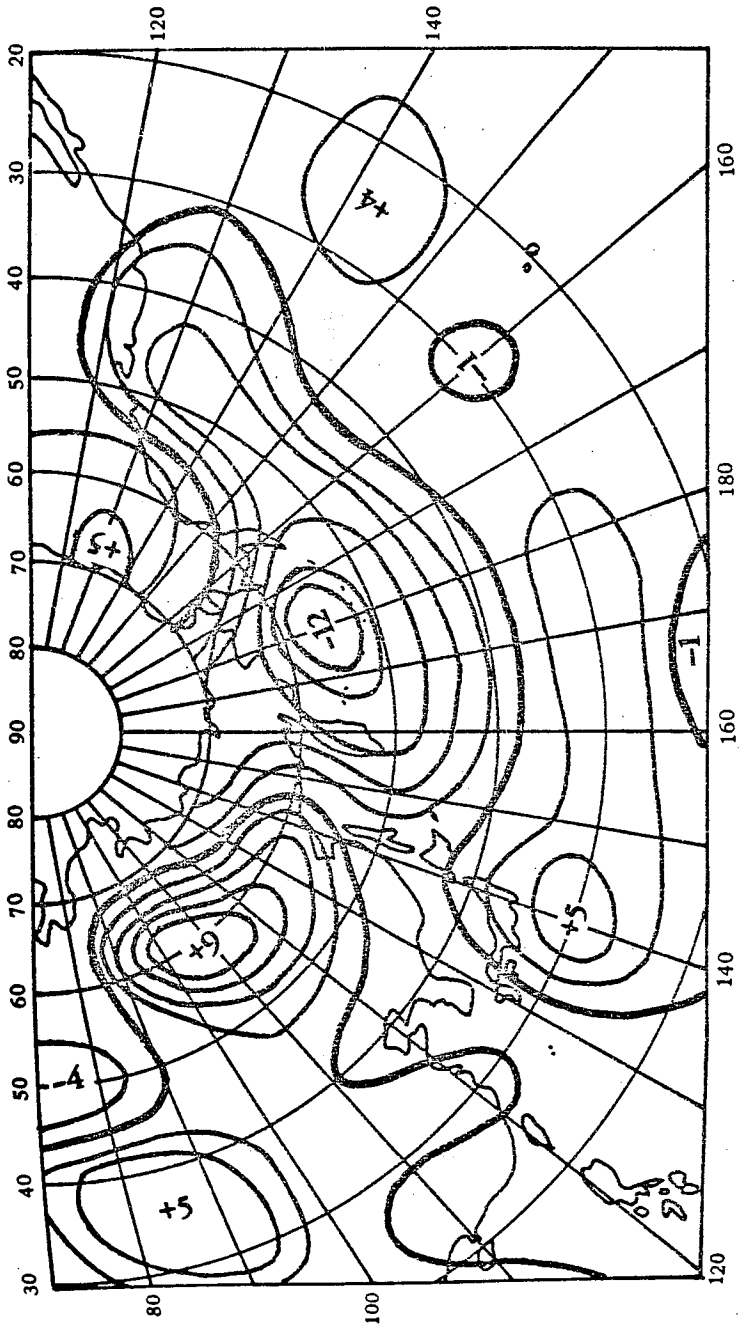

Figure 36. Mean 700-mb height anomalies of the North Pacific and East Asia associated with inactive typhoon months of August in Taiwan.

3. The mid-Pacific trough is well developed. An area of deep negative anomalies is centered on the Bering Sea and extends westward over the Sea of Okhotsk. The area of negative anomalies penetrates southward into tropical latitudes approximately along 130°E.
4. The monsoon trough weakens as evidenced by positive anomalies over the South China Sea.
5. The subtropical ridges over the Tibetan Plateau and the North Pacific slightly intensify.

Rainfall Associated with the Typhoon Visiting Taiwan

Typhoons visiting Taiwan include two groups, i.e., the northern and southern types, as defined in Chapter I. The northern-type typhoons contribute greater amounts of mean annual rainfall to the north and northeast than to the south and southwest of the island, whereas the southern-type contributes more mean annual rainfall to the south than to the north. With the exception of the southwestern and southeastern sectors of the island, the northern-type contributes more mean annual rainfall than the southern-type. Typhoons visiting Taiwan contribute greater rainfall to the south and east than to the north and west. The

mean annual rainfall contributed by typhoons visiting Taiwan ranges from about 815 mm (32.09 inches) at Hengchun to about 411 mm (16.18 inches) at Taichung. At Hengchun, about 46% of mean annual rainfall is derived from typhoons visiting Taiwan, whereas at Keelung it is only 19% (Figure 10 and Tables 22a and 22b in Appendix B). The northern-type contributes greatest amounts of rainfall to the south and southwest in July and to the north and northeast in September. At Taichung and Alishan, the northern-type contributes greatest amounts of rainfall in August (Tables 44a and 44b in Appendix B). The southern-type contributes more rainfall to the south in August and to the north in September (Tables 45a and 45b in Appendix B).

The northern-type has lowest rainfall intensity in the southwest, whereas the southern-type has highest rainfall intensity in that area (Figures 11 and 12 and Tables 46a and 46b in Appendix B). It appears that the standard deviation of daily rainfall associated with the northern-type is higher in general than that associated with the southern-type (Figure 12). The maximum daily rainfall also shows a similar trend. The maximum daily rainfall in the lowland area reaches a highest value of 622 mm (24.49 inches) at Kaoshiung. At the mountain station of Alishan, it is 874 mm

(34.41 inches). Both values are contributed by the northern-type typhoons.

The probability of rainy days associated with the northern-type typhoons shows a pronounced spatial variation, with values higher in the north and lower in the southwest of the island (Figure 13 and Tables 47a and 47b in Appendix B). It reaches nearly 90% at Taipei but only 56% at Tainan. In contrast, the probability of rainy days associated with the southern-type shows less spatial variation. It varies from slightly more than 90% at Taitung, Kaoshiung, and Alishan, to about 73% at Tainan.

The probability of daily rainfall exceeding 76.2 mm is higher in the north and east than in the west and southwest for the northern-type typhoons. It varies from 16% at Yilan and Hwalien to only about 3% at Kaoshiung. The probability of daily rainfall exceeding 76.2 mm also shows a similar spatial variation pattern. It varies from 24% at Taitung and 22% at Hwalien to only about 5% at Taipei and 6% at Taichung (Figure 13 and Tables 47a and 47b in Appendix B).

Rainfall Associated with the Kyushu-type Typhoon

The Kyushu-type typhoon contributes rainfall mainly to the south and southwest of the island (Figure 10 and

Tables 22a and 22b in Appendix B). The percentage of mean annual rainfall contributed by it varies from about 7% at Tainan and Kaoshiung to only 0.5% at Keelung.

The Kyushu-type typhoon contributes significant amounts of rainfall to the southwest and south only in August (Table 48a in Appendix B). The percentage of mean August rainfall associated with it reaches about 26% at Taichung, Tainan, and Kaoshiung, but only 5% at Taipei (Table 48b in Appendix B).

The mean and the standard deviation of daily rainfall contributed by the Kyushu-type typhoon is highest in the southwest of the island (Figures 11 and 12 and Table 49 in Appendix B). At Taichung, Tainan, and Kaoshiung, the mean daily rainfall contributed by it is even higher than that contributed by the typhoon visiting Taiwan. It is notable that the maximum daily rainfall in lowland areas is highest at Taichung, about 660 mm (25.98 inches). This was associated with the Kyushu-type typhoon on August 8, 1959, a record-flood day in Taiwan in this century.

The probability of rainy days associated with the Kyushu-type typhoon is highest in the southwest of the island. It varies from about 83% at Kaoshiung to about 43% at Keelung. At Alishan, it reaches nearly 97%. The

probability of rainfall exceeding 76.2 mm is 20% at Kaoshiung (Figure 13 and Table 50 in Appendix B).

Rainfall Associated with the Monsoon Trough

The monsoon contributes a fairly large amount of rainfall to southern Taiwan. At Hengchun and Taitung, about 150 mm (5.91 inches) or 9% of mean annual rainfall is derived from the monsoon trough (Figure 10 and Tables 22a and 22b in Appendix B). The mean annual rainfall contributed by it is lowest at Keelung, only about 41 mm (1.61 inches) or 1%.

The monsoon trough contributes rainfall to Taiwan mainly from June through September (Tables 51a and 51b in Appendix B). The percentage of mean monthly rainfall contributed by it is highest in the northwest and east in July and in the south and southwest in September. In summer, June through September, the monsoon trough contributes about 10% or more of mean monthly rainfall at most stations.

The mean and the standard deviation of daily rainfall associated with the monsoon trough show distinct regional patterns with values higher in the southeast and lower in the southwest (Figures 11 and 12 and Table 52 in Appendix B). The mean daily rainfall varies from 21 mm (0.83 inches) at Taitung to about 8 mm (0.31 inches) at Tainan. In general,

the southeast wind dominates the island in connection with the proximity of a monsoon trough to the south of it. This favors high rainfall in the southeast due to windward position. Except for Keelung and Taipei, the maximum daily rainfall reaches more than 100 mm.

The probability of rainy days associated with the monsoon trough is higher in the south than in the north of the island. It varies from approximately 62% at Kaoshiung to about 32% at Keelung. The probability of daily rainfall exceeding 76.2 mm is smaller for the monsoon trough than for the Kyushu-type typhoon and the typhoon visiting Taiwan. At Keelung and Taipei, the monsoon trough has never contributed rainfall of more than 76.2 mm (Figure 13 and Table 53 in Appendix B).

Summary of Significant Results

In summary, typhoons tend to visit Taiwan during periods of the weak westerlies in summer. The previous chapters indicate that both the Mongolian anticyclone and the Taiwan low also favor Taiwan with more rainfall in February when the strength of the westerlies is at a minimum. It can be concluded that low zonal-index favors Taiwan with heavy rainfall in both winter and summer. Zonal-index thus can be used as an important guide for the forecasting of

daily weather and climatic variations over Taiwan.

The 700-mb height anomalous pattern is useful in the forecasting of the typhoon activity over Taiwan. Intense negative anomalies over Siberia and China, accompanying the deepening of the Siberian trough, favor the typhoon visiting Taiwan. The Siberian trough appears to be more important than the mid-Pacific trough in controlling the typhoon activity over Taiwan.

As with other synoptic flow types, rainfall associated with the typhoon visiting Taiwan, the Kyushu-type typhoon, and the monsoon trough also shows distinct spatial variations. As expected, the northern-type typhoon contributes more rainfall to the north than to the south, whereas the southern-type shows the reverse pattern. The Kyushu-type typhoon frequently caused floods over southwestern Taiwan, as seen by its high chance of daily rainfall exceeding 76.2 mm. It produces only a negligible amount of rainfall in northern Taiwan. The monsoon trough contributes rainfall mainly to southern Taiwan.

Typhoons are major rainfall sources at all Taiwan stations in summer, as evidenced by their high contributions of annual, monthly, and daily rainfall, and by their high chances of rainy days. In southern Taiwan, typhoons

contribute nearly 50% of mean annual rainfall. They contribute more than 60% of monthly rainfall to most stations in summer. Typhoon rains are highly variable as evidenced by their high standard deviation and maximum daily rainfall. In southern Taiwan, where almost all water needs are derived from summer rains, crop types are more diversified because of high risks of floods and droughts. In northern Taiwan, rice fields dominate the agricultural landscape, whereas in southern Taiwan, scattered rice, sugarcane, banana, and sweet potato fields are found.

Although typhoons frequently cause severe damages on crops due to their strong destructive forces and high rainfall intensities, they benefit Taiwan by supplying sufficient water for agriculture. Without typhoons, severe droughts would occur over Taiwan. The severe drought period over southern and western Taiwan from 1963 through 1965 resulted from a decrease in typhoon activity.

CHAPTER VII

STATISTICAL MODELS OF DAILY RAINFALL AND SYNOPTIC FLOW TYPE OCCURRENCES

The Simple Markov Chain Probability Model

The synoptic aspects of the probability of daily rainfall over Taiwan were discussed in preceding chapters. It has been found that statistical models of sequences of wet and dry days provide additional tools for weather forecasting. Gabriel and Neumann (1962) found that a simple Markov chain probability model fit Tel Aviv data of daily rainfall occurrences. Topil (1963) and Caskey (1963) recognized that theoretical probabilities derived from a simple Markov chain model agreed closely with the empirical values of probabilities of precipitation occurrences in intervals of various lengths at Denver. Weiss (1944) computed probabilities of sequences of duration of storm period and intervals between periods by the Markov chain probability model for four 10^{o} "squares" centered near England, Newfoundland, the Great Lakes, and the Aleutians. Weiss (1964) also pointed out that a Markov chain probability model is shown to fit sequences of wet and dry days in records of various lengths for

Kansas City and Fort Worth. Hershfield (1970) presented examples of the simple Markov chain probabilities of dry spells in Minnesota and the Washington, D.C. area. Green (1965), after examining Weiss' data of rainfall occurrences by exponential probability model, concluded that it gave expected frequencies similar to those by the simple Markov chain probability model.

The purpose of this section is to study sequences of wet and dry days of various lengths at the eight Taiwan stations by the simple Markov chain probability model so that the results can be used as a supplemental tool for daily rainfall forecasting.

The simple Markov chain probability model requires the computation of two variables, i.e., Po and Pl. Po refers to the conditional probability of wet days, given a previous dry day, and Pl is the conditional probability of a wet day, given a previous wet day. According to this probability model, a given day should fall in one of the following four categories, i.e., (W/W), (D/W), (W/D), (D/D); where W and D denote wet and dry days, respectively. The numerator represents today; the denominator, yesterday. A wet day is defined as one with rainfall equal to or exceeding 0.1 mm.

Thus

$$P1 = Pr(W/W) = \frac{N(W/W)}{N(W/W) + N(D/W)}$$

$$Po = Pr(W/D) = \frac{N(W/D)}{N(W/D) + N(D/D)}$$

where Pr refers to the conditional probability and N denotes the total number of days. The probability of a wet spell of length n is

$$(1 - P1)P1^{n-1},$$

and of a dry spell of length n is

$$Po(1 - Po)^{n-1}.$$

The cumulative distribution through n is, for wet sequences

$$1 - P1^{n},$$

and for dry sequences

$$1 - (1 - Po)^{n}.$$

The probability for wet sequences greater than n is

$$P1^{n},$$

and for dry sequences

$$(1 - Po)^{n} \quad .$$

Annual and monthly probabilities of wet and dry days of various lengths at eight Taiwan stations were calculated by these equations.

Table 8 shows the procedure for the calculation of the conditional probability of wet days on an annual basis by the simple Markov chain model at eight Taiwan stations. Both Pl and Po show distinct spatial variations with values higher in northern and eastern Taiwan than in western and southern Taiwan. Pl is very high at all stations; varying from nearly 0.73 at Keelung to about 0.59 at Kaoshiung. At all stations Po is much lower than Pl; it varies from 0.33 at Keelung to only about 0.13 at Kaoshiung. It can be con-concluded that the conditional probability that a wet day follows a wet day is much higher than that a wet day follows a dry day.

Since the conditional probability of dry days can be calculated by subtracting Pl and Po from 1, it shows a reverse spatial variation pattern to that of wet days with values higher in the southwest than in the northeast of the island.

TABLE 8

ESTIMATES OF WET-DAY (0.1 MM OR MORE) OCCURRENCES

	Preceding day	Actual day Wet	Actual day Total	Estimate of probability P1(W/W)	Estimate of probability Po(W/D)
Keelung	Wet	1552	2142	0.7245	
	Dry	592	1876		0.3155
Taipei	Wet	1256	1870	0.6716	
	Dry	613	2148		0.2853
Taichung	Wet	710	1188	0.5976	
	Dry	477	2830		0.1685
Kaoshiung	Wet	580	985	0.5888	
	Dry	406	3033		0.1338
Hengchun	Wet	706	1184	0.5962	
	Dry	478	2103		0.2272
Taitung	Wet	890	1534	0.5801	
	Dry	644	2484		0.2592
Hwalien	Wet	1307	1960	0.6668	
	Dry	651	2058		0.3163
Yilan	Wet	1574	2201	0.7151	
	Dry	628	1817		0.3456

Both P1 and Po show distinct seasonal variations (Table 9). Higher values are observed in winter than in summer at Keelung, Yilan, and Hwalien. It is notable that peak values of both P1 and Po reach maxima in February at those stations. As discussed in preceding chapters, both the Mongolian anticyclone and the Taiwan low contribute greatest amounts of rainfall in February. In contrast, values of both P1 and Po are higher in summer than in winter at Taipei, Taichung, Hengchun, and Taitung. All stations show peak values of P1 and Po in May and June, obviously associated with polar fronts.

Figure 37 shows the cumulative conditional probabilities derived from the simple Markov chain model and the unconditional probabilities of wet spells of various lengths at eight Taiwan stations for the period 1959 through 1969. The unconditional probability is defined as the ratio of the number of wet spells of a given length to the total number of wet spells. It appears that unconditional probabilities are higher for short spells and lower for long spells than conditional probabilities derived from the simple Markov chain model. For example, at Keelung, the unconditional probabilities of wet spells shorter than 6 days are higher than the conditional probabilities derived from the simple

TABLE 9

MONTHLY VARIATIONS IN CONDITIONAL PROBABILITIES OF WET-DAY OCCURRENCES

Month	1	2	3	4	5	6	7	8	9	10	11	12
Keelung	0.756	0.808	0.749	0.647	0.685	0.709	0.547	0.659	0.735	0.667	0.803	0.769
	0.365	0.408	0.307	0.344	0.444	0.351	0.175	0.193	0.294	0.307	0.393	0.440
Taipei	0.656	0.766	0.688	0.623	0.622	0.729	0.658	0.699	0.700	0.599	0.629	0.623
	0.288	0.285	0.271	0.216	0.330	0.333	0.265	0.259	0.265	0.314	0.284	0.324
Taichung	0.438	0.654	0.552	0.451	0.689	0.734	0.521	0.675	0.636	0.400	0.485	0.390
	0.153	0.174	0.195	0.205	0.196	0.299	0.327	0.314	0.164	0.044	0.064	0.090
Kaoshiung	0.250	0.381	0.381	0.392	0.605	0.740	0.609	0.719	0.592	0.471	0.400	0.235
	0.084	0.089	0.090	0.111	0.138	0.287	0.330	0.346	0.235	0.086	0.052	0.043
Hengchun	0.415	0.296	0.397	0.436	0.586	0.781	0.701	0.737	0.673	0.489	0.487	0.275
	0.133	0.195	0.163	0.149	0.239	0.313	0.409	0.435	0.430	0.233	0.219	0.145
Taitung	0.505	0.602	0.540	0.566	0.577	0.699	0.607	0.672	0.654	0.518	0.477	0.414
	0.190	0.295	0.319	0.324	0.376	0.255	0.210	0.217	0.339	0.225	0.238	0.201
Hwalien	0.621	0.733	0.665	0.708	0.704	0.711	0.559	0.667	0.662	0.629	0.659	0.581
	0.433	0.477	0.370	0.479	0.430	0.306	0.157	0.209	0.296	0.259	0.397	0.250
Yilan	0.697	0.770	0.659	0.644	0.726	0.746	0.594	0.693	0.738	0.721	0.777	0.726
	0.386	0.430	0.396	0.399	0.444	0.343	0.155	0.219	0.272	0.216	0.545	0.426

(Upper numbers indicate P1(W/W) and lower numbers indicate Po(W/D))

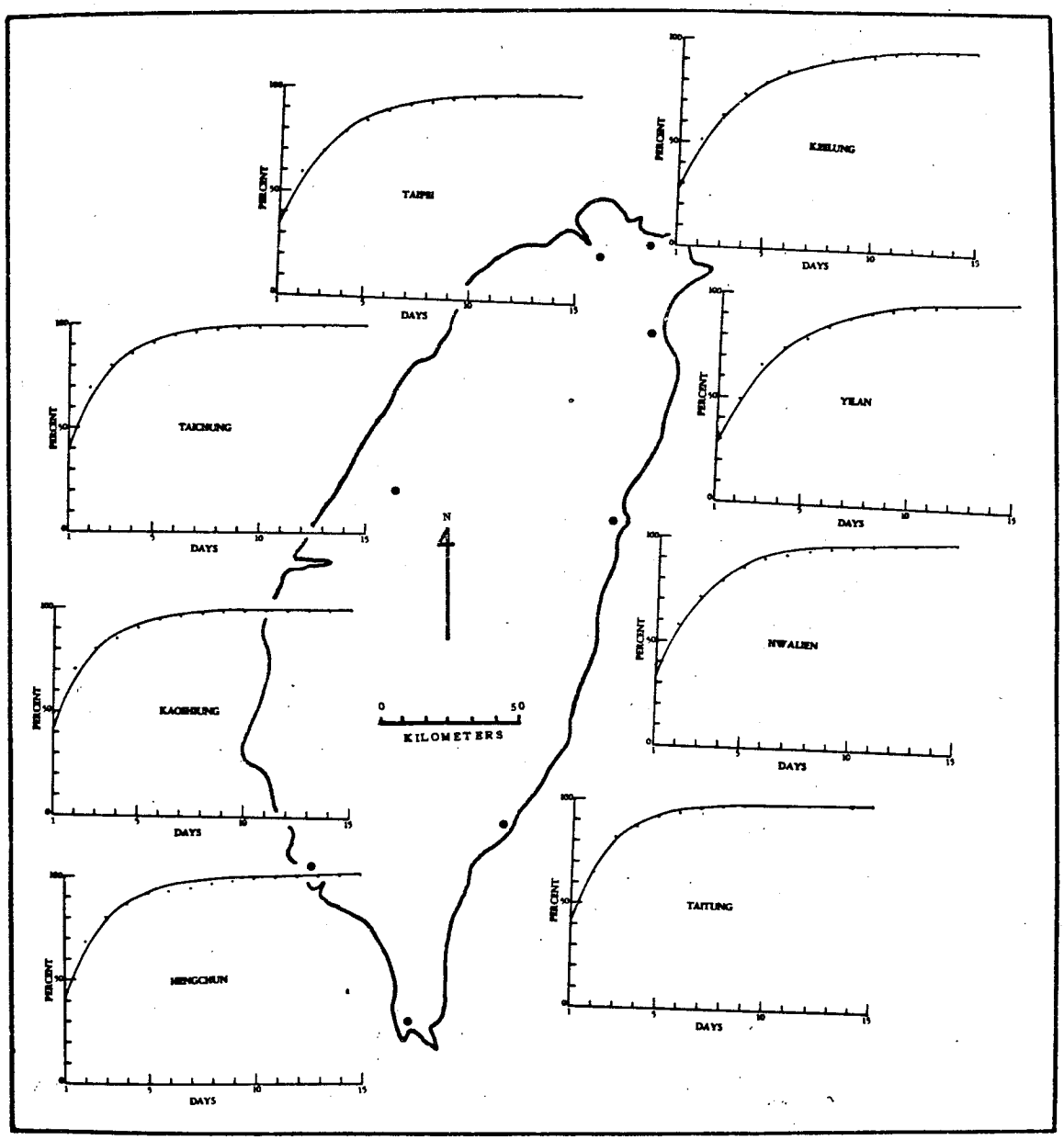

Figure 37. The cumulative conditional probabilities (curves) derived from the simple Markov chain model and the cumulative unconditional probabilities (dots) of wet-spells of various length.

Markov chain model, whereas the unconditional probabilities of wet spells longer than 6 days are lower than the conditional probabilities derived from the model. The same characteristic holds well for dry spells (Figure 38). The conditional probabilities agree well with the unconditional probabilities for wet spells at all stations. However, they deviate greatly from each other for dry spells at Taichung and Kaoshiung.

Figure 39 shows the observed and expected frequencies of wet spells of various lengths at eight Taiwan stations. Chi-square is used to test the "goodness" of fit of daily rainfall data to the simple Markov chain possibility model (Table 54 in Appendix C). Spells with expected frequencies of less than 5 are excluded from the computation of Chi-square values because of their large sampling variation. Consequently, degrees of freedom vary from station to station. With the exception of Kaoshiung and Hengchun, Chi-square indicates that the theoretical frequencies of wet spells, derived from the simple Markov chain probability model, agree with the observed frequencies at the 5% level for the other six stations. At Kaoshiung, the Chi-square value is significant at the 0.1% level, reflecting that the model is less successful in explaining daily rainfall

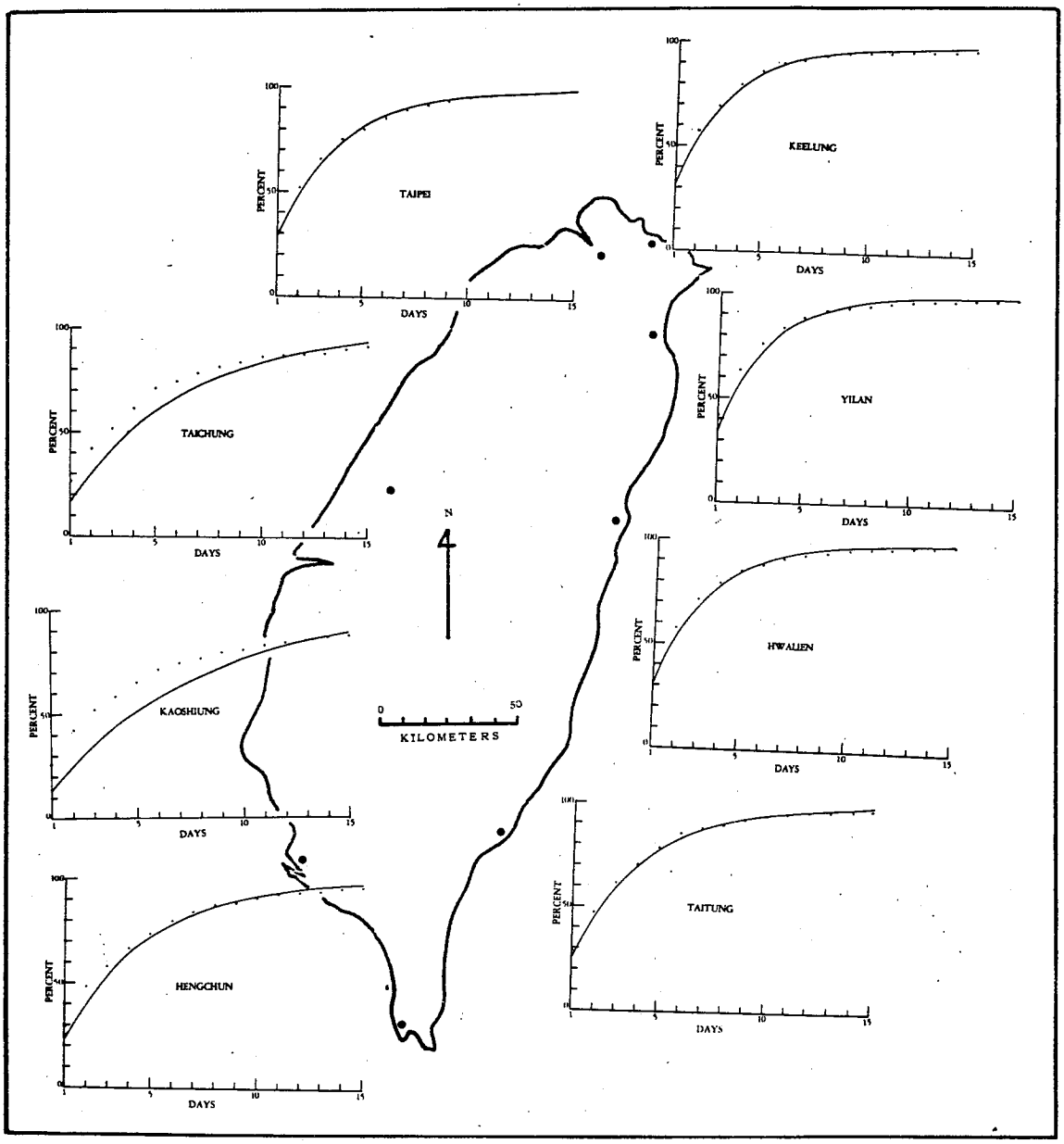

Figure 38. The cumulative conditional probabilities (curves) derived from the simple Markov chain model and the cumulative unconditional probabilities (dots) of dry-spells of various length.

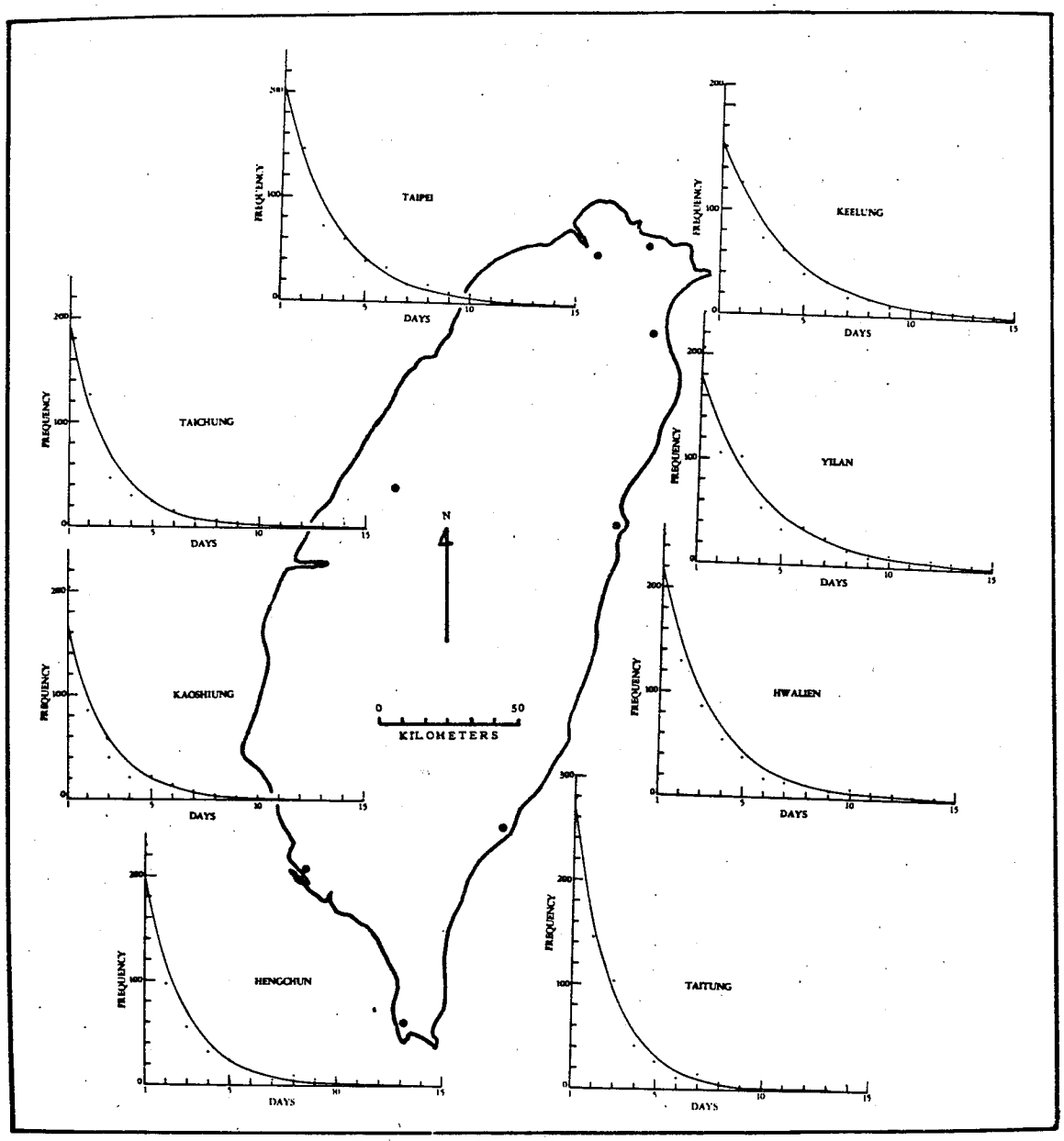

Figure 39. The frequency distribution of wet-spells by the simple Markov chain model (curves) and by observation (dots).

occurrences. At Hengchun, the Chi-square value exceeds the significant value, indicating that the model fails to explain the occurrence of wet spells.

In terms of dry spells, the model fits daily rainfall data at the 5% level at Taitung and at the 0.1% level at Keelung, Hengchun, Hwalien, and Yilan; it fails to fit data at Taipei, Taichung, and Kaoshiung. At those stations, the Chi-square values far exceed the significant values (Figure 40 and Table 55 in Appendix C).

The return period of sequences of daily rainfall is defined as the ratio of the number of days or years of record to the total number of sequences of more than n days in length. According to the simple Markov chain model, the return period, given in days, of sequences of greater than n days for wet days is

$$Tw = \frac{1-P1+Po}{Po(1-P1)P1^{n}},$$

and for dry days

$$Td = \frac{1-P1+Po}{Po(1-P1)(1-Po)^{n}}.$$

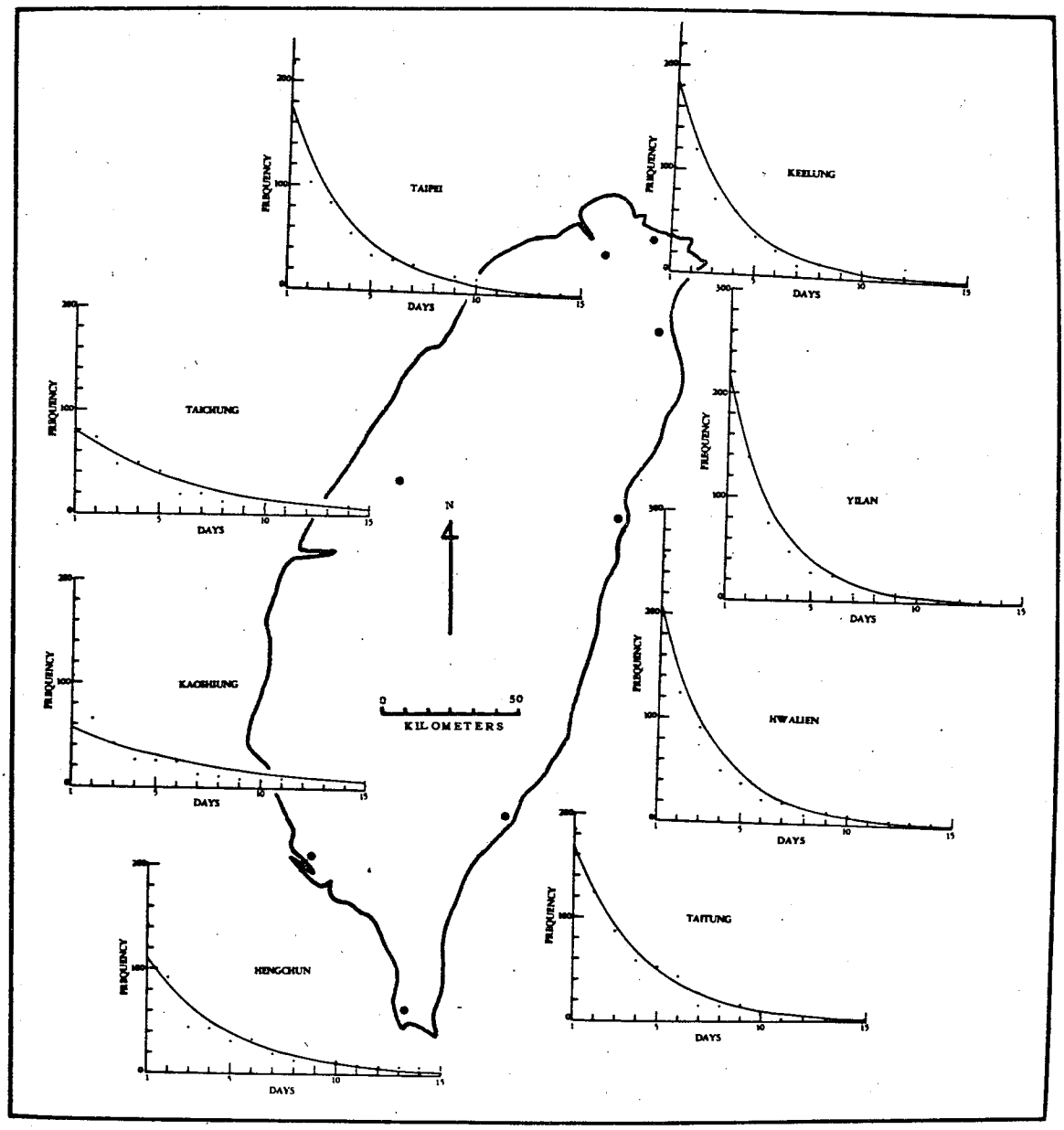

Figure 40. The frequency distribution of dry-spells by the simple Markov chain model (curves) and by observation (dots).

Tables 10 and 11 show return periods of wet and dry sequences of various lengths, respectively. These tables show that shorter spells tend to have shorter return periods than do longer spells. For example, once in almost every 9 days Keelung experiences a wet spell of more than one day, whereas only once in almost every 2.5 years does it experience a wet spell of more than 15 days. Distinct spatial variations in return periods of wet and dry spells are noted. Return periods of wet spells of various lengths are consistently lower in the northern and eastern sectors than in the western and southern sectors of the island. For example, at Keelung, the return period of a wet spell of more than one day is almost 9 days, whereas at Kaoshiung it is almost 17 days. At Kaoshiung, the return period of a wet spell of more than 15 days is about 149 years as contrasted with about 2.5 days at Keelung. This implies that southern and western Taiwan hardly experience long wet spells. In contrast, they tend to show shorter return periods of dry spells of more than 2 days duration than do northern and eastern Taiwan. For example, the return period of a dry spell of more than 15 days is about 11 years at Yilan and about 6 years at Keelung, but at Taichung, Kaoshiung, and Hengchun it is less than a year. On the other hand,

TABLE 10

RETURN PERIODS (IN DAYS) OF WET-SPELLS DERIVED FROM THE SIMPLE MARKOV CHAIN PROBABILITY MODEL

Spells	Keelung	Taipei	Taichung	Kaoshiung	Hengchun	Taitung	Hwalien	Yilan
1	9.4	9.8	14.1	16.8	11.5	10.8	9.2	9.0
2	13.0	14.5	23.6	28.7	19.4	18.5	13.9	12.5
3	17.9	21.6	39.5	48.6	32.5	32.0	52.5	17.5
4	24.7	32.1	66.0	82.5	54.5	55.1	31.1	24.5
5	34.2	48.0	120.7	140.1	91.5	95.7	46.8	34.3
6	47.3	71.4	185.5	238.2	153.5	164.2	70.2	47.9
7	65.7	105.8	310.8	1.1	257.7	283.7	105.4	67.1
8	90.9	157.4	1.4	1.9	1.2	1.4	158.0	93.9
9	125.7	236.5	2.4	3.2	2.0	2.3	237.0	131.5
10	173.8	361.0	4.1	5.6	3.3	4.1	356.3	184.0
11	246.3	1.4	6.8	9.7	5.7	7.1	1.5	258.3
12	347.7	2.1	11.6	17.2	9.9	13.2	2.2	361.9
13	1.2	3.3	21.1	30.5	17.3	24.8	3.4	1.4
14	1.7	5.0	39.1	55.3	32.0	43.3	5.1	2.0
15	2.4	7.5	78.2	149.3	64.0	88.6	7.7	2.7

(Values underlined are years)

TABLE 11

RETURN PERIODS (IN DAYS) OF DRY-SPELLS DERIVED FROM THE SIMPLE MARKOV CHAIN PROBABILITY MODEL

Spells	Keelung	Taipei	Taichung	Kaoshiung	Hengchun	Taitung	Hwalien	Yilan
1	9.9	9.2	10.1	11.4	8.7	8.4	9.0	9.8
2	14.5	12.8	12.2	13.2	11.5	11.4	13.2	15.0
3	21.2	18.0	14.7	15.2	14.9	15.4	19.3	22.9
4	31.0	25.1	17.6	17.6	19.3	20.7	28.2	34.9
5	45.3	35.2	21.2	20.3	25.0	28.0	41.3	53.4
6	66.2	49.2	25.5	23.5	32.3	37.8	60.4	81.7
7	96.9	68.9	30.7	27.1	41.8	51.0	88.4	123.9
8	141.7	96.5	36.9	31.3	54.1	69.0	129.5	191.2
9	207.4	135.1	44.4	36.1	70.0	93.1	189.6	292.4
10	303.7	189.4	53.4	41.7	90.7	125.8	277.7	1.3
11	1.2	265.2	64.2	48.2	117.6	170.0	1.1	1.9
12	1.7	1.0	77.3	55.6	152.2	230.3	1.6	2.9
13	2.6	1.4	92.9	60.7	197.1	312.1	2.4	4.5
14	3.9	2.0	118.8	84.2	255.8	1.2	3.6	7.0
15	5.9	2.9	134.5	85.7	332.5	11.6	5.3	11.0

(Values underlined are years)

southern and western Taiwan experience a dry spell of more than 15 days every year, whereas northern and eastern Taiwan hardly experience such a long dry spell.

Logarithmic Series

Williams (1952) found that the frequency distribution of sequences of fine days at Harpenden conforms very closely to a logarithmic series. Cooke (1953) indicated that dry-spell day data at Moncton, New Brunswick fit geometric progression very closely, while wet-spell data fit the logarithmic curve.

A wet- or dry-spell of length n by logarithmic series can be written as

$$\alpha \frac{x^n}{n}$$

The two constants, α and x, can be calculated once the total number of wet or dry days (N) and of spells of various lengths (S) are known:

$$S = \alpha \log_e (1 + N/\alpha)$$

$$N = \alpha x/(1 - x)$$

However, the solution of these two simultaneous equations is complicated and indirect. Fisher, et al. (1943) and Williams (1947) presented simple graphic and mathematic

methods to derive values of α and x. Values of log N/α corresponding to those of Log N/S can be found from Table 56 in Appendix C. Both N and S can be estimated from data samples. If the value of log N/S is smaller than 0.4 and α and x cannot be estimated from the log N/α table, Figure 58 in Appendix D can be used to estimate the value of x. The value of α can then be derived from the equation

$$\alpha = N\ (1 - x)/x$$

where x is consistently less than one.

Table 12 shows the four parameters, N, S, α, and x, for both wet- and dry-spells. Evidently, northern Taiwan has more wet days and more wet-spells than does southern Taiwan. Values of both α and x fail to show any distinct regional pattern for wet-spells. In contrast, all four parameters of dry spells show distinct spatial variation. Southern Taiwan shows more dry days but fewer dry-spells than does northern Taiwan. Values of α are higher in northern Taiwan than in southern Taiwan, whereas those of x are the reverse. Chi-square values are calculated to test the agreement between the observed and expected frequencies of wet- and dry-spells of various lengths (Tables 57 and 58 in Appendix C). It is found that the logarithmic series

TABLE 12

FOUR PARAMETERS FOR THE ESTIMATION OF WET-SPELLS AND DRY-SPELLS ACCORDING TO THE LOGARITHMIC SERIES

	Wet-spells			
	N	S	α	x
Keelung	2144	592	270.4	0.8879
Taipei	1869	611	316.0	0.8553
Taichung	1187	476	269.8	0.8034
Kaoshiung	986	408	246.5	0.8000
Hengchun	1184	478	277.6	0.8100
Taitung	1534	642	407.7	0.7900
Hwalien	1958	652	342.0	0.8513
Yilan	2202	628	293.5	0.8824
	Dry-spells			
	N	S	α	x
Keelung	1874	588	294.6	0.8642
Taipei	2149	613	286.4	0.8824
Taichung	2831	479	165.4	0.9448
Kaoshiung	3032	408	129.6	0.9598
Hengchun	2103	478	193.1	0.9159
Taitung	2484	646	283.6	0.8975
Hwalien	2060	653	329.7	0.8620
Yilan	1816	626	338.1	0.8430

fail to fit data of wet-spells at Keelung, Taipei, Taitung, and Yilan, but they do fit data of wet-spells at Taichung, Kaoshiung, Hengchun, and Hwalien. In terms of dry-spells, the expected frequencies, derived from the logarithmic series, agree with the observed frequencies at the 0.1% level at Keelung, Taichung, and Hengchun, and at the 5% level at Kaoshiung, Hwalien, and Yilan. It can be concluded that the logarithmic series fit data of dry-spells at the latter three stations. The relationship between the expected and observed frequencies of both wet- and dry-spells are presented in Figures 41 and 42.

Synoptic Flow Types

As already discussed in the previous sections, the theoretical frequencies of both wet- and dry-spells, whether derived from the Markov chain model or logarithmic series, agree well with the observed frequencies at most Taiwan stations. The "goodness" of fit of these two statistical models to daily rainfall shows distinct spatial variation. This may result from different rainfall mechanisms. An attempt is made to study whether surface synoptic flow types over Taiwan occur simply by chance or by pattern and hence can be predicted by statistical models.

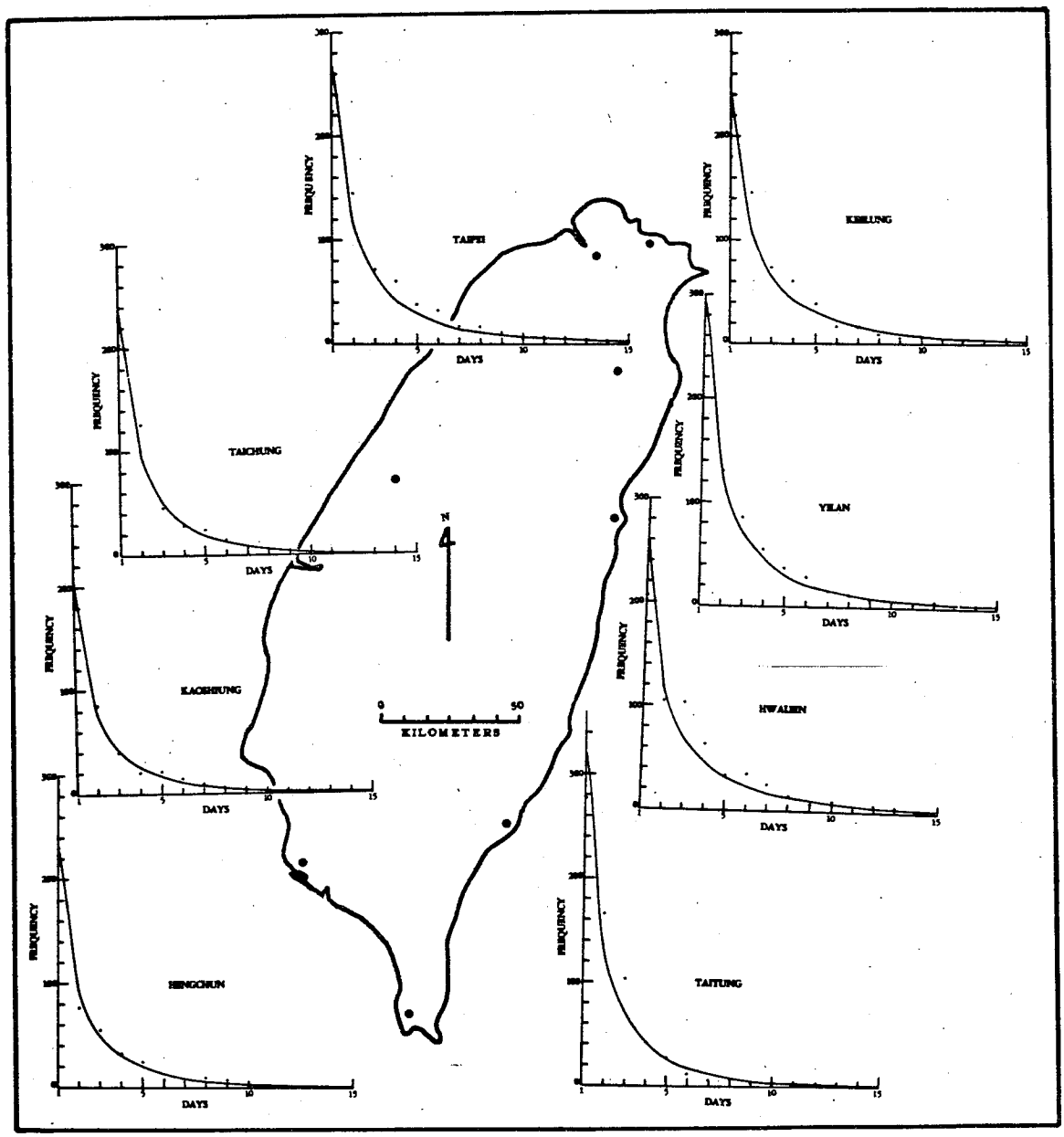

Figure 41. The frequency distribution of wet-spells by the logarithmic series (curves) and by observation (dots).

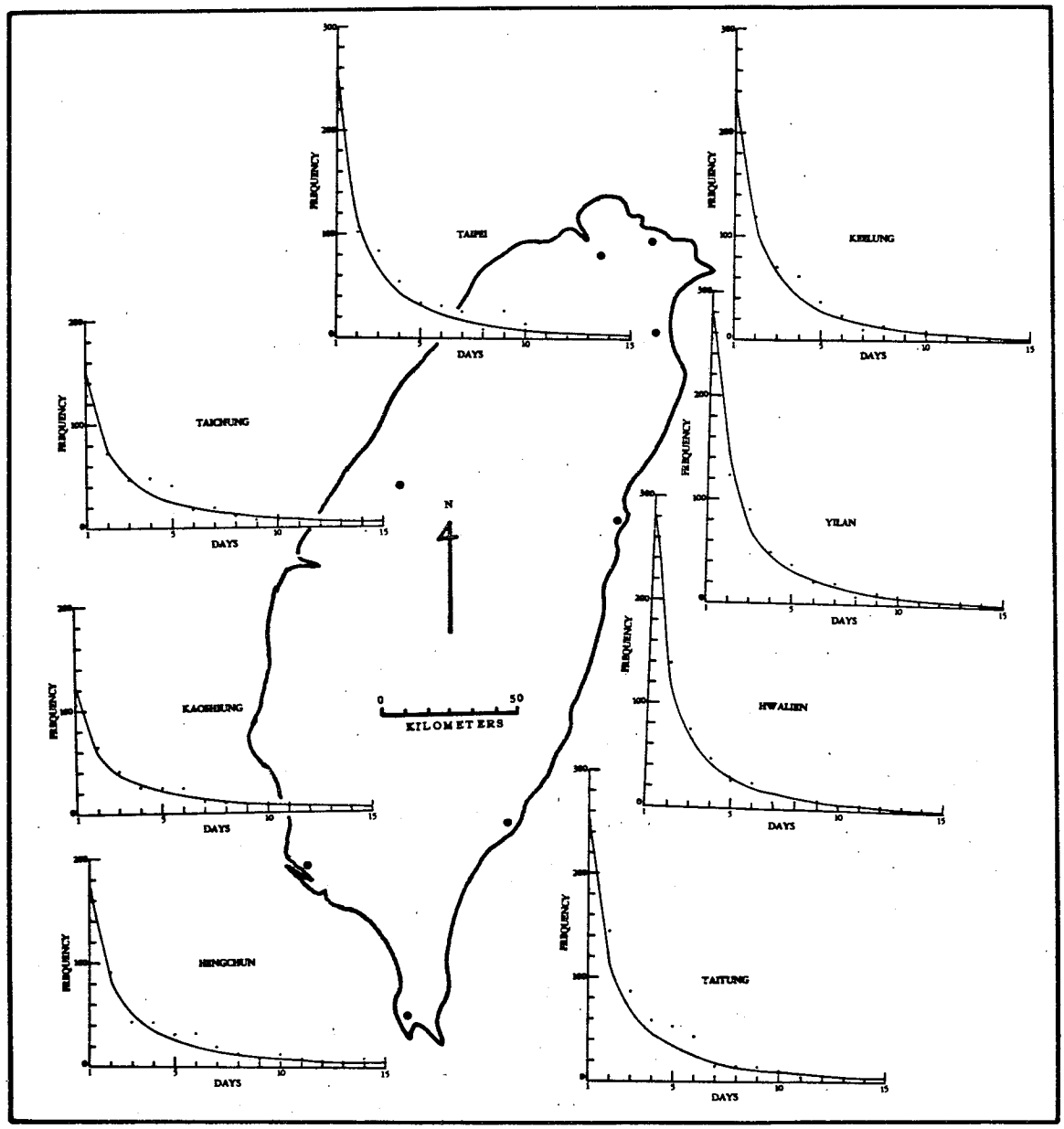

Figure 42. The frequency distribution of dry-spells by the logarithmic series (curves) and by observation (dots).

Figure 43 shows the cumulative probabilities of occurrences of different synoptic flow types derived from the simple Markov chain model. The Kyushu-type typhoon is excluded from Figure 43 due to its small sample size; its frequency is less than 5 in all spells. With the exception of the polar front, both over and south of Taiwan, and the northern-type typhoon, the conditional probabilites calculated by the model run close to the unconditional probabilities.

Figure 44 shows the observed and the expected frequencies of different synoptic flow types over Taiwan. Chi-square values are calculated to test the "goodness" of fit of the simple Markov chain model to the data sample of each synoptic flow type (Table 59 in Appendix C). It appears that the theoretical frequency distribution, derived from the model, agrees with the observed frequency distribution of all synoptic flow types.

Figure 45 shows the theoretical frequency distribution, derived from logarithmic series, and the observed frequency distribution of each synoptic flow type. Chi-square indicates that the two frequency distributions agree with each other for the polar front over Taiwan, the North Pacific subtropical anticyclone, the southwest monsoon, the

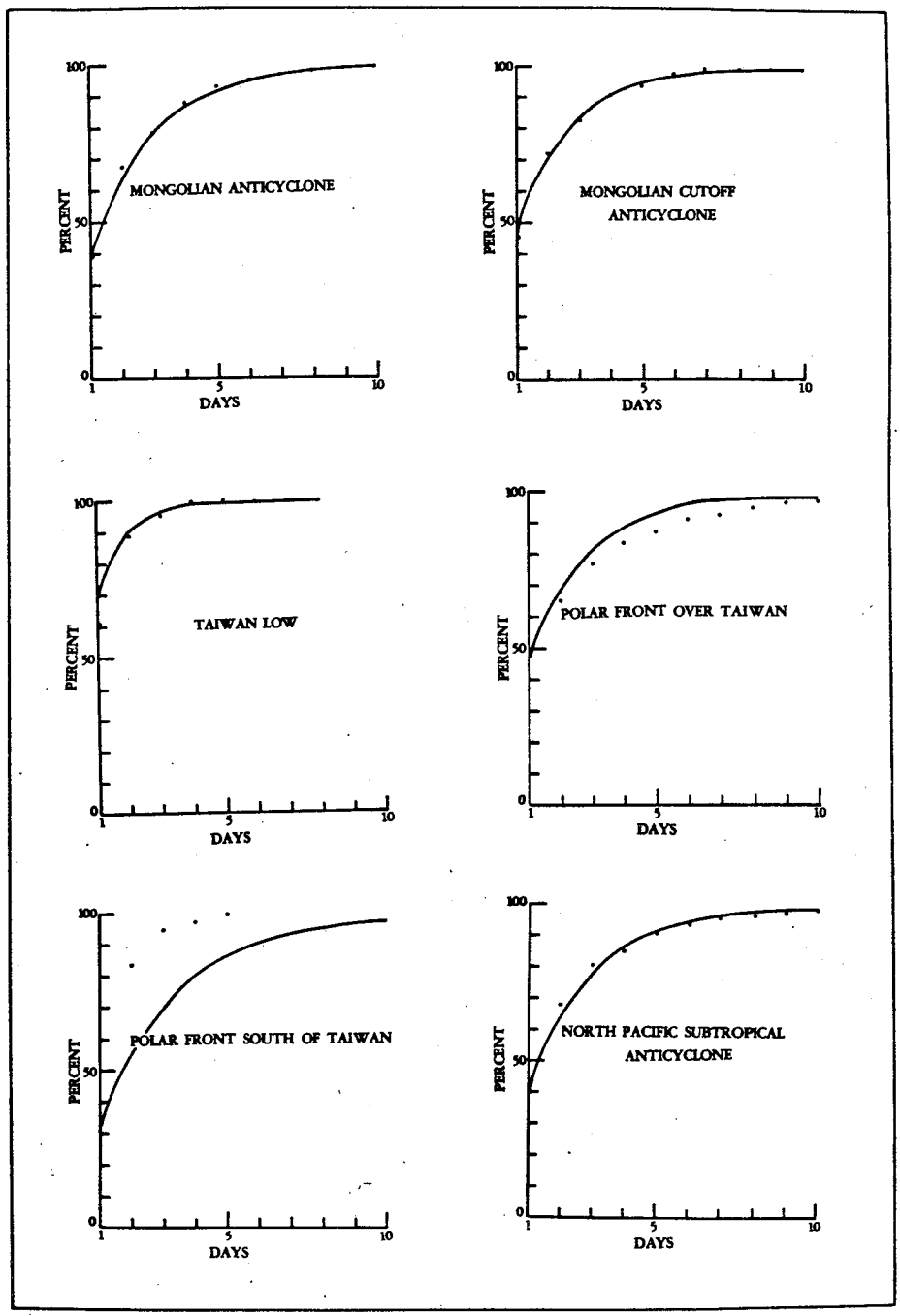

Figure 43. The cumulative conditional probabilities (curves) derived from the simple Markov chain model and the cumulative unconditional probabilities (dots) of occurrences of the eleven synoptic flow types.

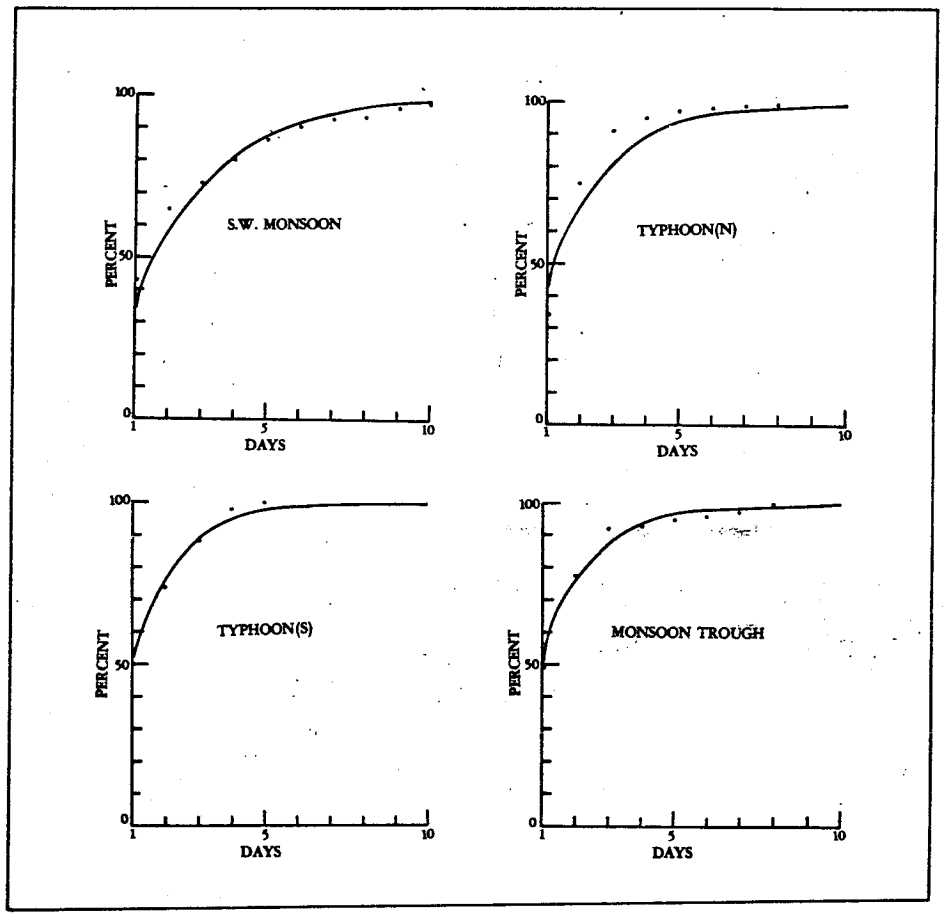

Figure 43. Continued.

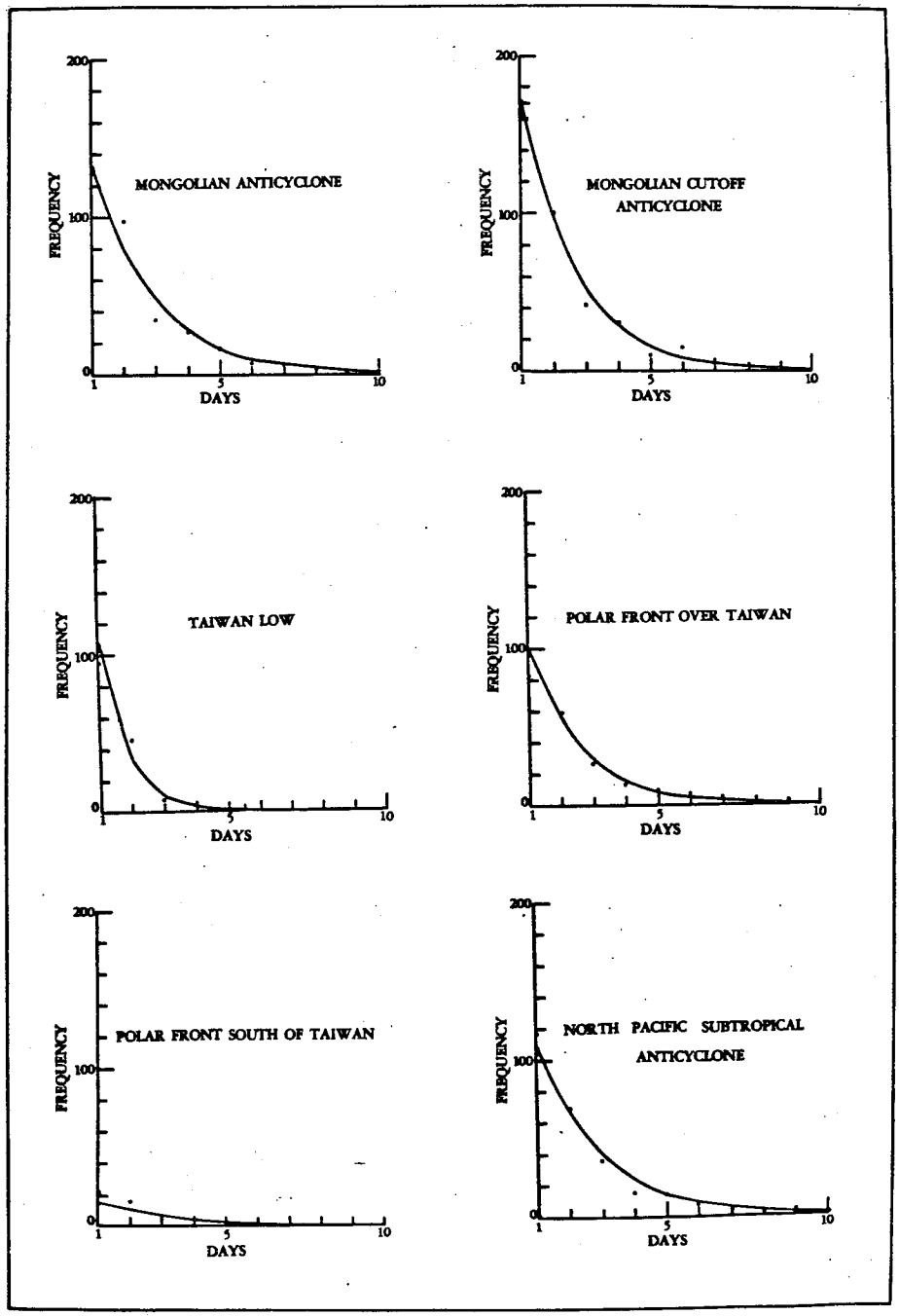

Figure 44. The frequency distribution of the eleven synoptic flow types by the simple Markov chain model (curves) and by observation (dots).

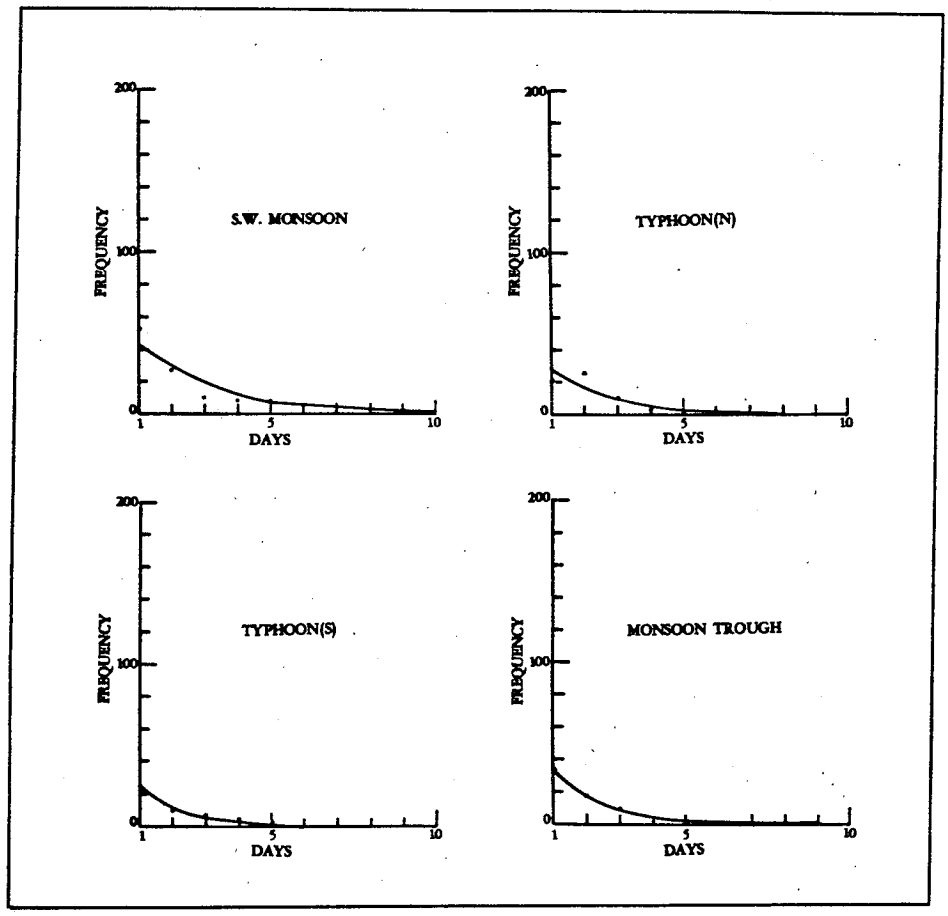

Figure 44. Continued.

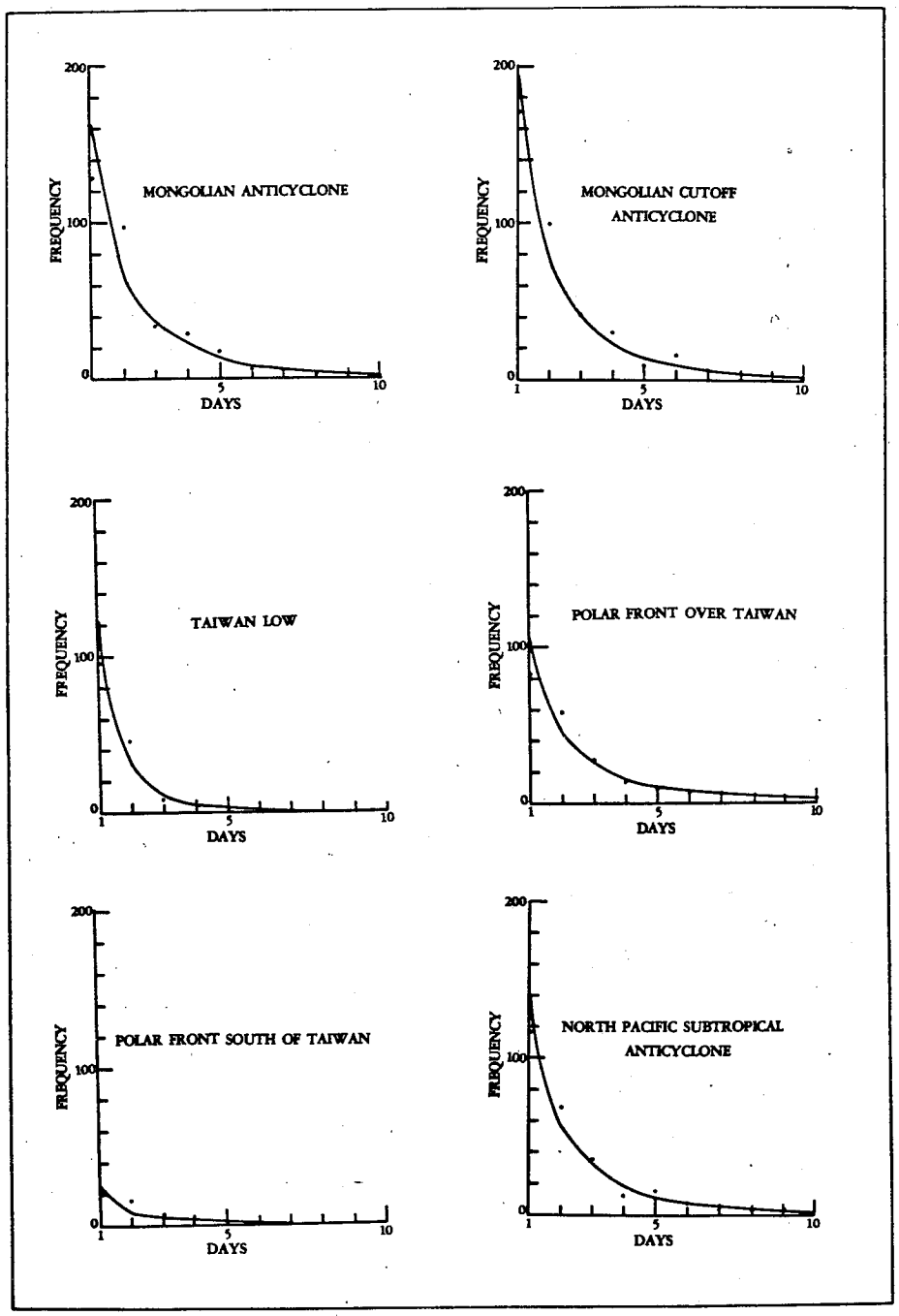

Figure 45. The frequency distribution of the eleven synoptic flow types by the logarithmic series (curves) and by observation (dots).

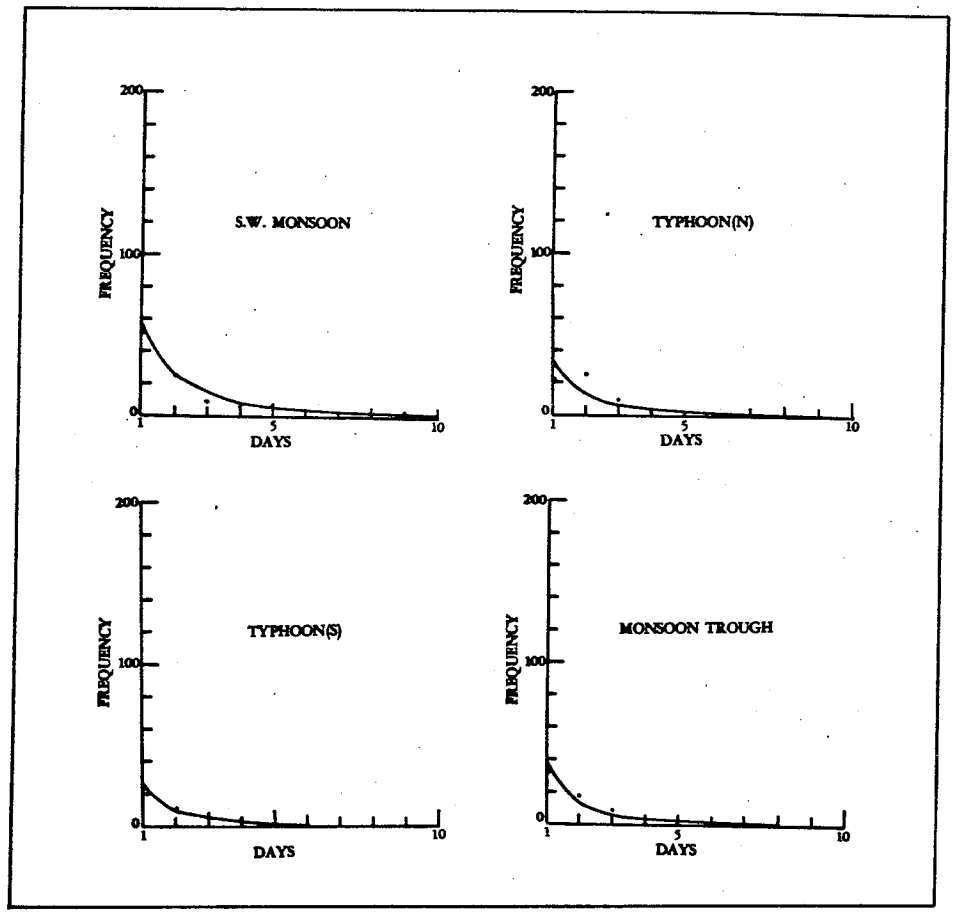

Figure 45. Continued.

southern-type typhoon, and the monsoon trough (Table 60 in Appendix C). Those synoptic flow types dominate Taiwan in summer and are major rainfall sources of southern Taiwan. Logarithmic series does not fit the frequency distribution of the winter synoptic flow types such as the Mongolian anticyclone, the Mongolian cutoff anticyclone, and the Taiwan low. It appears that there is a connection between the frequency distribution of wet- and dry-spells at various Taiwan stations and that of synoptic flow types over Taiwan. The Markov chain model explains well the frequency distribution of wet-spells and of synoptic flow types over Taiwan, but fails to explain the frequency distribution of dry-spells over southwestern Taiwan where rainfall concentration in summer is prominent. Logarithmic series explains the frequency distribution of both wet- and dry-spells over southwestern Taiwan and of summer synoptic flow types, but fails to explain that of wet-spells over northern and eastern Taiwan and of winter synoptic flow types.

Summary of Significant Results

The simple Markov chain probability model fits data of wet-spells at all stations except for Hengchun. It also fits data of dry-spells at Keelung, Hengchun, Taitung,

Hwalien, and Yilan. Logarithmic series fits data of wet-spells at Taichung, Kaoshiung, Hengchun, and Hwalien, and data of dry-spells at Keelung, Taichung, Kaoshiung, Hengchun, Hwalien, and Yilan. With the exception of Taipei, both wet- and dry-spells at other stations can be explained well by either or both statistical models. Neither of the two can explain the dry-spell data at Taipei. The Markov model explains well the frequency distribution of all synoptic flow types over Taiwan, whereas logarithmic series explains the frequency distribution of the summer synoptic flow types, but fails to explain that of the winter synoptic flow types. A summary of the "goodness" of fit of the two statistical models to occurrences of daily rainfall and synoptic flow types is presented in Tables 13 and 14.

The significant result of this study is that occurrences of daily rainfall and surface synoptic flow types are not random or by chance but, rather, are determined by conditions of the preceding day. The conditional probability derived from the simple Markov model thus can be used for the forecasting of daily rainfall occurrences. Persistence of rainfall or lack of rainfall has significant effects on agriculture. Hershfield (1970) stated that an extended period of little or no rain is one of the greatest natural

TABLE 14

THE AGREEMENT BETWEEN THE FREQUENCY DISTRIBUTION OF SYNOPTIC FLOW TYPES DERIVED FROM THE SIMPLE MARKOV CHAIN PROBABILITY MODEL OR FROM THE LOGARITHMIC SERIES AND THAT DERIVED FROM OBSERVATION

Flow Types	Markov Chain	Logarithmic Series
1	Yes	No
2	Yes	No
3	Yes	No
4	Yes	Yes
5	Yes	No
6	Yes	Yes
7	Yes	Yes
8	Yes	No
9	Yes	Yes
11	Yes	Yes

hazards to agriculture. On the other hand, a protracted rainy period can drastically reduce the final yield of crops. The current study indicates that wet- and dry-spells over Taiwan can be predicted either by the simple Markov chain model or by the logarithmic series for the estimation of water needs. Green (1965) pointed out that the statistical model may be helpfully suggestive regarding the mechanism of rainfall occurrences at places where it seems to apply. Gabriel and Neumann (1962) recognized that the fit of the Markov chain model to Tel Aviv rainfall, which is in connection with the passage of depressions and frontal systems, stands in contrast to data from England where persistence increases for the first few days of dry length. In Taiwan, the fit of the Markov chain model to both wet- and dry-spells at stations deriving their rainfall mostly from winter synoptic flow types, stands in contrast to data from stations deriving their rainfall mainly from summer synoptic flow types, where the logarithmic series is a better statistical model to fit wet- and dry-spell frequencies.

CHAPTER VIII

DIURNAL RAINFALL VARIATIONS

Theories

During the past thirty years, a number of studies have been made to investigate diurnal rainfall variations over various parts of the world. Distinct diurnal rainfall variations can be identified not only in the tropics where weather is often dominated by diurnal process (Nieuwolt, 1968), but also in the subtropics such as Hawaii (Leopold, 1948, 1949), Florida (Byers and Rodebush, 1948), and the eastern Mediterranean coast (Newmann, 1951). Even in the central United States (Means, 1944; Bleeker and Andre, 1951) and monsoon Asia (Ramage, 1952) where weather is complicated by the high frequency of cyclones and fronts, rainfall shows pronounced diurnal patterns.

Diurnal rainfall variations have been classified into continental and marine types, with rainfall maxima around afternoon and at night, respectively. However, the diurnal rainfall regime in a large continent is not so simple. The central United States has a pronounced nocturnal rainfall maximum (Bleeker and Andre, 1951; Means, 1944).

A popular theory regarding nocturnal rainfall is that the radiation cooling from the tops of clouds at night increases instability (Loveridge, 1924; Hewson, 1937). This is further substantiated by Kraus (1963) in his study of diurnal precipitation change over the sea. However, Dexter (1944) has considered this of secondary importance to the potential instability of warm air over land surface. The lapse rate in a cloud will not increase by more than 0.5°C per kilometer in 12 hours as a result of greater absorption of solar energy by the upper portion of a cloud than by the lower portion.

Some meteorologists (Hewson, 1937; Dexter, 1944) think that a warm front is usually associated with the nocturnal rainfall and thunderstorm activity as a result of the frontal uplifting of warm air in the night. This warm air becomes potentially unstable in late afternoon. The time lag between the development of the maximum potential instability of the surface air and thunderstorm activity is 6 to 10 hours (Dexter, 1944). Topography is also important in accounting for night rainfall over land surfaces. A downslope wind at night often establishes a convergent field in valleys and produces nighttime rainfall. The central United States, between the

Rocky Mountains and the Appalachians, is in a sense a large valley. At night the air in contact with the mountain slopes on both sides is colder than the air at the same level over the central plain. As a result, air from the slopes sinks and converges over the central plain producing strong vertical motion. This is responsible for the night-time rainfall and thunderstorm activity (Bleeker and Andre, 1951). Advection of warm air over land at night is also responsible for the nocturnal rainfall over the central plains of the United States (Means, 1944) and East China (Ramage, 1952).

Mountain areas normally show daytime rainfall maxima due to valley winds and thermal convection caused by strong solar radiation.

Over coastal stations, the diurnal rainfall regime is governed by various factors such as land and sea breezes, synoptic-scale circulations, topography, and the curvature of coastlines. Clouds that form at night over the ocean or along the coast may be blown inland or upslope by sea breezes and cause the post-dawn rainfall along the coast (Palmer, 1949). The Kona sea breeze of Hawaii Island is of this type (Leopold, 1949). In a study of the diurnal rainfall regime over Monsoon East Asia, Ramage (1952) has found that

warm air advection at low levels between midnight and sunrise favors the formation of convective clouds; radiation from cloud tops increases the vertical instability (Hewson, 1943). This often causes rainfall in early morning or post-dawn at tropical and subtropical stations.

A daytime rainfall maximum is attributed to strong convection caused by solar heating of land surface (Hewson, 1943; Dexter, 1944). Sea breezes also play an important role in favoring many coastal stations with daytime rainfall maxima. Orographic uplifting of sea breezes often leads to afternoon rainfall (Barry and Chorley, 1971). Interaction between local sea breezes and synoptic-scale prevailing winds, such as monsoon winds and trade winds, can create a sea-breeze front over land and thus causes daytime rainfall at coastal stations in the lee of a mountain.

In summer, the daytime rainfall maximum at the leeward stations of the islands of Molokai, Lanai, and Hawaii is attributable to the convergence between sea breezes and northeast trade winds. At the exposed windward stations in northern Hawaii Island, trade winds are strengthened by sea breezes, resulting in daytime rainfall maxima. Over subtropical peninsulas, such as Florida and Malaya, sea-breeze convergence in summer causes afternoon thunderstorm activity

(Byers and Rodebush, 1948; Ramage, 1964). Similar convergent wind fields of daytime sea breezes are also found over small islands such as Cyprus (Neumann, 1951) and Lanai (Leopold, 1948). In an extensive study of the relation between coastline curvature and thunderstorm activity at many coastal stations in the eastern Mediterranean and the United States, Neumann (1951) found a fairly consistent relation between convex coastlines and daytime thunderstorm activity, because sea breezes constitute a convergent wind field.

The characteristics of the sea breeze have been investigated extensively either by field observations or by numerical simulations. Defant (1951) has presented a detailed description of the life cycle of the sea breeze. The sea breeze is caused orimarily by the diurnal differential heating between land and sea. The sea breeze considerably surpasses the land breeze in intensity, frequency, and extent. Usually, the sea breeze starts in the morning, reaches its maximum velocity in the afternoon, and subsides towards the evening, whence it is replaced by the land breeze. The sea breeze which develops in opposition to the synoptic-scale wind may delay its advance towards coasts until late in the afternoon. It often sets in with

considerable gustiness of a cold front like character. In the tropical coasts, the sea breeze can penetrate about 150 kilometers inland with a depth of about two kilometers. It occurs more frequently in clear days than in cloudy days. The wind directions start at a right angle to the coast and then turn to the right in the northern hemisphere due to the coriolis effect. According to Estoque's (1961) two-dimensional numerical model of the sea breeze along a straight shoreline, a low level convergence zone is generated at the leading edge of the landward current in the afternoon. This is the sea breeze front created by the convergence between the synoptic-scale wind and the sea breeze. In nature, the linear pattern of cumulus parallel to shorelines in the afternoon is a manifestation of this feature. A return flow is also generated at an elevation of 1.0 to 1.5 kilometers. In addition, the model exhibits that at night onshore wind velocity increases farther inland. Estoque has ascribed this behavior to the force convection associated with the turbulent mixing. In the area immediately adjacent to the shoreline, the free convection ceases at night but the sea breeze has not dissipated. Both advective and turbulent cooling in this area is more effective than the area farther inland, where the winds are much lighter and surface is still

warm so that turbulent heat flux to the ground is negligible, permitting less cooling above the boundary layer inversion. This horizontal differential cooling produces the acceleration of the air towards the interior region in the surface layer. Yu and Wagner (1970) have actually observed such a wind regime on the Texas coast. McPherson (1970) has presented a three-dimensional numerical model of the sea breeze on an irregular coastline with a square model bay. He has demonstrated that in the early stage of the life cycle of the sea breeze, the convergence zone caused by the coastal configuration is distorted about the bay, with two centers of strong ascending motion on both sides of the bay and subsidence directly inland from the bay. Neumann (1951) has pointed out that sea breezes will be convergent and land breezes divergent along a coast that is convex towards the sea, and that the reverse is true along a concave coast. A square bay exhibits concavity in its upper reaches, while the junctions of the sides of the bay with the main water body constitute convex coasts. The symmetric distribution of the vertical motion about the bay is caused by the coriolis force which acts in opposition to the pressure gradient on the west side and in concert on the east side. In the late stage of the life cycle, only one center of the strongest ascending

motion is generated farther inland in the northeast. Winds rotate clockwise with the time of evolution, a reflection of the coriolis effect. The three-dimensional model also shows the tendency of prolonged onshore flow at low levels for several hours beyond the time when the surface temperature gradient is reversed. Based on field observations along the upper Texas coast, Hsu (1970) has found the distortion of the motion and thermal fields due to Galveston Bay and Sabine Lake. This confirms McPherson's numerical model. Hsu (1973) has also studied the dynamics of the sea breeze in the atmospheric boundary layer on the Gulf coast near Fort Walton Beach, Florida. He has concluded that the sea breeze is in the atmospheric free-convection regime and that its wind and temperature profiles in the surface boundary layer can be represented by the equations used in Estoque's two-dimensional and McPherson's three-dimensional models.

Winter

Taiwan is an elongated island in an area where monsoon and trade winds interact. The circulation over the island is further complicated by high mountain ranges extending north-south and irregular coastline configuration. Distinct

diurnal rainfall patterns can be identified at various stations during different seasons.

Average hourly rainfall for January and July during 11 years (1959-1969) was calculated for nine stations; Keelung, Taipei, Taichung, Kaoshiung, Hengchun, Taitung, Hwalien, Yilan, and Alishan. These stations were selected to represent different rainfall regimes and different exposures with respect to prevailing winds. The diurnal rainfall patterns at those stations are shown in Figure 46.

In January, Keelung shows a nocturnal rainfall maximum. Mean hourly rainfall increases abruptly between 1900 and 2100 (local time) and then decreases to a minimum at 0800. The nocturnal maximum at Keelung is a common characteristic of all winter months, November to March (Figure 47). Keelung has a wet winter because it is located in the exposed northern coast of the island (Figure 48). The convergence between land breezes and northeast monsoon winds is probably the primary cause of the nocturnal rainfall maximum in winter. In addition, the concave coastline at Keelung may also favor the formation of a convergent wind field by nighttime land breezes and hence may increase a rainfall amount. Radiation cooling from cloud tops may enhance the nocturnal rainfall maximum. This factor is

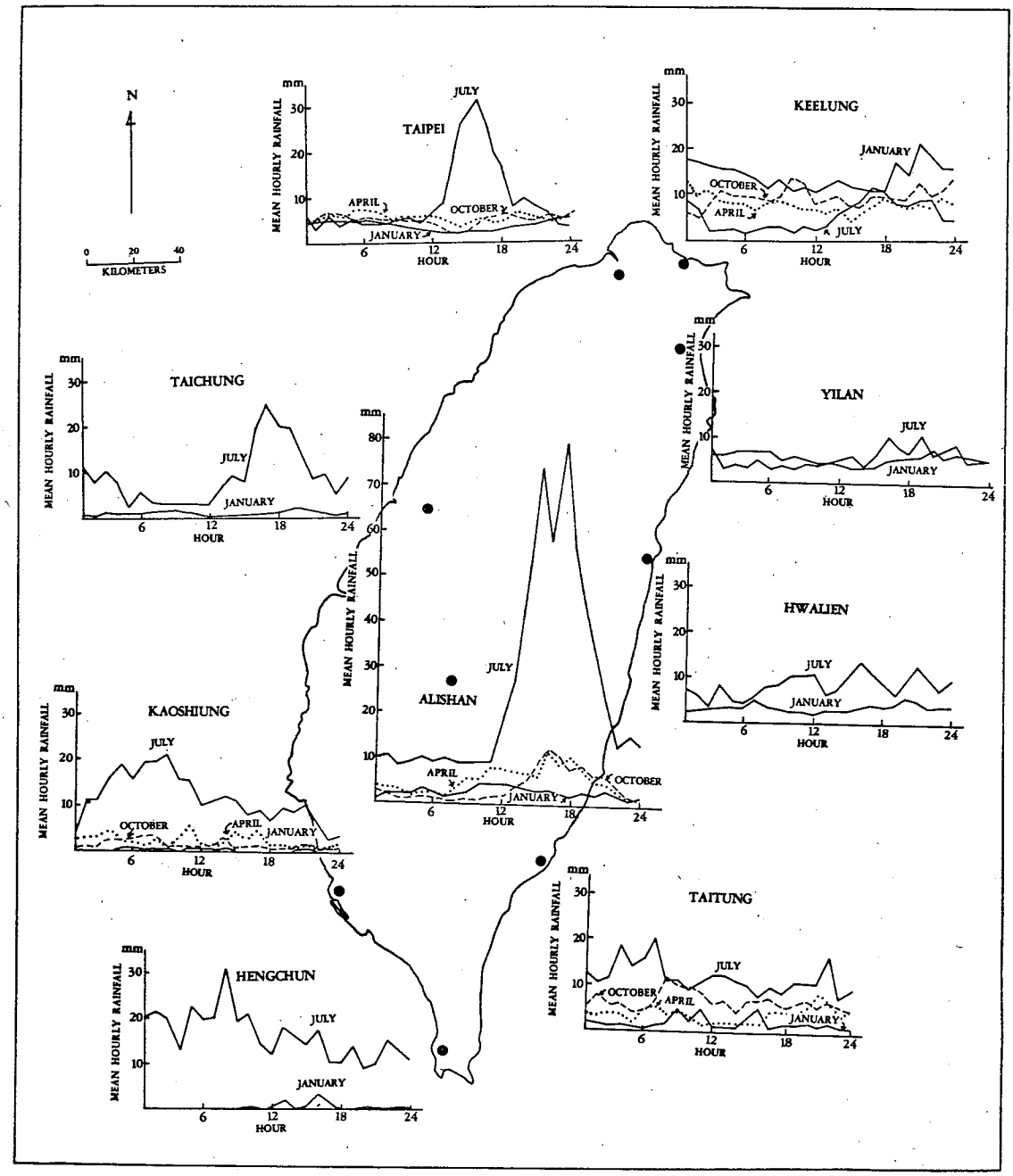

Figure 46. Diurnal rainfall variations at various Taiwan stations.

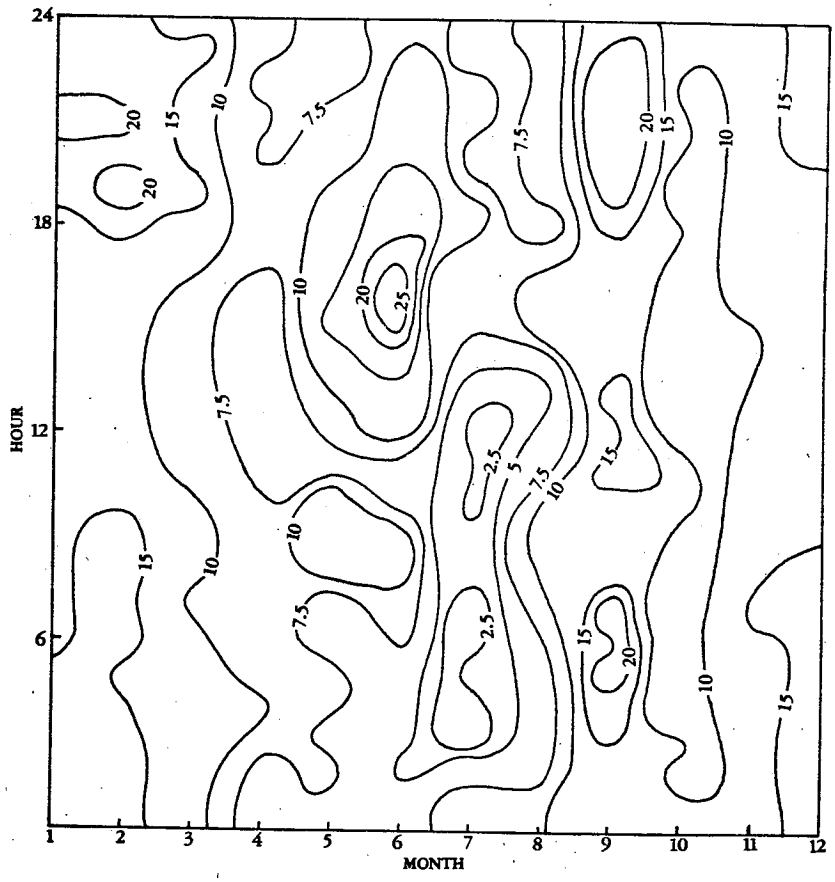

Figure 47. Diurnal rainfall variations at Keelung.

probably responsible for the large-scale nocturnal rainfall maxima over the entire northern half of Taiwan.

Taipei is located on a basin in northern Taiwan, with two river valleys facing northeast and west, respectively. The convergent wind field over the basin created by downslope winds from surrounding mountains at night accounts for the nocturnal rainfall in January. Similarly, Taichung, in a basin in the central west of the island, is also characterized by a nocturnal rainfall maximum in January.

Winter is a dry season at Kaoshiung due to its leeward position with respect to the northeast monsoon (Figure 48). Mean hourly rainfall is too slight to show any significant diurnal pattern.

Hengchun, at the southern end of the island, is also in a leeward position with respect to the northeast monsoon, and its winters are dry. Although mean hourly rainfall is very small, it shows a slight rainfall maximum in January in late afternoon. This may be caused by solar heating, a common characteristic at tropical stations. In addition, convergence between sea breezes and the northeast monsoon winds is probably also responsible for an afternoon rainfall maximum.

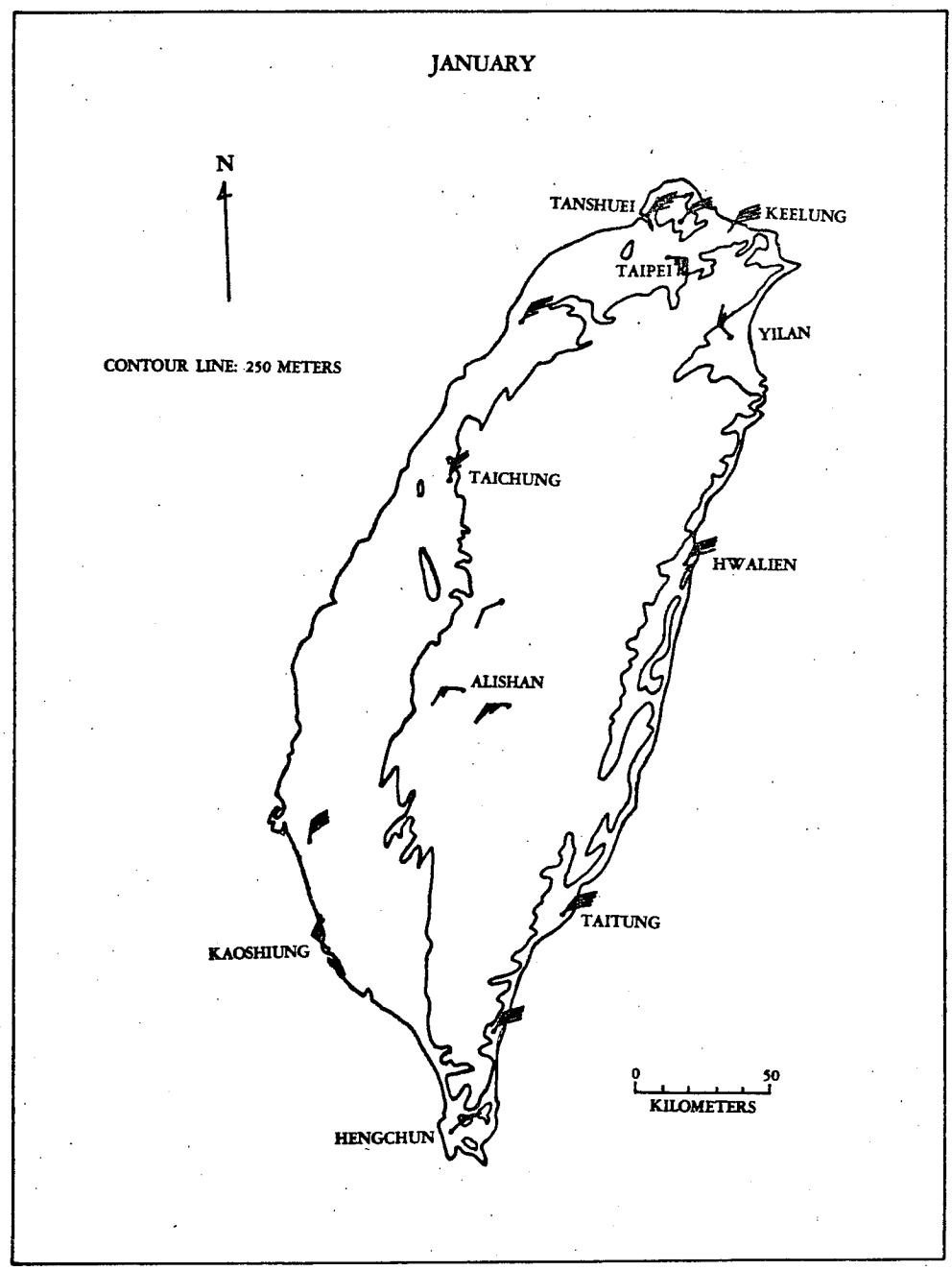

Figure 48. The prevailing winds over Taiwan in January. Each Barb represents 1 m/sec and each triangle 5 m/sec.

Taitung, on the southeast coast of the island, appears to have two peaks in the January mean hourly rainfall curve, perhaps caused by sea breezes in the morning and late afternoon. The topographic rainfall which is usually caused by the uplifting of monsoon or trade winds may be increased by the strengthening of daytime sea breezes. In addition, the convex coastline at Taitung also favors the development of a convergent wind field by daytime sea breezes. Strong afternoon solar heating is also responsible for late afternoon rainfall maxima.

Hwalien, on the central east coast of the island, appears to have a mean hourly rainfall maximum in late afternoon and early evening. The concave coastline at Hwalien favors land-breeze convergence.

As the case at Keelung, at Yilan, on the northeast coastal plain, mean hourly rainfall is higher at night in January. Land-breeze convergence associated with the concave coastline probably accounts for a nocturnal rainfall maximum in January.

Alishan, on the central mountain area of the island, shows a morning rainfall maximum in January, probably caused by valley winds and thermal convection.

Spring

With the advent of spring, the northeast monsoon weakens and wind directions become more variable. Hence, mean hourly rainfall decreases in the north and increases in the south. The diurnal rainfall pattern in April is not so pronounced as that in January at Keelung and Taipei. However, it is still characterized by nocturnal maxima at these two stations. In contrast to Keelung and Taipei, mean hourly rainfall at Kaoshiung increases and reaches a maximum in late morning and late afternoon, probably caused by an increase in daytime convective activity in spring.

At Taitung, the daytime rainfall maximum in January is replaced by a nocturnal rainfall maximum in April. The shift in the synoptic-scale circulation is probably responsible for the significant change in the diurnal rainfall pattern in April. In January, the northeast monsoon blows almost parallel to the coastline along Taitung and a land-breeze front is absent at night. In April, the southeast trades are frequent in Taiwan, intersecting the coastline near Taitung. The land-breeze front which develops from convergence between trades and land breezes at night is responsible for the nocturnal rainfall maximum in April at Taitung.

Summer

In summer, Taiwan is alternately dominated by the southwest monsoon and the southeast trades. The start of the southwest monsoon is frequently accompanied by the passage of a slow-moving front, which often produces heavy rains over the entire island. Rainfall in southern Taiwan increases abruptly in May and continues until September. In contrast, the northern end of the island, in the lee of both the southwest monsoon and the southeast trades, is much drier (Figure 49). Mean hourly rainfall increases significantly and diurnal rainfall patterns are more pronounced in July than in January at most stations except for Keelung, Yilan, and Hwalien. Mean hourly rainfall occurences at these three stations reach maxima in the late afternoon and the early evening due to increasing thermal convection and the effect of evening land breezes converging off the concave coastline.

The inland stations, such as Taipei, Taichung, and Alishan, appear to have intense mean hourly rainfall in the afternoon due to their basin or mountain location which favors strong daytime convection in summer. The diurnal rainfall variation on the southwest and southeast coasts, such as Kaoshiung, Hengchun, and Taitung, is characterized

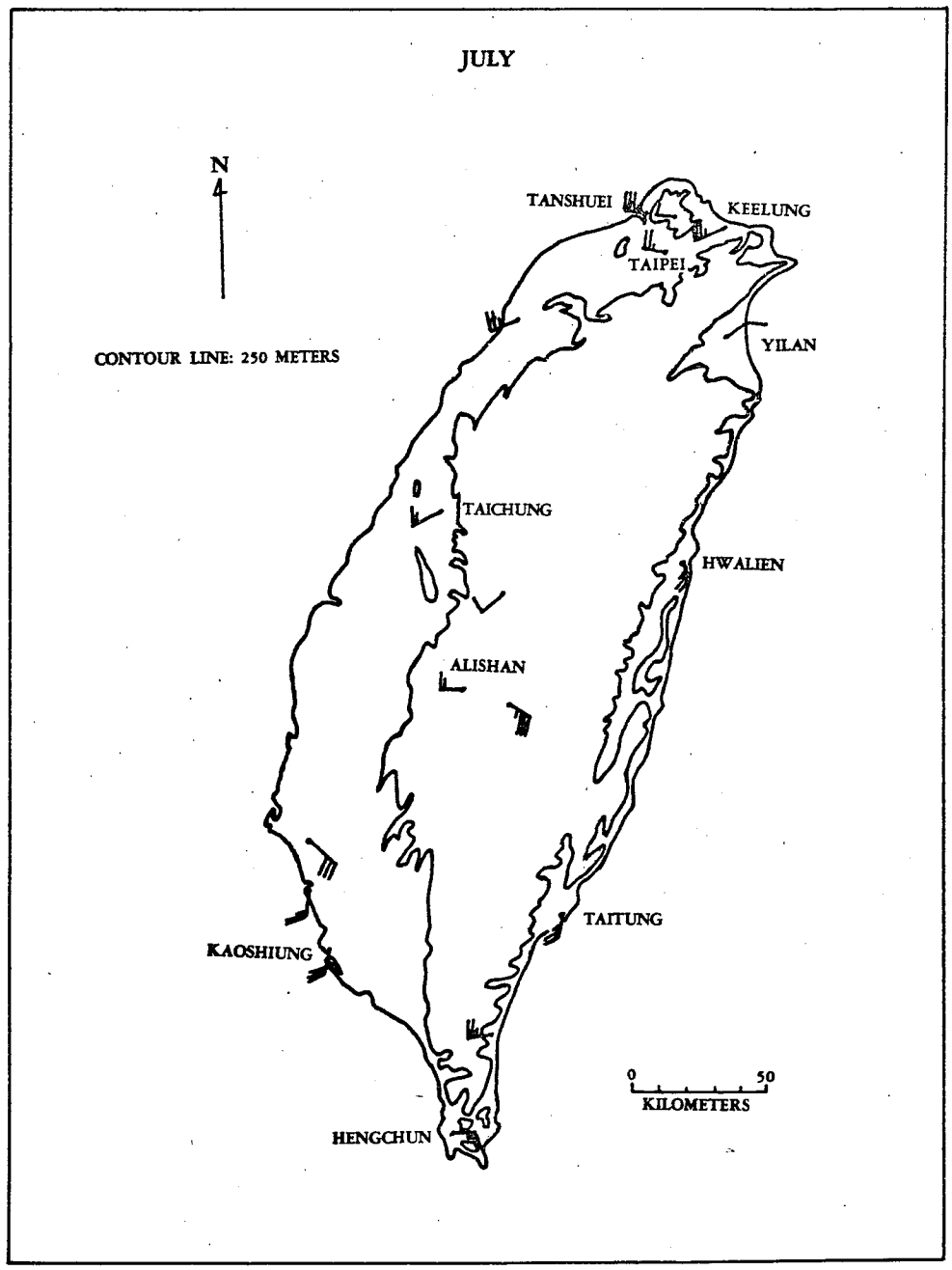

Figure 49. The prevailing winds over Taiwan in July, Legend is the same as in Figure 48.

by early morning rainfall maxima, apparently as a result of convergence between land breezes and monsoons or trades. In addition, shower clouds which are formed over the sea at night may be transported onshore by morning sea breezes. Hence, they may contribute early morning rainfall maxima to those tropical coastal stations. A mean hourly rainfall maximum at dawn is common at tropical and subtropical stations during the summer monsoon season, mainly caused by warm air advection in the lower troposphere between midnight and sunrise.

Fall

In October, the frequency of the northeast monsoon over the island increases, whereas that of the southwest monsoon decreases. However, surface temperatures remain warm and thunderstorms are still active. The diurnal rainfall variation in October is similar to that in January and April at most stations except for Alishan, where the diurnal rainfall shows a pronounced afternoon maximum, similar to that in July.

Summary of Significant Results

The diurnal rainfall pattern shows pronounced regional and seasonal variations over Taiwan. In winter, stations on the northern and eastern coasts, exposed to the northeast monsoon, show nocturnal rainfall maxima, as do stations

within a basin. Mean hourly rainfall in winter in the southwestern sector of the island is too slight to reveal any diurnal pattern.

In spring and fall, diurnal rainfall variation shows a similar pattern to that in winter at most stations except for Alishan, where mean hourly rainfall reaches a maximum at midday throughout the year because it is in the inland high-mountain area.

Several factors may account for distinct regional and seasonal variations in diurnal rainfall in Taiwan. The land-breeze front, concave coastlines, and warm-air advection at night, and radiation cooling from cloud tops, are responsible for nocturnal rainfall maxima observed at various coastal stations in Taiwan. At basin stations, the convergent wind field established by downslope winds and warm-air advection at night are responsible for nocturnal rainfall maxima. Morning onshore transport of convective clouds, formed over the sea at night, by sea breezes accounts for the early morning rainfall maxima at coastal stations in southern Taiwan.

The sea-breeze front and convex coastline are responsible for daytime rainfall maxima at many coastal stations. Valley winds and thermal convection contribute

to daytime rainfall maxima at mountain stations. Strong daytime convection in summer accounts for the pronounced afternoon rainfall maxima at basin stations.

The seasonal shift in the synoptic-scale circulation is responsible for the seasonal change in diurnal rainfall patterns. In winter, convergence between land breezes and northeast monsoon winds accounts for nocturnal rainfall maxima at windward stations in northern Taiwan. In summer, convergence between land breezes and southwest monsoon winds or southeast trade winds accounts for nocturnal rainfall maxima at windward stations in southern Taiwan. In spring and fall, winds are variable and weaker. The magnitude of diurnal rainfall is reduced.

In this study, the diurnal rainfall variation over Taiwan is investigated in the light of some theories proposed by climatologists. It is found that land and sea breezes explain well the diurnal rainfall pattern over Taiwan. No statistical data are available to justify the occurrence of such meso-scale circulation systems over Taiwan. However, it is reasonable to hypothesize their occurrence because they are common characters of coastal areas, especially in the tropics and subtropics. Defant (1951) has indicated that land and sea breezes occur in the

tropical coasts with a high degree of regularity.

Hourly rainfall is important in the study of the basin hydrological cycle which aims at the estimation of river runoff for flood forecasting. Rainfall characteristics over a basin must be understood before any hydrological study can be carried out. It is found that diurnal rainfall patterns over various sectors of the island are related to the synoptic-scale circulation, land and sea breezes, thermal convection, and topography. This study can be extended to investigate diurnal rainfall variations at various rainfall stations on a basin. The relationship between diurnal rainfall and runoff patterns can be studied by some hydrological techniques such as water-budget equations, unit hydrographs, and regression methods. The time lag between peak hourly rainfall and peak river runoff is of particular importance in flood forecasting. The mean rainfall-runoff relation should be understood so that it provides the necessary information for the study of the dispersion from the mean condition under individual storms.

CHAPTER IX

ANNUAL RAINFALL

The Stability of Means and Medians

Mean and median are two values commonly used to represent rainfall normals. Questions have been raised regarding the number of years required to obtain representative monthly and annual rainfall normals. Landsberg (1951) has proposed that in many areas of the world, a 20-year period is considered satisfactory for establishing monthly rainfall normals. However, monthly rainfall means in Hawaii reach stability only when a period of 45 years or longer is taken into account. For Djakarta, Indonesia, the January normal is reached only after a minimum of 30 years (Sandy, 1960). Usuaully, 30 to 40 years of records are recommended for annual rainfall means, and 60 to 70 years for monthly rainfall means (Biel, 1929).

In truth, however, rainfall means vary from decade to decade; the period of reference should, therefore, be specified to allow for possible changes. The 30-year average, 1901-1930, is the first "standard climatological normal," and that of 1931-1960 is the second "standard climatological normal" for this century. Several studies of climatic

changes adopted the 40-year average, 1900-1939, as the standard normal (Lamb and Johnson, 1959).

Landsberg (1951) has suggested a method to determine the number of years needed to obtain a normal by calculating successive means or medians by one-year increments. A mean or median is considered normal when the addition of one successive year does not change the value substantially. Figure 50 indicates the number of years needed to reach the stability of means or medians of annual rainfall at the seven stations in Taiwan. The rainfall normal is obtained when the absolute change in mean or median is less than 100 mm by adding rainfall of one successive year, and the situation continues for more than 30 years, i.e., the mean or median of the 30-year increments loses one-way trend, either rising or declining. Except for Taipei where 18-year records are needed to obtain both a stable mean and median, a lesser number of years is satisfactory at other stations to obtain a stable median than to obtain the mean. For example, at Tainan, 41-year records are needed to obtain a stable mean, but only 21-year records are needed for a stable median. More years are required to obtain a stable mean in the south than in the north, probably because rainfall is more variable in the south than in the north. But

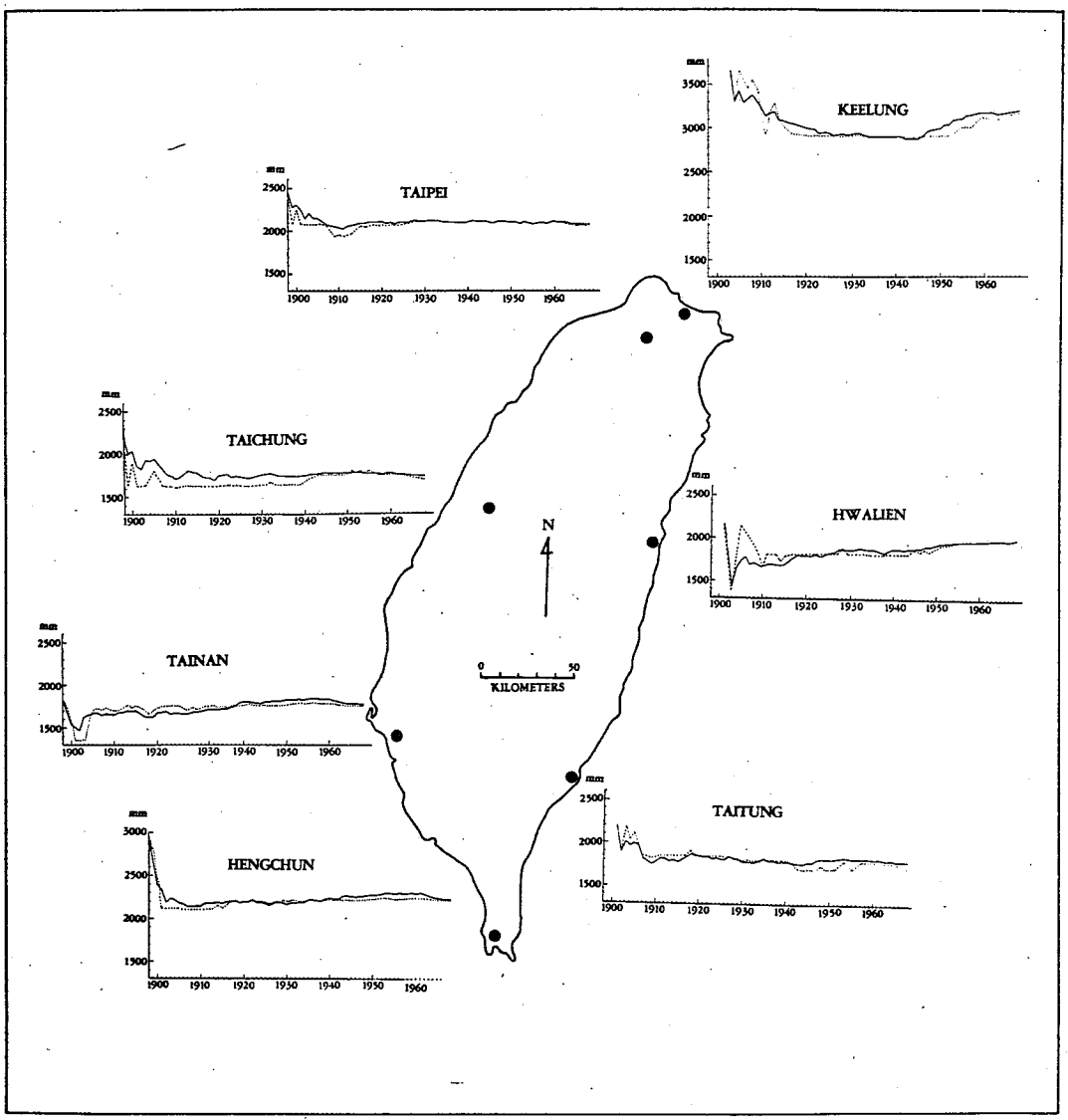

Figure 50. The stability of mean and median at various Taiwan stations.

the median does not behave similarly. No stable mean or median could be obtained for the entire study period at Keelung and Hwalien. The mean is stable only for the period 1923-1947 at Keelung, and 1918-1946 at Hwalien. Both the mean and median have increased substantially since the late 1940's at those two stations. At Taichung and Taitung, the median is stable only in the period 1907-1941; it has been fluctuating since the early 1940's. It appears that in the 1960's both the mean and median decreased over western and southern Taiwan, but in the same period they increased over northern and eastern Taiwan.

Skewness and Rainfall Probability Chart

In a normal distribution, mean and median are equal, but the sample median may be a better indication of the centrality, because extreme values will not affect the median as much as the mean. In Taiwan, both the monthly and annual rainfall means are greater than the monthly and annual medians at all stations (Table 15). The distribution of monthly rainfall means or medians is more skewed than that of annual rainfall means or medians, so the difference between mean and median is greater for monthly rainfall than for annual rainfall.

TABLE 15

MEAN AND MEDIAN VALUES OF ANNUAL AND MONTHLY RAINFALL (UNIT: MM)

	1	2	3	4	5	6	7	8	9	10	11	12	Annual
Keelung	322.4	322.6	292.8	213.1	260.4	281.7	131.2	175.0	273.2	268.1	300.3	338.4	3187.3
	322.3	308.6	287.5	194.0	243.2	247.8	94.2	164.7	235.6	225.1	261.4	324.7	3175.4
Taipei	89.2	138.8	167.0	162.5	212.5	301.3	241.4	279.6	233.6	115.2	68.0	73.3	2079.3
	78.3	126.0	154.1	133.8	195.3	275.4	202.9	258.3	196.3	95.7	60.0	67.0	2064.1
Taichung	32.2	64.8	98.3	124.2	222.2	375.1	281.1	328.3	145.3	20.0	15.6	25.8	1740.7
	20.0	48.8	89.7	101.9	196.2	321.2	227.9	252.3	77.3	5.4	10.5	17.8	1700.0
Tainan	17.5	31.3	49.7	67.4	174.0	384.7	408.3	420.5	165.6	32.7	18.4	16.4	1774.8
	8.3	18.1	35.5	46.8	135.2	374.1	315.4	345.1	118.5	12.5	4.9	6.2	1753.6
Hengchun	28.2	25.7	23.4	48.8	169.6	405.9	509.5	524.3	299.5	134.9	56.2	19.3	2238.3
	13.6	13.9	16.8	21.3	132.9	363.6	422.1	475.9	263.2	84.5	23.2	13.4	2217.4
Taitung	36.8	41.4	57.6	80.4	161.4	231.0	308.4	293.9	298.8	165.4	87.8	43.3	1811.4
	28.2	37.0	49.7	56.5	131.7	154.3	255.2	230.7	194.4	112.7	55.4	29.4	1728.0
Hwalien	66.6	87.2	103.9	117.6	197.9	208.4	229.8	238.7	305.3	255.7	154.2	77.1	2010.4
	54.3	72.0	93.0	101.6	163.3	168.0	160.6	209.3	248.9	149.7	104.6	61.8	2006.3

(Upper values denote means and lower values medians)

Skewness of rainfall distribution is evident by examining the cumulative frequency distribution of rainfall at various Taiwan stations. Figure 51 shows the cumulative frequency distribution of annual rainfall at six Taiwan stations plotted on a normal probability paper.

Skewness of rainfall frequency distribution can also be expressed by a quantity, $(100/12) \times |Ci - Mi| / Mi$, where Ci is the median and Mi is the mean of individual monthly rainfall. In a symmetrical frequency distribution, Ci = Mi, and skewness is zero (Landsberg, 1951).

Figure 52 shows the areal distribution of skewness of annual rainfall in Taiwan based on 51 stations with records of 30 years or more. Skewness is greatest along the southwest coastal plain, where more than 90% of mean annual rainfall occurs during the six summer months, April through September. Winter rainfall is almost negligible in this area and a few extreme values may raise the mean far above the median. On the other hand, skewness is least in northern Taiwan where maximum mean monthly rainfall occurs in winter, although summer is by no means dry. The total rainfall of six summer months accounts for about 40%, or slightly more, of annual total. Low skewness is also found in mountain areas where the seasonal concentration of

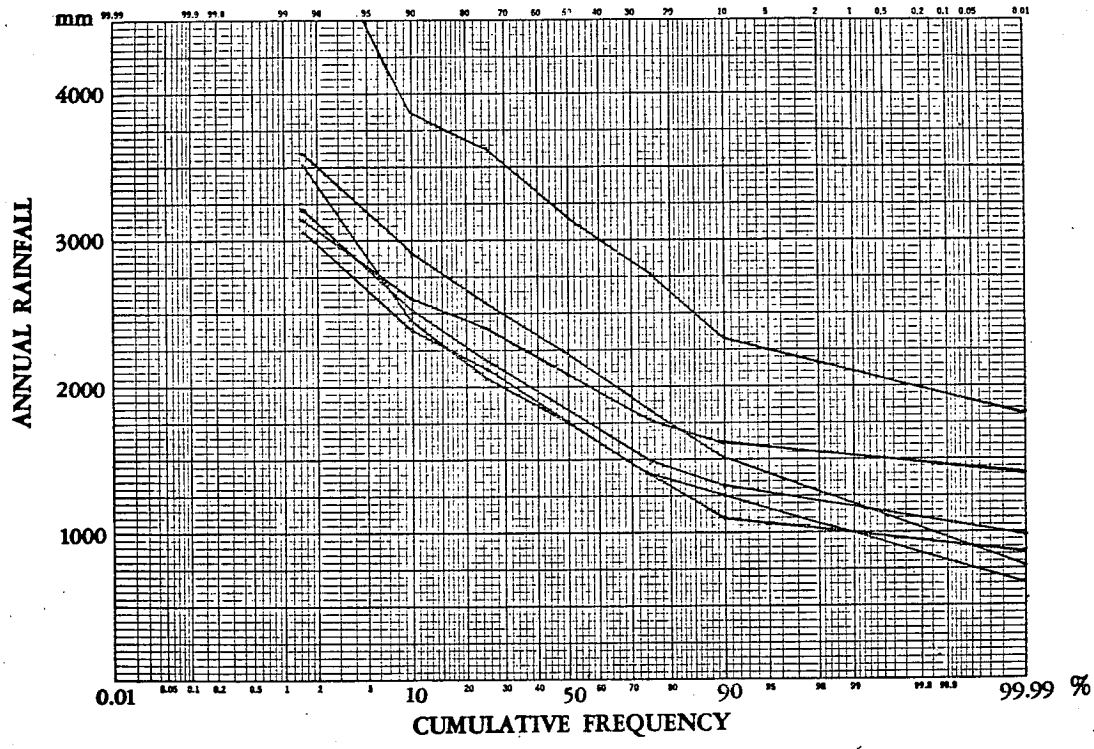

Figure 51. Cumulative frequency distribution of the mean annual rainfall at the six Taiwan stations.

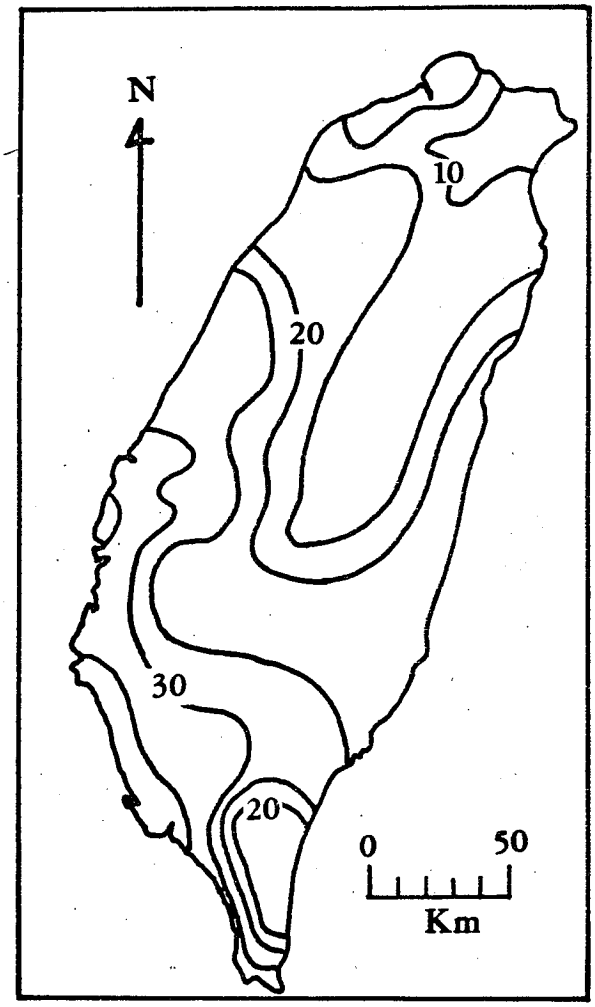

Figure 52. Spatial variations in the skewness of rainfall.

rainfall is not as distinct as in the southwest coastal plain. This conforms Sandy's (1960) finding that the mean is a better measure of the rainfall normal during the rainy season than during the dry season. The regional contrast of rainfall skewness over Taiwan can be explained by the variability of the frequency of synoptic flow types and by rainfall characteristics associated with them. As discussed in previous chapters, the winter synoptic flow types, which are main rainfall sources in northern Taiwan, show smaller frequency variabilities than do the summer synoptic flow types, which contribute almost all annual rainfall to southwestern Taiwan. In addition, rainfall characteristics associated with summer synoptic flow types are more variable as evidenced by higher mean, standard deviation, and maximum of daily rainfall associated with them.

Perhaps rainfall at the various Taiwan stations is caused by non-uniform weather systems, modified locally by topography. To investigate this hypothesis, a rainfall probability chart was constructed by plotting median or mean annual rainfall against the probability of individual annual rainfall of less than a given quantity. Such probability curves for stations within a region should appear as

straight lines, if annual rainfall at all stations is uniformly caused by the same weather systems, and variation in amounts is a function only of topography, exposure, and other local peculiarities (Landsberg, 1951).

Figure 53 shows the rainfall probability chart based on annual rainfall at eight Taiwan stations. As seen, annual rainfall at the various Taiwan stations appears to be the result of different weather systems, and not a function only of topography.

Synoptic Aspects of Inter-annual Rainfall Variations

In order to understand the relationship between the inter-annual rainfall variations at various Taiwan stations and the inter-annual frequency variations of synoptic flow types, a stepwise multiple regression analysis is employed to calculate the coefficients of determination. The coefficient of determination is defined as the percentage deviation from the mean annual rainfall explained by the annual frequency of a certain synoptic flow type. Annual rainfall is a dependent variable and annual frequencies of synoptic flow types are independent variables. The results are presented in Table 16. Although the Mongolian anticyclone is the main rainfall source in winter, it accounts

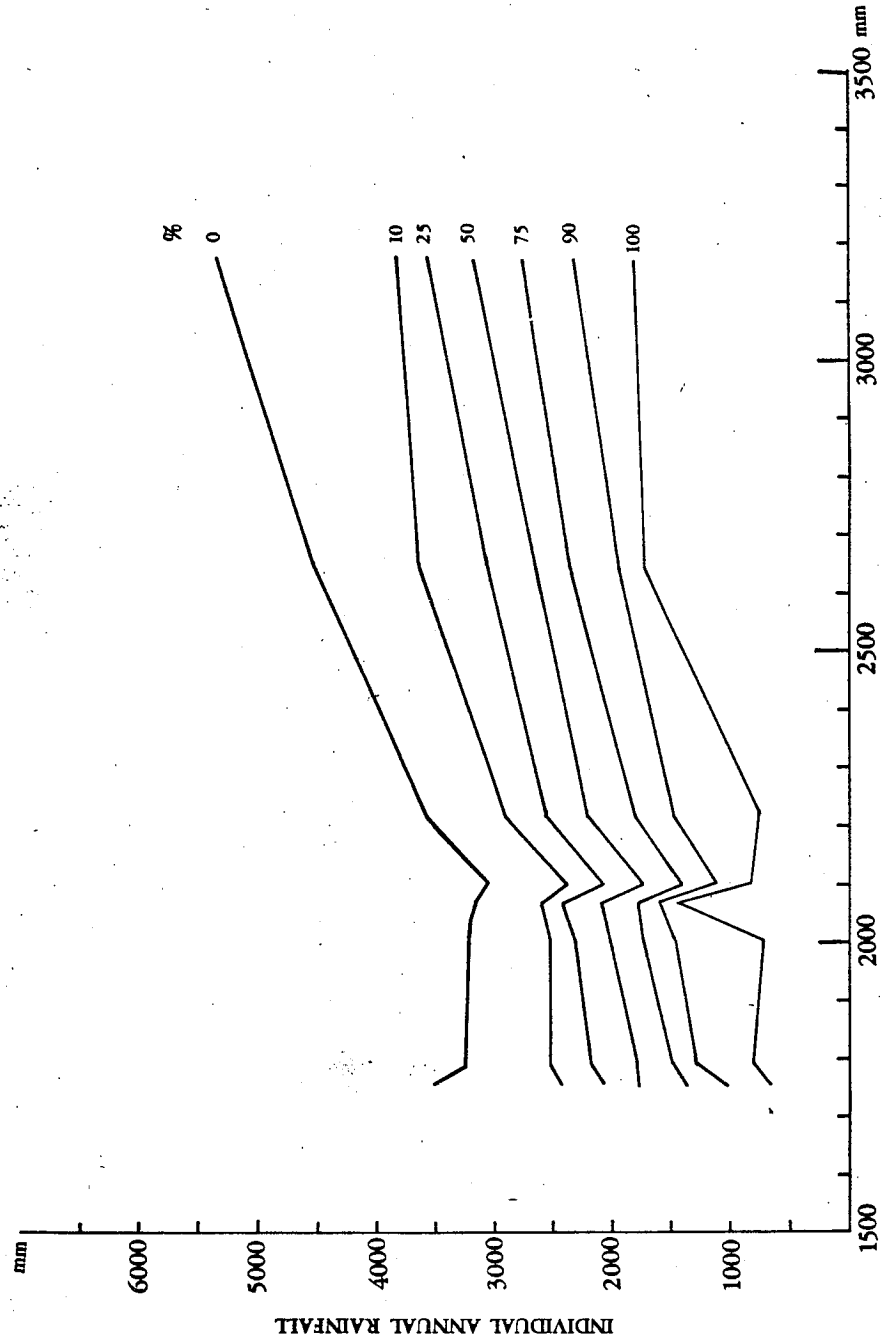

Figure 53. The rainfall probability chart based on the eight Taiwan stations.

TABLE 16

COEFFICIENTS OF DETERMINATION BETWEEN ANNUAL FREQUENCIES OF SYNOPTIC FLOW TYPES AND ANNUAL RAINFALL

Steps	1	2	3	4	5	6	7	8	9	Total
Keelung	0.5536 6	0.1941 2	0.0461 5	0.1191 1	0.0298 11	0.0267 7	0.0216 10	0.0078 3	0.0016 9	0.9993
Taipei	0.4542 11	0.2412 2	0.0987 8	0.0925 3	0.0242 4	0.0078 9	0.0406 5	0.0288 1		0.9880
Taichung	0.3771 11	0.1287 10	0.1184 7	0.0474 9	0.0572 8	0.0176 4	0.0128 6	0.0294 1	0.0870 5	0.9916
Kaoshiung	0.3876 9	0.2319 4	0.2179 3	0.0677 7	0.0570 8	0.0147 6	0.0070 5	0.0155 2	0.0008 1	1.0000
Hengchun	0.5060 2	0.0811 7	0.2798 8	0.0209 4	0.0609 1	0.0232 9	0.0256 6			0.9974
Taitung	0.2100 2	0.1240 8	0.1310 3	0.1046 5	0.0984 11	0.0741 10	0.0918 4	0.1082 9	0.0476 1	0.9896
Hwalien	0.3694 3	0.3026 4	0.1597 11	0.0610 8	0.0423 10	0.0212 9	0.0038 1	0.0200 2	0.0157 6	0.9958
Yilan	0.4569 2	0.3048 4	0.0427 10	0.0331 11	0.0438 7	0.0082 3	0.0181 8	0.0087 5	0.0778 9	0.9941
Alishan	0.3789 11	0.1520 3	0.1416 9	0.1327 8	0.0149 5	0.0462 6	0.0489 7	0.0750 2	0.0031 4	0.9933

(Lower numbers indicate synoptic flow types)

for only about 12% of the total inter-annual rainfall variation at Keelung, and about 6% at Hengchun. At the other stations, it accounts for almost negligible percentages of the inter-annual rainfall variation. This is also reflected by low correlations between its annual frequency and the annual rainfall at those stations (Table 17). The Mongolian anticyclone is a rather dependable rainfall source over Taiwan as also evidenced by its low frequency variability (Chapter II). On the other hand, the Mongolian cutoff anticyclone appears to be a more dominant variable than the Mongolian anticyclone in explaining inter-annual rainfall variations at most stations. It is the most important variable accounting for the inter-annual rainfall at Hengchun, Yilan, and Taitung. At Hengchun and Yilan about 50% of the total inter-annual rainfall variation is due to the inter-annual frequency variation of the Mongolian cutoff anticyclone. This is also reflected by significantly high correlation coefficients between the annual frequency of the Mongolian cutoff anticyclone and the annual rainfall at those two stations (Table 17). At Keelung and Taipei, the Mongolian cutoff anticyclone is the second important variable in explaining the total inter-annual rainfall variations.

TABLE 17

COEFFICIENTS OF CORRELATION BETWEEN ANNUAL FREQUENCIES OF SYNOPTIC FLOW TYPES AND ANNUAL RAINFALL

Flow Types	1	2	3	4	5	6	7	8	9	10	11
Keelung	0.14	-0.56	0.23	0.65	0.30	-0.74	0.46	0.12	-0.14	0.05	0.13
Taipei	0.02	-0.49	0.27	0.19	-0.04	0.09	-0.13	0.48	0.34	0.01	-0.67
Taichung	-0.32	-0.03	0.07	0.11	0.02	0.11	-0.15	0.28	0.41	0.40	-0.61
Kaoshiung	0.38	-0.34	-0.28	0.11	0.11	-0.35	-0.05	0.46	0.62	0.15	-0.29
Hengchun	0.50	-0.71	-0.05	0.01	-0.08	-0.24	0.15	0.65	0.39	0.18	-0.17
Taitung	0.31	-0.46	-0.08	0.32	0.05	-0.33	0.22	-0.01	0.13	0.11	0.22
Hwalien	0.50	-0.07	-0.61	0.33	-0.21	-0.34	0.48	-0.14	-0.46	-0.22	0.53
Yilan	0.07	-0.68	0.45	0.64	0.39	-0.53	0.07	0.13	-0.18	-0.14	0.17
Alishan	-0.43	-0.01	0.51	-0.02	0.30	0.04	-0.26	0.15	0.51	0.12	-0.62

At Hwalien, the Taiwan low is the most important variable accounting for the total inter-annual rainfall variation; i.e., about 37% of its total inter-annual rainfall variation is explained by the inter-annual frequency variation of the Taiwan low.

Although the polar front over Taiwan contributes large amounts of annual rainfall to all stations, its annual frequency accounts for about 30% of the total inter-annual rainfall variation at Yilan and Hwalien, and about 23% at Kaoshiung. At the other stations, the coefficients of determination are very low. The correlation coefficient between the annual rainfall and the annual frequency of the polar front over Taiwan is highest at Keelung: 0.64. However, the variable of the polar front over Taiwan is excluded from the regression equation. This suggests that the explanative power of the polar front over Taiwan is masked by the North Pacific subtropical anticyclone due to the high correlation coefficient between those two synoptic flow types (Table 18). The coefficients of determination for the polar front south of Taiwan are very low at all stations. It is a poor variable for explaining the total inter-annual rainfall variation over Taiwan.

The North Pacific subtropical anticyclone is the most

TABLE 18

COEFFICIENTS OF CORRELATION AMONG ALL SYNOPTIC FLOW TYPES

	1	2	3	4	5	6	7	8	9	10	11
1	1.00	-0.42	-0.59	-0.38	-0.57	0.01	0.17	0.33	0.25	-0.11	0.36
2		1.00	0.60	-0.14	-0.14	-0.16	0.17	-0.17	-0.27	-0.25	-0.01
3			1.00	0.32	0.60	-0.19	-0.17	0.18	-0.02	0.02	-0.22
4				1.00	0.62	-0.67	0.32	-0.21	-0.49	-0.17	-0.06
5					1.00	-0.68	-0.06	-0.07	0.01	-0.06	-0.21
6						1.00	-0.54	-0.61	0.13	0.19	-0.25
7							1.00	-0.56	-0.49	-0.47	0.43
8								1.00	0.53	0.42	-0.54
9									1.00	0.38	-0.30
10										1.00	-0.07
11											1.00

dominant variable accounting for the total inter-annual rainfall variation at Keelung. About 55% of the total variation is attributable to the inter-annual frequency variation of the North Pacific subtropical anticyclone. This is also reflected by the high correlation coefficient (-0.74) between the annual rainfall at Keelung and the annual frequency of the North Pacific subtropical anti-cyclone.

The annual frequency of the southwest monsoon appears to be a poor variable in explaining the total inter-annual rainfall variation over Taiwan. It accounts for only about 12% of the total inter-annual rainfall variation at Taichung and less than 10% at the other stations. This is also reflected in the low correlation coefficients between the annual frequency of the southwest monsoon and the annual rainfall at all Taiwan stations.

Although typhoons are main rainfall sources in summer at all stations, they are significant only at Kaoshiung and Hengchun in the explanation of total inter-annual rainfall variation. At Kaoshiung, nearly 40% of the total inter-annual rainfall variation is attributable to the inter-annual frequency variation of the southern-type typhoon. At Hengchun, the inter-annual frequency variation of the

northern-type typhoon accounts for about 28% of the total inter-annual rainfall variation. At the other stations, less than 15% of the total inter-annual rainfall variation is attributable to the inter-annual frequency variation of either the northern-type or southern-type typhoon. The explanative ability of typhoons may be masked by other synoptic flow types which correlate highly with them.

The Kyushu-type typhoon is the second significant variable accounting for the total inter-annual rainfall variation at Taichung, but it explains only 13% of the total variation.

It is surprising to find that the monsoon trough is the most significant variable in the explanation of the total inter-annual rainfall variations at Taipei, Taichung, and Alishan. The coefficient of determination is about 45% at Taipei, and nearly 40% at Taichung and Alishan. The correlation coefficients between the annual frequency of the monsoon trough and the annual rainfall at those three stations are significantly high.

Regression equations which show the relationship between the annual rainfall at the nine Taiwan stations and the annual frequencies of the eleven synoptic flow types are presented in Appendix E. Since the inter-annual frequency

variations of synoptic flow types explain almost all inter-annual rainfall variations at the nine stations (Table 16), the computed annual rainfall almost equals the observed annual rainfall for the period 1959-1969. This is also evidenced by very small residuals between computed and observed annual rainfall in every year at all stations (Table 19). The residuals appear to be largest at Taitung but they varied only from 5.2% in 1959 to -4.8% in 1960. It can be concluded that annual rainfall over Taiwan can be predicted well from the annual frequencies of the eleven synoptic flow types by stepwise multiple regression equations.

Floods and Droughts

Floods and droughts have various definitions. Climatologists may define floods and droughts by precipitation anomalies. Hydrologists usually define floods and droughts by stream flow anomalies. Agriculturists would be more concerned with soil moisture as a criterion to define floods and droughts. Since floods and droughts greatly affect agriculture, their physical causes have attracted much attention. The occurrence of floods and droughts over an area is frequently attributed to variations in the atmospheric circulation and solar activity. The purpose of this section

TABLE 19

RESIDUALS BETWEEN THE COMPUTED AND OBSERVED ANNUAL RAINFALL (UNIT: MM)

	Keelung	Taipei	Taichung	Kaoshiung	Hengchun	Taitung	Hwalien	Yilan	Alishan
1959	6.9	-1.2	11.2	-0.1	20.6	96.0	-29.0	-25.0	-54.9
1960	6.7	7.0	-3.2	0.4	2.9	-69.3	-12.0	22.6	39.0
1961	9.7	-8.0	19.4	-0.5	-10.0	56.3	53.2	-33.4	-38.2
1962	-9.8	1.5	-21.3	-0.9	-51.1	-7.8	-13.8	64.6	-11.4
1963	-1.2	-0.1	1.7	0.1	-5.0	-46.3	4.2	-5.5	3.0
1964	-8.6	-1.4	-32.4	-1.5	-7.2	-27.3	13.6	25.8	-136.7
1965	17.5	2.6	54.1	0.8	27.5	27.6	1.7	-26.5	35.4
1966	-6.8	1.0	-75.9	0.1	-32.3	4.7	-14.4	29.1	16.2
1967	18.4	5.1	24.9	2.0	54.6	33.3	-34.3	-21.4	126.2
1968	-26.4	-6.0	38.6	-0.8		-37.9	35.2	-8.3	-51.5
1969	-6.2	-0.3	-17.0	0.7		-29.6	-4.3	-22.0	72.6

is to investigate physical causes of floods and droughts over Taiwan for the period 1897 through 1969. A flood year is defined as one with annual rainfall two standard deviations above normal, whereas a drought year is defined as one with annual rainfall two standard deviations below normal.

Table 20 shows frequencies of floods and droughts over Taiwan, locations of centers of action, and the strength of the westerlies. Data of locations of centers of action and zonal index were obtained from Wang (1964). Zonal index is defined as the percentage deviation of surface pressure difference between 40°N and 70°N from the long-term mean. It appears that Keelung has experienced fewest floods and droughts; whereas Taichung has suffered the most from floods and Taichung and Taipei have experienced more droughts than any of the other stations.

Table 20 shows that the center of the Aleutian low is located more southward and eastward during flood years than during drought years. Southern and eastern Taiwan tend to suffer from droughts when the Aleutian low is close to its normal latitudinal position. The relationship does not hold so well for the Siberian anticyclone and the equatorial trough. The Siberian anticyclone is located farther north

TABLE 20

THE FREQUENCIES OF FLOODS AND DROUGHTS OVER TAIWAN AND THEIR RELATIONS TO THE POSITIONS OF THE ALEUTIAN LOW, THE SIBERIAN ANTICYCLONE, THE MONSOON TROUGH, AND TO ZONAL-INDEX

	Frequency	Aleutian Low		Siberian Anticyclone		Monsoon Trough	Zonal Index (%)
		N	W	N	W	S	E	40-70°N
Keelung	7	49.2	174.2	50.8	100.8	6.0	147.0	-68.4
	9	53.1	170.6	53.1	102.5	12.5	144.3	3.4
Taipei	10	53.0	173.6	53.5	103.5	10.5	148.5	-44.9
	15	52.7	172.7	52.3	100.0	9.5	146.3	1.5
Taichung	14	51.1	176.1	52.5	104.6	11.4	147.5	-34.6
	15	53.3	166.6	50.4	101.7	10.4	150.4	0.1
Tainan	9	52.2	175.6	54.4	102.2	11.1	150.0	-41.9
	12	53.3	174.2	51.7	105.0	13.3	147.5	3.2
Hengchun	9	51.7	170.6	51.1	102.2	8.9	143.3	-13.0
	13	54.4	170.6	53.8	104.4	12.8	146.7	-13.7
Taitung	11	51.0	174.0	51.5	101.0	12.0	141.0	-35.2
	11	54.4	175.6	52.5	100.0	10.6	152.5	19.0
Hwalien	12	50.6	175.0	53.9	102.2	11.7	141.1	-35.1
	13	52.8	170.0	50.8	102.1	11.3	152.9	13.6
Normal (1897-1960)		54.6	172.9	51.2	104.0	10.0	148.6	-1.2

(Upper values refer to floods and lower values refer to droughts)

when Taipei, Taichung, Tainan, and Hwalien experience floods, than when those stations suffer droughts. The reverse pattern occurs at Keelung, Hengchun, and Taitung. The Siberian anticyclone is located farther east during flood years than during drought years at Taipei, Taichung, Taitung, and Hwalien, whereas at Keelung, Tainan, and Hengchun it is located farther west during these periods respectively. At the latter three stations, flood years are associated with more northerly location of the equatorial trough than drought years. At Keelung, Taipei, and Tainan, the equatorial trough is farther east during flood years than during drought years.

It is notable that zonal-index correlates well with frequencies of flood and drought years. With the exception of Hengchun, where both flood and drought years are associated with almost equal strength of the westerlies, the other six stations indicate that flood years are accompanied by high zonal index, whereas drought years are associated with low zonal index. As discussed before, low zonal index favors typhoons, the Taiwan low, and the Mongolian anticyclone producing heavy rainfall over Taiwan. In contrast, the North Pacific subtropical anticyclone and the Mongolian cutoff anticyclone invade Taiwan more frequently during the high zonal-index circulation pattern. The prominent drought

period 1963 through 1967 over western and southern Taiwan was associated with decreased frequency of typhoons and with increased frequency of the North Pacific subtropical anticyclone.

Figures 54 and 55 show inter-annual variation in Wolf's sun-spot number and flood and drought years at seven stations for the period 1897-1969. The 11-year sun-spot cycle is evident. Solar activity also shows a secular trend. It increased from the turn of this century, reaching a maximum in the 1950's and has decreased since then. Figures 54 and 55 also show that at least one station experienced flood or drought almost every year. However, large-scale floods and droughts rarely occurred. Floods covering four stations or more occurred only in 1939, 1947, and 1953. The 1939 and 1947 floods were associated with sun-spot maxima, whereas the 1953 flood was accompanied by a sun-spot minimum. On the other hand, droughts covering four stations or more occurred in 1923, 1933, 1963, 1964, and 1965, all associated with sun-spot minima. Hence it can be tentatively concluded that large-scale floods and droughts over Taiwan tend to occur during periods of extreme solar activity. Perhaps the response of the atmospheric circulation to solar activity is most significant during periods of sun-spot maxima and minima.

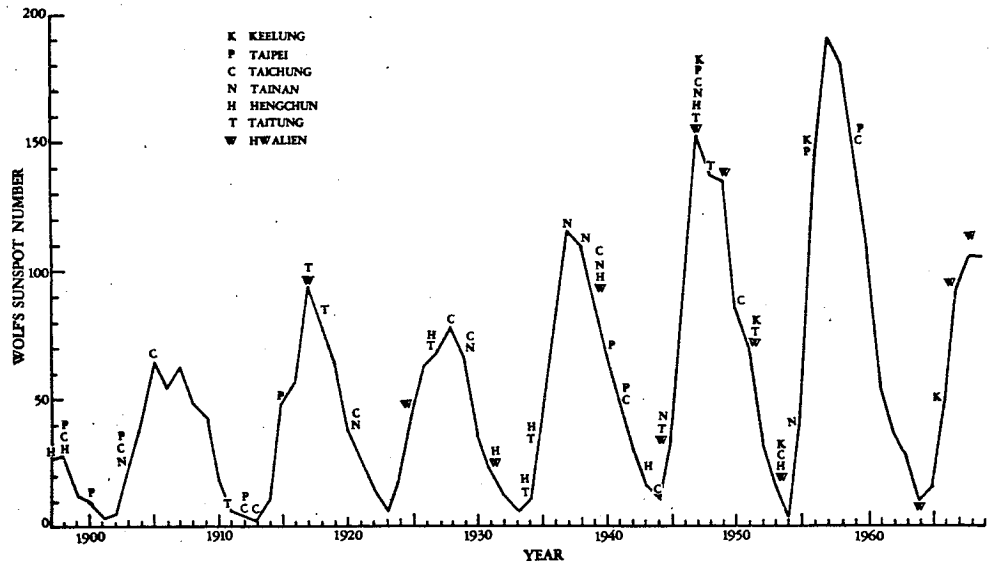

Figure 54. The inter-annual variation in Wolf's sunspot number and flood years at various Taiwan stations.

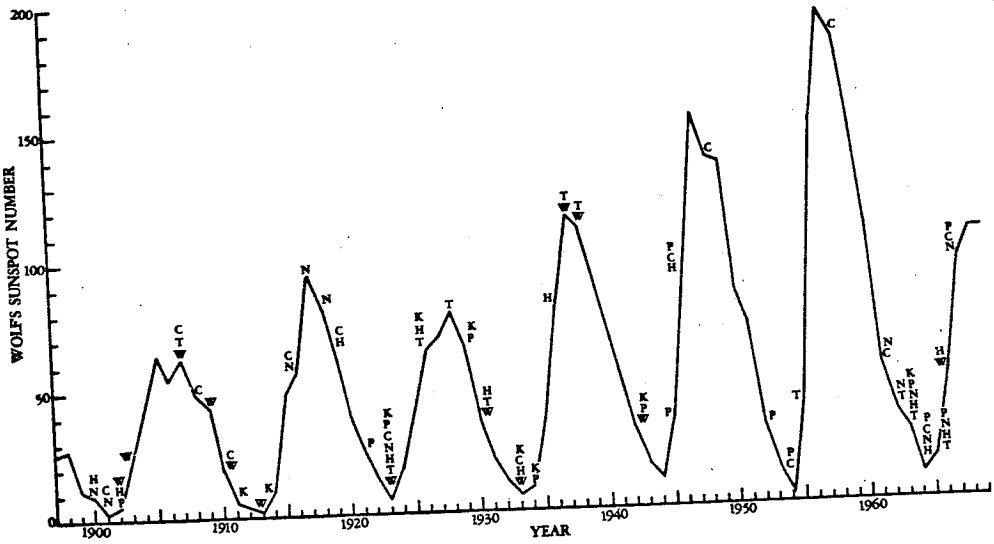

Figure 55. The inter-annual variation in Wolf's sunspot number and drought years at various Taiwan stations.

Frequencies of floods and droughts over Taiwan show distinct secular trends. Droughts occurred more frequently during the first three decades of this century and during the 1960's, whereas floods occurred more frequently during the 1940's and the 1950's.

Summary of Significant Results

The number of years required to obtain a stable mean or median varies from station to station over Taiwan. It required at least 18 years to obtain a stable mean or median. At Keelung and Hwalien, no stable mean or median can be obtained for the 73-year period 1897-1969. Annual rainfall is extremely skewed over southern Taiwan where rainfall concentration in summer is pronounced. The rainfall probability chart indicates that annual rainfall over Taiwan results from different weather systems and is not a simple function of topography.

Stepwise multiple regression analysis suggests that the total inter-annual rainfall variation over Taiwan is attributable to the inter-annual frequency variation of synoptic flow types, as reflected by very small residuals between the computed and observed annual rainfall. The most powerful variable accounting for the total inter-annual rainfall variation is the North Pacific subtropical

anticyclone at Keelung, the monsoon trough at Taipei, Taichung, and Alishan, the southern-type typhoon at Kaoshiung, the Mongolian cutoff anticyclone at Hengchun, Taichung, and Yilan, and the Taiwan low at Hwalien. It appears that the center of action such as the North Pacific subtropical anticyclone is the most important physical cause of the climatic fluctuation over Taiwan. Both the Mongolian cutoff anticyclone and the monsoon trough are associated with the extension of the North Pacific subtropical anticyclone over or near Taiwan, a high zonal-index circulation. The explanative ability of the polar front and the typhoon may be masked by the North Pacific subtropical anticyclone, the Mongolian cutoff anticyclone, and the monsoon trough.

Floods and droughts over Taiwan are found to be significantly related to the position of the Aleutian low and to zonal-index. Floods tend to occur over Taiwan when the Aleutian low is displaced southward and eastward of its normal position. This conforms the previous finding that the North Pacific subtropical anticyclone is the most important variable accounting for climatic fluctuation over Taiwan. Long-term annual positions of the North Pacific subtropical anticyclone are not available and the direct investigation of the relationship between its position and

floods and droughts over Taiwan is not possible. However, it is a well known fact that the position of the Aleutian low is closely related to that of the North Pacific sub-tropical anticyclone. Droughts tend to occur over Taiwan when the Aleutian low is close to its normal latitudinal position. No consistent relationship is found between the meridional position of the Aleutian low and droughts over Taiwan. Zonal-index correlates well with flood and drought frequencies over Taiwan. High zonal-index favors Taiwan with droughts, whereas low zonal-index favors Taiwan with floods. There is at least one area suffering from flood or drought almost every year. Large-scale floods and droughts tend to occur during periods of extreme solar activity. Large-scale floods may occur during periods of either sun-spot maxima or minima, whereas large-scale droughts occur consistently during periods of sun-spot minima.

CHAPTER X

SECULAR RAINFALL VARIATIONS

Method

Secular rainfall variation comprises a topic of interest to many scholars. Kraus (1955a and b) found that an abrupt rainfall decrease occurred at the end of the 19th century in the tropics and along east coasts of the subtropics, e.g., east coasts of North America and Australia. This dry condition terminated during the 1930's and 40's at different stations. In contrast, Arakawa (1956a and b) pointed out that a wet period in higher latitudes, e.g., China, Korea, and Japan, began around 1900 and ended about 1930. Both Kraus' and Arakawa's findings have been confirmed by Lamb and Johnson (1959, 1961) and Lamb (1966) in their sequential studies relating climatic variations to the general circulation. Though neither Kraus nor Lamb studied the rainfall variation over Taiwan, located off China's southeast coast, a trend similar to that of eastern North America and Australia can be expected. In a study of the secular variation of precipitation over monsoon Asia, Yoshimura (1971) places Taiwan in a single region in terms of the amplitude of the secular rainfall variation for

January, but in two regions for July. However, the secular rainfall variation on Taiwan is more complicated than that. The complexity of combined elements of varied landforms, transitional location between a large continent and the ocean, and unique monsoon and trade systems create a distinct regional pattern of secular rainfall variation. The purpose of this chapter is to discuss the regionality of that variation on Taiwan and to relate it to the general circulation. Agreement will be sought with the findings of others regarding the secular rainfall variation over other regions of the world.

In climatology, the word "secular" usually refers to modern instrumental meteorological observations which cover a span of more than a decade to a few centuries (W.M.O., 1966). Two common methods applied to long-term rainfall records to study these variations over various regions of the world are (1) moving average, and (2) residual masses.

Ten and thirty-year moving-average curves of rainfall have been frequently used to smooth out short variations so that longer variations can be revealed more clearly. This method is quite helpful in revealing the form of well-defined long-period variations in a series (W.M.O., 1966). However, the moving-average technique suffers certain serious

disadvantages when long-term variations in a series are ill-defined. Grant (1952) has pointed out that the moving-average method when applied to a random series gives rise to a series which is no longer random in character. It also tends to shift the phase of some of the short fluctuations and results in a reverse trend of the original series. Moreover, each subsequent value is given the same weight. Thus a single extreme value may considerably affect the long-term mean.

In contrast, a residual-mass curve tends to suppress amplitudes of short variations and to show long-term trends more clearly (W.M.O., 1966). The secular rainfall variation over the island of Taiwan was studied by constructing annual and seasonal rainfall residual-mass curves for seven stations for which 72 years (1897-1968) of records are available. An effort was made to first identify long-term dry and wet periods for different sectors of the island through trends of rainfall residual-mass curves at various stations. Stations dominated by the same climatic controls were assumed to show similar changes in trends of residual-mass curves, from which groupings of stations could be achieved.

A final purpose was to seek those physical factors such as the strength and pattern of the general circulation and solar activity, which are responsible for any significant

change in rainfall series of the island and/or regional pattern in secular rainfall trends. Kraus (1955a and b) has pointed out that the confirmation of various hypotheses regarding causes of climatic changes and of confusing features of rainfall records over many areas can be solved successfully from a systematic investigation of a long series of synoptic weather charts. No attempt was made to analyze series of synoptic weather charts for the 72-year study period due to the lack of accurate weather maps. However, surface synoptic flow types were studied in detail to seek their relation to rainfall from 1959 through 1969. It was found that low zonal-index favors Taiwan with heavy rainfall.

Residual-mass curves are used in hydrology to calculate the storage or deficit of stream flow and reservoirs over a long period. As early as 1919, this technique was used by Barnes (1919) to determine the true long-period average rainfall in England. Later, Kraus (1955a and b) used it to study secular rainfall variations in the tropics. Some Japanese climatologists (Sekiguti, 1964; Kukuchi, 1970) used residual-mass curves to study the spatial variation in the secular rainfall pattern over Japan.

One advantage of using the residual-mass curve is that the fixed mean used for calculation need not be a true long-term average. Attention is paid to the shape of the curves. A period with an average rainfall above the chosen mean is reflected in rising or concave curve, whereas a period with an average rainfall below the chosen mean is reflected in a descending or convex curve (Barnes, 1919).

A residual mass can be expressed either by the cumulative amount of rainfall deviation from a chosen mean or by the cumulative percentual deviation. The advantage of the latter is that a single extreme value will not affect the whole series significantly. In the present study, the cumulative percentual deviation from a chosen mean rainfall is calculated by the following formula (Kraus, 1955a and b):

$$Y_n = 100 \sum_{l=1}^{n} \left(\frac{r_l}{\bar{r}} - 1 \right) - 100 \sum_{l=1}^{n^*} \left(\frac{r_l}{\bar{r}} - 1 \right)$$

where

Y_n : cumulative percentual deviation from mean for the nth year.

r_l : rainfall for the nth year.

$\bar{r}$: mean rainfall for the standard 60-year period, 1909-1968.

n^* : represents the year 1908.

Annual and seasonal rainfall residual-mass curves at seven stations are shown in Figures 56 and 57, respectively. The sum of monthly rainfall from October to April was used to calculate winter residual masses and that from May to September was used to calculate summer residual masses.

Regionalization

Figure 56 shows residual-mass curves of annual rainfall at seven stations in different climatic regimes of the island. Except for Taipei and Taitung, the curves show a pronounced dry period around the start of the 20th century, continuing until the 1930's at Taichung, Tainan, and Hengchun, and until the 1940's at Keelung and Hwalien.

A wet period has been observed since then but terminated around 1960 at Taichung, Tainan, and Hengchun. On the other hand, a wet period extended from 1946 to 1968 at Keelung. The trend of the annual residual-mass curve at Hwalien is similar to that at Keelung except that the curve flattens out between 1937 and 1946.

The contrast in secular variations of annual rainfall between stations in the south and those in the north reflects their different rainfall sources. Keelung and Hwalien, on the northern and eastern coasts, windward location with respect to the northeast monsoon, have maximum mean monthly

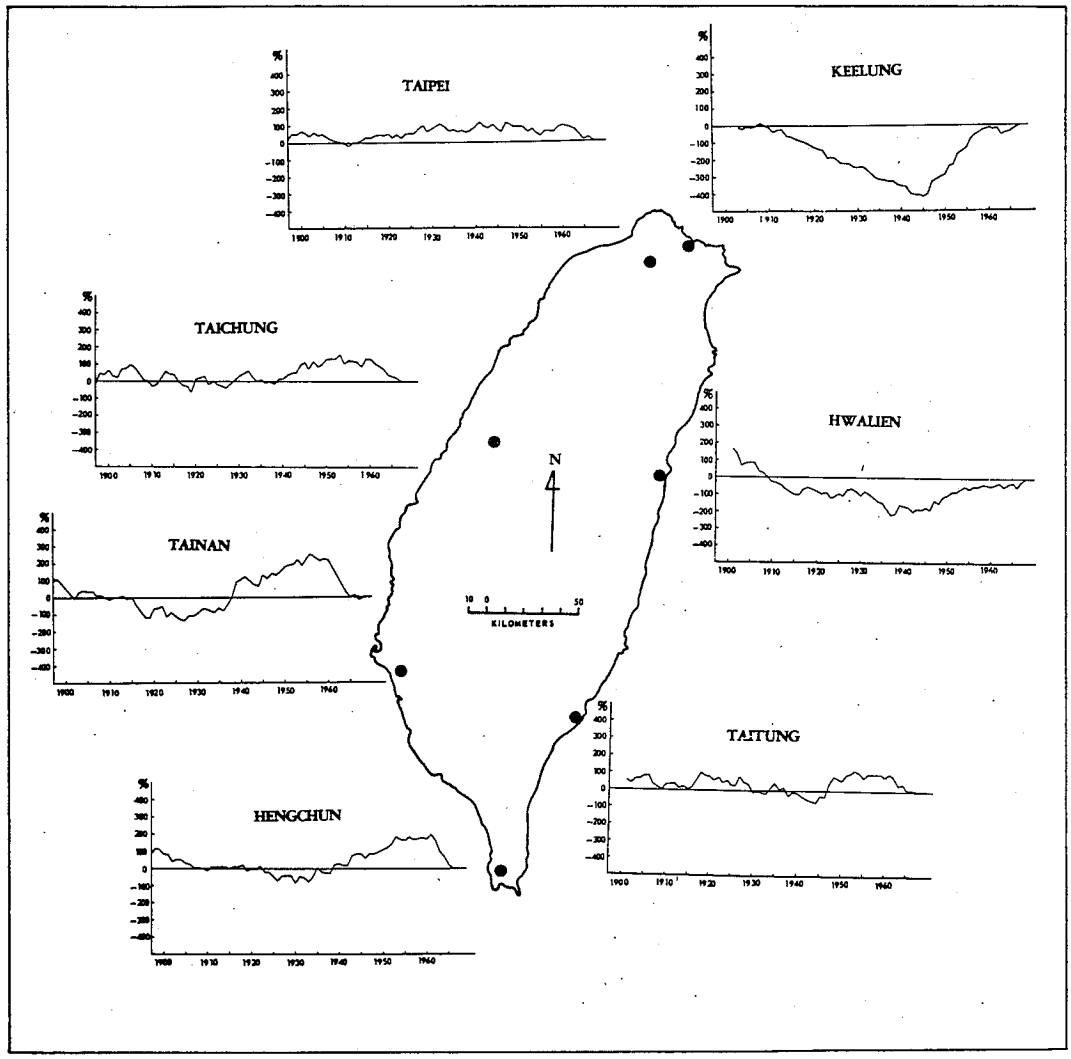

Figure 56. The annual rainfall residual-mass curves at various Taiwan stations.

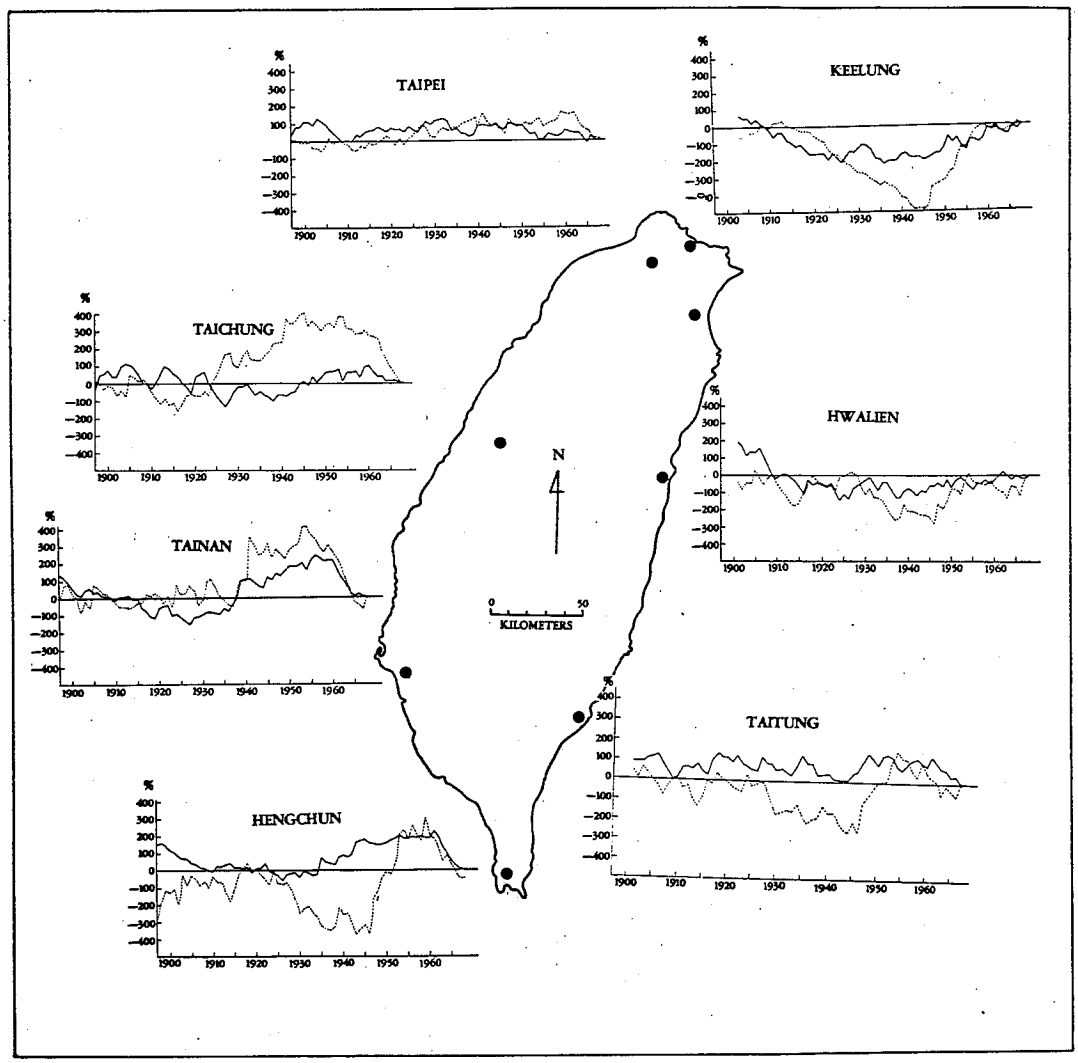

Figure 57. The rainfall residual-mass curves in summer (full lines) and in winter (dotted lines).

rainfall in winter and late fall, respectively. On the other hand, Taichung, Tainan, and Hengchun, respectively in the middle west, southwest, and south of the island, suffer dry winters due to their leeward location with respect to the northeast monsoon. Summer is a wet season at those stations when the northeast monsoon gives way to the southwest monsoon or the southeast trade. It is interesting to note that the annual residual-mass curves indicate that both dry and wet periods commenced and stopped ten years earlier in the south and southwest, a summer rainfall regime, than in the north and northeast, a winter rainfall regime. The long-term rainfall fluctuation on Taiwan seems to follow the so-called Bruckner cycle with a periodicity of 30-35 years. For example, the dry period at Keelung occurred from 1909 to 1945, and at Tainan from 1897 to 1930.

The secular rainfall variation on Taiwan appears to be a part of worldwide patterns. Kraus (1955a and b) has pointed out that the tropical rainfall regime is characterized by a pronounced wet period during the late half of the 19th century, followed by an abrupt decrease in rainfall in the late 1890's. This dry period ended approximately in the 1930's and a wet period has prevailed since then. Kraus attributed this dry period in the tropics to the shrinking of

the equatorial rainy zone and the shortening of the wet season. Unfortunately, pre-1897 rainfall records at the seven stations are not available and direct comparison with Kraus study is not possible. However, rainfall records around 1900 at various stations were much higher than the 1909-1968 mean. This can be seen both from the residual-mass curves (Figures 56 and 57) and from the curves of increments of annual rainfall means (Figure 50). In terms of shorter rainfall variations, the "hump" in the curves of the annual residual mass in 1918 at Hengchun, Tainan, and Hwalien, and in 1922 at Taitung and Tainan, and the tendency of a wet period from 1913 to 1918 at Taipei, Tainan, Hengchun, Taitung, and Hwalien, were all concurrent with those at other tropical stations, such as Honolulu, Georgetown, and Bogota (Kraus, 1955a and b).

As with annual residual-mass curves, seasonal residual-mass curves at the seven stations also show distinct regional patterns. The trend of the annual residual-mass curve is similar to that of the winter residual-mass curve at Keelung and Hwalien because mean monthly rainfall is higher there in winter than in summer. In contrast, the trend of the annual residual-mass curve is similar to that of the summer residual-mass curve at Taichung, Tainan, and Hengchun

due to the higher concentration of rainfall at those locations in summer.

At all the stations, the secular rainfall variations in summer are similar to each other. The change from a dry to a wet period came in 1926 or 1927 at all the stations. No corresponding pattern is found in the secular rainfall variation in winter, perhaps because summer weather systems influence rainfall over the entire island to a greater degree than do the winter ones. Typhoons contribute a significant amount of rainfall to the entire island, whereas the northeast monsoon contributes a significant amount of rainfall only to a limited area in the north of the island.

At Taipei and Taitung, the secular rainfall variation shows a transitional type between that at Keelung and Hwalien and that at Taichung, Tainan, and Hengchun. At Taipei, both summer and winter contribute a significant amount of rainfall to the annual total. Although mean monthly rainfall reaches a maximum in summer, winter is by no means dry. The annual residual-mass curve shows no significant dry or wet period, because seasonal rainfall variation is not always in phase. A wet season may be compensated by a dry season in the same year. However, the annual residual-mass curve resembles the summer curve more than the winter curve.

The annual residual-mass curve at Taitung shows a dry period from 1906 to 1944, a trend similar to that at Keelung and Hwalien. But the dry period was interrupted by a short wet-period around 1918. Sekiguti (1964) found the similar characteristic for the Pacific side of Japan. The annual residual-mass curve at Taitung rose from 1943 to 1960, in contrast to its trend at Keelung and Hwalien, but similar to its trend at Taichung, Tainan, and Hengchun. At Taitung, mean monthly rainfall reaches a maximum in September when the southeast trade dominates the island. The winter secular rainfall variation at Taitung is similar to that at Hwalien, but the summer secular rainfall variation reveals no significant dry and wet periods as it does at Hwalien.

The previous discussion shows that the island of Taiwan displays four different types of the secular rainfall variation:

1. The winter-monsoon type shows a dry period from the start of this century to the 1940's, and a wet period since then: Keelung, Hwalien.
2. The summer-monsoon type shows a dry period from the late 1890's into the 1930's, a wet period between the 1930's and about 1960, and a dry period since then: Taichung, Tainan, and Hengchun.

3. The trade-wind type shows rainfall peaks in 1918 and 1950, a trend similar to the Pacific-side of Japan (Sekiguti, 1964): Taitung.
4. The intermediate-type shows no significant dry or wet period: Taipei.

Physical Causes

The regional diversity of the secular rainfall variation on Taiwan is attributable to the combined effect of the large-scale circulation and topography.

In a study of the secular change in rainfall of south-east Australia, Kraus (1954) has concluded that the change in rainfall is associated with the intensity of the upper westerlies. The strength of the westerlies is normally expressed by zonal index, defined by Rossby (1939) as the surface-pressure difference between the 35° and 55° of latitude. The variation in zonal index is associated with the intensity and position of the centers of action at ground surface. During periods of low zonal-index, the Aleutian low usually has two centers, one of which shifts toward the west and is located close to Kamachatka. The North Pacific subtropical anti-cyclone weakens and shifts toward the east with its axis oriented north-south. Meanwhile, the Mongolian anticyclone is well developed with an increase in polar outbreaks over

China. Therefore, a considerable mass is transferred across the subtropical area (Willett, 1959).

Taiwan is located in a subtropical area where rainfall increases during periods of low zonal-index. Liu (1966) has stated that heavy rainfall over Taiwan is always associated with an increase in speeds of westerly winds at upper levels. This confirms Namias' (1950) study that low zonal-index is characterized by the displacement of the belt of the strongest westerlies towards the subtropical latitudes. The variation in zonal-index reflects a shift in the latitudinal distribution of momentum rather than a decrease or increase in absolute values because of the conservative nature of the total momentum of the mid-tropospheric westerlies for a given time. Wei (1968) has also found that over Taipei the average wind-speed at 200 mb during the wet January of 1957-1958 exceeded that of the dry January of 1963-1965 by 18.2 m/sec.

The dry periods from the start of this century to the 1930's at stations in the west and south, and to the 1940's at those in the north and east of the island, as well as the subsequent wet periods with a peak during the 1950's at all the stations, are found to be related to the strength of the westerlies. Lamb and Johnson (1959, 1961) and Lamb (1966) have recognized that indices of zonal circulation in most

parts of the world increased since 1895 to a maximum around 1925. Apparently, a period of abnormal strength of the westerlies was centered about 1925 ± 20 years. As a result, an abrupt decline in rainfall in the tropics and subtropics occurred during the first three or four decades of this century when the westerlies were most strengthened. On the other hand, the wet periods from the 1930's to the 1950's at the stations in the west and south, and from the 1940's to the 1950's at those in the north and east, were associated with the decline in the strength of the westerlies.

The wet period terminated in 1960 at stations in the south and west, but appears to have continued further into the 1960's at stations in the north and east (Figures 56 and 57). The increase in rainfall during the 1960's in northern and eastern Taiwan can be attributed to the continued drop in zonal index accompanied by an increase in frequency of blocking situations in high latitudes (Lamb, 1966). Since 1960, the meridional flow has become more prevalent (Wahl, 1972; Figure 5). Wang (1964) has found that the center of the Siberian anticyclone has been displaced towards low latitudes since 1944. On the other hand, the monsoon trough was displaced northward from 1931 to 1960 (Wang, 1964) in

connection with an increase in rainfall over Taiwan. Since 1960, the monsoon trough has probably been displaced southward in accordance with the weakening and southward displacement of the North Pacific subtropical anticyclone (Lamb, 1966). This is reflected by a decline in the frequency of typhoons in the western North Pacific and Taiwan accompanied by the decreased trend in rainfall in southern and western Taiwan during the 1960's.

The secular rainfall variation over Taiwan appears to follow the 80-year solar-climatic cycle postulated by Willett (1961). During the first quarter of the minimum solar activity, approximately from the 1880's to the 1890's, the zonal circulation prevailed over low latitudes. This low zonal-index circulation was responsible for a wet period at most tropical and subtropical stations. During the second and third quarters of the irregularly increased solar activity (Figure 54), approximately from the 1900's to the 1930's, the zonal circulation shifted poleward to middle latitudes, a high zonal-index pattern. The low latitudes suffered a dry period due to the weakening of the westerlies, whereas the high latitudes experienced a wet period due to the strengthening of the westerlies. During the fourth quarter of the peak solar activity, approximately from the 1940's to the 1950's, the

atmospheric circulation was characterized by low zonal-index pattern with pronounced cellular blocking highs. The subtropical latitudes experienced a wet period. This is reflected by a pronounced increase in rainfall over the entire island of Taiwan. During the 1960's, the beginning of the first quarter of the current 80-year cycle, solar activity declined (Figure 54). The westerlies became zonal and strengthened over the low latitudes. As a result, rainfall in the subtropics increased. Keelung and Hwalien show increased secular rainfall trends during the 1960's. In contrast, at Taipei, Taichung, Tainan, Hengchun, and Taitung, rainfall decreased during the 1960's, perhaps associated with the shrinking of the monsoon trough, and the southward displacement of the North Pacific subtropical anticyclone, accompanied by the decrease in typhoon activity.

Climatic changes in the geological time were evidenced by the great glacial epochs. Climatologists have devoted their attention to seek for possible physical mechanisms of such changes. Milankovich (1930) indicated that the great glacial periods corresponded to the time of radiation reduction during warm season in middle and high latitudes. He attributed such a radiation decrease to the change in the position of the earth's surface in relation to the sun.

Budyko (1972) has agreed with Milankovich's theory and has demonstrated, by a numerical heat-balance model, that the extent of the polar ice depends on the insolation on the outer boundary of the atmosphere. His model has showed that the present climatic regime is highly sensitive to a very small change of incoming radiation. The polar ice would cover the whole globe with a decrease in solar radiation by 2%, whereas it would completely melt with an increase by several tenths of 1%. A slight change in the earth's surface temperature, not more than $1^{o}C$, would lead to a noticeable displacement of the ice cover limit.

The variation in the polar ice extent has been found to be related to the variation in the atmospheric concentration of carbon dioxide, aerosols, and water vapor. Budyko (1972) has indicated that the small change in carbon dioxide concentration would consistently affect the mean earth's surface temperature which in turn would lead to the shift in the polar ice cover over long distances. Complete ice-melting may occur when the carbon dioxide concentration increases by 50% of its present value. The role of carbon dioxide, aerosols, and water vapor in climatic changes has been a matter of debate and a subject of numerical experiments. It has been found that the earth's mean annual surface

temperature increased by about 0.6°C from 1880 to 1940. Since 1940, it has been decreasing and is now about 0.3°C lower than in 1940 (Hobbs, et al., 1974). The carbon dioxide concentration has been increasing significantly since 1880, but without any interruption in 1940. Bryson and Petterson (1968) has attributed the recent global cooling to the man-generated turbidity. Mitchell (1970) has proposed that the umbrella of fine dusts cast into the stratosphere by recent volcanism must have accounted for the global cooling trend since 1940. Frisken (1971) has indicated that increasing backscattering from high-layer aerosols results in the cooling of the near surface environment. Möller (1963) has recognized that 1% increase of general cloudiness would complete mask the warming trend caused by the increase in carbon dioxide concentration. The increase in carbon dioxide concentration would lead to an increase in the earth's surface temperature which in turn would increase evaporation from the sea. As a result, the increased water vapor would reinforce the warming trend. However, the mean cloudiness would also increase, buffering the warming trend due to the increase in albedo. According to Manabe and Wetherald's (1967) numerical model, doubling of carbon dioxide concentration would only increase the

earth's surface temperature by 2.4°C, which could be masked by a 3% increase in low cloud. Frisken (1971) concluded that the earth's surface temperature may increase and then decrease as a result of the increasing atmospheric concentration of carbon dioxide, aerosols, and water vapor.

It has been found that the polar ice boundary shows year-to-year and secular variations and is significantly related to climatic fluctuations. The polar ice extent affects the surface albedo and hence the amount of solar energy absorbed. It covers part of the sea surface available for air-sea interaction. Ice cover is not only the consequence of cold climatic conditions, but also, to some extent, the cause of them (Budyko, 1972). There is a possibility of a sharp increase in small climatic fluctuations due to a change in the polar ice area. Because of its high albedo, more than 80%, a large extent of ice cover tends to maintain cold conditions which may lead to self-amplifying process (Brooks, 1949). Fletcher (1969) has found that the extent of the Antarctic sea ice may have caused change in the strength of the general circulation on a short-time scale. Kukla (1974) recognized that in 1972 the anomalous circulation pattern and the low global surface temperature were associated with a large increase in the extent of the Arctic sea ice, which

can be detected by satellite photographs. He has concluded that the role of snow and ice in year-to-year weather variations seems to be substantiated. Lamb (1972) has noted that the Arctic sea ice shrunk during the first half of this century. The total area of the Arctic sea ice is estimated to have shrunk by more than 10% between 1920 and 1938. Since the late 1950's and the early 1960's, the Arctic sea ice has been noticeably increasing, perhaps in response to a decline in radiation budget in high latitudes accompanied by the intensification of the polar anticyclone or the northerly wind, bringing cold Arctic currents towards low latitudes.

It appears that there is a strong association between the secular rainfall variation in Taiwan and the variation in the extent of the Arctic sea ice. The entire island of Taiwan suffered a distinct dry period from about 1920 to 1940, the years in which the Arctic sea ice melted at a most rapid rate. The strength of the westerlies and air and ocean temperatures in the northern hemisphere reached maxima in this period. On the other hand, the entire island of Taiwan experienced distinct wet periods in the 1940's and the 1950's, concurrent with the time the westerlies weakened with active blocking situations. The limit of the Arctic sea ice had withdrawn far to the north, but must have a lower melting

rate than in the preceding period. The time of the late 1950's and the early 1960's marked a significant climatic change in this century. This is evidenced by a sharp decline in rainfall at most Taiwan stations, by a significant weakening of the westerlies with the mainstream shifting towards the subtropics, and by the cooling of ocean surface temperatures. Climatologists have also noted a considerable decline in tree-ring width in western America (LaMarche, 1974). The Arctic sea ice has increased since the late 1950's. By 1964-1968, it advanced to the position similar to what they had been in the 19th century before the decades of its shrinking (Lamb, 1972).

Summary of Significant Results

Some climatologists have recognized that climatic changes may be only part of a random fluctuation in the time series of meteorological elements. Yevjevich (1968) stated that in the analysis of the longest series of annual values of precipitation and runoff, no statistically significant climatic changes could be detected. In contrast, Bean (1964) has insisted that weather data are not random but governed by a high degree of law and order. Numerous efforts have been devoted to investigate the hidden periodicity and physical causes of

fluctuations in the time series of meteorological elements in hope that they can be used for forecasting. Secular climatic changes are hemispheric phenomena and thus show pronounced teleconnections. Moving average and residual-mass curves are frequently used to study climatic changes. Climatic changes were often linked to the variations in the strength and pattern of the atmospheric circulation, in the ocean-surface temperatures, in the extent of the polar ice, and in solar activity. The current study employed the residual-mass curves to identify the regional pattern in the secular rainfall variation over Taiwan. It appears that the secular rainfall variation over Taiwan is closely related to the strength and pattern of the westerlies and is part of a worldwide phenomenon. The low zonal-index circulation patterns favor Taiwan with wet periods, whereas the high zonal-index patterns favor Taiwan with dry periods. The secular rainfall variation over Taiwan was found to follow the 80-year solar-climatic cycle. During the first four decades of this century, e.g., the second and third quarters of the last 80-year cycle, the strength of the westerlies increased in association with the irregular increases in the sun-spot numbers. As a result, dry periods prevailed at all the Taiwan stations. The sun-spot numbers in the 1940's and

1950's are associated with the sharp decreases in the strength of the westerlies which were characterized by pronounced blocking situations. Therefore, wet periods occurred over Taiwan. In the 1960's, the first quarter of the current 80-year cycle, the sun-spot numbers decreased accompanied by the continuing decrease in the strength of the westerlies. But the westerlies were not characterized by blocking highs as they were in the 1940's and 1950's. Instead, they were governed by the zonal circulation with the belt of the strongest westerlies shifting from middle to low latitudes. Rainfall increased in northern and eastern Taiwan but decreased in western and southern Taiwan. Lamb (1972) has indicated that the circulation pattern in the 1960's is the recurrence of the period of the weak circulation right before 1900. There is no doubt that climatic changes must be linked to fluctuations in the ocean-surface temperatures. Rasool and Hogan (1969) have indicated that the mass and heat capacity of the oceans is so large that small changes in mean ocean temperature over large areas of the globe would significantly affect the heat budget of the overlying atmosphere and hence may be capable of initiating climatic changes. They have suggested that the ocean temperatures in the equatorial Pacific influences the dynamics of the Intertropical

Convergence Zone which could influence the circulation patterns of the both hemispheres. The process of the air-sea interaction is complicated. Rossby (1959) has suggested that heat can be temporarily stored in the deep sea and may influence heat and water-vapor exchange after periods of the order of a few decades to a few centuries. Due to the lack of long-term ocean-surface temperature data in the North Pacific, the effect of the ocean-surface temperatures on the secular rainfall variation over Taiwan cannot be investigated. However, the pronounced drop in rainfall over southern and western Taiwan from the 1950's to the 1960's was apparently associated with below normal sea-surface temperatures over the entire North Pacific.

The secular rainfall variation in Taiwan is related to the variation in the extent of the Arctic sea ice. Taiwan suffered a dry period from 1920 to 1940, the years in which the Arctic sea ice melted at a most rapid rate. Since 1940, the Arctic sea ice had shrunk at a lower rate. Correspondingly, the westerlies weakened and Taiwan experienced a wet period. The Arctic sea ice has expanded since the early 1960's. Except for the northernmost section, Taiwan rainfall showed a significant decline.

In this chapter, the cumulative deviation from the annual rainfall mean has been used to examine the climatic changes in Taiwan during this century. It aims at the finding of physical mechanisms which have accounted for such changes. The use of cumulative process has been a subject of arguments. It has been found that long-term geophysical data tend to follow the Hurst phenomenon, which states that the rescaled range, Rn/Sn, depends on period of record n. Mathematically it can be expressed by $Rn/Sn \sim n,^{h}$ where $1.0 > h > 0.5$, and Rn and Sn are, respectively, the sample range of cumulative departure from the mean and the standard deviation of a time series of length n (Mandelbrot and Wallis, 1969b; Klemes, 1974). Many attempts have been made to apply statistical processes to fit the historical data exhibiting the Hurst phenomenon so that numerical models can be established to simulate time series. The Gauss-Markov process cannot account for a time series which show extreme values, the Noah effect, and long durations of values either above or below mean, the Joseph effect (Mandelbrot and Wallis, 1968). It has been found that the fractional Brownian noise, the autogressive integrated moving average, and broken line process are capable of modeling the phenomenon obeying the Hurst law (Mandelbrot and Wallis, 1969a; O'Connell, 1971;

Rodriguez-Iturbe, et al., 1972). These models describe well the statistical characteristics of long-run geophysical records, but disregard the physical mechanisms that produce processes exhibiting the Hurst phenomenon. The main properties of the fractional Brownian noise are (1) infinite memory, (2) self-similarity, and (3) stationarity in the mean. Klemes (1974) has demonstrated that the Hurst phenomenon is not necessarily an infinite memory process. It can also be caused by nonstationarity in the mean and by specific storage systems. He has further commented that the fractional Brownian noise is an operational not a physically founded model, and all the inferences about the physical properties of the modeled processes that are based on it can be misleading. Scheidegger (1970) has also commented that to extrapolate the correlated behavior from a finite time span to an asymptotically infinite one by using self-similarity is physically completely unjustified.

CHAPTER XI

SUMMARY

A review of literature and personal communication with climatologists in the Taiwan Weather Bureau indicate that the following analyses regarding Taiwan rainfall have not been carried out:

1. A systematic classification of synoptic flow patterns over Taiwan into types based on long-term records; the tabulation of frequencies of those types and the interpretation of their relationships with the spatial and temporal variation in rainfall over Taiwan.
2. The study of temporal variation in frequencies of synoptic flow types in terms of ocean-surface temperatures in the North Pacific, the extent of the Arctic sea ice, and solar activity.
3. The forecasting of the "plum rains" over Taiwan by the latitudinal position of polar fronts, the 500-mb geopotential heights and temperatures, and wind variations in the lower stratosphere and the troposphere.

4. The forecasting of the typhoon activity over Taiwan by the 700-mb anomalous circulation patterns with a focus on the strength of the Siberian trough.
5. Statistical models of daily rainfall and synoptic flow type occurrences over Taiwan.
6. The diurnal rainfall variation over Taiwan in relation to the synoptic-scale prevailing winds, land and sea breezes, and topography.
7. The numerical prediction of annual rainfall from frequencies of synoptic flow types by a stepwise multiple regression analysis.
8. Flood and drought frequencies in relation to centers of action and the strength of the westerlies.
9. The stability of annual rainfall mean and median, the skewness, and rainfall probability curves.
10. The secular rainfall variation over Taiwan from 1897 through 1968; its trends, its regional patterns, and its physical causes.

Berry and Perry (1973) have stated that synoptic climatology is the study of local or regional climate in relation to the atmospheric circulation. Its aim is to interpret the spatial and temporal climatic patterns in terms of large-scale weather processes and events. Two stages towards

a synoptic climatology study are (1) the determination of categories of atmospheric circulation patterns; (2) the assessment of weather elements in relation to these categories. In this study, eleven synoptic flow types over Taiwan were recognized, based on the daily weather maps for the period 1959 to 1969. The spatial variation in rainfall characteristics, such as mean annual, monthly, and daily rainfall, the standard deviation and the maximum of daily rainfall, and the probability of rainy days, associated with each synoptic flow type were presented in Chapters III through VI. The forecasting of the "plum rains" and the typhoon activity over Taiwan was also discussed. In Chapter VII, effort was devoted to the investigation of statistical models of daily rainfall and synoptic flow type occurrences which are supplemental tools for weather forecasting and are particularly important in agriculture and water resources management. In Chapter II, attention was paid to the investigation of temporal patterns of frequencies of synoptic flow types in terms of the general circulation, the ocean-surface temperatures, and solar activity. The temporal patterns of rainfall ranging in scale from diurnal to secular variations were presented in Chapters VIII through X.

Rainfall characteristics associated with synoptic flow types over Taiwan show distinct regional patterns because of topographic effects. The Mongolian anticyclone, the cutoff anticyclone, and the Taiwan low contribute significant amounts of rainfall to northern and eastern Taiwan but negligible amounts to western and southern Taiwan. Polar fronts become stationary in May and June and cause the "plum rains" over the entire island. Their occurrence is associated with an abrupt change in the atmospheric circulation, the downward penetration of the easterly winds and an increase in temperature and geopotential height at the 500-mb level. The north Pacific subtropical anticyclone, the southwest monsoon, typhoon, and monsoon trough dominate Taiwan in summer. They contribute rainfall to the entire island with a higher intensity to the south than to the north. Typhoons tend to visit Taiwan when a large negative anomaly area occurs over Siberia and the east China seaboard.

In Taiwan, the annual frequencies of different synoptic flow types have been found to be related to the strength of the westerlies, solar activity, ocean-surface temperatures in the eastern equatorial Pacific and the central North Pacific. The Mongolian anticyclone and typhoons tend to visit Taiwan most frequently during years of the weakening of the

westerlies in the Northern Hemisphere, associated with low sun-spot number and warming of ocean-surface temperatures in the central North Pacific. In contrast, the frequencies of the Mongolian cutoff anticyclone and the North Pacific subtropical anticyclone increase during the same periods. In addition, the Mongolian anticyclone tends to visit Taiwan most frequently when ocean-surface temperatures in the eastern equatorial Pacific increase, whereas the Mongolian cutoff anticyclone behaves in the reverse manner. The winter synoptic flow types are more dependable than the summer synoptic flow types, as evidenced by their smaller coefficients of variation in annual frequencies.

With the exception of southern Taiwan, the frequency distribution of wet spells agrees well with that of the simple Markov probability model. Therefore, daily rainfall probabilities in different months calculated by the simple Markov chain model can be used for forecasting. In southern Taiwan, logarithmic series appears to fit data of daily rainfall occurrences. Except for Taipei, the frequency distribution of dry spells agrees well with that of either the simple Markov chain model or the logarithmic series. The frequency distribution of all synoptic flow types follows the simple Markov chain probability model; but only that of

summer synoptic flow types, such as the polar front over Taiwan, the North Pacific subtropical anticyclone, the southwest monsoon, the southern-type typhoon, and the monsoon trough, follows the logarithmic series.

In Taiwan, diurnal rainfall variations show distinct regional patterns and correlate well with the synoptic-scale prevailing winds, land and sea breezes, coastal configurations, and other elements of topography. At lowland and coastal stations, there are reverse diurnal rainfall patterns between winter and summer. This can be attributed to the shift in the synoptic-scale prevailing winds caused by the change of different synoptic flow types from one season to another.

Statistical analysis indicates that in Taiwan rainfall skewness is higher in southern coastal plains where rainfall is mainly contributed by summer synoptic flow types, whereas it is lower in northern Taiwan and mountain areas where both summer and winter synoptic flow types contribute significant amounts of rainfall. It requires at least eighteen years to obtain a stable mean or median, and at some stations no stable mean or median can be obtained for the entire study period 1897 to 1968.

Annual rainfall at various Taiwan stations can be satisfactorily estimated from annual frequencies of synoptic flow types by stepwise multiple regression equations. The most significant variable accounting for the year-to-year rainfall variations over the entire study period at Keelung, is the North Pacific subtropical anticyclone, at Taipei, Taichung, and Alishan, the monsoon trough, at Kaoshiung, the southern-type typhoon, at Hengchun, Taitung, and Yilan, the Mongolian cutoff anticyclone, and at Hwalien, the Taiwan low. It is found that floods and droughts over Taiwan are closely related to the position of the Aleutian low and to zonal-index. Floods tend to occur over Taiwan when the Aleutian low is displaced eastward and southward of its normal position, whereas droughts tend to occur when the Aleutian low is close to its normal position. Low zonal-index brings Taiwan floods, whereas high zonal-index brings Taiwan droughts.

The secular rainfall variation over Taiwan is part of a worldwide phenomenon and resembles that at various subtropical and tropical stations. It shows distinct regional patterns and appears to be related to the strength of the westerlies, ocean temperatures, the extent of the Arctic sea ice, and solar activity. In general, high zonal-index or

strong westerlies favor Taiwan with low rainfall. In contrast, low zonal-index with pronounced cellular blocking-highs in the westerlies favors the entire island with heavy rainfall. Low zonal-index with the strengthening of the zonal circulation over low latitudes favors only northern and eastern Taiwan with heavy rainfall while it brings the other sectors of the island low rainfall. The secular rainfall variation over Taiwan appears to follow the 80-year solar-climatic cycle. The first four decades of this century coincide with the second and third quarters of the last 80-year cycle. Sun-spot number showed an irregular increased trend, accompanied by a pronounced increase in the strength of the westerlies. As a result, the entire island of Taiwan suffered dry periods. The 1940's and 1950's coincided with the fourth quarter of the last cycle, with an increase in sun-spot number; but the strength of the westerlies weakened sharply with pronounced blocking-highs. The entire island thus experienced wet periods. In the 1960's, the beginning of the first quarter of the current cycle, sun-spot number decreased in association with the continuing decrease in the strength of the westerlies. The belt of the maximum strength of the westerlies was displaced from middle to low latitudes. Northern and eastern Taiwan enjoyed wet periods, but western

and southern Taiwan suffered dry periods. The Arctic sea ice shrunk poleward most rapidly from about 1920 to 1940, and has advanced equatorward since 1960. These two periods coincide, respectively, with the high- and low-zonal index in the northern hemisphere.

The application of synoptic climatology lies in several fields. Agriculture is of most concern to geographers. The classical study usually correlates climatic zones with agricultural land-use patterns. Temperature, rainfall, and moisture-index are frequently used to show climatic and crop distribution relations. Recently, numerical approaches have been used to estimate crop yields from meteorological elements. Watson (1963) has stated that climate determines what types of crops can be grown in a certain area and that weather determines the annual yield. It is commonly believed that solar radiation determines the potential crop productivity and that water-use affects the actual yield. Many studies link fluctuations in annual crop yields to variations in annual rainfall. In Australia, there is a strong association between fluctuations in some aspects of total Australian agricultural production and the variations in the proportion of Australia experiencing above-average rainfall (Maunder, 1970). Shaw and Thompson (1964) have found that

there is a close association between crop and rainfall variations in the midwest of the United States. Thompson (1964) used the multiple regression technique to estimate the corn yield trend in Iowa by weather variables, and claimed that improved weather accounted for almost a third of the increase in yield from 1930 to 1962. Mather (1968) has found a significantly high correlation coefficient between corn yield and moisture deficit in Cumberland County, New Jersey.

In Taiwan, crop distribution shows pronounced regional patterns and is closely related to climatic conditions. Rice fields dominate the cultivated land in northern Taiwan where winter synoptic flow types produce significant amounts of rainfall. In contrast, southern Taiwan is characterized by more diverse croplands. Due to long dry winters in that region, cash crops, such as sugarcane, pineapple, and bananas, also account for large proportions of cultivated lands. The boundary separating these two land-use types coincides approximately with the zero water-deficit line derived from Thornthwaite's method (Chen, 1959). In Taiwan, the variation in annual rice yield appears to be affected by large-scale droughts (Figure 59 in Appendix C). The rice yield has increased since the early years of this century, largely due to improved technology and an increase in

cultivated lands. The secular rice-yield trend showed a significant decline from 1938 to 1945 because of World War II. Moreover, the pronounced decreases in rice yields in 1923, 1933, and 1963 were associated with the occurrences of large-scale droughts over Taiwan. The 1963 drought caused a pronounced reduction not only in rice yield but also in many other crop yields. Synoptic studies indicated that the pronounced drought in 1963 was attributable to the significant increase in the frequency of the North Pacific subtropical anticylone in contrast to the decrease in the frequency of the Mongolian anticyclone, polar fronts, and typhoons. The stepwise multiple regression analysis indicates that the annual frequency of the northern-type typhoon accounts for about 57% of the total variation in the annual rice yield over the study period. The Mongolian cutoff anticyclone is the second important variable; its annual frequency accounts for about 14% of the total variation in the annual rice yield. The coefficient of determination between annual rice yields and frequencies of synoptic flow types almost reaches 100%, reflecting the fact that the former can be successfully estimated from the latter (Table 61 in Appendix F).

Synoptic climatology is also important in the study of water balance over a certain area. Water balance varies in scale ranging from the whole globe to individual stations. In any case, rainfall is one of the major variables in water-balance equations. The spatial and temporal patterns of rainfall provide basic data for the study of water balance. In Taiwan, water deficit and surplus calculated from Thornthwaite's method (Chen, 1959) indicate pronounced regional and seasonal patterns which are closely related to different rainfall regimes resulting from different synoptic flow types. Northern Taiwan shows pronounced water deficit in summer and water surplus in winter, because winter synoptic flow types contribute abundant rainfall to that region. In contrast, southern and southwestern Taiwan show pronounced water deficits in winter and water surpluses in summer, because rainfall in those regions is concentrated in summer. Northwestern Taiwan shows significant water deficit in fall, probably due to its leeward position with respect to the east and southeast winds associated with the Mongolian cutoff anticyclone which dominates Taiwan in that season.

The primary concern of synoptic climatology is weather and climate forecasting. Although the construction of weather maps is the daily routine work in the Taiwan Weather

Bureau, rainfall forecasts issued to the public are still restricted to qualitative description due to the lack of statistical guides. Rainfall forecasting is mainly based on the weathermen's intuitive experiences; it would be more objective if forecast from the probability, mean, standard deviation, and maximum of daily rainfall under each synoptic flow type. The Markov chain model was proven useful for objective forecasting of the probability of daily rainfall occurrences. Such statistical methods are particularly helpful for the hydrologists in forecasting river runoff. The study of the rainfall-runoff relation by hydrographs and multi-varient models requires information of the daily and hourly rainfall. The diurnal rainfall pattern may be helpful in forecasting the time and amount of peak runoff. The author, during his service for the Taiwan Weather Bureau in 1966, recognized that the forecast rainfall data provided to hydrologists by weathermen may change several times in a day due to a lack of statistical values such as those presented in this study. This drawback can be avoided by forecasting mean, standard deviation, and maximum daily rainfall.

In conclusion, this study enhances the understanding of spatial and temporal characteristics of rainfall over

Taiwan in terms of synoptic and general circulation, air-sea interaction, and solar activity. It postulates various means for the forecasting of rainfall varying in temporal scale from diurnal to secular patterns over different sectors of the island. These are important in estimating the water resource potential for agricultural and hydrological applications.

APPENDIX A

TABLE 21

MEAN MONTHLY FREQUENCY OF SYNOPTIC FLOW TYPES OVER TAIWAN (%)

Types	1	2	3	4	5	6	7	8	9	10	11	12
1	49.8	39.8	17.5	9.3	0.8				9.0	26.0	38.7	52.1
2	26.0	26.3	25.5	22.1	14.3	0.9	0.5	7.0	17.5	45.7	31.5	26.0
3	13.4	15.4	13.4	9.6	1.7					2.3	6.3	11.7
4	2.6	7.7	21.1	23.9	43.1	49.6	1.1	2.9	17.8	8.7	6.3	1.1
5	0.2	0.3	1.7	4.8	7.0	3.6	0.8		3.3		2.7	1.1
6	7.6	10.2	20.5	26.6	19.3	14.2	28.9	27.8	22.7	11.4	11.8	7.0
7				1.8	10.8	25.4	40.1	21.1	2.1	0.2		
8				0.3	1.4	2.4	11.7	11.4	10.1	3.8	2.1	0.5
9				0.6	0.8	1.5	5.8	9.1	6.0	1.4	0.3	
10						0.3		7.9	0.6			
11				0.6	0.2	1.8	11.1	12.3	10.6			

APPENDIX B

TABLE 22a

AMOUNT OF MEAN ANNUAL RAINFALL ASSOCIATED WITH DIFFERENT SYNOPTIC FLOW TYPES
(UNIT: MM)

Flow types	1	2	3	4	5	6	7	8	9	8+9	10	11
Keelung	945.4	235.8	378.5	926.9	73.0	18.3	68.6	454.7	160.9	615.6	17.8	40.8
Taipei	271.0	39.3	144.3	677.4	39.4	42.9	143.4	436.5	145.3	581.8	22.0	68.6
Taichung	86.3	10.5	54.9	648.8	34.3	65.4	97.0	278.5	132.4	410.9	96.7	85.5
Tainan	49.3	6.5	17.9	413.1	12.4	52.0	134.6	223.0	237.5	460.5	95.2	53.4
Kaoshiung	39.1	9.4	20.3	508.5	18.8	40.6	129.3	227.2	230.4	457.6	109.0	82.6
Hengchun	32.5	37.4	20.7	400.0	19.6	104.3	117.1	446.4	368.4	814.8	71.7	150.3
Taitung	91.8	87.6	41.1	424.3	25.7	132.5	46.2	322.8	389.0	711.8	28.4	147.6
Hwalien	270.1	192.3	80.2	560.9	41.0	84.4	45.3	487.0	300.3	787.3	20.8	86.5
Yilan	483.9	263.6	162.0	624.8	61.0	40.1	65.2	491.7	264.9	756.8	25.1	68.3
Alishan	221.9	115.7	83.7	1236.9	97.1	310.1	286.8	884.3	416.9	1303.9	139.1	159.7

APPENDIX B

TABLE 22b

PERCENTAGE OF MEAN ANNUAL RAINFALL ASSOCIATED WITH DIFFERENT SYNOPTIC FLOW TYPES
(UNIT: %)

Flow types	1	2	3	4	5	6	7	8	9	8+9	10	11
Keelung	28.5	7.1	11.4	27.9	2.2	0.6	2.1	13.7	4.8	18.5	0.5	1.2
Taipei	13.3	1.9	7.1	33.4	1.9	2.1	7.1	21.5	7.2	28.7	1.1	3.4
Taichung	5.4	0.7	3.4	40.8	2.2	4.1	6.1	17.5	8.3	25.8	6.1	5.4
Tainan	3.8	0.5	1.4	31.9	1.0	4.0	10.4	17.2	18.3	35.5	7.3	4.1
Kaoshiung	2.8	1.3	1.4	35.9	1.3	2.9	9.1	16.1	16.3	32.4	7.7	5.8
Hengchun	1.8	2.1	1.2	22.6	1.1	5.9	6.6	25.2	20.8	46.0	4.1	8.5
Taitung	5.3	5.0	2.4	24.4	1.5	7.6	2.7	18.6	22.4	41.0	1.6	8.5
Hwalien	12.5	8.9	3.7	25.9	1.9	3.9	2.1	22.5	13.8	36.3	1.0	4.0
Yilan	19.0	10.3	6.4	24.5	2.4	1.6	2.6	19.3	10.4	29.7	1.0	2.7
Alishan	5.6	~~7.3~~ 2.9	2.1	31.3	2.5	7.8	7.3	22.4	10.5	32.9	3.5	4.0

APPENDIX B

TABLE 23a

AMOUNT OF MEAN MONTHLY RAINFALL ASSOCIATED WITH THE MONGOLIAN ANTICYCLONE
(UNIT: MM)

Months	1	2	3	4	5	6	7	8	9	10	11	12
Keelung	199.8	215.1	63.0	31.3	3.3				9.3	63.6	146.2	213.8
Taipei	44.6	73.7	30.8	23.5	2.4				9.3	22.2	28.3	36.3
Taichung	8.9	34.3	17.0	14.7	1.2					0.2	6.2	3.7
Tainan	3.3	13.2	10.3	12.5	0.5				0.5	0.3	8.0	0.9
Kaoshiung	3.2	6.0	12.7	5.5	0.2				1.6	0.8	7.6	1.5
Hengchun	4.5	4.6	1.2	1.8					3.7	9.8	3.8	3.2
Taitung	11.9	16.0	6.2	10.0	8.1				3.6	10.8	19.0	6.3
Hwalien	43.7	60.1	21.5	17.5	2.2				11.2	41.6	34.5	37.8
Yilan	73.3	88.9	18.3	13.0	0.2				16.8	69.7	100.3	103.3
Alishan	32.3	63.5	34.3	23.0	0.4				4.8	16.0	26.0	21.6

APPENDIX B

TABLE 23b

PERCENTAGE OF MEAN MONTHLY RAINFALL ASSOCIATED WITH THE MONGOLIAN ANTICYCLONE
(UNIT: %)

Months	1	2	3	4	5	6	7	8	9	10	11	12
Keelung	58.1	57.0	21.8	16.6	1.5				2.4	27.2	49.3	60.9
Taipei	52.4	53.6	20.8	17.1	1.4				2.7	19.4	39.3	63.1
Taichung	40.1	53.0	20.4	17.7	0.7					1.6	38.7	36.2
Tainan	34.9	64.5	32.0	21.0	0.5				0.4	6.0	40.4	46.4
Kaoshiung	48.9	48.3	25.6	8.7	0.2				1.3	2.1	36.8	42.9
Hengchun	29.1	32.7	3.5	3.6					1.4	11.9	7.5	34.1
Taitung	24.4	34.1	10.7	10.8	5.5				1.1	6.7	21.1	30.0
Hwalien	52.0	52.5	23.4	13.3	1.0				2.7	18.8	19.7	60.3
Yilan	53.1	51.9	16.4	13.4	0.1				3.6	22.0	35.9	65.0
Alishan	51.6	65.3	23.5	15.4	0.1				0.8	16.4	43.1	61.8

APPENDIX B

TABLE 24

MEAN, STANDARD DEVIATION, AND MAXIMUM OF DAILY RAINFALL ASSOCIATED WITH THE MONGOLIAN ANTICYCLONE (UNIT: MM)

	Mean	Standard Deviation	Maximum
Keelung	16.5	16.9	129.0
Taipei	5.9	8.1	80.4
Taichung	4.9	8.6	61.9
Tainan	4.9	10.2	58.5
Kaoshiung	4.7	8.8	52.9
Hengchun	2.1	5.1	53.7
Taitung	4.0	7.9	88.7
Hwalien	6.6	9.6	66.3
Yilan	8.8	14.0	110.2
Alishan	8.6	11.0	63.5

APPENDIX B

TABLE 25

PROBABILITY OF RAINY DAYS WITH DIFFERENT INTENSITIES FOR THE MONGOLIAN ANTICYCLONE (UNIT: %)

mm	0.1 - 12.6	12.7 - 25.3	25.4 - 50.8	50.9 - 76.2	76.3 and greater	Total
Keelung	40.8	20.0	12.9	3.1	0.7	77.5
Taipei	53.6	6.5	2.1	0.0	0.1	62.3
Taichung	20.3	2.1	0.6	0.2	0.0	23.3
Tainan	9.9	0.7	0.4	0.1	0.0	11.1
Kaoshiung	10.5	0.2	0.5	0.1	0.0	11.3
Hengchun	17.1	0.2	0.0	0.1	0.0	17.5
Taitung	28.8	1.6	0.6	0.0	0.1	18.2
Hwalien	18.3	5.0	2.0	0.6	0.0	55.9
Yilan	58.9	8.7	4.6	1.1	0.7	74.0
Alishan	26.6	4.7	3.2	0.2	0.0	34.7

APPENDIX B

TABLE 26a

AMOUNT OF MEAN MONTHLY RAINFALL ASSOCIATED WITH THE MONGOLIAN CUTOFF ANTICYCLONE
(UNIT: MM)

Months	1	2	3	4	5	6	7	8	9	10	11	12
Keelung	41.5	30.7	10.9	8.9	8.7		0.4	1.3	14.2	32.7	33.8	53.3
Taipei	3.9	4.8	4.2	1.2	1.5	2.0		1.6	4.5	8.3	2.9	4.3
Taichung	0.8	3.0	2.8	2.4			0.2		0.4	0.3	0.2	0.3
Tainan	0.3	1.1	1.4	2.0	*		0.3		0.4	0.6	0.1	*
Kaoshiung	0.1	0.4	0.8	0.8	0.6	0.6		0.1	0.1	4.0	*	
Hengchun	0.9	3.1	1.7	0.3	4.8		0.9	0.6	14.3	8.6	2.0	0.2
Taitung	2.9	10.4	11.6	8.7	7.6			1.4	10.7	23.2	7.4	3.7
Hwalien	16.9	22.2	12.6	11.1	14.6	0.1		2.4	28.3	51.3	25.6	6.9
Yilan	27.7	23.7	12.4	5.7	12.4		2.4	4.9	17.9	70.4	61.0	25.1
Alishan	2.3	6.0	12.6	7.6	16.8	1.4	1.6	12.3	15.9	32.9	4.7	2.2

*Indicates mean monthly rainfall less than 0.1 mm.

APPENDIX B

TABLE 26b

PERCENTAGE OF MEAN MONTHLY RAINFALL ASSOCIATED WITH THE MONGOLIAN CUTOFF ANTICYCLONE (UNIT: %)

Months	1	2	3	4	5	6	7	8	9	10	11	12
Keelung	12.1	8.1	3.8	4.7	3.9		0.3	0.7	3.7	13.8	11.4	15.2
Taipei	4.5	3.5	2.8	0.9	0.9	0.7		0.6	1.4	7.2	4.1	7.5
Taichung	3.4	4.7	3.3	2.9			0.1		0.3	2.8	1.3	2.9
Tainan	3.7	5.5	4.4	3.4	0.1		0.1		0.4	13.0	0.7	1.2
Kaoshiung	1.4	3.3	1.6	1.3	0.5	0.2		0.3	0.9	10.7	0.1	
Hengchun	6.1	21.5	5.0	0.6	3.1		0.2	0.1	5.7	10.5	4.0	1.9
Taitung	6.0	22.2	20.0	9.4	5.2			0.6	3.4	14.3	8.2	17.7
Hwalien	20.2	19.4	13.7	8.4	6.4			1.1	7.1	23.2	14.7	11.0
Yilan	20.1	13.8	11.1	5.9	6.7		1.7	2.2	3.8	22.2	31.9	15.8
Alishan	3.7	6.2	8.6	5.1	3.8	0.2	0.3	1.4	2.8	33.8	7.7	5.1

APPENDIX B

TABLE 27

MEAN, STANDARD DEVIATION, AND MAXIMUM OF DAILY RAINFALL ASSOCIATED WITH THE MONGOLIAN CUTOFF ANTICYCLONE (UNIT: MM)

	Mean	Standard Deviation	Maximum
Keelung	8.2	13.5	124.3
Taipei	2.7	4.5	30.0
Taichung	2.3	4.3	22.0
Tainan	2.0	3.4	16.6
Kaoshiung	2.4	2.8	12.6
Hengchun	2.4	5.6	40.7
Taitung	4.7	7.9	53.4
Hwalien	6.4	14.5	201.4
Yilan	7.7	13.2	145.3
Alishan	7.0	10.1	47.0

APPENDIX B

TABLE 28

PROBABILITY OF RAINY DAYS WITH DIFFERENT INTENSITIES FOR THE MONGOLIAN CUTOFF ANTICYCLONE (UNIT: %)

mm	0.1 - 12.6	12.7 - 25.3	25.4 - 50.8	50.9 - 76.2	76.3 and greater	Total
Keelung	30.6	4.9	3.1	0.0	0.4	39.0
Taipei	18.9	0.6	0.1	0.0	0.0	19.6
Taichung	5.9	0.2	0.0	0.0	0.0	6.1
Tainan	3.4	0.1	0.0	0.0	0.0	3.5
Kaoshiung	5.3	0.0	0.0	0.0	0.0	5.3
Hengchun	16.7	0.1	0.5	0.0	0.0	17.3
Taitung	22.6	2.1	0.6	0.1	0.0	25.4
Hwalien	35.2	3.8	1.1	0.2	0.2	40.5
Yilan	38.0	4.5	3.1	0.7	0.1	46.4
Alishan	18.5	2.3	1.6	0.0	0.0	22.4

APPENDIX B

TABLE 29a

AMOUNT OF MEAN MONTHLY RAINFALL ASSOCIATED WITH THE TAIWAN LOW (UNIT: MM)

Months	1	2	3	4	5	6	7	8	9	10	11	12
Keelung	83.3	89.5	74.7	41.8	2.6					4.0	13.5	69.1
Taipei	27.4	37.8	32.5	23.1	1.3					1.1	5.7	15.5
Taichung	7.2	20.3	11.5	9.1	0.2						0.7	5.8
Tainan	3.3	4.1	3.8	6.2							0.1	0.3
Kaoshiung	1.7	5.6	4.7	6.8								1.6
Hengchun	7.0	1.2	4.1	4.7						0.2	0.7	2.9
Taitung	10.2	13.3	4.2	4.5	1.7					0.3	1.5	5.4
Hwalien	13.4	21.6	13.4	12.7	0.2					0.1	7.7	11.1
Yilan	32.3	49.4	23.8	18.4	1.0					1.4	13.2	22.3
Alishan	13.9	23.5	14.3	18.3	1.7					0.3	1.6	10.1

APPENDIX B

TABLE 29b

PERCENTAGE OF MEAN MONTHLY RAINFALL ASSOCIATED WITH THE TAIWAN LOW (UNIT: %)

Months	1	2	3	4	5	6	7	8	9	10	11	12
Keelung	24.3	23.7	25.8	22.1	1.2					1.7	4.6	19.7
Taipei	32.2	27.5	22.0	16.9	0.7					0.9	7.9	26.9
Taichung	32.4	31.3	13.7	11.0	0.1						4.6	56.7
Tainan	34.8	20.1	11.9	10.4							0.7	18.7
Kaoshiung	26.9	44.6	9.4	10.7								46.3
Hengchun	45.2	8.5	11.9	9.6						0.2	1.5	30.4
Taitung	20.9	28.3	7.2	4.9	1.2					0.2	1.7	25.7
Hwalien	15.9	18.9	14.6	9.6	0.1					0.1	4.4	17.6
Yilan	23.4	28.8	21.3	18.9	0.6					0.5	4.7	14.1
Alishan	22.2	24.2	9.8	12.2	0.4					0.3	2.6	29.0

APPENDIX B

TABLE 30

MEAN, STANDARD DEVIATION, AND MAXIMUM OF DAILY RAINFALL ASSOCIATED WITH THE TAIWAN LOW (UNIT: MM)

	Mean	Standard Deviation	Maximum
Keelung	21.0	23.9	116.1
Taipei	9.3	12.5	61.3
Taichung	6.2	9.1	57.9
Tainan	4.3	8.4	31.5
Kaoshiung	5.9	9.9	44.8
Hengchun	3.3	6.4	32.9
Taitung	4.3	7.2	53.5
Hwalien	6.0	7.8	36.6
Yilan	10.4	17.3	107.7
Alishan	9.0	11.5	57.5

APPENDIX B

TABLE 31

PROBABILITY OF RAINY DAYS WITH DIFFERENT INTENSITIES FOR THE TAIWAN LOW
(UNIT: %)

mm	0.1 - 12.6	12.7 - 25.3	25.4 - 50.8	50.9 - 76.2	76.3 and greater	Total
Keelung	40.7	16.9	15.6	4.9	3.3	81.4
Taipei	51.0	13.6	3.7	1.6	0.0	69.9
Taichung	34.2	4.1	1.2	0.4	0.0	39.9
Tainan	13.2	1.2	0.8	0.0	0.0	15.2
Kaoshiung	13.2	1.6	0.8	0.0	0.0	15.6
Hengchun	21.8	0.4	0.8	0.0	0.0	23.0
Taitung	38.7	4.1	0.0	0.4	0.0	43.2
Hwalien	50.2	7.8	2.5	0.0	0.0	60.5
Yilan	56.0	7.4	4.5	1.2	1.6	70.7
Alishan	32.5	5.8	3.3	0.4	0.0	42.0

APPENDIX B

TABLE 32a

AMOUNT OF MEAN MONTHLY RAINFALL ASSOCIATED WITH POLAR FRONTS OVER TAIWAN
(UNIT: MM)

Months	1	2	3	4	5	6	7	8	9	10	11	12
Keelung	13.8	40.4	131.0	87.4	159.4	276.2	0.7	6.5	122.8	52.6	34.3	1.7
Taipei	8.2	21.1	74.8	75.8	128.5	228.5	1.6	6.2	89.6	20.7	17.5	0.3
Taichung	5.3	7.1	46.8	44.8	145.0	343.3	8.3	17.5	22.1	4.7	3.9	
Tainan	2.5	2.0	14.4	25.4	55.3	253.0	18.4	7.1	25.9	0.9	8.2	
Kaoshiung	1.4	0.4	27.3	30.5	84.7	288.2	18.4	8.2	28.4	11.7	9.3	
Hengchun	2.7	3.0	23.2	23.8	79.6	173.1	8.3	3.7	43.8	26.0	12.6	
Taitung	19.2	0.7	26.6	25.6	68.4	122.5	2.6	4.3	79.6	51.4	32.8	0.1
Hwalien	7.6	6.9	37.3	34.8	113.1	179.6	1.6	1.1	109.1	34.2	35.8	
Yilan	3.5	9.4	51.2	38.7	94.2	210.3	0.8	2.9	114.7	57.8	41.1	0.1
Alishan	13.5	4.1	71.6	76.2	300.6	597.1	24.2	30.0	79.5	24.1	16.0	

APPENDIX B

TABLE 32b

PERCENTAGE OF MEAN MONTHLY RAINFALL ASSOCIATED WITH POLAR FRONTS OVER TAIWAN
(UNIT: %)

Months	1	2	3	4	5	6	7	8	9	10	11	12
Keelung	4.1	10.7	45.3	46.2	71.1	88.3	0.6	3.4	31.6	22.5	11.6	0.5
Taipei	9.7	15.4	50.5	58.7	74.6	83.6	0.7	2.3	26.4	18.2	24.3	0.5
Taichung	23.7	11.0	56.0	53.8	80.9	88.1	3.9	4.7	14.9	44.5	24.1	
Tainan	26.5	9.9	44.6	42.8	58.8	82.2	6.5	2.0	23.2	20.0	41.8	
Kaoshiung	22.3	3.4	55.2	48.2	77.4	83.0	6.6	2.2	24.4	30.7	45.0	
Hengchun	17.2	21.3	67.1	48.8	51.5	54.7	2.2	0.9	17.6	31.8	25.1	
Taitung	39.2	1.5	37.5	22.6	47.0	55.7	0.9	1.8	24.9	31.6	36.3	0.6
Hwalien	9.1	6.0	40.5	26.5	49.8	75.7	0.8	0.5	27.3	13.4	20.4	
Yilan	2.6	5.5	45.8	39.7	51.3	83.2	0.6	1.3	24.4	18.2	14.7	0.1
Alishan	21.5	4.2	49.1	51.0	67.3	76.6	3.9	3.4	14.0	24.7	26.6	

APPENDIX B

TABLE 33

MEAN, STANDARD DEVIATION, AND MAXIMUM OF DAILY RAINFALL ASSOCIATED WITH POLAR FRONTS OVER TAIWAN (UNIT: MM)

	Mean	Standard Deviation	Maximum
Keelung	19.7	24.2	199.3
Taipei	15.3	24.3	243.3
Taichung	20.8	30.7	211.4
Tainan	17.9	28.9	235.3
Kaoshiung	20.6	29.7	237.7
Hengchun	16.1	21.6	150.8
Taitung	13.6	22.7	198.3
Hwalien	13.4	22.7	207.0
Yilan	13.6	23.9	295.9
Alishan	31.8	47.0	347.9

APPENDIX B

TABLE 34

PROBABILITY OF RAINY DAYS WITH DIFFERENT INTENSITIES FOR POLAR FRONTS OVER TAIWAN
(UNIT: %)

mm	0.1 - 12.6	12.7 - 25.3	25.4 - 50.8	50.9 - 76.2	76.3 and greater	Total
Keelung	45.7	14.6	13.0	6.9	2.7	82.9
Taipei	50.4	12.7	9.6	3.5	1.9	78.1
Taichung	33.1	8.3	6.3	3.9	3.5	55.1
Tainan	21.0	4.2	5.0	1.6	1.4	33.2
Kaoshiung	25.0	5.3	8.5	3.2	1.6	43.6
Hengchun	21.8	5.1	6.1	2.1	0.6	35.7
Taitung	37.2	8.8	5.8	2.4	0.8	55.0
Hwalien	54.7	8.3	6.7	2.4	1.9	74.0
Yilan	54.9	12.5	9.6	2.6	1.4	81.0
Alishan	32.3	10.8	13.2	5.3	7.2	68.8

APPENDIX B

TABLE 35a

AMOUNT OF MEAN MONTHLY RAINFALL ASSOCIATED WITH POLAR FRONTS SOUTH OF TAIWAN
(UNIT: MM)

Months	1	2	3	4	5	6	7	8	9	10	11	12
Keelung	3.5	1.5	9.0	6.6	20.3	3.2	*		15.5		6.0	7.1
Taipei	1.1	*	5.0	4.7	20.1	2.0	0.3		0.8		2.4	1.0
Taichung	*		5.2	5.0	13.1	2.0	4.4		1.5		2.7	0.4
Tainan			*	4.8	2.8	0.8	0.5		2.8		0.2	0.5
Kaoshiung			2.4	3.6	2.6	3.5	2.6		3.4		0.2	0.4
Hengchun				5.6	0.6	1.6	8.3		2.8		0.1	0.5
Taitung			3.5	5.2	4.4	3.2	2.1		4.8		0.4	2.1
Hwalien	1.2		3.8	6.5	16.3	2.8			7.6		0.9	1.9
Yilan	1.2		0.7	3.7	22.6	1.7	*		14.7		7.3	4.6
Alishan	0.1		11.9	9.4	37.4	5.3	9.9		7.8		4.4	1.1

*Indicates mean monthly rainfall less than 0.1 mm.

APPENDIX B

TABLE 35b

PERCENTAGE OF MEAN MONTHLY RAINFALL ASSOCIATED WITH POLAR FRONTS SOUTH OF TAIWAN
(UNIT: %)

Months	1	2	3	4	5	6	7	8	9	10	11	12
Keelung	1.0	0.4	3.1	3.5	9.0	1.0	*		4.0		2.0	2.0
Taipei	1.3	*	3.4	3.4	11.7	0.7	0.2		0.8		3.3	1.7
Taichung	0.3		6.3	6.0	7.3	0.5	2.1		1.0		16.6	3.9
Tainan			0.1	8.0	3.0	0.3	0.2		2.5		0.9	26.5
Kaoshiung			4.9	5.8	2.4	1.0	1.0		2.9		0.8	10.9
Hengchun				11.5	0.4	0.5	2.2		1.1		0.3	5.7
Taitung			6.0	5.7	3.0	1.5	0.8		1.5		0.4	10.0
Hwalien	1.4		4.1	4.9	7.2	1.2			1.9		0.5	3.0
Yilan	0.9		4.7	3.8	12.3	0.7	*		3.1		2.6	2.9
Alishan	0.1		8.1	6.3	8.4	2.0	1.6		1.4		7.4	3.3

*Indicates percentage of mean monthly rainfall less than 0.1%.

APPENDIX B

TABLE 36

MEAN, STANDARD DEVIATION, AND MAXIMUM OF DAILY RAINFALL ASSOCIATED WITH POLAR FRONTS SOUTH OF TAIWAN (UNIT: MM)

	Mean	Standard Deviation	Maximum
Keelung	13.8	20.7	118.3
Taipei	9.2	14.9	85.0
Taichung	11.4	13.1	53.3
Tainan	4.7	8.9	41.5
Kaoshiung	6.7	9.8	39.7
Hengchun	6.7	11.9	52.0
Taitung	6.6	9.2	34.4
Hwalien	8.3	8.5	34.3
Yilan	11.4	18.3	109.1
Alishan	18.4	18.5	71.0

APPENDIX B

TABLE 37

PROBABILITY OF RAINY DAYS WITH DIFFERENT INTENSITIES FOR POLAR FRONTS SOUTH OF TAIWAN (UNIT: %)

mm	0.1 - 12.6	12.7 - 25.3	25.4 - 50.8	50.9 - 76.2	76.3 and greater	Total
Keelung	43.2	12.5	8.0	0.0	2.3	66.0
Taipei	39.8	10.2	2.3	0.0	1.1	53.4
Taichung	25.0	8.0	3.4	1.1	0.0	37.5
Tainan	23.9	2.3	1.1	0.0	0.0	26.3
Kaoshiung	28.4	4.5	2.3	0.0	0.0	35.2
Hengchun	23.9	3.4	1.1	1.1	0.0	29.5
Taitung	37.5	0.1	2.3	0.0	0.0	48.9
Hwalien	46.6	12.5	2.3	0.0	0.0	61.4
Yilan	45.5	17.0	1.1	2.3	1.1	67.0
Alishan	36.4	11.4	13.6	4.5	2.0	65.9

APPENDIX B

TABLE 38a

AMOUNT OF MEAN MONTHLY RAINFALL ASSOCIATED WITH THE NORTH PACIFIC SUBTROPICAL ANTICYCLONE (UNIT: MM)

Months	1	2	3	4	5	6	7	8	9	10	11	12
Keelung	0.1	0.4	0.6	5.5	4.5	0.3	1.3	2.0	1.4	0.3	1.8	0.1
Taipei	*	*	0.3	2.5	4.6	3.2	14.2	17.0	1.1			
Taichung	*	*	0.3	6.3	2.3	17.5	26.6	6.0	4.7	1.6	*	*
Tainan	*	*	2.2	*	0.2	4.9	23.8	9.4	11.2	*	*	*
Kaoshiung	*	*	1.5	8.0	0.2	4.7	11.8	10.5	3.4	0.2	0.4	
Hengchun	0.4	2.2	4.2	0.7	9.3	24.3	20.5	21.2	19.6	0.1	1.3	0.5
Taitung	4.7	6.5	10.2	23.6	11.1	20.8	16.9	22.1	8.2	1.8	4.0	2.7
Hwalien	1.2	3.7	3.5	26.1	25.4	3.3	1.5	4.6	5.3	1.4	3.5	5.1
Yilan	0.1	0.1	0.8	6.2	15.3	3.8	1.8	2.0	4.1	0.9	3.3	1.8
Alishan	0.5	0.1	1.4	11.5	37.1	38.0	99.5	83.9	34.6	3.0	*	0.3

*Indicates mean monthly rainfall less than 0.1 mm.

APPENDIX B

TABLE 38b

PERCENTAGE OF MEAN MONTHLY RAINFALL ASSOCIATED WITH THE NORTH PACIFIC SUBTROPICAL ANTICYCLONE (UNIT: %)

Months	1	2	3	4	5	6	7	8	9	10	11	12
Keelung	*	0.1	0.2	2.9	2.0	0.1	1.0	1.1	0.4	0.2	0.6	*
Taipei	*	*	0.2	1.8	2.7	1.2	6.3	6.3	0.3			
Taichung	*	*	0.4	7.6	1.3	4.5	12.4	1.6	3.2	15.2	0.1	0.3
Tainan	0.1	*	7.0	*	0.2	1.6	8.4	2.7	10.3	0.5	0.4	7.2
Kaoshiung	0.4	0.4	3.1	12.7	0.2	1.4	4.3	2.8	2.8	0.4	1.8	
Hengchun	2.4	16.0	12.3	1.3	6.0	7.7	5.5	5.0	7.9	0.2	2.6	5.3
Taitung	9.5	13.9	17.6	25.6	7.6	9.5	5.9	9.0	2.6	1.0	4.3	12.7
Hwalien	1.4	3.2	3.8	19.9	11.2	1.4	0.8	2.1	1.3	0.6	2.0	8.1
Yilan	*	*	0.8	6.4	8.3	1.5	1.2	0.9	0.9	0.3	1.2	1.1
Alishan	0.9	0.1	1.0	7.7	8.3	4.9	15.9	9.5	6.1	3.1	*	0.9

*Indicates percentage of mean monthly rainfall less than 0.1%.

APPENDIX B

TABLE 39

MEAN, STANDARD DEVIATION, AND MAXIMUM OF DAILY RAINFALL ASSOCIATED WITH THE NORTH PACIFIC SUBTROPICAL ANTICYCLONE (UNIT: MM)

	Mean	Standard Deviation	Maximum
Keelung	2.5	4.9	31.7
Taipei	6.6	11.6	66.8
Taichung	7.4	14.5	68.0
Tainan	4.7	8.8	54.2
Kaoshiung	4.7	9.9	84.0
Hengchun	5.2	8.4	65.7
Taitung	6.0	10.1	72.6
Hwalien	5.3	9.9	60.6
Yilan	3.9	7.9	67.0
Alishan	12.4	15.2	92.6

APPENDIX B

TABLE 40

PROBABILITY OF RAINY DAYS WITH DIFFERENT INTENSITIES FOR THE NORTH PACIFIC SUBTROPICAL ANTICYCLONE (UNIT: %)

mm	0.1 - 12.6	12.7 - 25.3	25.4 - 50.8	50.9 - 76.2	76.3 and greater	Total
Keelung	11.2	0.4	0.1	0.0	0.0	11.7
Taipei	8.5	1.2	0.6	0.1	0.0	10.4
Taichung	11.2	1.7	0.3	0.7	0.0	13.9
Tainan	12.8	0.7	0.6	0.1	0.0	14.2
Kaoshiung	12.7	0.9	0.1	0.0	0.1	13.8
Hengchun	22.9	2.6	0.4	0.1	0.0	26.0
Taitung	30.5	2.9	1.2	0.4	0.0	35.0
Hwalien	22.6	1.3	0.7	0.4	0.0	25.0
Yilan	15.0	1.2	0.0	0.1	0.0	16.3
Alishan	26.2	6.5	5.9	0.9	0.3	39.8

APPENDIX B

TABLE 41a

AMOUNT OF MEAN MONTHLY RAINFALL ASSOCIATED WITH THE SOUTHWEST MONSOON
(UNIT: MM)

Months	1	2	3	4	5	6	7	8	9	10	11	12
Keelung			*	*	6.7	20.8	22.0	1.8	0.6			
Taipei			0.4	*	6.2	17.9	79.8	35.0	3.9			
Taichung					12.8	16.2	42.2	25.1	0.7			
Tainan					9.9	34.6	40.9	42.1	7.1			
Kaoshiung					8.0	22.0	44.5	51.6	2.9	0.2		
Hengchun			0.1	0.2	14.0	18.7	48.2	28.6	7.0	0.2		
Taitung			0.6		3.1	6.0	26.1	10.5	*			
Hwalien				0.1	5.1	16.9	8.0	15.3				
Yilan					7.9	20.9	9.3	26.7	0.2			
Alishan					26.9	40.3	131.2	83.2	5.2			

*Indicates mean monthly rainfall less than 0.1 mm.

APPENDIX B

TABLE 41b

PERCENTAGE OF MEAN MONTHLY RAINFALL ASSOCIATED WITH THE SOUTHWEST MONSOON
(UNIT: %)

Months	1	2	3	4	5	6	7	8	9	10	11	12
Keelung			*	*	3.0	6.6	17.3	9.8	0.2			
Taipei			0.3	*	3.6	6.6	35.5	13.0	1.1			
Taichung					7.1	4.2	19.8	6.8	0.5			
Tainan					10.5	11.3	14.4	12.1	6.4			
Kaoshiung					7.3	6.3	16.0	14.0	2.5	0.6		
Hengchun			0.3	0.5	9.1	5.9	13.0	6.8	2.8	0.2		
Taitung			1.0	*	2.1	2.7	9.1	4.3	*			
Hwalien				0.1	2.2	7.1	4.0	6.9				
Yilan				0.1	4.3	8.3	6.4	11.9	0.1			
Alishan					6.4	5.2	21.0	9.4	0.9			

*Indicates percentage of mean monthly rainfall less than 0.1%.

APPENDIX B

TABLE 42

MEAN, STANDARD DEVIATION, AND MAXIMUM OF DAILY RAINFALL ASSOCIATED WITH THE SOUTHWEST MONSOON (UNIT: MM)

	Mean	Standard Deviation	Maximum
Keelung	7.9	12.1	64.8
Taipei	11.8	21.0	145.9
Taichung	8.1	13.7	114.2
Tainan	10.4	17.5	109.6
Kaoshiung	11.0	16.2	86.1
Hengchun	8.2	14.8	120.1
Taitung	8.1	16.6	94.1
Hwalien	7.3	12.1	64.1
Yilan	7.1	12.0	70.9
Alishan	16.4	21.5	166.3

APPENDIX B

TABLE 43

PROBABILITY OF RAINY DAYS WITH DIFFERENT INTENSITIES FOR THE SOUTHWEST MONSOON
(UNIT: %)

mm	0.1 - 12.6	12.7 - 25.3	25.4 - 60.8	50.9 - 76.2	76.3 and greater	Total
Keelung	22.5	3.2	1.4	0.6	0.0	27.7
Taipei	28.5	4.6	4.0	0.3	1.2	38.6
Taichung	29.4	6.1	1.7	0.3	0.3	37.8
Tainan	25.9	3.7	2.0	1.4	0.3	33.3
Kaoshiung	28.8	3.5	3.2	1.2	0.6	37.3
Hengchun	30.8	3.2	2.6	0.3	0.3	37.2
Taitung	15.6	1.4	0.6	0.0	0.6	18.2
Hwalien	16.4	1.7	1.2	0.3	0.0	19.6
Yilan	24.2	2.9	1.4	0.6	0.0	29.1
Alishan	33.1	11.0	8.4	1.4	1.4	63.3

APPENDIX B

TABLE 44a

AMOUNT OF MEAN MONTHLY RAINFALL ASSOCIATED WITH NORTHERN-TYPE TYPHOONS
(UNIT: MM)

Months	1	2	3	4	5	6	7	8	9	10	11	12
Keelung				1.2	17.7	3.8	77.5	101.8	140.3	46.0	60.6	5.8
Taipei				0.4	6.4	9.5	90.0	122.8	138.3	53.6	15.3	0.1
Taichung				0.2	1.0	2.2	75.3	128.4	66.9	2.0	2.3	
Tainan					0.9	4.6	118.8	69.6	25.5	0.6	3.0	
Kaoshiung					1.6	7.6	129.2	61.6	20.5	3.7	3.0	
Hengchun				0.2	20.3	57.0	179.0	84.8	60.0	13.4	29.6	2.1
Taitung					20.3	22.5	80.3	58.0	76.8	39.1	25.0	0.7
Hwalien				2.8	30.4	11.0	107.0	85.6	116.1	67.5	66.7	
Yilan				4.8	26.6	4.3	86.8	105.1	129.1	80.4	53.0	1.7
Alishan				0.2	13.1	7.4	236.1	305.1	302.4	12.4	7.6	

APPENDIX B

TABLE 44b

PERCENTAGE OF MEAN MONTHLY RAINFALL ASSOCIATED WITH NORTHERN-TYPE TYPHOONS
(UNIT: %)

Months	1	2	3	4	5	6	7	8	9	10	11	12
Keelung				0.6	7.9	1.2	61.0	54.0	36.1	19.7	0.4	1.7
Taipei				0.3	3.7	3.5	40.0	45.6	40.8	46.8	21.2	0.2
Taichung				0.3	0.5	0.6	35.2	34.9	45.2	18.8	14.5	
Tainan					0.9	1.5	41.7	30.0	22.8	14.0	15.0	
Kaoshiung					1.4	2.2	46.4	16.6	17.6	9.7	14.5	
Hengchun				0.4	13.1	18.0	48.2	20.1	24.0	16.4	58.8	22.7
Taitung					13.9	10.2	28.1	23.7	24.0	24.1	27.7	3.4
Hwalien				2.1	13.4	4.6	53.2	38.7	29.0	30.4	38.1	
Yilan				4.9	14.5	1.7	60.1	46.7	27.4	25.4	19.0	1.1
Alishan				0.2	2.9	1.0	37.7	34.5	53.0	12.7	12.6	

APPENDIX B

TABLE 45a

AMOUNT OF MEAN MONTHLY RAINFALL ASSOCIATED WITH SOUTHERN-TYPE TYPHOONS
(UNIT: MM)

Months	1	2	3	4	5	6	7	8	9	10	11	12
Keelung				6.3	0.9	2.0	8.3	36.6	70.9	35.0	0.4	
Taipei				1.1	1.2	3.7	14.5	40.4	75.9	8.5		
Taichung				0.7	3.8	7.5	28.7	52.2	38.1	1.5		
Tainan				8.5	24.5	4.1	54.8	120.6	23.1	2.0		
Kaoshiung				7.9	11.5	3.9	49.5	104.8	35.8	16.8	0.2	
Hengchun				11.1	25.4	15.0	69.7	181.9	33.9	19.4	0.1	
Taitung				19.4	18.7	23.3	107.3	95.6	88.6	35.9	0.3	
Hwalien				20.0	19.8	7.4	61.4	84.2	81.8	25.3	0.4	
Yilan				6.8	3.3	2.6	29.6	41.4	144.7	36.5		
Alishan				3.0	12.3	45.5	63.4	190.1	93.7	8.9		

APPENDIX B

TABLE 45b

PERCENTAGE OF MEAN MONTHLY RAINFALL ASSOCIATED WITH SOUTHERN-TYPE TYPHOONS
(UNIT: %)

Months	1	2	3	4	5	6	7	8	9	10	11	12
Keelung				3.4	0.4	0.6	6.5	19.4	18.3	15.0	0.1	
Taipei				0.8	0.7	1.3	6.5	15.0	22.4	7.4	0.1	
Taichung				0.8	2.1	1.9	13.4	14.2	25.7	14.4	0.2	
Tainan				14.3	26.0	1.3	19.2	34.5	20.7	46.5	0.2	
Kaoshiung				12.4	10.5	1.1	17.8	28.3	30.8	44.2	1.1	
Hengchun				22.6	16.4	4.7	18.8	43.2	16.6	28.9	0.3	
Taitung				21.0	12.8	10.6	37.5	39.0	27.7	22.1	0.3	
Hwalien				15.2	8.7	3.1	30.5	38.1	20.4	11.4	0.2	
Yilan				6.9	1.8	1.0	20.4	18.4	30.8	11.5		
Alishan				2.0	2.8	5.9	10.1	21.5	16.4	9.1		

APPENDIX B

TABLE 46a

MEAN, STANDARD DEVIATION, AND MAXIMUM OF DAILY RAINFALL ASSOCIATED WITH NORTHERN-TYPE TYPHOONS (UNIT: MM)

	Mean	Standard Deviation	Maximum
Keelung	39.4	54.2	294.1
Taipei	36.1	49.8	332.1
Taichung	36.0	69.2	431.1
Tainan	24.5	48.2	292.6
Kaoshiung	26.0	75.5	621.5
Hengchun	38.3	54.2	273.0
Taitung	35.5	53.5	219.4
Hwalien	51.5	72.4	360.3
Yilan	44.0	61.7	300.0
Alishan	79.7	161.1	874.3

APPENDIX B

TABLE 46b

MEAN, STANDARD DEVIATION, AND MAXIMUM OF DAILY RAINFALL ASSOCIATED WITH SOUTHERN-TYPE TYPHOONS (UNIT: MM)

	Mean	Standard Deviation	Maximum
Keelung	26.8	50.0	323.5
Taipei	21.3	39.7	230.3
Taichung	21.1	38.0	243.3
Tainan	33.4	42.7	200.4
Kaoshiung	30.9	39.4	232.6
Hengchun	46.0	57.2	256.6
Taitung	53.5	60.8	289.4
Hwalien	44.6	57.7	284.3
Yilan	42.2	86.7	460.5
Alishan	56.6	93.4	508.0

APPENDIX B

TABLE 47a

PROBABILITY OF RAINY DAYS WITH DIFFERENT INTENSITIES FOR NORTHERN-TYPE TYPHOONS
(UNIT: %)

mm	0.1 - 12.6	12.7 - 25.4	25.4 - 50.8	50.9 - 76.2	76.3 and greater	Total
Keelung	37.8	12.2	15.5	8.1	12.2	85.8
Taipei	34.5	19.6	14.9	8.1	12.8	89.9
Taichung	35.1	4.7	7.4	2.7	7.4	57.8
Tainan	35.8	6.1	6.1	0.7	6.8	55.5
Kaoshiung	43.2	8.1	6.8	3.4	3.4	64.9
Hengchun	35.1	5.4	11.5	7.4	11.5	70.9
Taitung	35.8	10.1	6.1	2.7	12.8	67.5
Hwalien	29.1	12.8	4.1	8.8	15.5	70.3
Yilan	30.4	16.2	13.5	7.4	15.5	83.0
Alishan	38.5	15.5	6.1	5.4	16.9	82.4

APPENDIX B

TABLE 47b

PROBABILITY OF RAINY DAYS WITH DIFFERENT INTENSITIES FOR SOUTHERN-TYPE TYPHOONS

mm	0.1 - 12.6	12.7 - 25.3	25.4 - 50.8	50.9 - 76.2	76.3 and greater	Total
Keelung	39.8	13.6	10.2	4.5	6.8	74.9
Taipei	53.4	12.5	10.2	4.5	4.5	85.1
Taichung	46.6	13.6	11.4	1.1	5.7	78.4
Tainan	33.0	11.4	10.2	10.2	8.0	72.8
Kaoshiung	42.0	13.6	19.3	6.8	11.4	93.1
Hengchun	27.3	14.8	15.9	11.4	12.5	81.8
Taitung	29.5	9.1	20.5	8.0	23.9	91.0
Hwalien	38.6	9.1	12.5	2.3	21.6	84.1
Yilan	42.0	14.8	6.8	5.7	9.1	78.4
Alishan	26.1	17.0	26.1	9.1	13.6	91.9

APPENDIX B

TABLE 48a

AMOUNT OF MEAN MONTHLY RAINFALL ASSOCIATED WITH THE KYUSHU-TYPE TYPHOON
(UNIT: MM)

Months	1	2	3	4	5	6	7	8	9	10	11	12
Keelung						6.3		11.4	0.1			
Taipei						6.2		13.9	2.0			
Taichung						0.7		95.3	0.6			
Tainan						0.7		92.5	1.9			
Kaoshiung						9.5		96.6	2.8			
Hengchun						14.1		57.2	0.4			
Taitung						4.4		23.9				
Hwalien						6.3		14.5				
Yilan						3.8		21.3				
Alishan						18.5		120.4	0.7			

APPENDIX B

TABLE 48b

PERCENTAGE OF MEAN MONTHLY RAINFALL ASSOCIATED WITH THE KYUSHU-TYPE TYPHOON
(UNIT: %)

Months	1	2	3	4	5	6	7	8	9	10	11	12
Keelung						2.0		6.8				
Taipei						2.3		5.2	0.6			
Taichung						0.2		25.9	0.4			
Tainan						0.2		26.5	1.7			
Kaoshiung						2.7		26.1	2.4			
Hengchun						4.5		13.6	0.2			
Taitung						2.0		9.8				
Hwalien						2.7		6.5				
Yilan						1.5		9.4				
Alishan						2.4		13.6	0.1			

APPENDIX B

TABLE 49

MEAN, STANDARD DEVIATION, AND MAXIMUM OF DAILY RAINFALL ASSOCIATED WITH THE KYUSHU-TYPE TYPHOON (UNIT: MM)

	Mean	Standard Deviation	Maximum
Keelung	15.1	23.1	69.6
Taipei	14.3	17.7	68.2
Taichung	46.2	136.1	660.2
Tainan	35.7	57.1	234.6
Kaoshiung	48.0	57.1	240.3
Hengchun	28.1	33.7	126.9
Taitung	19.5	16.7	48.6
Hwalien	12.0	21.0	69.4
Yilan	17.3	34.8	137.8
Alishan	35.7	57.1	234.6

APPENDIX B

TABLE 50

PROBABILITY OF RAINY DAYS WITH DIFFERENT INTENSITIES FOR THE KYUSHU-TYPE TYPHOON
(UNIT: %)

mm	0.1 - 12.6	12.7 - 25.3	25.4 - 50.8	50.9 - 76.2	76.3 and greater	Total
Keelung	33.3	0.0	3.3	6.7	0.0	43.3
Taipei	33.3	10.0	10.0	3.3	0.0	56.6
Taichung	43.3	13.3	10.0	3.3	6.7	76.6
Tainan	50.0	0.0	10.0	13.3	6.7	80.0
Kaoshiung	26.7	13.3	16.7	6.7	20.0	83.4
Hengchun	36.7	10.0	16.7	3.3	10.0	76.7
Taitung	23.3	10.0	20.0	0.0	0.0	53.3
Hwalien	50.0	3.3	3.3	6.7	0.0	63.3
Yilan	40.0	0.0	10.0	0.0	3.3	53.3
Alishan	46.7	10.0	20.0	6.7	13.3	96.7

APPENDIX B

TABLE 51a

AMOUNT OF MEAN MONTHLY RAINFALL ASSOCIATED WITH MONSOON TROUGHS
(UNIT: MM)

Months	1	2	3	4	5	6	7	8	9	10	11	12
Keelung						0.3	16.7	10.6	13.2			
Taipei						0.4	24.4	32.1	11.7			
Taichung						0.2	28.2	43.7	13.1	0.03		
Tainan						4.9	27.6	7.8	13.2			
Kaoshiung						7.3	22.1	45.8	16.7	0.06		
Hengchun				0.5	25.4	15.0	36.7	43.3	56.6			
Taitung				0.1	2.2	17.3	51.0	29.0	48.1			
Hwalien						10.1	21.8	13.5	40.8	0.03		
Yilan						5.4	13.9	20.9	28.1			
Alishan						45.5	69.9	58.1	25.8			

APPENDIX B

TABLE 51b

PERCENTAGE OF MEAN MONTHLY RAINFALL ASSOCIATED WITH MONSOON TROUGHS
(UNIT: %)

Months	1	2	3	4	5	6	7	8	9	10	11	12
Keelung						0.1	13.1	5.6	3.4			
Taipei						0.2	10.8	11.9	3.5			
Taichung						0.1	13.2	11.9	8.9	2.6		
Tainan						1.6	9.7	2.2	12.8			
Kaoshiung						2.1	8.0	9.7	14.4	1.6		
Hengchun				1.0	0.4	4.0	9.9	10.3	22.7			
Taitung				0.1	1.5	7.9	17.8	11.8	15.0			
Hwalien						4.3	10.8	6.1	10.2	0.1		
Yilan						2.1	9.6	9.3	6.0			
Alishan						2.0	9.6	6.5	4.5			

APPENDIX B

TABLE 52

MEAN, STANDARD DEVIATION, AND MAXIMUM OF DAILY RAINFALL ASSOCIATED WITH MONSOON TROUGHS (UNIT: MM)

	Mean	Standard Deviation	Maximum
Keelung	11.2	16.9	74.2
Taipei	13.0	16.1	67.2
Taichung	13.6	19.6	84.0
Tainan	8.4	17.9	119.0
Kaoshiung	11.6	24.0	138.9
Hengchun	17.3	20.7	102.5
Taitung	20.8	29.4	149.7
Hwalien	15.8	25.3	106.2
Yilan	13.4	19.3	99.6
Alishan	17.6	17.6	101.9

APPENDIX B

TABLE 53

PROBABILITY OF RAINY DAYS WITH DIFFERENT INTENSITIES FOR MONSOON TROUGHS
(UNIT: %)

mm	0.1 - 12.6	12.7 - 25.3	25.4 - 50.8	50.9 - 76.2	76.3 and greater	Total
Keelung	24.4	2.4	2.4	2.4	0.0	31.6
Taipei	29.1	6.3	8.7	1.6	0.0	45.7
Taichung	37.8	6.3	7.1	3.1	0.8	55.1
Tainan	38.7	4.8	1.6	0.0	0.8	46.0
Kaoshiung	46.5	9.4	3.1	0.8	2.4	62.2
Hengchun	37.8	5.5	13.4	2.4	2.4	61.5
Taitung	34.6	11.8	6.3	6.3	2.4	61.4
Hwalien	32.3	7.1	3.9	2.4	2.4	48.1
Yilan	29.1	7.1	6.3	1.6	0.8	44.9
Alishan	37.8	20.5	17.3	2.4	0.8	78.8

APPENDIX C

TABLE 54

FREQUENCY DISTRIBUTION OF WET-SPELLS BY THE SIMPLE MARKOV CHAIN PROBABILITY MODEL (Fe) AND BY OBSERVATION (Fo)

Spells	Keelung		Taipei		Taichung		Kaoshiung	
	Fe	Fo	Fe	Fo	Fe	Fo	Fe	Fo
1	163	180	201	224	192	204	168	203
2	118	126	134	126	114	127	99	85
3	86	73	91	72	68	47	58	40
4	62	61	61	61	41	30	34	21
5	45	39	41	39	24	25	20	22
6	33	33	27	33	15	16	12	15
7	24	18	18	18	9	8	7	9
8	17	17	12	17	5	7	4	5
9	12	10	8	10	3	5	2	3
10	9	5	5	5	2	1	1	0
11	7	7	4	7	1	1	1	0
12	5	5	2	5	1	2	0	0
13	4	3	2	4	0	1	0	1
14	3	2	1	3	0	0	0	0
15	3	2	1	3	0	1	0	1
15+	9	5	2	9	0	1	0	3
Chi-square	7.94		9.98		12.69		21.35	

APPENDIX C

TABLE 54

CONTINUED

Spells	Hengchun		Taitung		Hwalien		Yilan	
	Fe	Fo	Fe	Fo	Fe	Fo	Fe	Fo
1	193	230	270	278	217	252	179	206
2	115	97	156	146	145	130	128	105
3	68	56	91	103	97	86	91	104
4	41	33	53	42	64	55	65	54
5	24	24	30	27	43	38	47	34
6	14	4	18	12	29	29	33	36
7	9	6	10	16	19	15	24	27
8	5	10	6	7	13	12	17	15
9	3	7	3	4	8	8	12	9
10	2	6	2	4	6	6	9	11
11	1	0	1	1	4	7	6	4
12	1	1	1	1	3	5	4	8
13	0	1	0	1	2	2	3	6
14	0	0	0	0	1	3	2	4
15	0	0	0	0	1	1	2	3
15+	0	2	0	0	2	3	4	3
Chi-square	26.73		10.81		11.20		18.27	

APPENDIX C

TABLE 55

FREQUENCY DISTRIBUTION OF DRY-SPELLS BY THE SIMPLE MARKOV CHAIN PROBABILITY MODEL (Fe) AND BY OBSERVATION (Fo)

Spells	Keelung		Taipei		Taichung		Kaoshiung	
	Fe	Fo	Fe	Fo	Fe	Fo	Fe	Fo
1	186	219	175	217	81	129	55	106
2	127	119	125	102	67	73	47	66
3	87	72	89	84	56	47	41	42
4	59	62	64	55	46	49	35	26
5	41	37	46	34	39	41	31	26
6	28	24	33	31	32	19	27	25
7	19	11	23	26	27	20	23	12
8	13	13	17	9	22	12	20	11
9	9	6	12	17	18	8	17	9
10	6	1	8	15	15	10	15	5
11	4	3	6	5	13	8	13	9
12	3	4	4	3	11	2	11	5
13	2	1	3	3	9	6	10	4
14	1	0	2	3	7	9	8	4
15	1	4	2	2	6	6	7	4
15+	2	12	4	7	30	40	47	54
Chi-square	18.59	31.64			60.38		87.68	

APPENDIX C

TABLE 55

CONTINUED

Spells	Hengchun		Taitung		Hwalien		Yilan	
	Fe	Fo	Fe	Fo	Fe	Fo	Fe	Fo
1	109	142	167	184	207	255	216	259
2	84	92	124	125	141	123	141	139
3	65	44	92	87	97	91	92	76
4	50	43	68	59	66	50	61	48
5	39	31	50	53	45	39	40	28
6	30	33	37	44	31	23	26	25
7	23	20	28	16	21	20	17	8
8	18	13	20	17	14	9	11	8
9	14	8	15	17	10	11	8	9
10	11	12	11	10	7	9	5	4
11	8	9	8	4	5	4	3	2
12	6	2	6	6	3	4	2	5
13	5	2	5	1	2	4	1	4
14	4	8	3	2	2	2	1	0
15	3	1	3	4	1	2	1	2
15+	10	18	7	17	2	8	1	8
Chi-square	29.4		15.85		23.25		23.64	

APPENDIX C

TABLE 56

VALUES OF LOG N/α FOR DIFFERENT VALUES OF LOG N/S FOR SOLVING EQUATION $S = \alpha \text{ LOGe } (1-N/\alpha)$

$\log_{10}N/S$	0	1	2	3	4	5	6	7	8	9
0.4	0.61	0.63	0.65	0.66	0.68	0.70	0.72	0.74	0.76	0.77
0.5	0.79	0.81	0.83	0.85	0.86	0.88	0.90	0.91	0.93	0.95
0-6	0.96	0.98	0.99	1.01	1.03	1.04	1.06	1.07	1.09	1.11
0-7	1.12	1.14	1.15	1.17	1.18	1.20	1.21	1.23	1.24	1.26
0-8	1.27	1.29	1.30	1.31	1.33	1.34	1.36	1.37	1.39	1.40
0-9	1.41	1.43	1.44	1.46	1.47	1.48	1.50	1.51	1.53	1.54
1-0	1.55	1.57	1.58	1.59	1.61	1.62	1.63	1.65	1.66	1.67
1-1	1.69	1.70	1.71	1.73	1.74	1.75	1.77	1.78	1.79	1.81
1-2	1.82	1.83	1.85	1.86	1.87	1.88	1.90	1.91	1.92	1.94
1-3	1.95	1.96	1.97	1.99	2.00	2.01	2.03	2.04	2.05	2.06
1-4	2.08	2.09	2.10	2.11	2.13	2.14	2.15	2.16	2.18	2.19

APPENDIX C

TABLE 56

CONTINUED

$\log_{10} N/S$	0	1	2	3	4	5	6	7	8	9
1-5	2.20	2.21	2.23	2.24	2.25	2.26	2.28	2.29	2.30	2.31
1-6	2.32	2.34	2.35	2.36	2.37	2.39	2.40	2.41	2.42	2.43
1-7	2.45	2.46	2.47	2.48	2.50	2.51	2.52	2.53	2.54	2.56
1-8	2.57	2.58	2.59	2.60	2.62	2.63	2.64	2.65	2.66	2.68
1-9	2.69	2.70	2.71	2.72	2.74	2.75	2.76	2.77	2.78	2.79
2-0	2.81	2.82	2.83	2.84	2.85	2.87	2.88	2.89	2.90	2.91
2-1	2.92	2.94	2.95	2.96	2.97	2.98	2.99	3.01	3.02	3.03
2-2	3.04	3.05	3.06	3.08	3.09	3.10	3.11	3.12	3.13	3.15
2-3	3.16	3.17	3.18	3.19	3.20	3.22	3.23	3.24	3.25	3.26
2-4	3.27	3.28	3.30	3.31	3.32	3.33	3.34	3.35	3.36	3.38
2-5	3.39	3.40	3.41	3.42	3.43	3.45	3.46	3.47	3.48	3.49

APPENDIX C

TABLE 56

CONTINUED

$\log_{10}N/S$	0	1	2	3	4	5	6	7	8	9
2-6	3.50	3.51	3.53	3.54	3.55	3.56	3.57	3.58	3.59	3.60
2-7	3.62	3.63	3.64	3.65	3.66	3.67	3.68	3.70	3.71	3.72
2-8	3.73	3.74	3.75	3.76	3.77	3.79	3.80	3.81	3.82	3.83
2-9	3.84	3.85	3.86	3.88	3.89	3.90	3.91	3.92	3.93	3.94
3-0	3.95	3.97	3.98	3.99	4.00	4.01	4.02	4.03	4.04	4.06
3-1	4.07	4.08	4.09	4.10	4.11	4.12	4.13	4.15	4.16	4.17
3-2	4.18	4.19	4.20	4.21	4.22	4.23	4.25	4.26	4.27	4.28
3-3	4.29	4.30	4.31	4.32	4.33	4.35	4.36	4.37	4.38	4.39
3-4	4.40	4.41	4.42	4.43	4.45	4.46	4.47	4.48	4.49	4.50
3-5	4.51	4.52	4.53	4.55	4.56	4.57	4.58	4.59	4.60	4.61

(After Fisher, *et al.*, 1943)

APPENDIX C

TABLE 59

FREQUENCY DISTRIBUTION OF SYNOPTIC FLOW TYPES BY THE SIMPLE MARKOV CHAIN PROBABILITY MODEL (Fe) AND BY OBSERVATION (Fo)

Spells	1		2		3		4		5	
	Fe	Fo	Fe	Fo	Fe	Fo	Fe	Fo	Fe	Fo
1	132	129	170	170	108	96	103	83	15	22
2	79	97	93	100	33	46	55	59	10	16
3	47	34	51	42	10	9	29	27	7	5
4	28	29	28	30	3	6	15	14	4	1
5	17	17	15	10	1	1	8	9	3	1
6	9	8	8	15	0	0	4	7	2	0
7	6	6	4	5	0	0	2	5	1	0
8	4	3	2	0	0	0	1	5	1	0
9	2	2	1	0	0	0	1	3	1	0
10	1	2	1	0	0	0	0	2	0	0
Chi-square	7.91		10.06		6.55		4.52		7.44	

APPENDIX C

TABLE 59

CONTINUED

Spells	6		7		8		9		11	
	Fe	Fo	Fe	Fo	Fe	Fo	Fe	Fo	Fe	Fo
1	108	117	42	52	27	22	24	23	32	32
2	66	69	28	27	16	26	11	11	16	18
3	40	36	18	10	9	10	5	7	8	9
4	24	13	12	8	5	3	3	4	4	1
5	14	15	8	8	3	1	1	1	2	1
6	9	8	5	5	2	0	0	0	1	1
7	5	4	3	2	1	0	1	0	1	1
8	3	3	2	2	1	0	0	0	0	1
9	2	4	1	3	0	1	0	0	0	0
10	1	1	1	2	0	0	0	0	0	0
Chi-square	6.71		7.31		8.08		0.84		0.38	

APPENDIX C

TABLE 60

FREQUENCY DISTRIBUTION OF SYNOPTIC FLOW TYPES BY THE LOGARITHMIC SERIES (Fe) AND BY OBSERVATION (Fo)

Spells	1		2		3		4		5	
	Fe	Fo	Fe	Fo	Fe	Fo	Fe	Fo	Fe	Fo
1	162	129	196	170	122	96	106	83	26	22
2	65	97	74	100	30	46	44	59	9	16
3	35	34	38	42	10	9	24	27	4	5
4	21	29	22	30	4	6	15	14	2	1
5	13	17	13	10	2	1	10	9	1	1
6	9	8	8	15	1	0	7	7	1	0
7	6	6	5	5	0	0	5	5	0	0
8	4	3	4	0	0	0	4	5	0	0
9	3	2	2	0	0	0	3	3	0	0
10	2	2	2	2	0	0	2	2	0	0
Chi-square	26.98		22.74		14.00		10.31		20.60	

APPENDIX C

TABLE 60

CONTINUED

Spells	6		7		8		9		11	
	Fe	Fo	Fe	Fo	Fe	Fo	Fe	Fo	Fe	Fo
1	139	117	55	52	31	22	27	23	38	32
2	56	69	24	27	12	26	9	11	13	18
3	30	36	13	10	6	10	4	7	6	9
4	18	13	8	8	4	3	3	4	3	1
5	11	15	6	8	2	1	1	1	2	1
6	8	8	4	5	2	0	0	0	1	1
7	5	4	3	2	1	0	0	0	1	1
8	4	3	2	2	0	0	0	0	0	1
9	3	4	2	3	0	1	0	0	0	0
10	2	1	1	2	0	0	0	0	0	0
Chi-square	10.73		1.90		21.60		1.03		4.37	

APPENDIX D

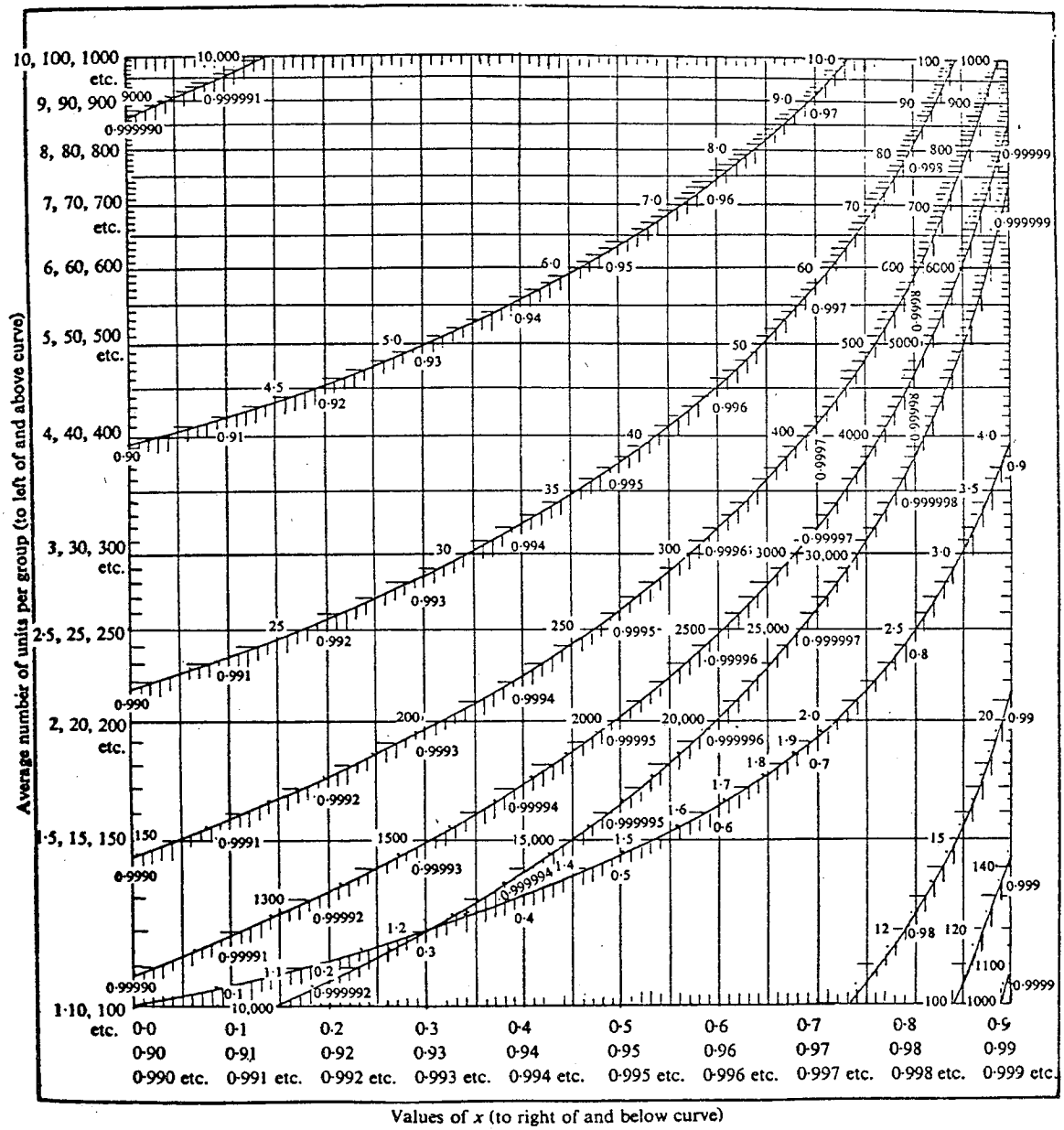

Figure 58. The relation between N/S and x for all values of the former from 1 to 70,000 (after Williams, 1947).

APPENDIX E

REGRESSION EQUATIONS FOR THE ESTIMATION OF ANNUAL RAINFALL

Keelung	$Y = 18489.6 - 156.6X_1 - 45.9X_2 - 784.4X_5 - 397.1X_6 - 88.9X_{11}$
Taipei	$Y = 709.9 + 1.3X_2 + 100.3X_3 + 119.4X_4 - 143.4X_{11}$
Taichung	$Y = 7288.8 - 29.2X_7 + 58.9X_8 + 367X_9 - 122.1X_{10} - 52.0X_{11}$
Kaoshiung	$Y = -2743.7 - 150.1X_3 + 84.0X_4 + 235.4X_7 + 43.0X_8 + 384.0X_9$
Hengchun	$Y = 9203.8 - 157.7X_1 - 98.2X_2 - 282.7X_4 + 332.4X_7 + 407.2X_8$
Taitung	$Y = 36115.2 + 765.4X_5 - 745.4X_2 - 767.0X_3 - 916.3X_8 - 641.3X_{11}$
Hwalien	$Y = 12088.9 - 299.2X_3 - 35.0X_7 - 154.5X_5 + 36.9X_8 - 357.6X_{10}$
Yilan	$Y = -8132.1 + 156.4X_2 + 272.8X_4 - 40.1X_7 - 456.6X_{10} + 378.3X_{11}$
Alishan	$Y = 11354.5 + 550.4X_3 - 1312.1X_5 - 162.8X_8 + 503.1X_9 - 431.9X_{11}$

APPENDIX F

TABLE 61

COEFFICIENTS OF DETERMINATION (R^2) BETWEEN ANNUAL RICE YIELDS AND ANNUAL FREQUENCIES OF SYNOPTIC FLOW TYPES

Steps	Flow Types	R^2	ΣR^2
1	8	0.5716	0.5716
2	2	0.1345	0.7061
3	5	0.0826	0.7887
4	3	0.0916	0.8802
5	6	0.0577	0.9380
6	10	0.0264	0.9644
7	7	0.0209	0.9853
8	1	0.0044	0.9897
9	8+9	0.0101	0.9998

APPENDIX G

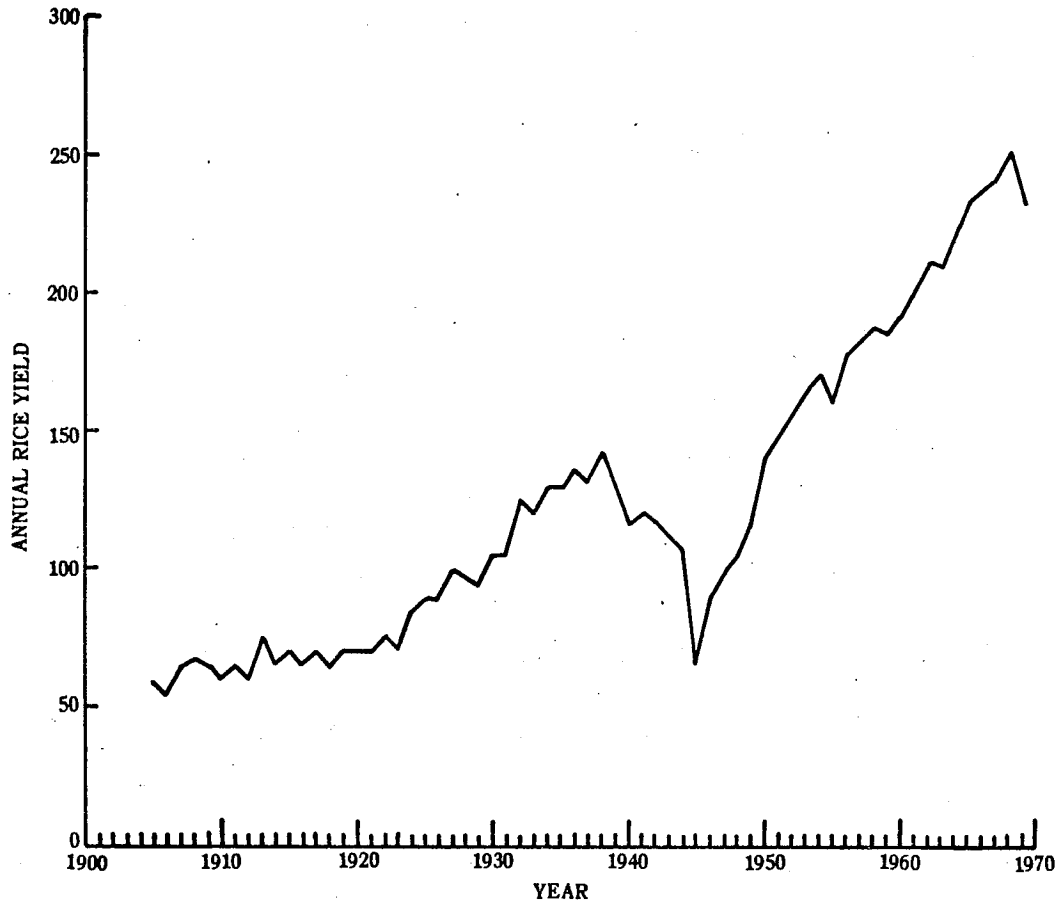

Figure 59. The secular variation in annual rice yields in Taiwan (rice yield unit: 1000 m.t., after Chen, 1959 and The Republic of China, 1970).

BIBLIOGRAPHY

Abbott, D.A., 1973, "Scale interactions of forced quasi-stationary planetary waves at low latitudes," Report 73-2, Department of Meteorology, Florida State University, Tallahassee, 190 pp.

Arakawa, H., 1956a, "On the secular variation of annual totals of rainfall at Seoul from 1770 to 1944," Archiv für Meteorologie, Geophysik und Bioklimatologie, Series B, Vol. 7, pp. 205-211.

Arakawa, H., 1956b, "Two minima of the average rainfall at about 1940 in the Far East," Archiv für Meteorologie, Geophysik und Bioklimatologie, Series B, Vol. 7, pp. 406-412.

Ballenzweig, E.M., 1959, "Relation of long-period circulation anomalies to tropical storm formation and motion," Journal of Meteorology, Vol. 16, pp. 121-139.

Barnes, A.A., 1919, "Rainfall in England: the true long-average as deduced from symmetry," Quarterly Journal of the Royal Meteorological Society, vol. 45, pp. 209-232.

Barry, R.G., and Chorley, R.J., 1971, Atmosphere, Weather and Climate, Methuen & Co. Ltd., London, 379 pp.

Barry, R.G., and Perry, A.H., 1973, Synoptic Climatology: Methods and Applications, Methuen & Co. Ltd., London, 555 pp.

Baur, F., 1941, "Haufigkeit und Aufeinanderfolge der Grund-formen der Boden Luftdruckverteilung über Westeuropa im Sommer auf grund 55-jähriger Beubachtungen (1885-1939)," Reichsamt für Wetterdienst, Forschungs--und Erfahrungs-berichte, Reihe B, no. 5.

Bean, L.H., 1964, "The predictability of cycle, trends and annual fluctuations in weather and crops," Weather and Our Food Supply, CAED Report 20, Iowa State University of Science and Technology, pp. 153-171.

Bell, G.J., 1969, The Monsoon Trough Near the South China Coast, Royal Observatory, Hong Kong, 23 pp.

Biel, E., 1929, "Die Veränderlichkeit der Jahresume des Niederschlages auf der Erde," Geogr. Jahresbericht aus Oesterreich, vol. 14-15, pp. 150-180.

Bjerknes, J., 1966, "A possible response of the atmospheric Hadley circulation to equatorial anomalies of ocean temperature," Tellus, vol. 18, pp. 820-829.

Bjerknes, J., 1969, "Atmospheric teleconnections from the equatorial Pacific," Monthly Weather Review, vol. 97, pp. 163-172.

Bleeker, W., and Andre, M.I., 1951, "On the diurnal variation of precipitation, particularly over central U.S.A. and its relation to large-scale orographic circulations systems," Quarterly Journal of the Royal Meteorological Society, vol. 77, pp. 260-282.

Bowie, E.H., and Weightman, R.H., 1914, "Types of storms of the United States and their average movement," Monthly Weather Review, Supplement No. 1.

Brooks, C.E.P., 1949, Climate through the Ages, London (benn), 2nd edition, 395 pp.

Bryson, R.A., and Lowry, W.P., 1955, "Synoptic climatology of the Arizona summer precipitation singularity," Bulletin of the American Meteorological Society, vol. 36, pp. 329-339.

Bryson, R.A., and Peterson, J.T., 1968, "Atmospheric aerosols: increased concentration during the last decades," Science, vol. 162, pp. 120-121.

Budyko, M.I., 1972, "The future climate," Transactions, American Geophysical Union, vol. 53, pp. 868-874.

Burger, 1952, Klimatologische Studie über die Temperaturverhältnisse der Grosswetterlagen Mitteleuropas, Berichte, des Deutschen Wetterdienstes in der US-Zone.

Byers, H.R., and Rodebush, H.R., 1948, "Causes of thunderstorms of the Florida Peninsula," Journal of Meteorology, vol. 15, pp. 275-280.

Caskey, J.E. Jr., 1963, "A Markov chain model for the probability of precipitation occurrence in intervals of various length," Monthly Weather Review, vol. 91, pp. 298-301.

Caviedes, C.N., 1973, "Secas and El Nino Two simultaneous climatical hazards in South America," Proceedings, Association of American Geographers, vol. 5, pp. 44-49.

Chang, J.H., 1959, "Zonal indices as related to the winter climate in East Asia," Annals, Association of American Geographers, vol. 49, pp. 156-163.

Chang, J.H., 1972, Atmospheric Circulation Systems and Climates, The Oriental Publishing Company, Honolulu, 328 pp.

Chang, X., and Sh, G.E., 1957, "The activity of the anticyclone in Eastern Asia," Acta Meteorologica Sinica, vol. 28, pp. 167-174.

Chen, C.S., 1959, A Geography of Taiwan, vol. 1, 400 pp.

Chen, H.Y., 1957, "The circulation characteristics during the 1954 flood period in the Yangtze and Hwai Basins," Acta Meteorologica Sinca, vol. 28, pp. 1-12.

Chen, L.S., 1965, "Flow patterns in the westerlies in relation to the East Asia typhoon tracks," Acta Meteorologica Sinica, vol. 35, pp. 476-485.

Cheng, C.S., 1949, Chinese Synoptic Weather Patterns, Shanghai Observatory, 114 pp.

Cheng, T.C., 1959, "A discussion on great inundation in the middle and southern parts of Taiwan in relation to the promotion on the study of geophysical science," Meteorological Bulletin of Taiwan, vol. 5, no. 2, pp.1-15.

Chi, C.H., 1964, "Plum rains in Taiwan," Meteorological Bulletin of Taiwan, vol. 10, no. 2, pp. 1-12.

Chi, C.H., 1969, "The distribution of rainfall in Taiwan," Meteorological Bulletin of Taiwan, vol. 15, no. 3, pp. 26-47.

Chiang, P.J., 1954, Meteorology of Taiwan, Bank of Taiwan, 221 pp.

Chin, P.C., 1969, Cold Surges Over South China, Royal Observatory, Hong Kong, Technical Note, no. 28, 19 pp.

Chow, M.D., and Cheng, J.M., 1971, "A preliminary statistical study on meteorological minima at Taipei international airport," Chinese American Air Forces Technical Meteorological Workshop, Second Session Program, published by the First Weather Wing, 576 pp. (see pp. 541-557).

Chu, C.C., 1926, "A preliminary study on the weather types of East China," Proceedings of the First Pan-Pacific Science Congress, Tokyo, Japan.

Chu, P.H., 1962, "Climate of China," Science Publications, Peking (English translation, 1967, U.S. Department of Commerce, Joint Publication Research Service).

Cooke, D.S., 1953, "The duration of wet and dry spells at Moncton, New Brunswick," Quarterly Journal of the Royal Meteorological Society, vol. 79, pp. 536-538.

Dao, S.Y., and Chen, L.S., 1957, "The structure of the general circulation over the Asiatic continent in summer," Acta Meteorologica Sinica, vol. 28, pp. 234-247.

Dao, S.Y., and Chu, F.K., 1964, "Variations of the 100-mb flow pattern over southern Asia in summer and its relation to the advance and retreat of the west Pacific subtropical anticyclone," Acta Meteorologica Sinica, vol. 34, pp. 385-396.

Dao, S.Y., et al., 1958, "The relationship between the Mai-yü period in the Far East and the seasonal variation of the upper-air circulation over Asia," Acta Meteorologica Sinica, vol. 29, pp. 119-134.

Defant, F., 1951, "Local Winds," Compedium of Meteorology, American Meteorological Society, pp. 655-672.

Dexter, R.V., 1944, "The diurnal variation of warm-frontal precipitation and thunderstorms," Quarterly Journal of the Royal Meteorological Society, vol. 70, pp. 129-137.

Dzerdzeevskii, B., 1962, "Fluctuations of climate and of general circulation of the atmosphere in extra-tropical latitudes of the Northern Hemisphere and some problems of dynamic meteorology," Tellus, vol. 14, pp. 328-336.

Dzerdzeevskii, B., 1963, "Fluctuations of general circulation of the atmosphere and climate in the twentieth century," Changes of Climate, UNESCO, pp. 285-295.

Elliott, R.D., 1949, "Forecasting the Weather," Weatherwise, vol. 2, pp. 15-18, 40-43, 64-67, 86-88, 110-113, 136-138.

Estoque, M.A., 1961, "A theoretical investigation of the sea breeze," Quarterly Journal of the Royal Meteorological Society, vol. 87, pp. 136-146.

Fett, R.W., 1966, "Upper-level structure of the formative tropical cyclone," Monthly Weather Review, vol. 99, pp. 9-18.

Fett, R.W., 1968, "Typhoon formation within the zone of the intertropical convergence," Monthly Weather Review, vol. 96, pp. 106-117.

First Weather Wing, USAF, 1966, Taiwan Low Study, Technical study 1, 36 pp.

Fisher, R.A., et al., 1943, "The relation between the number of species and the number of individuals in a random sample of an animal proportion," Journal of Animal Ecology, vol. 12, pp. 42-58.

Fletcher, R.D., 1945, "The general circulation of the tropical and equatorial atmosphere," Journal of Meteorology, vol. 2, pp. 167-174.

Flohn, H., 1960a, "Monsoon winds and general circulation," in Monsoons of the World, India Meteorological Department, pp. 65-74.

Flohn, H., 1960b, "Recent investigations on the mechanism of the summer monsoon of southern and eastern Asia," in Monsoons of the World, India Meteorological Department, pp. 75-88.

Forsdyke, A.G., 1958, "Zonal and other indices," Meteorological Magazine, vol. 80, pp. 156-161.

Frisken, W.R., 1971, "Extended industrial evolution and climatic change," Transactions, American Geophysical Union, vol. 52, pp. 500-508.

Gabriel, K.R., and Neumann, J., 1962, "A Markov chain model for daily rainfall occurrence at Tel Aviv," Quarterly Journal of the Royal Meteorological Society, vol. 88, pp. 90-95.

Gangopadhyaya, M., et al., 1963, "Some characteristics of the average monsoon along the coasts of India and Burma," Australia Meteorological Magazine, no. 40-43, pp.

Grant, A.M., 1952, "Some properties of runs in smoothed random series," Biometrik, vol. 39, pp. 198-204.

Gray, W.M., 1968, "Global view of the origin of tropical disturbances and storms," Monthly Weather Review, vol. 96, pp. 669-700.

Gray, W.M., 1970, A Climatology of Tropical Cyclones And Disturbances Of the Western Pacific---With A Suggested Theory For Their Genesis/Maintenance, NAVWEARSCHIFAC, Technical paper, no. 19-70, 226 pp.

Green, J.R., 1965, "Two probability models for sequences of wet or dry days," Monthly Weather Review, vol. 93, pp. 155-156.

Hershfield, D.M., 1970, "The frequency and intensity of wet and dry seasons and their interrelationships," Water Resources Bulletin, vol. 6, pp. 87-93.

Hess, P. and Brezowsky, 1952, Katalog der Grosswetterlagen Europas, Berichte, des Deutscher Wetterdienstes in der US-Zone.

Hewson, E.W., 1937, "The application of wet-bulb potential temperature to air mass analysis, III Rainfall in depressions," Quarterly Journal of the Royal Meteorological Society, vol. 63, pp. 323-335.

Hewson, E.W., 1943, "The reflection, absorption and transmission of solar radiation by fog and cloud," Quarterly Journal of the Royal Meteorological Society, vol. 69, pp. 47-62.

Hobbs, P.V., et al., 1974, "Atmospheric effects of pollutants," Science, vol. 183, pp. 909-915.

Howell, W.E., 1954, "A study of the rainfall of central Cuba," Journal of Meteorology, vol. 10, pp. 270-278.

Hsu, C.H., 1969, "A study of forecasting cyclogenesis in Taiwan and front movement by 700-1000mb thickness charts," Meteorological Bulletin of Taiwan, vol. 15, no. 1, pp. 1-16.

Hsu, S.A., 1970, "Coastal air-circulation system: observations and empirical model," Monthly Weather Review, vol. 98, pp. 487-509.

Hsu, S.A., 1973, "Dynamics of the sea breeze in the atmospheric boundary layer: A case study of the free convection regime," Monthly Weather Review, vol. 101, pp. 187-194.

Hsu, S.Y., and Kao, Y.S., 1962, "The onset and retreat of the Chinese monsoon and the determination of their dates," Acta Geographica, vol. 28, pp. 1-18.

Hsu, Y.H., and Wang, S.T., 1956, "The formation of the middle tropospheric jet stream in relation to the Siberian polar outbreak over East Asia," Meteorological Bulletin of Taiwan, vol. 2, no. 1, pp. 1-10.

Hsu, Y.H., and Wang, S.T., 1958, "A discussion on forecasting a polar outbreak," Meteorological Bulletin of Taiwan, vol. 4, no. 3, pp. 6-14.

Hsueh, C.H., 1963a, "A study on East Asia weather types," Science Reports, Department of Geography, National Taiwan University, vol. 1, pp. 48-63.

Hsueh, C.H., 1963b, "On the application of East Asia winter weather types in forecasting weather," Science Reports, Department of Geography, National Taiwan University, vol. 2, pp. 1-12.

Julian, P. R., 1966, "The index cycle: a cross-spectral analysis of zonal index data," Monthly Weather Review, vol. 94, pp. 283-293.

Kang, Y.C., 1968, "On the characteristics of the precipitation in Taiwan," Science Reports, Department of Geography, National Taiwan University, vol. 5, pp. 25-47.

Kikuchi, R., 1970, "Fluctuation of winter precipitation in northern Honshu," Japanese Progress in Climatology, pp. 67-84.

Klemes, V., 1974, "The Hurst phenomenon: a puzzle?" Water Resources Research, vol. 10, pp. 675-688.

Koteswaram, P., 1960, "The Asian summer monsoon and the general circulation over the tropics," in Monsoons of the World, India Meteorological Department, pp. 105-110.

Kraus, E. B., 1954, "Secular changes in the rainfall regime of SE. Australia," Quarterly Journal of the Royal Meteorological Society, vol. 80, pp. 591-601.

Kraus, E.B., 1955a, "Secular changes of tropical rainfall regimes," Quarterly Journal of the Royal Meteorological Society, vol. 81, pp. 198-210.

Kraus, E.B., 1955b, "Secular changes of east coast rainfall regimes," Quarterly Journal of the Royal Meteorological Society, vol. 81, pp. 430-439.

Kraus, E.B., 1963. "The diurnal precipitation change over the sea," Journal of the Atmospheric Science, Vol. 20, pp. 551-556.

Krishnamurti, T.N., et al., 1973a, "Tropical east-west circulations during the northern winter," Journal of the Atmospheric Sciences, vol. 30, pp. 780-787.

Krishnamurti, T.N., et al., 1973b, "Tibetan high and upper tropospheric circulations during northern summer," Bulletin of the American Meteorological Society, vol. 54, pp. 1234-1249.

Krueger, A.F., and Gray, T.I., 1969, "Long-term variations in equatorial circulation and rainfall," Monthly Weather Review, vol. 97, pp. 700-711.

Kukla, G.J., and Kukla, H.J., 1974, "Increased surface albedo in the Northern Hemisphere," Science, vol. 183, pp. 709-714.

Lamb, H.H., 1966, "Climate in the 1960's: changes in the world's wind circulation reflected in prevailing temperatures, rainfall patterns and the levels of the African lakes," Geographical Journal, vol. 132, pp. 183-212.

Lamb, H.H., 1972, Climate: Present, Past and Future, Methuen & Co. Ltd., London, 612 pp.

Lamb, H.H., and Johnson, A.I., 1959, "Climatic variation and observed changes in the general circulation," Geografiska Annaler, vol. 41, pp. 94-134.

Lamb, H.H., and Johnson, A.I., 1961, "Climatic variation and observed changes in the general circulation," Geografiska Annaler, vol. 43, pp. 363-400.

Landsberg, H.E., 1951, "Statistical investigation into climatology of rainfall on Oahu," Meteorological Monograph, vol. 1, pp. 7-23.

Lee, C.B.M., 1967, A Preliminary Study of Thunderstorms In Hawaii, Unpublished Master's Thesis, Department of Meteorology, University of Hawaii.

Lee, T.L., 1971, "A study of fog forecast for Pingtung Area," Chinese American Air Forces Technical Meteorological Workshop, Second Session Program, published by the First Weather Wing, 576 pp. (see pp. 532-539).

Leopold, L.B., 1948, "Diurnal weather patterns on Oahu and Lanai, Hawaii," Pacific Science, vol. II, no. 2, pp. 81-93.

Leopold, L.B., 1949, "The interaction of trade wind and sea breeze, Hawaii," Journal of Meteorology, vol. 6, pp. 312-320.

Liu, H.S., 1966, "A study of weather forecasting in Taiwan," Geographical Studies, Department of Geography, Taiwan Normal University, no. 1, pp. 26-52.

Liu, K.N., and Wu, H.H., 1956, "A preliminary study on the determination of the nature synoptic summer season over the Asiatic natural synoptic region and the prevailing weather process in this season," Acta Meteorologica Sinica, vol. 27, pp. 219-241.

Loveridge, D.H., 1924, "Diurnal variation of precipitation at Honolulu," Monthly Weather Review, vol. 52, pp. 584-585.

Manabe, S., and Wetherald, R.T., 1967, "Thermal equilibrium of the atmosphere with a given distribution of relative humidity," Journal of the atmosphere sciences, vol. 24, pp. 241-259.

Manabe, S., and Hahn, D.C., 1973, "The general circulation of the tropics as simulated by the time integration of a global model of the atmosphere with an annual cycle of solar radiation," to be published.

Mandelbrot, B.B., and Wallis, J.R., 1968, "Noah, Joseph, and operational hydrology," Water Resources Research, vol. 4, pp. 909-918.

Mandelbrot, B.B., and Wallis, J.R., 1969a, "Computer Experiments with Fractional Gaussian Noises, Part I, average and variances," Water Resources Research, vol. 5, pp. 228-241.

Mandelbrot, B.B., and Wallis, J.R., 1969b, "Some long-run properties of Geophysical Records," Water Resources Research, vol. 5, pp. 321-340.

Mason, R.B., and Anderson, C.E., 1963, "The development and decay of the 100-mb summertime anticyclone over southern Asia," Monthly Weather Review, vol. 91, pp. 3-12.

Mather, J.R., 1968, "Irrigation agriculture in humid areas," in Eclectic Climatology, edited by Arnold Court, Oregon State University Press, Corvallis, Oregon, 184 pp. (see pp. 107-122).

Maunder, W.T., 1970, The Value of the Weather, Methuen & Co. Ltd., 388 pp. (see p. 58).

McPherson, R.D., 1970, "A numerical study of the effect of a coastal irregularity on the sea breeze," Journal of Applied Meteorology, vol. 5, pp. 767-777.

Means, L.L., 1944, "The nocturnal maximum occurrence of thunderstorms in the mid-western states," Department of Meteorology, University of Chicago, Miscellaneous Reports, no. 16, 38 pp.

Milankovich, M., 1930, "Mathematische klimaletore und astronomische theorie der klimaschwankungen," in W. Köppen and R. Geiger, Handbuch der Ulimalogoe, Berlin.

Mintz, Y., 1965, "Very long-term global integration of the primitive equations of atmospheric motion," World Meteorological Organization, Technical Note no. 66, pp. 141-147, also in Meteorological Monograph, vol. 8, 1968, pp. 20-36.

Mitchell, J.M., Jr., 1970, "A preliminary evaluation of atmospheric pollution as a cause of the global temperature fluctuation of the past century," in Global Effects of Environmental Pollution, edited by S.F. Singer and D. Reidel, Dordrecht, Holland.

Mizukoshi, M., 1962, "Distribution of rainfall related to the activities of Baiu-fronts," Geographical Review of Japan, vol. 35, pp. 35-44.

Möller, F., 1963, "On the influence of changes in the CO_2 concentration in air on the radiation balance of the earth's surface, and on the climate," Journal of Geophysical Research, vol. 68, pp. 3877-3886.

Namias, J., 1950, "The index cycle and its role in the general circulation," Journal of Meteorology, vol. 7, pp. 130-139.

Namias, J., 1955a, "Long range factors affecting the genesis and paths of tropical cyclones," Proceedings of the UNESCO symposium on typhoons, pp. 213-219.

Namias, J., 1955b, "Secular fluctuations in vulnerability to tropical cyclones in and off New England," Monthly Weather Review, vol. 83, pp. 155-162.

Namias, J., 1959, "Recent seasonal interactions between North Pacific waters and the overlying atmospheric circulation," Journal of Geophysical Research, vol. 64, pp. 631-646.

Namias, J., 1963, "Large-scale air-sea interactions over the North Pacific from summer 1962 through the subsequent winter," Journal of Geophysical Research, vol. 68, pp. 6171-6186.

Namias, J., 1965, "Macroscopic association between mean monthly sea-surface temperature and the overlying winds," Journal of Geophysical Research, vol. 70, pp. 2307-2318.

Namias, J., 1968, "The Labile Gulf of Alaska cyclone--key to large-scale weather modification elsewhere," Proceedings of the international conference on cloud physics, Toronto, August 26-30, 1968, pp. 735-743.

Namias, J., 1969a, "Autumnal variations in the North Pacific and North Atlantic anticyclones as manifestations of air-sea interaction," Deep Sea Research, Supplement to vol. 16, pp. 153-164.

Namias, J., 1969b, "Seasonal interaction between the North Pacific Ocean and the atmosphere in 1960's," Monthly Weather Review, vol. 97, pp. 173-192.

Namias, J., 1969c, "On the causes of the small number of Atlantic hurricanes in 1968," Monthly Weather Review, vol. 97, pp. 346-348.

Namias, J., 1972, "Large-scale and long-term fluctuations in some atmospheric and ocean variables," Proceedings of the 20th Nobel Symposium, Gothenburg, Sweden, pp. 27-48.

Namias, J., 1973, "Response of the equatorial countercurrent to the subtropical atmosphere," Science, vol. 181, pp. 1244-1245.

Namias, J., and Clapp, P., 1949, "Confluence theory of the high tropospheric jet stream," Journal of Meteorology, vol. 6, pp. 330-336.

Neumann, J., 1951, "Land breezes and nocturnal thunderstorms," Journal of Meterology, vol. 8, pp. 60-67.

Neyama, Y., 1963, "On the dates of the transition of wind direction from west to east in the lower stratosphere at Marcus Island in late spring and of the setting-in of Bai-u, the rainy season in Japan," Geophysical Magazine, vol. 31, pp. 633-651.

Nieuwolt, S., 1968, "Diurnal rainfall variation in Malaya," Annals of the Association of American Geographers, vol. 58, pp. 313-326.

O'Connell, P.A.P., 1971, "A simple stochastic modeling of Hurst's law," in Proceedings of the International Symposium on Mathematical models in Hydrology, International Association of Scientific Hydrology, Warsaw, pp. 327-358.

Orgill, M.M., 1960, "An investigation into the relationship of monthly circulation indices and anomalies to typhoon development in the western Pacific," Hawaii Institute of Geophysics, Scientific Report, no. 2.

Orgill, M.M., 1961, "Anomalous mean monthly circulation and typhoon development," Paper presented at First Western National Meeting of American Geophysical Union, Meteorological Section, Los Angeles, December 27-29, 1961.

Palmen, E., 1951, "The role of atmospheric disturbances in the general circulation," Quarterly Journal of the Royal Meteorological Society, vol. 77, pp. 337-354.

Palmer, C.E., 1949, "Notes on tropical meteorology," Technical Bulletin, 2143rd Weather Wing, vol. 1, no. 2, pp. 1-49.

Ramage, C.S., 1952, "Diurnal variation of summer rainfall over East China, Korea, and Japan," Journal of Meteorology, vol. 9, pp. 83-86.

Ramage, C.S., 1954, "Non-frontal crachin and cool season clouds of the China Seas," Bulletin of the American Meteorological Society, vol. 35, pp. 404-411.

Ramage, C.S., 1959, "Hurricane development," Journal of Meteorology, vol. 16, pp. 227-237.

Ramage, C.S., 1964, "Diurnal variation of summer rainfall of Malaya," Journal of Tropical Geography, vol. 19, pp. 62-68.

Ramage, C.S., 1968, "Role of tropical maritime continent in the atmospheric circulation," Monthly Weather Review, vol. 96, pp. 365-369.

Ramage, C.S., 1971, Monsoon Meteorology, International Geophysics Series, vol. 15, Academic Press, New York, 297 pp.

Rasool, S.I., and Hogan, J.S., 1969, "Ocean circulation and climatic changes," Bulletin of the American Meteorological Society, vol. 50, pp. 130-134.

Reed, T.R., 1932, "Weather types of the North Pacific Ocean as related to the weather on the North Pacific coast," Monthly Weather Review, vol. 60, pp. 246-252.

Republic of China, 1970, Taiwan Statistical Data Book, 217 pp.

Riehl, H., and Schacht, E., 1947, "Some aspects of Puerto Rican rainfall," Transactions of the American Geophysical Union, vol. 28, pp. 401-406.

Riehl, H., and Shafer, R.J., 1944, "The recurvature of tropical storms," Journal of Meteorology, vol. 1, pp. 42-54.

Rodriguez-Iturbe, E., et al., 1972, "Stream flow simulation, 1. A new look at Markovian models, fractional Gaussian noise and crossing theory; 2. The broken line process as a potential model for hydrological simulation," Water Resources Research, vol. 8, pp. 921-941.

Rossby, C.G., 1939, "Relation between variation in the intensity of the zonal circulation of atmosphere and displacements of the semi-permanent centers of actions," Journal of Marine Research, vol. 2, pp. 38-55.

Rossby, C.G., 1959, "Current problem in meteorology," The Atmosphere and Sea in Motion, The Rockefeller Institute Press and Oxford University Press, p. 9.

Rowntree, P.R., 1972, "The influence of tropical east Pacific temperatures on the atmosphere," Quarterly Journal of the Royal Meteorological Society, vol. 98, pp. 290-321.

Sadler, J.C., 1964, "Tropical cyclones of the eastern North Pacific as revealed by Tiro observation," Journal of Applied Meteorology, vol. 3, pp. 347-366.

Saito, N., 1968, "A preliminary study of the summer monsoon of southern and eastern Asia," Journal of the Meteorological Society of Japan, vol. 44, pp. 44-59.

Samarakkody, A., 1969, Synoptic Climatology of the Hawaiian Region, Unpublished Master's Thesis, Department of Meteorology, University of Hawaii, 110 pp.

Sandy, I.M., 1960, A Preliminary Statistical Investigation of the Rainfall of Java, Unpublished Ph.D. Dissertation, Department of Geography, Clark University, 153 pp.

Scheidegger, A.E., 1970, "Stochastic models in hydrology," Water Resources Research, vol. 6, pp. 750-755.

Sekiguti, T., 1964, "Secular change patterns of Japanese rainfall," Geographical Review of Japan, vol. 37, pp. 217-225.

Shaw, R.H., and Thompson, L.M., 1964, "Grain yields and weather fluctuations," Weather And Our Food Supply, CAED Report 20, Iowa State University, pp. 9-21.

Shieh, Y.P., et al., 1963, "A preliminary statistic and synoptic study about the basic currents over southeastern Asia and the initiation of typhoons," Acta Meteorologica Sinica, vol. 33, pp. 206-217.

Simpson, R.H., et al., 1968, "Atlantic tropical disturbances, 1967," Monthly Weather Review, vol. 96, pp. 251-259.

Simpson, R.H., et al., 1969, "Atlantic tropical disturbances, 1968," Monthly Weather Review, vol. 97, pp. 240-255.

Staff Members, Academia, 1958, "On the general circulation over East Asia (II)," Tellus, vol. 10, pp. 58-75.

Stark, L.P., 1960, "The weather and circulation of August 1960, a month dominated by a circulation reversal," Monthly Weather Review, vol. 88, pp. 286-294.

Subbaramayya, I., and Ramanadham, R., 1966, "The Asian summer-monsoon circulation," Journal of the Meteorological Society of Japan, vol. 44, pp. 167-172.

Suda, K., and Asakura, A., 1955, "A study in the unusual Baiu season in 1954 by means of northern hemispheric upper-air mean charts," Journal of the Meteorological Society of Japan, vol. 33, pp. 233-244.

Thompson, L.M., 1964, "Multiple regression techniques in the evaluation of weather and technology in crop production," Weather And Our Food Supply, CAED Repprt 20, Iowa State University, pp. 75-92.

Topil, A.G., 1963, "Precipitation probability at Denver related to length of period," Monthly Weather Review, vol. 91, pp. 293-297.

VanderMeer, C., 1968, "Changing water control in a Taiwanese rice-field irrigation system," Annals of Association of American Geographers, vol. 58, pp. 720-747.

Vowinckel, E., 1956, "Ein Beitrag zur Witterungsklimatologie des Suedlichen Mozambiquekanals," Miscelanea Geofisca Publicada Pelo Servico Meteorologie de Angola em Comemoracaco do X Aniversario do Servico Meteorologico Nacional (Luanda), pp. 63-68.

Wahl, E.W., 1972, "Climatological studies of the large-scale circulation in the Northern Hemisphere," Monthly Weather Review, vol. 100, pp. 553-564.

Wang, P. I., 1971, A Study of the Formation and Development of Taiwan Cyclones in Winter, Unpublished Master's Thesis, College of Chinese Culture, Taiwan, 100 pp.

Wang, S.T., 1958a, "A discussion on forecasting a polar outbreak," Meteorological Bulletin of Taiwan, vol. 4, no. 3, pp. 6-14.

Wang, S.T., 1958b, "An analysis of the severe cold outbreaks over China," Meteorological Bulletin of Taiwan, vol. 4, no. 4, pp. 15-22.

Wang, S.W., 1964, "Fluctuating in atmospheric circulation during the recent 90 years," Acta Meteorologica Sinica, vol. 34, pp. 486-506.

Watson, D.T., 1963, "Weather and plant yield," in Evans, C.T., ed., Environmental control of plant growth, Academic Press, New York, pp. 337-349.

Wei, Y.H., 1968, "A study of the winter precipitation in Taiwan and its relation with cold polar air outbreak, Meteorological Bulletin of Taiwan, vol. 4, no. 4, pp. 1-19.

Weiss, L.L., 1944, "Preliminary report on duration of stormy periods at selected localities and intervals between periods," Research Paper, no. 3, U.S. Weather Bureau, Washington.

Weiss, L.L., 1964, "Sequences of wet or dry days described by a Markov chain probability model," Monthly Weather Review, vol. 92, pp. 169-176.

Willett, H.C., 1931, "Ground plan of a dynamic climatology," Monthly Weather Review, vol. 59, pp. 219-223.

Willett, H.C., 1949, Final Report of the Weather Bureau--M.I.T. Extended forecasting project for the Fiscal Year July 1, 1948-June 30, 1949, Cambridge, Mass.

Willett, H.C., 1959, "Climatic trends of temperature and precipitation in the continental United States," Proceedings of the Eastern Snow Conference, pp. 55-75.

Willett, H.C., 1961, "The pattern of solar climatic relationship," Annals, New York Academic Sciences, vol. 95, pp. 89-96.

Willett, H.C., 1965, "Solar-climatic relationships in the light of standardized climatic data," Journal of the Atmospheric Sciences, vol. 22, pp. 120-136.

Williams, C.B., 1947, "The logarithmic series and its application to biological problems," Journal of Ecology, vol. 34, pp. 253-272.

Williams, C.B., 1952, "Sequences of wet and dry days considered in relation to the logarithmic series," Quarterly Journal of the Royal Meteorological Society, vol. 78, pp. 91-96.

World Meteorological Organization (W.M.O.), 1966, Climatic Change, Technical Note no. 79, 79 pp.

Worthley, L.E., 1967, "Synoptic Climatology of Hawaii," Part I, Weather Phenomena in Hawaii, Hawaii Institute of Geophysics, University of Hawaii, no Cwb 11373, 39 pp.

Wu, T.Y., 1971, "Relationships of the continental migratory highs to the weather in Taiwan during winter season," Chinese American Air Forces Technical Meteorological Workshop, Second Season Program, published by First Weather Wing, 576 pp.

Wyrtki, K., 1973, "Teleconnections in the equatorial Pacific Ocean," Science, vol. 180, pp. 66-68.

Yeh, T.C., 1950, "Circulation of the high-troposphere over China in winter, 1945-1946," Tellus, vol. 2, pp. 173-183.

Yeh, T.C., et al., 1951a, "A study of rainfall over Oahu," Meteorological Monographs, American Meteorological Society, vol. 1, pp. 34-46.

Yeh, T.C., et al., 1951b, "On the relation between circumpolar westerly current and rainfall over the Hawaiian Islands," Meteorological Monographs, vol. 1, pp. 47-55.

Yeh, T.C., et al., 1952, "A study on jet stream development over South Asia and Southwest North America during the period 1945-1946," Acta Meteorologica Sinica, vol. 23, pp. 1-32.

Yeh, T.C., et al., 1958, "The abrupt change of circulation over Northern Hemisphere during June and October," Acta Meteorologica Sinica, vol. 29, pp. 249-263.

Yeh, T.C., et al., 1959, "The abrupt change of circulation over the Northern Hemisphere during June and October," The Atmosphere And The Sea In Motion, Oxford University Press (Rossby memorial volume), pp. 249-267.

Yevjevich, V., 1968, "Misconception in hydrology and their consequences," Water Resources Research, vol. 4, pp. 225-232.

Yin, M.T., 1949, "A synoptic-aerologic study of the onset of the summer monsoon over India and Burma," Journal of Meteorology, vol. 6, pp. 393-400.

Yoshimura, M., 1971, "Regionality of secular variation in precipitation over monsoon Asia and its relation to general circulation," in Water Balance of Monsoon Asia, ed. by M.M. Yoshino, University of Hawaii Press, pp. 195-215.

Yoshino, M.M., 1965a, "Four stages of the rainy season in early summer over East Asia (Part I)," Journal of the Meteorological Society of Japan, vol. 43, pp. 231-245.

Yoshino, M.M., 1965b, "Frontal zones and precipitation distribution in the rainy season over East Asia," Geographical Review of Japan, vol. 38, pp. 14-28.

Yoshino, M.M., 1966, "Four stages of the rainy season in early summer over East Asia (Part II)," Journal of the Meteorological Society of Japan, vol. 44, pp. 209-217.

Yu, S.H., 1965, "A preliminary study on the dynamic stable layers over South China in winter," Acta Meteorologica Sinica, vol. 35, pp. 63-74.

Yu, T.W., and Wagner, N.K., 1970, "Diurnal variation of onshore wind speed near a coastline," Journal of Applied Meteorology, vol. 5, pp. 760-766.

Zou, H., et al., 1964, "An analysis of the 500-mb circulation in the middle and lower Yangtze Valley during the Mai-yü period," Acta Meteorologica Sinica, vol. 34, pp. 174-184.